

2013

# A NOVEL BIORELEVANT IN VITRO SYSTEM TO PREDICT THE IN VIVO PERFORMANCE OF ORAL TRANSMUCOSAL PRODUCTS

Poonam Delvadia

*Virginia Commonwealth University*

Follow this and additional works at: <http://scholarscompass.vcu.edu/etd>

 Part of the [Pharmacy and Pharmaceutical Sciences Commons](#)

© The Author

---

Downloaded from

<http://scholarscompass.vcu.edu/etd/3173>

This Dissertation is brought to you for free and open access by the Graduate School at VCU Scholars Compass. It has been accepted for inclusion in Theses and Dissertations by an authorized administrator of VCU Scholars Compass. For more information, please contact [libcompass@vcu.edu](mailto:libcompass@vcu.edu).

**© Poonam Renish Delvadia, 2013  
All Rights Reserved**

**A NOVEL BIORELEVANT *IN VITRO* SYSTEM TO PREDICT THE *IN VIVO*  
PERFORMANCE OF ORAL TRANSMUCOSAL PRODUCTS**

A dissertation submitted in partial fulfillment of the requirements for the degree of Doctor of  
Philosophy at Virginia Commonwealth University.

by

POONAM R. DELVADIA

M.PHARM., Gujarat University, India, 2006

B.PHARM., Gujarat University, India, 2004

Director: H. THOMAS KARNES, Ph.D.,

Professor & Graduate Program Director,  
Department of Pharmaceutics, School of Pharmacy

Virginia Commonwealth University  
Richmond, Virginia  
August 2013

**DEDICATION**

*To My Late Grandfather*

## ACKNOWLEDGEMENTS

There are number of individuals to whom I am greatly indebted and without whom this dissertation would not have been possible. First and foremost, I would like to express my immense gratitude to my major advisor Dr. H. Thomas Karnes. This dissertation could not have happened without Dr. Karnes' support, advice, insightful discussions and encouragement. I consider it as an honor to work with Dr. Karnes who is a source of inspiration for me to have a work-life balance. I owe my thanks to him for encouraging and allowing me to pursue extracurricular activities which helped me to gain confidence for leadership roles in addition to academic goals. Once again, I would like to show my appreciation to my advisor for his patience and motivation.

I would like to extend my sincerest thanks to my Graduate Committee members for their feedback, direction and assistance: Drs. William Barr, Mohamadi Sarkar, Sarah Rutan, Jurgen Venitz, Phillip Gerk and Don Farthing. Their advice and guidance has been instrumental in shaping this research project. I am deeply grateful to Dr. William Barr for his valuable advice on the biorelevant related work of my Ph.D. A very special thanks to Dr. Jurgen Venitz for his inputs on the pharmacokinetic aspects of my Ph.D. research work. I would also like to thank Dr. Sarah Rutan for her suggestions and guidance on the experimental designs. I owe my thanks to Dr. Sarkar for his efforts in collecting the information on the pharmacokinetic data of smokeless tobacco (snus) from The Center of Research and Technology, Altria, and making it available quickly for this research. I would like to thank Drs. Farthing and Gerk for their suggestions, advice and help. I appreciate Dr. Michael Kotlyar (College of Pharmacy, University of Minnesota) for sharing pharmacokinetic data on Stonewall with us.

My gratitude goes to the Bioanalytical Research Group: Dr. Randy James, Dr. Matthew Halquist, Dr. Kumar Shah, Dr. John Miller, Dr. Darren Desoi, Celeste Wilkinson, Dr. Yakun chen, Morse Faria, Brian Parris and Jaime Jenkel for their support and help. I would like to take this opportunity to deeply thank Dr. Matthew Halquist for his suggestions, being always available to answer my questions and help in instrument troubleshooting.

I thank the VCU Graduate School and School of Pharmacy for financial support. I gratefully acknowledge the financial support from The Center of Research and Technology, Altria, Richmond-VA that funded parts of the research discussed in this dissertation. I wish to express my thanks to the Pharmaceutics Department and Dean's Office staff: Keyetta, Laura and Karen for their assistance in orders and administrative work. I am also thankful to the PharTech staff for their immediate help.

It gives me a great pleasure in acknowledging the support and care I received from all my friends in the Department of Pharmaceutics: Apoorva, Morse, Gopichand, Clara, Ruba, Sayeed, Min, Li, Christine and Abdullah. Thank you friends for all the fond memories and graduate experience that you have left me with to cherish forever (Will miss our "lunch time"). The list is not complete without mention of my special friends: Kumar, Mrugaya, Lokesh, Rati, Parth, Lathika, Juni, Kunal, Aditi, Kshitij, Varsha, Ankit, Ranu and Amit. Thank you all my friends for your support and love in good as well as difficult times.

Most importantly, I would like to devote my heartfelt gratitude to my parents (Yogeshkumar S Aghara and Aartiben Y Aghara) for being a constant source of love, care and strength. I would not have made this far without their sacrifices. Thank you very much Dad and Mom for encouraging me throughout this endeavor and supporting me in all my pursuits. I warmly appreciate the love, support, patience and understanding of my parents in law (Ramniklal G Delavdia and Geetaben R Delvadia). My special thanks to other members in my family – Uncle (Kamlesh S Aghara), Aunt (Nipa K Aghara), Brothers (Love and Keval) and Sister (Shreena) who have supported me throughout. Last but certainly not least, I am deeply indebted to my incredible husband, Renish. This dissertation could not have been accomplished without the endless support, trust, love and encouragement offered by Renish. Thank you for always being there for me through all of my ups and downs.

## TABLE OF CONTENTS

	Page
<b>ACKNOWLEDGEMENTS</b> .....	iii
<b>LIST OF TABLES</b> .....	xiii
<b>LIST OF FIGURES</b> .....	xvi
<b>ABBREVIATIONS</b> .....	xxi
<b>ABSTRACT</b> .....	xxiv
<b>CHAPTER</b>	
<b>1 BACKGROUND AND SIGNIFICANCE</b> .....	1
<b>2 SELECTIVITY INVESTIGATION AND LIQUID CHROMATOGRAPHIC METHOD FOR THE ANALYSIS OF NICOTINE IN TOBACCO EXTRACTS</b>	18
<b>2.1 INTRODUCTION</b> .....	18
<b>2.2 MATERIALS AND METHODS</b> .....	20
2.2.1 MATERIALS.....	20
2.2.2 DESCRIPTION OF THE SNUS AND BIORELEVANCE .....	21
2.2.3 HIGH PERFORMANCE LIQUID CHROMATOGRAPHIC (HPLC) MTHOD .....	22
2.2.3.1 CHROMATOGRAPHY.....	22
2.2.3.2 PREPARATIONS OF STANDARDS AND QUALITY CONTROL SAMPLES .....	22
2.2.3.3 METHOD VALIDATION.....	23
2.2.3.4 STABILITY.....	24

2.2.4	SELECTIVITY OF THE HPLC METHOD FOR NICOTINE ANALYSIS).....	24
2.2.4.1	STANDARD ADDITION METHOD.....	25
2.2.4.2	PEAK PURITY TESTING.....	26
2.2.4.3	PEAK TRAPPING AND IDENTIFICATION BY THE MASS SPECTROMETRIC METHOD.....	27
2.2.5	LEACHING STUDY.....	29
2.2.6	PDA SPECTRUM AND CHROMATOGRAM OF THE LEACHED STUDY SAMPLE.....	30
<b>2.3</b>	<b>RESULTS AND DISCUSSION.....</b>	<b>31</b>
2.3.1	METHOD VALIDATION.....	31
2.3.1.1	LINEARITY AND LOQ.....	31
2.3.1.2	ACCURACY AND PRECISION.....	33
2.3.1.3	SYSTEM SUITABILITY PARAMETERS.....	33
2.3.2	STABILITY.....	35
2.3.3	SELECTIVITY OF THE HPLC METHOD FOR NICOTINE ANALYSIS.....	35
2.3.3.1	STANDARD ADDITION METHOD.....	35
2.3.3.2	PEAK PURITY TESTING.....	38
2.3.3.3	PEAK TRAPPING AND IDENTIFICATION BY THE MASS SPECTROMETRIC METHOD.....	41
2.3.4	LEACHING STUDY.....	44



2.3.5	PDA SPECTRUM AND CHROMATOGRAM OF THE LEACH STUDY SAMPLES.....	47
2.4	CONCLUSIONS.....	49
3	<b>A BIORELEVANT <i>IN VITRO</i> RELEASE/PERMEATION SYSTEM FOR ORAL TRANSMUCOSAL PRODUCTS.....</b>	50
3.1	INTRODUCTION.....	50
3.2	MATERIALS AND METHODS.....	53
3.2.1	MATERIALS.....	53
3.2.2	DESCRIPTION OF THE SNUS.....	54
3.2.3	MEDIUM FOR RELEASE AND PERMEATION STUDY.....	55
3.2.4	APPARATUSES.....	55
3.2.4.1	MODIFIED USP IV FLOW THROUGH APPARATUS (USP IV).....	56
3.2.4.2	VERTICAL DIFFUSION CELL (VDC) .....	59
3.2.4.3	NOVEL BIDIRECTIONAL TRANSMUCOSAL APPARATUS (BTA) .....	59
3.2.5	<i>IN VITRO</i> RELEASE/PERMEATION STUDY .....	62
3.2.5.1	EXPERIMENTAL SET-UP/CONDITIONS.....	62
3.2.5.2	BIORELEVANCE.....	63
3.2.5.3	BIDIRECTIONAL TRANSMUCOSAL APPARATUS ORIENTATION.....	64
3.2.5.4	MEMBRANE SELECTION.....	65

3.2.5.5	NICOTINE ADSORPTION STUDY ON ACRYLIC BIDIRECTIONAL TRANSMUCOSAL APPARATUS.....	66
3.2.6	<i>IN VIVO</i> STUDY.....	66
3.2.7	DATA ANALYSIS/PHARMACOKINETIC ASSESSMENT....	67
<b>3.3</b>	<b>RESULTS AND DISCUSSION.....</b>	<b>69</b>
3.3.1	VALIDATION OF THE SYSTEM.....	69
3.3.1.1	BIDIRECTIONAL TRANSMUCOSAL APPARATUS ORIENTATION.....	69
3.3.1.2	MEMBRANE SELECTION.....	73
3.3.1.3	ADSORPTION OF NICOTINE ON THE ACRYLIC BIDIRECTIONAL TRANSMUCOSAL APPARATUS AND ASSEMBLY COMPONENTS.....	78
3.3.2	<i>IN VITRO</i> RELEASE/PERMEATION STUDY.....	80
3.3.3	<i>IN VIVO</i> STUDY.....	82
3.3.4	<i>IN VITRO IN VIVO</i> RELATIONSHIP (IVIVR) .....	84
3.3.5	COMPARISON OF THE THREE APPARATUSES.....	85
<b>3.4</b>	<b>CONCLUSIONS.....</b>	<b>88</b>
<b>4</b>	<b>SCREENING AND SELECTION OF PHYSIOLOGICAL AND <i>IN VITRO</i> VARIABLES TO OPTIMIZE THE <i>IN VITRO IN VIVO</i> RELATIONSHIP (IVIVR) FOR SMOKELESS TOBACCO (SNUS) USING BIDIRECTIONAL TRANSMUCOSAL APPARATUS .....</b>	<b>89</b>
<b>4.1</b>	<b>INTRODUCTION.....</b>	<b>89</b>
<b>4.2</b>	<b>MATERIALS AND METHODS.....</b>	<b>91</b>

4.2.1	MATERIALS.....	91
4.2.2	SELECTION OF VARIABLES TO OPTIMIZE IVIVR FOR SMOKELESS TOBACCO (SNUS) .....	92
4.2.2.1	ORAL CAVITY PHYSIOLOGICAL VARIABLES....	94
4.2.2.2	<i>IN VITRO</i> VARIABLES.....	96
4.2.3	<i>IN VITRO</i> RELEASE AND PERMEATION TESTING.....	100
4.2.4	APPARTUS FOR AGITATION STUDY.....	109
4.2.5	EFFECT OF SNUS ON SALIVA pH.....	111
4.2.6	DATA ANALYSIS.....	111
<b>4.3</b>	<b>RESULTS AND DISCUSSION.....</b>	<b>112</b>
4.3.1	EFFECT OF ORAL CAVITY PHYSIOLOGICAL VARIABLES ON NICOTINE RELEASE/PERMEATION.....	112
4.3.2	EFFECT OF <i>IN VITRO</i> VARIABLES ON NICOTINE RELEASE/PERMEATION.....	118
<b>4.4</b>	<b>CONCLUSIONS.....</b>	<b>130</b>
<b>5</b>	<b>OPTIMIZATION OF THE <i>IN VITRO IN VIVO</i> RELATIONSHIP (IVIVR) FOR SMOKELESS TOBACCO (SNUS) EMPLOYING STIMULATED SALIVA SWALLOWING RATE (SSSR) AND MEDIA TEMPERATURE AS VARIABLES .....</b>	<b>131</b>
<b>5.1</b>	<b>INTRODUCTION.....</b>	<b>131</b>
<b>5.2</b>	<b>MATERIALS AND METHODS.....</b>	<b>133</b>
5.2.1	MATERIALS.....	133
5.2.2	EXPERIMENTAL DESIGN .....	134

5.2.3	<i>IN VITRO</i> RELEASE AND PERMEATION TESTING.....	134
5.2.4	DATA ANALYSIS.....	138
<b>5.3</b>	<b>RESULTS AND DISCUSSION.....</b>	<b>140</b>
5.3.1	EFFECT OF SSSR AND MEDIA TEMPERATURE ON <i>IN VITRO</i> NICOTINE PERMEATION RATE.....	140
5.3.2	EFFECT OF SSSR AND MEDIA TEMPERATURE ON THE RATIO OF <i>IN VITRO</i> NICOTINE PERMEATION TO <i>IN VIVO</i> NICOTINE ABSORPTION RATE .....	146
5.3.3	EFFECT OF SSSR AND MEDIA TEMPERATURE ON NICOTINE RELEASE AT 10 MIN FROM SNUS.....	150
5.3.4	OPTIMIZATION OF <i>IVIVR</i> FOR SNUS.....	156
<b>5.5</b>	<b>CONCLUSIONS.....</b>	<b>160</b>
<b>6</b>	<b>APPLICATION OF THE BIORELEVANT BIDIRECTIONAL TRANSMUCOSAL APPARATUS FOR THE PREDICTION OF THE <i>IN VIVO</i> PERFORMACE OF DISSOLVABLE COMPRESSED TOBACCO.....</b>	<b>161</b>
<b>6.1</b>	<b>INTRODUCTION.....</b>	<b>161</b>
<b>6.2</b>	<b>MATERIALS AND METHODS.....</b>	<b>163</b>
6.2.1	MATERIALS.....	163
6.2.2	DESCRIPTION OF STONEWALL.....	164
6.2.3	SELECTION OF VARIABLES FOR OPTIMIZATION OF <i>IVIVR</i> FOR STONEWALL.....	165
6.2.4	<i>IN VITRO</i> RELEASE AND PERMEATION TESTING.....	166

6.2.5	<i>IN VIVO</i> STUDY AND PHARMACOKINETIC ASSESSMENT OF STONEWALL.....	168
6.2.6	SAMPLE ANALYSIS.....	171
6.2.7	DATA ANALYSIS.....	172
<b>6.3</b>	<b>RESULTS AND DISCUSSION.....</b>	<b>173</b>
6.3.1	SAMPLE ANALYSIS.....	173
6.3.2	EFFECT OF DONOR MEDIA FLOW RATE AND MEDIA TEMPERATURE ON NICOTINE RELEASE/PERMEATION FROM STONEWALL .....	177
6.3.3	RELATIONSHIP BETWEEN NICOTINE RELEASE AND PERMEATION RATE .....	185
6.4	CONCLUSIONS.....	187
<b>7</b>	<b>SUMMARY AND GENERAL CONCLUSIONS.....</b>	<b>188</b>
	<b>REFERENCES.....</b>	<b>192</b>
	<b>APPENDICES.....</b>	<b>203</b>
	<b>APPENDIX A</b> METHOD VALIDATION RESULTS FOR THE HPLC METHOD REPORTED IN CHAPTER 2.....	204
	<b>APPENDIX B</b> DATA ON VALIDATION OF THE NOVEL BIDIRECTIONAL TRANSMUCOSAL APPARATUS DESIGNED FOR OTPs REPORTED IN CHAPTER 3.....	216
	<b>APPENDIX C</b> REPLICATE AND MEAN DATA ON SCREENING OF VARIABLES FOR THE OPTIMIZATION OF IVIVR FOR SNUS REPORTED IN CHAPTER 4.....	228

<b>APPENDIX D</b> REPLICATE AND MEAN DATA ON OPTIMIZATION OF THE IVIVR FOR SNUS REPORTED IN CHAPTER 5 .....	248
<b>APPENDIX E</b> REPLICATE AND MEAN DATA FOR NICOTINE RELEASE/PERMEATION, RATES AND LAG TIME OBTAINED WITH EXPERIMENTS REPORTED IN CHAPTER 6.....	268

## LIST OF TABLES

	Page
Table 1.1	Few examples of commercially available OTPs for drug delivery through oral cavity mucosa..... 3
Table 1.2	Physiological conditions of oral cavity for OTPs..... 14
Table 2.1	Accuracy and precision data for nicotine QCs in Hanks' media ..... 34
Table 2.2	System suitability parameters for nicotine (n=5)..... 34
Table 2.3	Peak purity testing on the nicotine standards and <i>in vitro</i> samples by autothreshold method..... 40
Table 2.4	Peak purity testing on the nicotine standards and <i>in vitro</i> samples by noise+solvent method..... 40
Table 3.1	Effect of apparatus orientation on nicotine permeation in receptor chambers (n=3)..... 72
Table 3.2	Nicotine release, cumulative nicotine permeation and nicotine adsorption with polyethersulfone (PES) and regenerated incellulose (RC) membranes..... 76
Table 3.3	Mean pharmacokinetic parameters (n=18) after administration of snus 1.0 g (8 mg nicotine)..... 82
Table 3.4	Simulation of oral cavity conditions by apparatuses..... 87
Table 4.1	Possibilities of the simulation and adjustment of oral cavity physiological and <i>in vitro</i> variables with the bidirectional transmucosal apparatus (BTA) and vertical diffusion cell (VDC)..... 93

Table 4.2	Anticipated effect of oral cavity physiological and <i>in vitro</i> variables on the permeation rate of nicotine from smokeless tobacco (snus) using BTA	99
Table 4.3	Conditions for experiments employing oral cavity physiological variables in the bidirectional transmucosal apparatus.....	104
Table 4.4	Conditions for experiments employing <i>in vitro</i> variables in the bidirectional transmucosal apparatus.....	105
Table 4.5	Artificial saliva preparation.....	107
Table 4.6	Nicotine release/permeation rate from snus as a function of physiological variables.....	116
Table 4.7	Nicotine release/permeation rate from snus as a function of <i>in vitro</i> variables.....	120
Table 5.1	A 3 <sup>2</sup> full multifactorial design for the optimization of IVIVR for snus using the bidirectional transmucosal apparatus.....	136
Table 5.2	Experimental conditions for 3 <sup>2</sup> factorial design.....	137
Table 5.3	<i>In vitro</i> nicotine permeation rate and the ratio of <i>in vitro</i> nicotine permeation to the <i>in vivo</i> nicotine absorption rate obtained from the 3 <sup>2</sup> factorial experiment.....	141
Table 5.4	Statistical validation of the second-order model for the <i>in vitro</i> nicotine permeation rate (ANOVA).....	141
Table 5.5	Statistical validation of the second-order model for the ratio of <i>in vitro</i> nicotine permeation to the <i>in vivo</i> nicotine absorption rate (ANOVA).....	147
Table 5.6	Cumulative <i>in vitro</i> nicotine release at 10 min obtained from the 3 <sup>2</sup> factorial experiments.....	153



Table 5.7	Statistical validation of the second-order model for <i>in vitro</i> nicotine release at 10 min (ANOVA).....	153
Table 5.8	Cumulative amount of nicotine permeated (mg), <i>in vitro</i> nicotine permeation rate (mg/min) and the ratio of <i>in vitro</i> nicotine permeation to <i>in vivo</i> nicotine absorption rates from snus at the optimal levels for SSSR 0.55 mL/min and media temperature 43 °C.....	158
Table 6.1	Experiments to optimize IVIVR for Stonewall using the BTA.....	167
Table 6.2	Peak purity testing on the nicotine standards and <i>in vitro</i> samples using the autothreshold method.....	176
Table 6.3	Nicotine permeation rate from Stonewall as a function of donor media flow rate and media temperature.....	180
Table 6.4	The ratio of <i>in vitro</i> nicotine permeation to the <i>in vivo</i> absorption rate from Stonewall as a function of donor media flow rate and media temperature.....	180
Table 6.5	Nicotine release rate from Stonewall as a function of donor media flow rate and media temperature.....	184

## LIST OF FIGURES

	Page
Figure 1.1 A pictorial representation of the oral cavity mucosal linings for drug delivery.....	4
Figure 1.2 A pictorial representation of <i>in vitro</i> devices for OTPs.....	10
Figure 1.3 A pictorial representation of <i>in vitro</i> devices for OTPs.....	10
Figure 2.1 Beaker set-up for nicotine permeation studies from snus.....	29
Figure 2.2 Representative chromatograms of blank and nicotine external standards.	32
Figure 2.3 Representative chromatogram of the <i>in vitro</i> nicotine sample.....	34
Figure 2.4 Comparison of the standard addition and external calibration curves.....	37
Figure 2.5 Mass spectra of peak trapped HBSS blank and external nicotine standard.	42
Figure 2.6 Mass spectra of peak trapped receptor and beaker <i>in vitro</i> sample at 60 min.....	43
Figure 2.7 Mass spectra of non-peak trapped blank and apparatus-assembly components.....	45
Figure 2.8 Mass spectra of non-peak trapped Neoprene O ring in Hanks' media sample.....	46
Figure 2.9 PDA chromatograms.....	48
Figure 2.10 Chromatogram of neoprene O ring in Hanks' media sample.....	48
Figure 3.1 The smokeless tobacco: Snus.....	54
Figure 3.2 Experimental set-up with three apparatuses.....	57
Figure 3.3 The novel bidirectional transmucosal apparatus.....	61

Figure 3.4	Effect of apparatus orientation on nicotine permeation in the receptor chambers.....	71
Figure 3.5	Effect of membrane type on nicotine permeation with the vertical diffusion cell and bidirectional transmucosal apparatus.....	77
Figure 3.6	Nicotine amount time profile for the nicotine adsorption study with the acrylic bidirectional transmucosal apparatus and assembly components...	79
Figure 3.7	The mean cumulative nicotine permeation/release time profiles with all three apparatuses.....	81
Figure 3.8	Deconvolution of plasma nicotine concentration time profile of snus by Wagner-Nelson modeling.....	83
Figure 3.9	<i>In vitro in vivo</i> relationships (IVIVR) for snus with three apparatuses.....	86
Figure 4.1	Bidirectional transmucosal apparatus assembly.....	102
Figure 4.2	Components of the bidirectional transmucosal apparatus for agitation study.....	110
Figure 4.3	The mean cumulative nicotine release at three saliva pH levels.....	115
Figure 4.4	Effect of snus on saliva pH at different volumes of saliva.....	116
Figure 4.5	The mean cumulative nicotine permeation at three stimulated saliva swallowing rate.....	117
Figure 4.6	The mean cumulative nicotine permeation at three receptor media flow rates.....	121
Figure 4.7	The mean cumulative nicotine permeation at three donor media flow rates	122
Figure 4.8	The mean cumulative nicotine permeation time profile at three receptor to donor media volume ratios.....	123

Figure 4.9	The mean cumulative nicotine permeation at three receptor dead volumes.	126
Figure 4.10	The mean cumulative nicotine permeation at three media temperatures...	127
Figure 4.11	The mean cumulative nicotine permeation as a function of agitation.....	128
Figure 5.1	The mean cumulative nicotine permeation time profile as a function of SSSR (mL/min) and media temperature (°C).....	142
Figure 5.2	The residual (predicted permeation rate – observed permeation rate) versus predicted <i>in vitro</i> nicotine permeation plot for the validation of the second-order model built to define the relationship between <i>in vitro</i> nicotine permeation rate (mg/min) and SSSR (mL/min) along with media temperature (°C).....	142
Figure 5.3	Three dimensional response surface plot for the <i>in vitro</i> nicotine permeation rate as a function of SSSR (mL/min) and media temperature (°C).....	145
Figure 5.4	The residual (predicted ratio of rates – observed ratio of rates) versus predicted ratio of rates plot for the validation of the second-order model built to define the relationship between ratio of rates and SSSR (mL/min) and media temperature (°C).....	147
Figure 5.5	Three dimensional response surface plot for the ratio of <i>in vitro</i> nicotine permeation to <i>in vivo</i> nicotine absorption rate as a function of SSSR (mL/min) and media temperature (°C).....	149
Figure 5.6	The mean cumulative <i>in vitro</i> nicotine release time profile as a function of SSSR (mL/min) and media temperature (°C).....	154

Figure 5.7	Residual nicotine release (predicted nicotine release – observed nicotine release) versus predicted nicotine release at 10 min for the validation of the second-order model built to define the relationship between the release of nicotine at 10 min and SSSR (mL/min) and media temperature (°C)...	154
Figure 5.8	Interaction plot for the effect of SSSR (mL/min) and media temperature (°C) on the release of nicotine at 10 min.....	155
Figure 5.9	Three dimensional response surface plot for <i>in vitro</i> nicotine release at 10 min as a function of SSSR (mL/min) and media temperature (°C).....	155
Figure 5.10	Contour plot of the ratio of <i>in vitro</i> nicotine permeation to <i>in vivo</i> nicotine absorption rate as a function of SSSR (mL/min) and media temperature (°C).....	157
Figure 5.11	The mean cumulative <i>in vitro</i> nicotine permeation time profile at optimal levels of of SSSR (0.55 mL/min) and media temperature (43 °C).....	159
Figure 5.12	The <i>in vitro in vivo</i> relationship (IVIVR) plot for snus at optimal levels of SSSR (0.55 mL/min) and media temperature (43 °C) using the BTA...	159
Figure 6.1	Compressed dissolvable tobacco: Stonewall.....	164
Figure 6.2	Deconvolution of plasma nicotine concentration time profile for Stonewall by Wagner-Nelson modeling.....	170
Figure 6.3	Comparison of the standard addition and external calibration curves.....	175
Figure 6.4	The mean cumulative nicotine permeation time profile for Stonewall at different donor media flow rates (DFR; mL/min) and media temperatures (T; °C).....	179

Figure 6.5	The mean cumulative nicotine release time profile for Stonewall at different donor media flow rates (DFR; mL/min) and media temperatures (T; °C).....	183
Figure 6.6	The relationship between nicotine release rate and permeation rate from Stonewall in the bidirectional transmucosal apparatus.....	186

## ABBREVIATIONS

%DFN	Percent deviation from nominal
%RSD	Percent relative standard deviation
®	Registered trademark
°C	Degree celsius
$\alpha$	Alpha
$\beta$	Buffer capacity
$\mu\text{g}$	Microgram
$\mu\text{m}$	Micrometer
ANOVA	Analysis of variance
AUC <sub>0-<math>\infty</math></sub>	Area under the curve from time 0 to time $\infty$
AUC <sub>0-t</sub>	Area under the curve from time 0 to time t
BLOQ	Below limit of quantification
BTA	Bidirectional transmucosal apparatus
cm	Centimeter
cm <sup>3</sup>	Cubic centimeter
C <sub>max</sub>	Maximum or peak plasma drug concentration
CV	Coefficient of variation
df	Degrees of freedom
DFR	Donor media flow rate
et al.	and others
F	Absolute bioavailability

FDA	Food and drug administration
FEP	Fluorinated ethylene propylene
FIP/AAPS	Federation Internationale Pharmaceutique/American Association of Pharmaceutical Scientists
FSPTC	Family Smoking Prevention and Tobacco Control Act
g	Gram
HBSS	Hanks' balanced salt solution
HEPES	N-(2-Hydroxyethyl)piperazine-N-(2-ethanesulfonic acid)
HPLC	High Performance Liquid Chromatography
HQC	High quality control
HSD	Honest Significant Difference
i.e.	That is
IR	Infrared
IV	Intravenous
IVIVR	In vitro in vivo relationship
KDa	Kilo dalton
Ke	Elimination rate constant
LOQ	Limit of quantification
LQC	Low quality control
mg	Milligram
mg/cm <sup>2</sup>	Milligram per centimeter square
Min	Minute
mL	Milliliter



mM/L/pH unit	Millimolar/liter/pH unit
MQC	Middle quality control
MS	Mass spectrometry
MUC	Modified Ussing chamber
MWCO	Molecular weight cut off
nm	Nanometer
OTPs	Oral transmucosal products
PDA	Photodiode array
PEEK	Polyether ether ketone
PMMA	Polymethyl methacrylate
QC	Quality control
R <sup>2</sup>	Coefficient of determination
rpm	Revolution or rotation per minute
SD	Standard deviation
SEM	Standard error of mean
SSSR	Stimulated salivary swallowing rate
SUPAC	Scale-up and post approval related changes
T <sub>max</sub>	Time to reach C <sub>max</sub>
USP	United States Pharmacopeia
USP IV	USP IV flow through apparatus
UV	Ultraviolet
VDC	Vertical diffusion cell
vs.	Versus

## ABSTRACT

### **A NOVEL BIORELEVANT *IN VITRO* SYSTEM TO PREDICT THE *IN VIVO* PERFORMANCE OF ORAL TRANSMUCOSAL PRODUCTS**

By Poonam R. Delvadia, B. Pharm., M.Pharm.

A dissertation submitted in partial fulfillment of the requirements for the degree of Doctor of Philosophy at Virginia Commonwealth University

Virginia Commonwealth University, 2013

Major Director: H. Thomas Karnes, Ph.D.  
Professor & Graduate Program Director,  
Department of Pharmaceutics, School of Pharmacy

In *vitro* dissolution, release and permeation testing is a common practice during drug product research and development. These *in vitro* tests, if predictive, are referred to as biorelevant tests and can play diverse roles to facilitate and expedite product development in a cost effective manner. Oral transmucosal products (OTPs) are currently tested using compendial and modified *in vitro* tests which may or may not be good predictors of *in vivo* performance due to a lack of biorelevance. A critical need for a broadly applicable and biorelevant *in vitro* system for OTPs has been expressed in the literature and the goal of this research was the development and

validation of a biorelevant *in vitro* method that can facilitate accurate prediction of the *in vivo* behavior of OTPs.

A combined strategy of appropriate apparatus design and relevant physiological and *in vitro* variable adjustment was investigated to incorporate biorelevance into evaluation of OTPs. A novel *in vitro* device, the bidirectional transmucosal apparatus (BTA), was designed and fabricated which allowed simulation of the oral cavity and its physiological variables to evaluate OTPs in a more realistic fashion. The BTA was tested using snus (a type of smokeless tobacco) as the OTP product. A simple and selective high performance liquid chromatographic (HPLC) method with photodiode array (PDA) detection was developed and validated to assess *in vitro* nicotine release and permeation (Linearity: 0.5 – 32 µg/mL; calibration curve accuracy (%recovery, n=5): 97.98-103.20%; calibration curve precision (%RSD, n=5): 0.15-3.14%). The performance of BTA was compared with the modified USP IV flow through apparatus (USP IV) and a commercially available vertical diffusion cell (VDC). The observed *in vitro in vivo* relationship (IVIVR) slopes with the USP IV, VDC and BTA were 0.27, 2.01 and 2.11 respectively. The BTA was selected over the VDC and USP IV devices because of better simulation and adjustment of variables to incorporate biorelevance in the test of OTPs. Additionally, the BTA allows study of permeation and release simultaneously unlike VDC and USP IV apparatuses. Further, the different BTA parameters were sequentially screened for their impact on *in vitro* rate of nicotine permeation that can be employed for the optimization of IVIVR for snus. Based on the results, stimulated saliva swallowing rate (SSSR) and media temperature were considered as significant factors affecting *in vitro* permeation of nicotine and used to further optimize IVIVR for snus. A 3<sup>2</sup> multifactorial experimental design integrating SSSR (0.32, 1.66 and 3 mL/min) and media temperature (25, 37 and 45 °C) was employed. Based on the response surface analysis, 0.55 mL/min SSSR and 43 °C

media temperature were identified as optimal BTA conditions that would give perfect IVIVR (i.e. IVIVR slope close to one) for snus. The experimental value of IVIVR slope (0.92) at these optimal conditions indicated that the BTA is a valid *in vitro* system for evaluation of OTPs in a biorelevant manner. The applicability of BTA for predicting nicotine permeation from ‘Stonewall’, a dissolvable compressed tobacco was also evaluated. However, comparable *in vitro* nicotine permeation and *in vivo* nicotine absorption profiles were not obtained (ratio of *in vitro* permeation to *in vivo* absorption rate ranged from 0.04 to 0.14 at different *in vitro* conditions) either due to the unavailability of reliable clinical data or due to inherently different *in vivo* behavior of Stonewall compared to snus that would require further modification in the BTA.

In conclusion, this research demonstrated the potential of the novel *in vitro* device to be a valuable tool for the prediction of *in vivo* performance of snus. The application of the novel bidirectional transmucosal apparatus for other types of OTPs will be an interesting subject for further investigation.

## **CHAPTER 1**

### **BACKGROUND AND SIGNIFICANCE**

The oral cavity provides an alternative route for efficacious systemic drug delivery through its mucosal linings (Washington et al. 2001; Madhav et al. 2009; Patel et al. 2011). Drug enters the systemic circulation through the oral cavity mucosa mainly by the passive transport mechanism (Washington et al. 2001; Patel et al. 2011). A profuse network of blood vessels present in this mucosal lining makes it a preferred route when quicker onset of action is required. The oral transmucosal route is an attractive option for delivery of drugs with gastric incompatibility and hepatic first pass metabolism (Madhav et al. 2009; Patel et al. 2011). With the advent of protein and peptide therapeutics which are susceptible to the gastric environment, the oral transmucosal route can be a favored delivery method for such drug candidates. The oral transmucosal route offers additional advantages of easy application of the product and its removal when required (Nicolazzo et al. 2008). The oral transmucosal route has been successfully explored for nicotine replacement therapy and smoking cessation (Zhang et al. 2002; Stead et al. 2008). This route is one of the options for nicotine consumer products (e.g. smokeless tobacco products). Because of the above multiple benefits of oral transmucosal products (OTPs) over traditional dosage forms like tablets and capsules, this route has attained considerable attention for drug delivery. Therefore,

many OTPs are on the market (Table 1.1) and many more are in the pipeline (Rathbone et al. 1996; Pather et al. 2008).

Therapeutic and non-therapeutic OTPs are formulated into tablets, patches, films, sprays, lozenges and chewing gums for delivery of drugs through mucosal linings of the oral cavity (Pfister et al. 2005; Patel et al. 2011). Figure 1.1 displays preferred oral transmucosal routes (sublingual, buccal and gingival) for drug delivery (Washington et al. 2001; Madhav et al. 2009). Table 1.1 lists a few of the sublingual, buccal and gingival OTPs commercially available for drug delivery. Each of these OTPs deliver drug by different release and permeation mechanisms (Dixit et al. 2009; Darwish et al. 2010; Sohi et al. 2010). The oral cavity environment plays a determinative role in the release of drug from the OTP to the delivery site and permeation of the drug through the oral mucosa for systemic delivery by influencing its operational mechanism (Patel et al. 2011). For example, the layer formed by mucus in saliva contributes to the formation of interfacial bonds based on intermolecular force with polymer chains of a bioadhesive OTP which aids in the adhesion of tablet to the oral cavity mucosal surface and helps with drug release and the permeation process (Duchêne et al. 1997). The components of saliva may also have an effect on the disintegration behavior of OTPs. An attempt was made for measuring the disintegration behavior of rapidly disintegration OTPs in simulated saliva (Abdelbary et al. 2005). The simulated saliva along with oral cavity temperature (37 °C) provided a better correlation between *in vitro* and *in vivo* disintegration time of rapidly disintegrating OTP in comparison to distilled water at room temperature (Abdelbary et al. 2005). The saliva variables and mucosal barriers may aid or hinder the release and absorption of drugs from OTPs (Nicolazzo et al. 2008). Therefore, it is critical to thoroughly evaluate oral transmucosal drug candidates and products by an appropriate *in vitro* system. The *in vitro* evaluation of products based on dissolution/release/permeation properties is

a common practice for the selection of an appropriate drug product for clinical studies and quality control purposes (Dressman et al. 1998; Wang et al. 2009).

**Table 1.1:** A few examples of commercially available OTPs for drug delivery through oral cavity mucosa

<b>Pharmaceutical OTPs</b>		
<b>Sublingual</b>	<b>Buccal</b>	<b>Gingival</b>
Nitroglycerin tablet (Nitrostat <sup>®</sup> )	Fentanyl Citrate tablet (Fentora <sup>®</sup> )	
Buprenorphine hydrochloride tablet (Subutex <sup>®</sup> )	Fentanyl Citrate dissolvable film (ONSOLIS <sup>®</sup> )	Lidocaine hydrochloride patch (Dentipatch <sup>®</sup> )
Buprenorphine hydrochloride and Naloxone hydrochloride film (Suboxone <sup>®</sup> )	Testosterone (Striant <sup>®</sup> )	
<b>Non pharmaceutical OTPs - Nicotine consumer products (Nicotine permeation through sublingual, buccal &amp; gingival membrane)</b>		
Nicotine chewing gum and lozenge (Nicorette <sup>®</sup> )		
Nicotine pouch (Zonnic <sup>®</sup> )		
Smokeless tobacco pouch (Marlboro)		
Smokeless tobacco dissolvable tablet (Stonewall)		

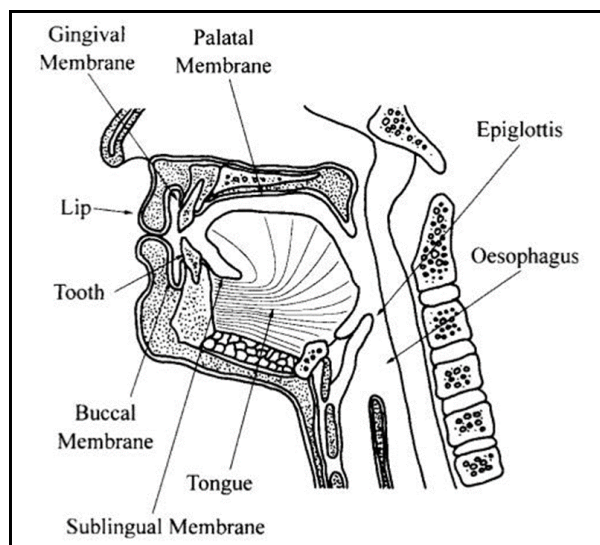


**Figure 1.1:** A pictorial representation of the oral cavity mucosal linings for drug delivery (Washington et al. 2001)

*In vitro* drug dissolution/release/permeation testing of dosage forms is a cost effective approach for pharmaceutical product quality and *in vivo* performance testing (Shah 2001). The *in vitro* test plays a vital role in the research and development phase for drug products and is an essential quality control tool (Wang et al. 2009). Specifically, with respect to research and development, *in vitro* testing should be able to predict the *in vivo* behavior of a drug product (Azarmi et al. 2007). The dissolution/release/permeation of drug from the product *in vivo* is one of the determinants of the systemic exposure of drug to the body in addition to its metabolism and excretion. The systemic exposure of drug to the body defined as the plasma drug concentration time profile or the amount of drug absorbed from the product is a measure of the *in vivo*



performance/behavior of the drug product and can be predicted by appropriate dissolution/release/permeation *in vitro* tests. The dissolution/release/permeation test can be a substitute for clinical studies; when the *in vitro* study can predict the *in vivo* performance of drug products (Dressman et al. 1998). When the *in vitro* test simulates relevant *in vivo* environment, it can accurately predict the *in vivo* behavior of drug products (Fotaki et al. 2010). Therefore, it would be of value to simulate physiological conditions like hydrodynamics, biological fluids and biological barriers in the *in vitro* system that affects the release and permeation properties of drugs from these products. The dissolution/release/permeation *in vitro* test that simulates relevant physiological conditions of the *in vivo* environment and successfully forecasts the *in vivo* performance of drug products is referred as a biorelevant test. Biorelevant tests can predict the *in vivo* behavior of a product through *in vitro in vivo* relationships (IVIVR) (Emami 2006; Wang et al. 2009; Fotaki et al. 2010). An IVIVR is defined as the predictive model that relates the *in vitro* drug dissolution/release/permeation time course and the *in vivo* response time course (Gillespie 1997). Biorelevant *in vitro* methods through IVIVR can provide predictive estimates of *in vivo* data and may be a surrogate for *in vivo* behavior of a drug product (Azarmi et al. 2007).

Biorelevant dissolution/release/permeation testing plays a versatile role at various stages of the drug product development process. Biorelevant *in vitro* testing is valuable in the selection of appropriate drug substance and optimal formulation for preclinical and clinical study, defining critical quality attributes and critical process parameters (Wang et al. 2009). The biorelevant approach also aids in gaining the approval of biowaivers after scale-up and post approval related changes in the drug products (SUPAC) (Emami 2006). A biowaiver is defined as the acceptance of *in vitro* testing as a surrogate for an *in vivo* bioequivalence study by the regulatory agency. Biorelevant drug release testing thus leads to fewer clinical studies, economizes and expedites the

drug development process by reducing the cost and time required for drug development and provides improved quality of the product (Emami 2006).

Significant advances have been made in the development of biorelevant *in vitro* systems for orally administered drug products (Dressman et al. 1998; Dressman et al. 2000; Vertzoni et al. 2005; Jantratid et al. 2008; Klein et al. 2008; Fang et al. 2010; Guhmann et al. 2013). The biorelevant methods that have been developed for oral products cannot be employed for novel dosage forms like subcutaneous implants, drug eluting stents, ocular systems, oral transmucosal products, etc., because novel dosage forms are designed for drug delivery in unique physiological environments. These require appropriate modification or design of novel *in vitro* devices for their evaluation. The standard/compendial methods do not simulate the physiological environment to which novel products are exposed *in vivo*. Therefore, efforts are underway to develop biorelevant *in vitro* systems to accurately characterize the dissolution/release/permeation of drugs from novel products (Crist 2009; Chidambaram et al. 1999; Kvist et al. 1999; Morjaria et al. 2004; Iyer et al. 2007a; Brown et al. 2011; Marques et al. 2011; Seidlitz et al. 2013).

Sublingual and buccal OTPs are traditionally evaluated by USP recommended methods employing a disintegration and dissolution apparatus. The USP monograph for ergoloid mesylate, ergotamine tartarate and nitroglycerine sublingual tablets suggests the use of the USP disintegration apparatus (an apparatus with a basket-rack assembly, a 1000 mL capacity glass beaker, a water bath and a device for up and down movement of the basket in the disintegration medium at a constant frequency); whereas, isosorbide dinitrate sublingual tablets are tested by USP II apparatus (an apparatus with paddle as a stirring element, a 1000 mL capacity glass vessel and a water bath) in 900 mL of water at 50 rpm (USP 2009a, b, c, d). Drug candidates for OTPs are currently evaluated by standard *in vitro* permeation devices such as a Franz cell, a Vertical

diffusion cell (VDC) or a Modified Ussing chamber (MUC) in the preclinical setting (Nicolazzo et al. 2008). The Franz cell and VDC both are vertical apparatuses and consists of a donor and receptor chamber separated by either an artificial or a mucosal membrane. The Franz cell has a static receptor compartment; whereas, the VDC provides a receptor chamber that can be maintained in a closed or open flow through condition (Nicolazzo et al. 2008). Unlike the Franz cell and VDC, the modified Ussing chamber is an apparatus that allows the flux of drug in a horizontal direction across the donor and receptor chamber of same volumes attributed to its design. The modified Ussing chamber is relatively a small volume apparatus (1.5 mL) in comparison to the Franz cell and VDC which are available in different volume capacity of the receptors compartments (Nicolazzo et al. 2008; Dezani et al. 2013). These standard/compendial and modified *in vitro* methods either utilize large volume of media or characterize products at conditions which do not reflect the *in vivo* physiological environment and hence may not be accurate predictors of *in vivo* performance of OTPs. A need to develop an appropriate *in vitro* model which simulates *in vivo* oral cavity conditions closely for the prediction of *in vivo* performance of OTPs has been documented (Patel et al. 2012). Several *in vitro* studies to simulate the low liquid surroundings of the oral cavity and other *in vivo* conditions to assess drug release and permeation from OTPs have been reported (Mumtaz et al. 1995; Luque-Pérez et al. 1999; Frenning et al. 2002; Hughes 2003; Nicolazzo et al. 2008; Lestari et al. 2009; Rachid et al. 2011).

Mumtaz and Ch'ng in 1995 developed a dissolution apparatus (Figure 1.2(A)) for a drug release study from bioadhesive buccal tablets using chicken buccal membrane and utilized this system for formulation optimization of triamcinolone acetonide (TAA) bioadhesive buccal tablet (Mumtaz et al. 1995). The apparatus was a closed flow through system that contained a dissolution cell and an assembly to hold the chicken buccal membrane for release testing of drug from the

bioadhesive buccal tablet. An attempt was made by Mumtaz et al. to simulation of buccal conditions; however, the system allowed only assessment of drug release in spite of the use of buccal membrane. The lack of receptor compartment in the apparatus did not allow study of drug permeation through the buccal membrane. The potential for modification of the system with respect to simulation of salivary variables (e.g. composition, secretion, swallowing) and incorporation of a receiver compartment for drug permeation existed. A method for determining drug release from OTPs in low liquid surroundings based on alternating ionic current measurements was developed (Frenning et al. 2002). A low liquid surrounding system developed by Frenning et al. is presented in Figure 1.2(B). The study was performed in two phases, Liquid absorption and drug release, utilizing a placebo and drug containing tablet respectively. For liquid absorption and drug release measurements, tablets were placed in water containing a conducting substance (sodium chloride) and distilled water respectively. The change in current as a function of time was related to the amount of liquid absorbed or drug released from the tablets. Liquid absorption was measured to determine the volume of liquid uptake which was further employed for the drug release measurement. The conclusions of this study indicated that large volume dissolution methods would not differentiate OTPs that were designed for fast release. The method simulates a low liquid environment which can be useful when developing biorelevant conditions for oral transmucosal drug release testing. However, this method does not study the contributions of drug in the liquid uptake process since a placebo tablet was used in the liquid absorption phase. The method relies on the assumption that both the processes of liquid absorption and drug release are well separated. In spite of the effort made to simulate oral cavity conditions, the system would not be compatible if simulated saliva was used due to the ionic components present in saliva which would contribute to the background current. Luque-Perez et al. developed a supported liquid

membrane system for the characterization of nicotine release and permeation from snuff in small volumes (Figure 1.2(C)) (Luque-Pérez et al. 1999). The system consisted of a small donor compartment separated from receptor chamber by a hydrophobic polypropylene porous membrane (20 nm) impregnated with n-undecane. A syringe with the bottom removed was filled with snuff and was placed in the donor chamber. A volume of 100  $\mu$ L of water was used as the donor media. A solution of sulfuric acid (pH 2.5) was employed as a receptor media which was maintained in an open flow through condition. Nicotine permeated into the receptor media was determined by inline spectrophotometric measurement saving time and resources. However, this may not be a selective analytical method because of the presence of the complex matrix in tobacco samples which could contribute to the spectrophotometric response of nicotine. Additionally, a study of the effect of saliva secretion and swallowing on the release and loss of drug, an important determinant of the bioavailability of drug, could not be studied due to limitations of the apparatus design.

A small volume buccal dissolution system for drug release from mouth dissolving OTPs was designed as shown in Figure 1.3(A) (Hughes et al. 2002). The system consisted of a single filtration cell of 10 mL capacity under continuous stirring and flow through conditions. Simulated saliva and the dissolution media, was circulated at a flow rate of 6 mL/min. The design lacked a permeation component which is a relevant variable in the availability of drug from mouth dissolving OTPs. This is because drug release is usually not a rate limiting step and therefore the buccal dissolution system may not be a suitable design for IVIVR.

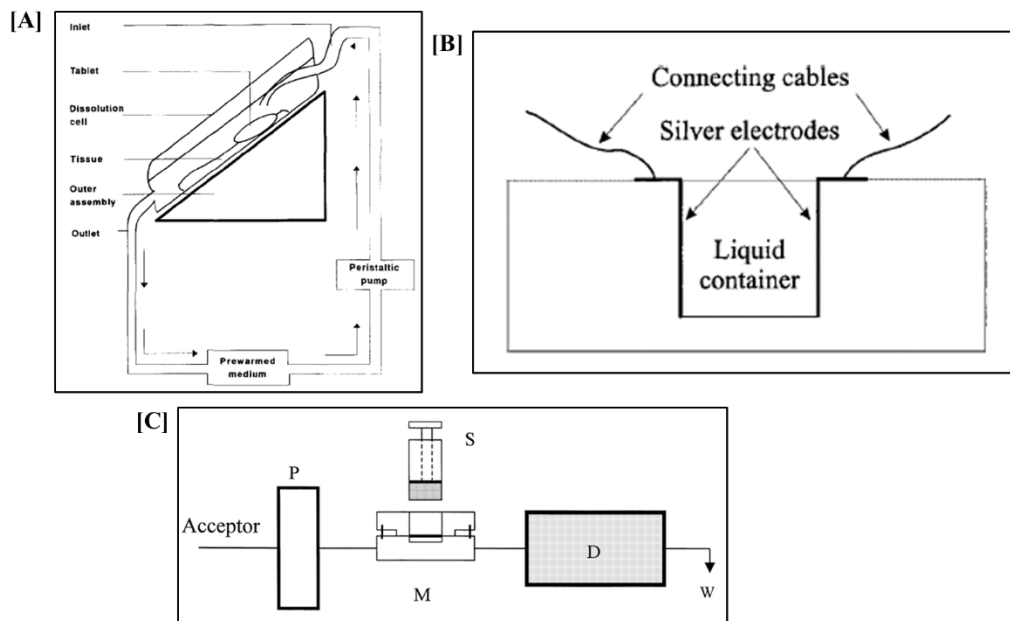


**Figure 1.2:** A pictorial representation of *in vitro* devices for OTPs; [A] Mumtaz et al. 1995; [B] Frenning et al. 2002; [C] Luque-Pérez et al. 1999. All pictures adopted from the respective references.

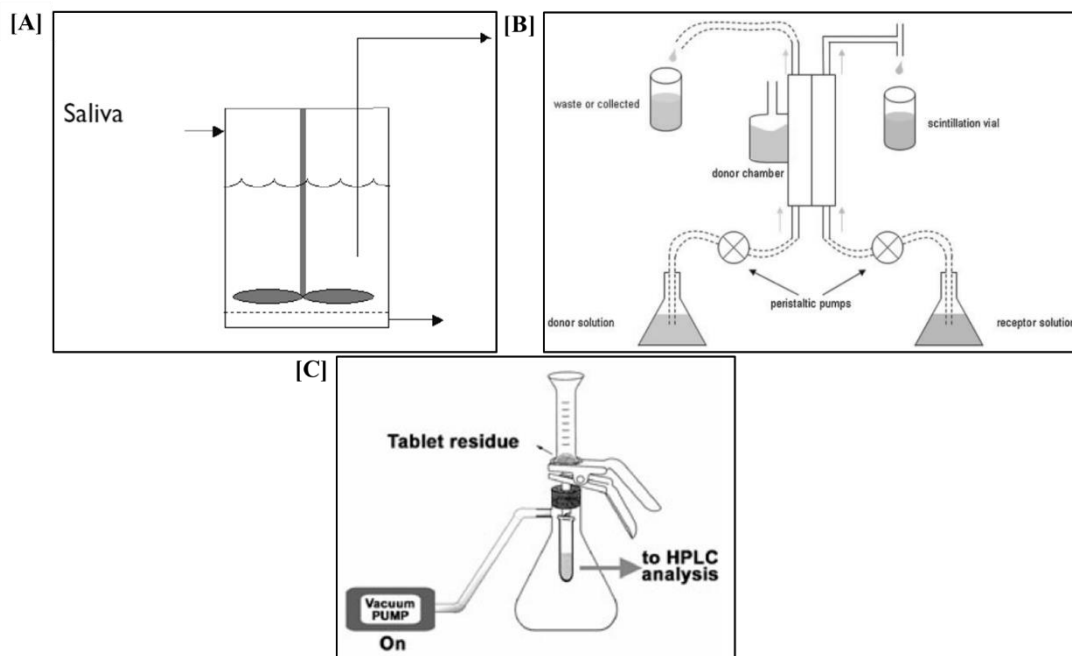


**Figure 1.3:** A pictorial representation of *in vitro* devices for OTPs; [A] Hughes et al. 2002; [B] Lestari et al. 2009; [C] Rachid et al. 2011. All pictures adopted from the respective references.

A flow through diffusion cell for study of drug permeation using porcine buccal mucosa was developed and evaluated employing drug in a solution (Figure 1.3(B)) (Lestari et al. 2009). The flow through diffusion cell comprised of a donor and receptor chamber both maintained under open flow through conditions. The permeation study was performed at a donor and receptor media flow rate of 1.2 mL/h which was very low and clinically not relevant. The diffusion cell was a reasonable model for screening drug candidates for oral transmucosal delivery in preclinical settings; however, an attempt to explore the applicability of the system to evaluate OTPs using artificial membranes was not made. The use of animal mucosal membranes may not be a practical approach for quality control and research purposes for OTPs due to the need of maintenance of viability of the oral cavity tissues throughout the experiment. In addition, the use of animal mucosal membranes would be an expensive approach. Furthermore, permeation of drug into receptors was measured unidirectionally which may not be true unless an OTP has an impermeable membrane on one side. Rachid et al. in 2011 built an apparatus for orally disintegrating tablets as presented in Figure 1.3(C) (Rachid et al. 2011). The system consisted of a glass funnel with a fritted glass base and a Buchner flask. A nylon filter membrane (0.45  $\mu\text{m}$ ) was placed between the funnel and glass base to retain solid particles after dissolution of sublingual tablets. A volume of 2 mL of distilled water was introduced into the glass funnel before the tablet was placed for dissolution studies. The flask was connected to vacuum with on and off switches for collecting fluid with dissolved drug. The filtrate was collected in a plastic tube below the filtration assembly for drug analysis. The system successfully simulated a small volume of oral cavity; however, other important saliva variables such as secretion and swallowing, which may be determining steps for drug release and permeation, could not be simulated.

The reported *in vitro* systems for OTPs simulated either small media volume or the membrane barrier or both; however, these systems did not simulate the physiological environment of the oral cavity completely and therefore these methods may be less predictive. Additionally, these systems provide fewer numbers of variables for simulation and adjustment and hence fewer options are available for optimization of IVIVR for OTPs. Some of these systems for OTPs utilized animal buccal mucosa for evaluation which may be tedious and present viability issues during the experiment which makes the use of animal mucosa impractical for quality control (QC) purposes. Furthermore, these systems were designed to suit specific types of products (bioadhesive or disintegrating OTPs or drug solution) and may not be universally applicable for all types of OTPs. Moreover, none of these devices have been validated by relating the *in vitro* with *in vivo* behavior. These methods, therefore, may or may not be able to predict the *in vivo* behavior of OTPs accurately. These limitations of the methods currently used for OTPs present a need of a biorelevant *in vitro* device that simulates oral cavity conditions completely and that facilitates the prediction of *in vivo* behavior of OTP product development in a cost effective manner which can also be employed as a quality control tool. An *in vitro* device which allows incorporating more number of physiological and *in vitro* variables would be beneficial as it will provide more options for adjustment and hence greater possibilities of establishing biorelevancy of the method. A need of a better *in vitro* device for OTPs was also recognized in the Federation Internationale Pharmaceutique/American Association of Pharmaceutical Scientists (FIP/AAPS) joint workshop report on Dissolution/*In vitro* Testing of Novel/Special Dosage Forms (Brown et al. 2011).

The development of biorelevant tests requires consideration of the physiological conditions of the drug product application site and then designing and/or modification of the apparatus accordingly. In order to test any formulation *in vitro*, in a biorelevant fashion, important factors



are design of the apparatus, dissolution/release/permeation medium, hydrodynamics (agitation, media flow, media viscosity, media volume), drug substance properties (solubility and permeability) and dosage form dissolution characteristics (Wang et al. 2009). Physiological factors of the oral cavity that may influence drug release and permeation from OTPs should be considered for biorelevant testing are presented in Table 1.2.

It is evident from the attempts in the literature that a method for the assessment of drug release and permeation as a function of oral cavity conditions is needed and would be useful. This research was therefore undertaken in order to develop and evaluate a novel biorelevant *in vitro* system to predict *in vivo* behavior of OTPs in a more physiologically realistic manner. In order to achieve this goal, a novel system that allows simulation of oral cavity physiological variables was designed. The possibility for adjustment of these *in vitro* variables for accurate prediction was also considered while designing the device. The research therefore, was carried out to build an apparatus that allows adjustment of certain *in vitro* variables in addition to simulation of the physiological environment. This should allow incorporation of biorelevance for OTPs that will improve *in vivo* predictability, economize the OTP development process and aid in product regulation.

**Table 1.2:** Physiological conditions of oral cavity for OTPs

<b>Physiological variable</b>	<b>Physiological variable subtype</b>	<b>Effect</b>	<b>Simulation strategy</b>
Low liquid surrounding of oral cavity	-	Drug release and sink condition	- Adjusting volume of media
Saliva	Composition (Ions, mucus, enzymes, etc.)	Drug release and stability	- Simulate relevant variables
	pH	Determinant of proportion of ionized and unionized form of drug	- Adjusting buffer composition and concentration
	Secretion and swallowing rate	Release and loss of drug	- Adjusting flow rate - Maintenance of flow in open or closed flow through pattern
Chewing	-	Drug release	- Adjusting agitation rate - Designing apparatus that allows simulation of chewing
Oral transmucosal barrier	Thickness	Drug permeability	- Use of multiple membranes
	Pore size and pore density	Drug permeability	- Use of appropriate artificial membranes
	Lipophilicity and hydrophilicity	Drug permeability	- Use of appropriate artificial membrane
	Barrier type (sublingual, buccal, gingival)	Drug permeability	- Use of appropriate artificial membranes
	Disease status (e.g. Leukoplakia)*	Drug permeability	- Use of appropriate artificial membranes - Use of multiple membranes

\* Leukoplakia in the oral cavity is the oral mucosal lesion caused by the use of smokeless tobacco which is associated with epithelial changes (thickening of epithelia) which might be one of the important physiological factors determining oral transmucosal drug permeation (Martin et al. 1999).

Snus, a smokeless tobacco product, was selected as a model OTP for evaluation of the novel bidirectional transmucosal apparatus (BTA). Snus is put under the upper lip for nicotine permeation through the buccal-labial and gingival membranes (Lunell et al. 2005). In addition to the oral transmucosal permeation, nicotine can also be available through the enteral route due to the swallowing of nicotine containing saliva. However, nicotine absorption through the enteral route is low in comparison to the oral transmucosal route due to its low oral absolute bioavailability (30%) attributed to the hepatic first pass effect (Benowitz et al. 1987; Jenner et al. 1973; Svensson 1987). The first pass effect leads to the metabolism of nicotine in liver and hence the low systemic availability. Primary metabolites of nicotine includes cotinine, nicotine N-oxide, N-methylnicotinium, nicointe-N-  $\beta$ -glucuronide and nornicotine formed by the activity of cytochrome P450 2A6 (CYP 2A6), aldehyde oxidase, flavin containing monooxygenase 3 (FMO 3), N-methyltransferase and uridine diphosphate-glucuronosyltransferase (UGT) enzymes (Hukkanen et al. 2005).

Snus was selected for the evaluation of the novel system due to the availability of *in vivo* nicotine pharmacokinetic data for comparison. Once validated the novel device can find application in the development and regulation of tobacco oral transmucosal products in addition to pharmaceutical OTPs. The U.S. Food and Drug Administration (FDA) regulates tobacco products following enactment of The Family Smoking Prevention and Tobacco Control Act (FSPTC) in June 2009. The development of a biorelevant *in vitro* system may be useful for regulation of tobacco products and as a research tool for predicting behavior of oral transmucosal tobacco products. These products include smokeless tobacco, dissolvable tobacco and other tobacco oral transmucosal formulations intended as less harm products. The system, once developed, may be helpful for predicting exposure to harmful tobacco component substances in

addition to exposure to nicotine. For these reasons, snus was selected as a model product for the development and evaluation of the newly designed biorelevant *in vitro* device for OTPs.

The first part of this research (Chapter 2) describes the development and validation of a high performance liquid chromatographic (HPLC) method for the analysis of nicotine in samples obtained from the *in vitro* experiments that employed the BTA, *in vitro* device. Dissolution/release/permeation testing is a quantitative measure which requires a quantitative analytical technique for the analyte of interest present in the product. Since the analytical method is a determinative step for the dissolution/release/permeation testing, it is important to validate the method. Therefore, the HPLC method for nicotine analysis in tobacco extract was validated for quantitative purpose and tested for its selectivity of nicotine analysis in the presence of tobacco components, the experimental environment and snus excipients.

In the second part of this research (Chapter 3), a novel *in vitro* device for OTPs was designed and developed that allowed better simulation and adjustment of physiological and *in vitro* variables for optimization of IVIVR for snus. The novel bidirectional transmucosal device was appropriately validated and its performance was compared to that of a widely used vertical diffusion cell (VDC) and a modified USP IV flow through apparatus (USP IV) for its evaluation.

Chapter 4 presents a study of the effect of physiological and *in vitro* variables on the *in vitro* behavior of snus using the novel *in vitro* device (BTA). The study was carried out to screen oral cavity physiological and *in vitro* variables that may be incorporated in the novel BTA device to add biorelevance and optimize IVIVR for snus.

Chapter 5 demonstrates application of multifactorial experimental design concepts for optimization of the relevant physiological and *in vitro* variables for accurately predicting *in vivo*

performance. This design was employed in determining optimal biorelevant conditions for the novel BTA device for optimization of IVIVR for snus.

Chapter 6 describes an effort to extend application of the biorelevant BTA to predict the *in vivo* performance of a dissolvable compressed tobacco product (Stonewall).

Chapter 7 summarizes the research findings and presents overall conclusion. This chapter also provides suggestions on potential modifications of the device that can be incorporated for broader application of the novel BTA device for OTPs.

## CHAPTER 2

### **SELECTIVITY INVESTIGATION AND LIQUID CHROMATOGRAPHIC METHOD FOR THE ANALYSIS OF NICOTINE IN TOBACCO EXTRACTS**

Drawn from a manuscript published in *J. Liq. Chromatogr. Relat. Technol.* (2013) 36: 1849-1868

#### **2.1 INTRODUCTION**

Selectivity testing of an analytical method for an analyte of interest is a primary step for method development and validation. Various approaches have been recommended to establish selectivity of an analytical method to identify and quantify the analyte in the presence of the matrix present in real samples (US Food and Drug Administration 2001; Karnes 2004; ICH 2005; USP 2009e). In addition, the standard addition approach and peak purity testing may be used to validate selectivity of the analytical method for an analyte when matrix cannot be replicated in standards or impurity and degradant standards are not available (Arce et al. 1998; Dunge et al. 2005; Sistla et al. 2005; Ribeiro et al. 2008).

The standard addition method is recommended for the confirmation of the presence of matrix effect (proportional effect) by comparison of slopes between the external calibration and standard addition curve (Karnes et al. 1991; Arce et al. 1998). In addition, it can be applied as the calibration approach over an external calibration method when matrix effects are present (Harvey

2002; Stüber et al. 2004; Basilicata et al. 2005; Fu et al. 2011). An interference (constant error) due to a component in the matrix caused by coelution cannot be corrected by the standard addition method (Karnes 2004; Ellison et al. 2008). The coeluant can be evaluated by baseline analysis or testing whether or not the intercept of the external calibration curve is significantly different from zero when an appropriate blank containing real matrix is available (Karnes et al. 1991; Karnes 2004). When an appropriate blank (real matrix or impurities and degradant standards) does not exist, peak purity testing can be a useful tool for the evaluation of coelution (ICH 2005). Peak purity testing with a photodiode array detector (PDA) is an approach that determines whether or not a matrix component coelutes and absorbs UV light similar to the analyte and thus contributing to the analyte response (Krull et al. 2001). Peak purity testing with the Waters 996 PDA detector and Waters Empower software analyzes absorbance spectra across the analyte peak and compares each spectrum of the peak with that of the apex spectrum of the same peak to determine if the spectra are similar (Waters 996 2002a, b, c). Similar spectra indicate a pure analyte peak; whereas a difference in the spectra indicates the presence of coeluting impurity. Elimination of the coeluant may not be possible when it is added into the sample during sample processing; however, the source of the coeluting compound can be determined by the analyte peak trapping followed by mass spectrometry (MS) which can help in avoiding the addition of the coeluting substance by appropriate steps. This approach can be a useful tool especially when the coeluant possess similar UV spectra to that of the analyte (Bryant et al. 1996).

In the present research, the above selectivity studies were applied for the validation of an HPLC method for nicotine analysis in samples obtained from a biorelevant *in vitro* release/permeation testing device of nicotine from smokeless tobacco (snus) which is described in Chapter 3. Biorelevant drug release/permeation testing are performed under simulated *in vivo*

conditions that allow better prediction of the *in vivo* behavior of the product (Emami 2006; Azarmi et al. 2007; Wang et al. 2009). A novel biorelevant *in vitro* system was developed for oral transmucosal products using smokeless tobacco (snus) as a model product (Chapter 3) (Delvadia et al. 2012).

A reported HPLC method for the analysis of nicotine in tablet dosage forms was appropriately modified for nicotine analysis in Hanks' balanced salt solution (HBSS) (Tambwekar et al. 2003; Iyer et al. 2007b). The modified HPLC method was validated using nicotine standards in Hanks' media as per the ICH guidance (ICH 2005). It was not possible to obtain blanks with matched matrix for the *in vitro* samples of smokeless tobacco (snus). Therefore, selectivity of the nicotine analysis was investigated as a part of validation using the standard addition method, peak purity testing and peak trapping with identification by MS and are described in detail in this Chapter.

## **2.2 MATERIALS AND METHODS**

### **2.2.1 MATERIALS**

(-)-Nicotine hydrogen tartrate was purchased from Sigma (St. Louis, MO, USA). Glacial acetic acid was obtained from EMD (Gibbstown, NJ, USA). HPLC grade ammonium acetate and ammonium formate were purchased from Fisher Scientific (Fair Lawn, NJ, USA) and Sigma (St. Louis, MO, USA), respectively. HPLC grade methanol and acetonitrile were purchased from Honeywell Burdick and Jackson (Muskegon, MI, USA). Hanks' Balanced Salt, N-(2-hydroxyethyl)piperazine-N'-(2-ethanesulfonic acid) (HEPES, 1M) buffer, formic acid and sodium hydroxide solution (10 N) were purchased from Sigma-Aldrich (St. Louis, MO, USA). Smokeless



tobacco (snus; non mentholated moist portion snus with natural flavor) was bought from Old Virginia Tobacco Co. (Richmond, VA, USA). SnakeSkin® regenerated cellulose membrane tubing for the permeation study was purchased from Thermo Scientific (Rockford, IL, USA). Fluorinated ethylene propylene (FEP) and Tygon® platinized silicon tubing were obtained from Cole-Parmer (Vernon Hills, IL, USA). Fittings (Delrin® Teflon unions, polypropylene luer fittings and ethylene tetrafluoroethylene adapt bodies) used for tubing connections were purchased from Upchurch Scientific (Oak Harbor, WA, USA). A 12-channel, 8-roller Masterflex® peristaltic pump was purchased from Cole-Parmer Instrument Company (Vernon Hills, IL, USA). Neoprene O rings for the apparatus to prevent leakage were purchased from Sutton Clark (Richmond, VA, USA).

## 2.2.2 DESCRIPTION OF THE SNUS AND BIORELEVANCE

Snus [ $0.98 \pm 0.03$  g (n=6)] used for the development of a biorelevant *in vitro* permeation system for OTPs is a smokeless tobacco product containing moist tobacco and excipients packed in a porous bag (Chapter 3). Each snus bag contained 8.0 mg of nicotine. The snus is placed under the upper lip for nicotine permeation through the buccal and gingival mucosa. A modified Hanks' Balanced Salt Solution (HBSS) was employed as both a biorelevant release (simulating saliva) and permeation medium (simulating plasma) for the study (Iyer et al. 2007b). The modified HBSS simulates the major inorganic components of saliva and plasma qualitatively (Krebs 1950; Rehak et al. 2000).

## 2.2.3 HIGH PERFORMANCE LIQUID CHROMATOGRAPHIC (HPLC) METHOD

### 2.2.3.1 CHROMATOGRAPHY

All experimental samples were analyzed using an HPLC method which was modified from a method reported for analysis of tablet dosage forms (Tambwekar et al. 2003). A Waters 600E multisolvent delivery system with a Waters 717 autosampler, a Shimadzu solvent degasser DGU-14A and a 996 Waters PDA detector were used for analysis. The separation of nicotine from other components in the *in vitro* samples was achieved using a reverse phase chromatographic column, Luna C18(2) (100 Å, 250 mm X 4.6 mm, 5 µm, Phenomenex, Torrance, CA) maintained at 45 °C. The chromatographic separation was isocratic and utilized premixed 10 mM ammonium acetate in 0.005% acetic acid (pH 5.5) : methanol (42:58, v/v) as the mobile phase at the flow rate of 1 mL/min. The sample injection volume was 20 µL. Detection was by absorption at 260 nm which was the wavelength maxima of nicotine using the PDA. Nicotine eluted at 4.3 min under the above chromatographic separation conditions.

### 2.2.3.2 PREPARATIONS OF STANDARDS AND QUALITY CONTROL SAMPLES

Nicotine hydrogen tartrate equivalent to nicotine (free base) was weighed and dissolved in methanol to obtain a 500 µg/ml nicotine stock solution. The above stock solution was used to prepare nicotine calibration standards in modified HBSS by appropriate dilutions ranging from 0.5 to 32 µg/mL. Quality control (QC) samples were prepared in Hanks' media at 1.5 (low quality control-LQC), 5 (middle quality control-MQC) and 28 (high quality control-HQC) µg/mL. A dilution quality control sample above the upper limit of quantification was prepared at a

concentration of 64 µg/mL. The above sample was diluted ten and twenty five times using Hanks' media to yield nicotine concentrations of 6.4 and 2.56 µg/mL, respectively. Standards and quality control samples were stored at -20 °C until analysis. The standards, quality control samples and *in vitro* samples were thawed at room temperature and directly injected for analysis.

### 2.2.3.3 METHOD VALIDATION

The modified HPLC method for nicotine analysis was validated for linearity, limit of quantification, repeatability and intermediate precision (precision), accuracy (inter and intra-day accuracy), system suitability, and selectivity (standard addition method and peak purity testing for the assessment of matrix and interference effect, respectively) (ICH 2005; USP 2009f).

Linearity of the nicotine HPLC analytical method was evaluated using seven nicotine calibrations standards (0.5, 1, 2, 4, 8, 16, 32 µg/mL); each was injected in replicates of five. Nicotine concentration was determined by linear regression of peak area versus concentration with 1/X weighting. The lower limit of quantification (LLOQ) was estimated based on a 10:1 signal to noise approach (ICH 2005). However, the lowest standard that provided acceptable accuracy and precision (n=5) was considered to be the established LLOQ. Intra-day accuracy and repeatability (n=6 during one day) were determined from the QC samples. Inter-day accuracy and intermediate precision (n=12 over 3 days) were similarly determined. Accuracy and precision (repeatability and intermediate precision) were represented by recovery (%) and percent relative standard deviation (%RSD), respectively. The system suitability parameters (resolution, tailing factor, and number of theoretical plates) were calculated for both the nicotine standard (4 µg/mL) and *in vitro* samples manually using appropriate equations recommended by the USP (USP 2009f). *In vitro* nicotine

samples were obtained from preliminary nicotine release and permeation studies reported in Chapter 3.

#### 2.2.3.4 STABILITY

The stability of nicotine in Hanks' media under different conditions was tested. Stability studies included storage stability, freeze thaw stability, and autosampler stability (Rosing et al. 2000). Storage and freeze thaw stability of nicotine in Hanks' salt solution was assessed at the low QC (1.5 µg/mL, n=6) and high QC (28 µg/mL, n=6) concentrations. Storage stability was carried out at -20 °C for 2 months. For the freeze thaw stability experiment, QC samples were stored at -20 °C for at least 24 hours in between two cycles. The nicotine concentrations in storage and freeze thaw stability samples were calculated from the calibration curve obtained from the analysis of freshly prepared standards with each run. Storage and freeze thaw stability were assessed by comparing the nicotine concentrations of stored and thawed samples with that of the concentration of same samples that were prepared and analyzed on day 0. Autosampler stability was performed by comparing the calibration standard concentrations at the start and end of the analytical day (10 hours). A paired t-test ( $\alpha = 0.05$ ) was performed to assess autosampler stability

#### 2.2.4 SELECTIVITY OF THE HPLC METHOD FOR NICOTINE ANALYSIS

*In vitro* nicotine samples for selectivity investigations were obtained from preliminary experiments using the novel *in vitro* bidirectional transmucosal device that will be described in Chapter 3 (Figure 3.2(C); Section 3.2.4.3; Section 3.2.5.1). *In vitro samples* were obtained from both donor and receptor chambers of the device. *In vitro* samples obtained from the

release/permeation study consisted of tobacco components and snus excipients in addition to nicotine. The apparatus-assembly components could also add leachables into the media during the experiment. These could cause errors in quantification which cannot be compensated for by the external calibration as it was not possible to produce standards with the matrix containing the above components. Various approaches for selectivity testing were therefore employed.

#### 2.2.4.1 STANDARD ADDITION METHOD

The donor and one receptor chamber *in vitro* samples at 60 min were used for the standard addition experiment. The donor sample was diluted 25 fold before spiking with the standards to represent the real situation where the donor sample is diluted for quantification within the calibration range. Nine hundred fifty microliters of the above *in vitro* samples were transferred to HPLC vials and spiked with 50  $\mu\text{L}$  of 20, 40, 80 and 160  $\mu\text{g}/\text{mL}$  of nicotine in Hanks' media and vortex mixed. The spiking was performed in replicates of five for both types of samples. Both the donor and receptor chamber samples were evaluated using standard addition. The external calibration curve was obtained from pure nicotine standards in Hanks' media (calibration samples) run in replicates of five with the standard addition experiment samples. The spiked samples and nicotine standards were analyzed using a wavelength range of 258-262 nm with 260 nm as the output wavelength. The plot of peak area responses as a function of true nicotine concentrations was constructed for spiked (donor and receptor chamber spiked samples) and calibration samples. A Student t-test ( $\alpha = 0.05$ ) was carried out to determine if the slopes (absolute values of slope) of both curves were significantly different (Arce et al. 1998). A significant difference (p-value  $< 0.05$ ) in the slope would indicate a proportional error or matrix effect.

#### 2.2.4.2 PEAK PURITY TESTING

Peak purity testing using the Waters 996 PDA detector and Empower software was performed on the donor and receptor chamber samples at 60 min. Donor samples were diluted 10 fold for HPLC peak purity analysis. Each sample was injected in triplicate. The peak purity testing using Waters Empower software provides purity angle and threshold angle values for each injection. Purity and threshold angle at the nicotine retention time estimates spectral heterogeneity (spectral differences between analyte and impurity) and spectral noise (spectral differences between analyte and solvent that contributes to the baseline noise), respectively (Krull et al. 2001; Waters 996 2002a, b, c). The presence of an impurity that is spectrally different and resolved to some extent from the analyte will increase the purity angle. A purity angle less than the threshold angle demonstrates the absence of a coeluant and that the analyte peak is pure and spectrally homogeneous. Whereas, a purity angle larger than the threshold angle is evidence for an impure analyte peak or a spectrally heterogenous peak and indicates the presence of more than one compound in the chromatographic peak. Peak purity plots with the threshold angle line and purity angle line were also studied. The purity angle line above the threshold angle line indicates the presence of a coeluant.

Peak purity testing was performed using the two methods available within the Empower software: Autothreshold and Noise+Solvent method. In the autothreshold method, the noise level was calculated automatically by the software from the run time window defined in the processing method. In the noise+solvent method, noise was defined as the maximum purity angle obtained from the peak purity analysis of replicate injections of the lowest standard. The noise+solvent method takes into account the solvent contribution for the threshold angle and is preferred over the autothreshold method. Peak purity testing with both methods for all samples was carried out

in the wavelength range of 200-300 and 250-270 nm with 260 nm representing the absorbance maxima of nicotine.

#### 2.2.4.3 PEAK TRAPPING AND IDENTIFICATION BY THE MASS SPECTROMETRIC METHOD

The presence of a coeluting compound was further confirmed using a triple quadrupole mass spectrometer (Waters Quattro API Micro with Masslynx 4.1 software for data acquisition, Waters Corporation, Milford, MA). The system was interfaced with a Shimadzu pumping system (Controller, SCL-10A VP; Pumps, LC 10 AT VP; and Solvent Degasser, DGU-14A, Shimadzu Scientific Instruments, Columbia, MD). Peak trapping was performed by collecting the nicotine peak at the elution time window of 4 to 4.8 min from the HPLC system waste outlet. The start and end time for peak collection was calculated based on the mobile phase flow rate and tubing dimensions of the PDA detector and waste line (length and diameter). Since, the HPLC-UV method utilized mobile phase with relatively high aqueous content and at high flow rate, the same solvent system could not be employed for identification of the coeluant in the peak trapped samples by mass spectrometry. Therefore, the coeluant in peak trapped samples was identified by use of a mass spectrometer compatible solvent system. The solvent system and mass spectrometer conditions optimized for nicotine analysis by the HPLC-MS-MS method reported in the literature was adopted and modified for coeluant identification (Cappendijk et al. 2010). The mass spectrometric method utilized premixed 10 mM ammonium formate in 0.05% formic acid (solvent system A): 0.05% formic acid in 1:1 methanol:acetonitrile (solvent system B) [5:95, v/v] at a flow rate of 0.2 mL/min. The source temperature, desolvation temperature, desolvation gas flow and cone gas flow were maintained at 150 °C, 350 °C, 200 L/h and 100 L/h, respectively. Peak trapped

samples were infused at a rate of 10  $\mu\text{L}/\text{min}$  and mixed with the above solvent system in a tee prior to infusion into the ionization chamber. A full scan study in the Q1 mode ( $m/z$  range 50-1300) was performed on the infusion of all peak trapped samples for the identification of coeluant.

Any coelutant can be attributed either to a smokeless tobacco (snus) component or a leachable substance from the apparatus-assembly. In addition to the *in vitro* study samples with the apparatus, samples were obtained from a nicotine permeation experiment conducted in a glass beaker and these samples were also subjected to peak trapping and MS identification to confirm whether or not a component of smokeless tobacco (snus) was the coeluting compound (Figure 2.1). For the beaker experiment, regenerated cellulose membrane tubing was sealed appropriately using a tubing clip from one end to avoid leakage. A snus with 5 mL of Hanks' media was placed in the tubing and the other side was sealed using another clip. The above was hung from a stand and immersed in a beaker containing 170 mL of Hanks' media maintained at 37  $^{\circ}\text{C}$ . The media in the beaker was stirred continuously using a magnetic stir bar. The experiment was carried out for an hour and media was sampled from the beaker at 60 min for MS identification.



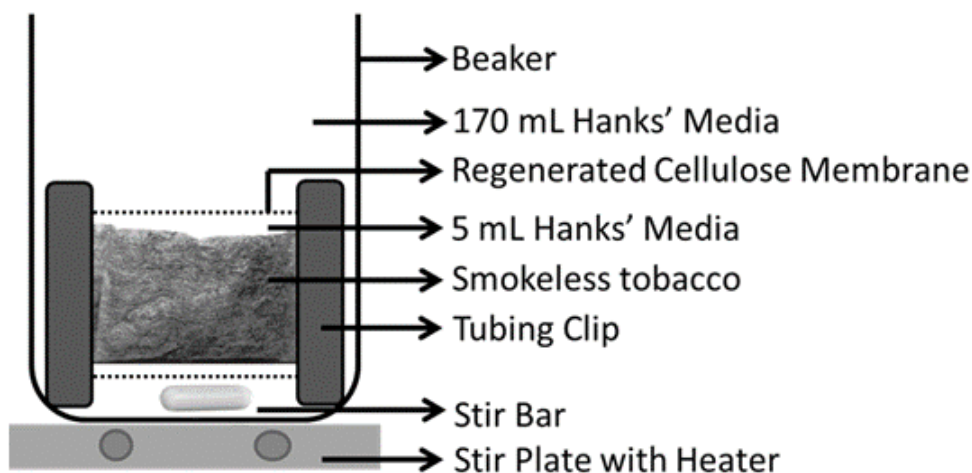


**Figure 2.1:** Beaker set-up for nicotine permeation studies from snus [Figure not to scale]

The mass spectra of trapped peaks for the *in vitro* apparatus and beaker samples were compared with those of the blank and nicotine standards in Hanks' media. The presence of any mass/charge ( $m/z$ ) peak in the mass spectrum of the peak trapped the *in vitro* samples different from that of the blank and nicotine standards indicated the presence of a coeluting substance. The presence of the coeluting substance in the mass spectrum of the beaker sample would provide evidence that a smokeless tobacco (snus) component is the contributing factor whereas, its absence would suggest the apparatus-assembly.

### 2.2.5 LEACHING STUDY

For further confirmation of whether or not the apparatus-assembly was the source of the coeluting substance, a leaching study was carried out. In this study, Hanks' media from three reservoirs maintained at 37 °C was re-circulated through the apparatus-assembly for 60 min without smokeless tobacco (snus) and regenerated cellulose membranes. The media re-circulation

sample from each reservoir was infused into the MS system for evaluation. In addition, in order to identify the source of the leachable substance, each component of the apparatus-assembly (Neoprene O ring, silicon tubing, FEP tubing, acetal resin unions, polypropylene male luer fittings and ethylene tetrafluoroethylene adapt body) was placed separately in beakers containing 10 mL of Hanks' media at 37 °C for 60 min. These samples were infused into the MS system and the mass spectra were compared to that of the blank. The mass spectrum of the component that provided the peak that was not present in the blank confirmed its contribution.

#### 2.2.6 PDA SPECTRUM AND CHROMATOGRAM OF THE LEACHED STUDY SAMPLE

A PDA spectrum from the leaching study sample was studied to confirm whether or not the leachable substance demonstrated absorbance at the wavelength of interest. The PDA spectrum was also compared to that of the nicotine standard. A chromatogram of the same sample was also studied to confirm whether or not the leachable substance coeluted with nicotine.

## 2.3 RESULTS AND DISCUSSION

### 2.3.1 METHOD VALIDATION

#### 2.3.1.1 LINEARITY AND LLOQ

The peak area response of nicotine versus its concentration demonstrated a linear relationship over the range of 0.5-32  $\mu\text{g/mL}$  [Peak area =  $(1.79 \times 10^4 \pm 83.47) \times$  nicotine concentration –  $(1.56 \times 10^3 \pm 333.87)$ , mean calibration curve equation for  $n=5$ ,  $R^2 > 0.99$ , weighting  $1/X$ ]. The calibration curve accuracy (%recovery) and precision (%RSD) for the mean back calculated values of the standards were 97.98-103.20% and 0.15-3.14%, respectively. Based on the 10:1 signal to noise approach, 0.4  $\mu\text{g/mL}$  was estimated to be the LLOQ; however, this lacked sufficient accuracy and precision. The LLOQ for the HPLC method was therefore 0.5  $\mu\text{g/mL}$  that showed acceptable accuracy and imprecision of 103.20% and 2.78% respectively. Figures 2.2(A), 2.2(B) and 2.2(C) represent chromatograms of the blank, lowest (0.5  $\mu\text{g/mL}$ ) and highest (32  $\mu\text{g/mL}$ ) nicotine standard respectively. The peak area and back calculated nicotine standard concentrations for individual injections are presented in Tables A1-A2 of Appendix A respectively.

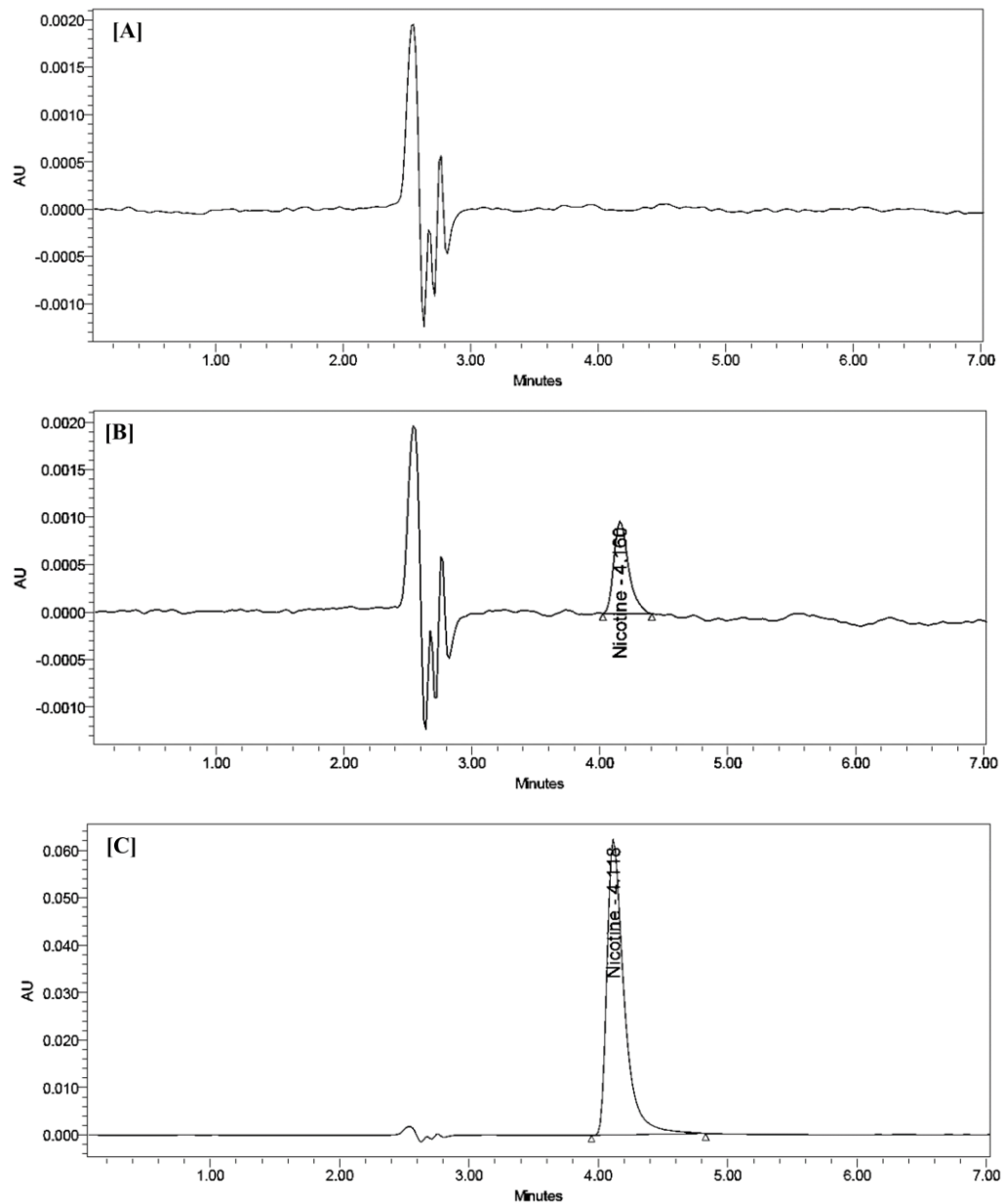


**Figure 2.2:** Representative chromatograms of blank and nicotine external standards; [A] Hanks' media blank; [B] Nicotine external standard in HBSS 0.5 µg/mL; [C] Nicotine external standard in HBSS 32 µg/mL.

### 2.3.1.2 ACCURACY AND PRECISION

Table 2.1 summarizes data on precision and accuracy, determined at five levels: LQC, MQC, HQC and two dilutions QCs. The intra- and inter- day precision was less than 4 % at all nicotine concentrations studied. The individual nicotine concentration at all QC levels for intra- and inter-day accuracy and precision are presented in Tables A3-A4 of Appendix A.

### 2.3.1.3 SYSTEM SUITABILITY PARAMETERS

System suitability parameters calculated according to USP for both nicotine standards and *in vitro* samples are tabulated in Table 2.2 (USP 2009f). System suitability parameters obtained were acceptable (US Food and Drug Administration 1994 ; Horacio et al. 2008; USP 2009f). Table A5 of Appendix A presents the system suitability parameters obtained from each individual injection of nicotine external standards and *in vitro* samples. The difference in the resolution of the nicotine peak from the solvent peak between the nicotine standard and *in vitro* sample was due to elution of unretained tobacco components in the *in vitro* sample. However, the nicotine peak was very well resolved from unretained tobacco components as shown in Figure 2.3.

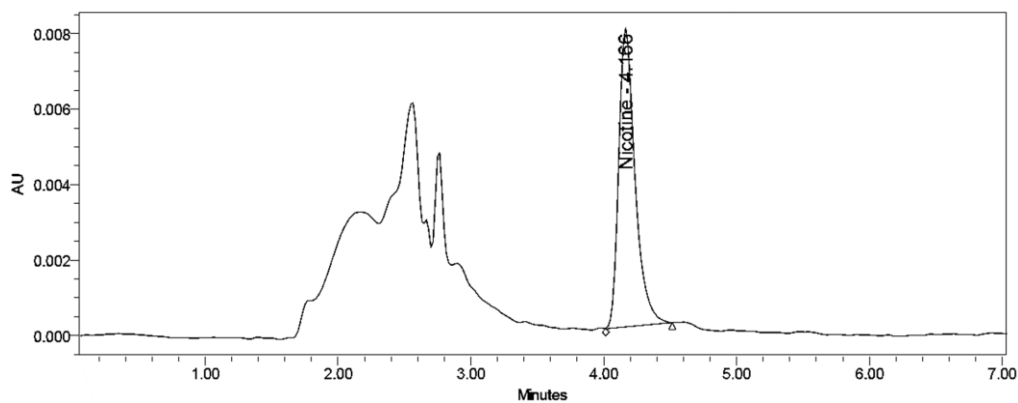
**Table 2.1:** Accuracy and precision data for nicotine QCs in Hanks' media

Nominal Concentration (µg/mL)	Intra-day(n=6)			Inter-day(n=12, 3 days)		
	Observed mean concentration (µg/mL)	Recovery (%)	RSD* (%)	Observed mean concentration (µg/mL)	Recovery (%)	RSD* (%)
1.5	1.53	101.80	3.26	1.53	102.13	3.18
5	4.93	98.50	2.15	4.85	97.04	2.30
28	27.94	99.80	0.29	28.43	101.54	2.40
64 (25 x dilution)	63.78	99.66	2.39	63.77	99.64	2.23
64 (10 x dilution)	63.50	99.21	1.59	63.32	98.94	1.47

\* Percent relative standard deviation (%RSD)

**Table 2.2:** System suitability parameters for nicotine (n=5)

Parameter	Mean (Standard)	Mean (In vitro sample)	Acceptance Limit
Resolution	11.3	4.9	> 2
Tailing factor	1.7	1.5	≤ 2
Number of theoretical plates	5849	5466	>2000
Retention time (min)	4.15	4.17	-

**Figure 2.3:** Representative chromatogram of the *in vitro* nicotine sample.

### 2.3.2 STABILITY

Nicotine calibration standards were stable in the autosampler based on statistically insignificant differences in the standard concentrations observed at the start and end of the analytical day (Paired t-test:  $t = 1.84$ ,  $df = 6$ ,  $p\text{-value} > 0.05$ ). LQC (1.5  $\mu\text{g/mL}$ ) and HQC (28  $\mu\text{g/mL}$ ) samples were stable for 2 months stored at  $-20\text{ }^{\circ}\text{C}$  with a maximum recovery of 94.13% and 100.63% and showed consistency with a RSD of 2.61% and 0.57% respectively. LQC and HQC samples were also stable after three freeze-thaw cycles based on the maximum recovery of 95% and 104.34% and RSD of 4.12% and 0.97% respectively. The short term and freeze-thaw stability data are shown in detail in Tables A6 and A7 respectively (Appendix A).

### 2.3.3 SELECTIVITY OF THE HPLC METHOD FOR NICOTINE ANALYSIS

#### 2.3.3.1 STANDARD ADDITION METHOD

Figure 2.4 represents the mean standard addition curve obtained with the spiked donor and receptor chamber samples ( $n=5$ ) along with the external calibration curve ( $n=5$ ). The external calibration curve represents the calibration curve obtained with the external standards of nicotine prepared in Hanks' media. The individual peak areas of the external standards and spiked donor and receptor chamber samples are presented in Tables A8-A9 of Appendix A. The fitted line for the external calibration curve shown in Figure 2.4(A) and 2.4(B) was represented by  $Y = [(1.75 \times 10^4 \pm 2.28 \times 10^2) \times X - (1.21 \times 10^3 \pm 2.93 \times 10^2)]$ . Whereas, the best fit lines for the standard addition curve for both the spiked donor and receptor chamber samples were  $Y = [(1.70 \times 10^4 \pm 1.00 \times 10^2) \times X - (1.11 \times 10^5 \pm 4.15 \times 10^2)]$  and  $Y = [(1.73 \times 10^4 \pm 1.11 \times 10^2) \times X - (5.44 \times 10^5 \pm$

4.71 × 10<sup>2</sup>], respectively. The slope of the peak area versus nominal nicotine concentration plot for the donor chamber spiked samples (Figure 2.4(A)) was statistically smaller than that of the respective external calibration curve (Figure 2.4(A)) (Equal variance t-test at α=0.05, donor *in vitro* sample: t = 4.86, df = 8, p-value = 0.0013); however, the difference in the slope was considered insignificant as both curves are parallel. The slope of the peak area versus nominal nicotine concentration plot for the receptor chamber *in vitro* spiked samples (Figure 2.4(B)) was not statistically different than that of the respective external calibration curve (Figure 2.4(B)) (Equal variance t-test at α=0.05, receptor *in vitro* sample: t = 1.93, df = 8, p-value = 0.0901) indicating the absence of a matrix effect in the receptor chamber samples.

The concentrations of nicotine in the donor and receptor samples obtained by extrapolation of the standard addition curves (x-intercept) were 6.52 and 31.51 µg/mL respectively. The nicotine concentrations in the same donor and receptor *in vitro* samples from the external calibration curve were 6.38 and 31.22 µg/mL respectively. This provided a positive deviation of 2.08% for the donor and 0.94% for the receptor compartments relative to the concentration obtained from the external calibration curve. These deviations were considered to be within an acceptable range. It was concluded that a proportional error was not present in the analysis of receptor *in vitro* samples and the error in the analysis of donor *in vitro* samples employing the external calibration curve was acceptable. A correction factor that accounts for the error involved in nicotine quantification by the external calibration method shown in Equation 2.1 can be employed in order to quantify nicotine in donor compartment more accurately. Overall, the external calibration was appropriate for *in vitro* nicotine sample analysis.

$$Nicotine\ Concentration_{Donor} = \frac{(Nicotine\ concentration_{EC} \times 2.08)}{100} + Nicotine\ concentration_{EC}$$

Eq. 2.1

where, EC is external calibration..



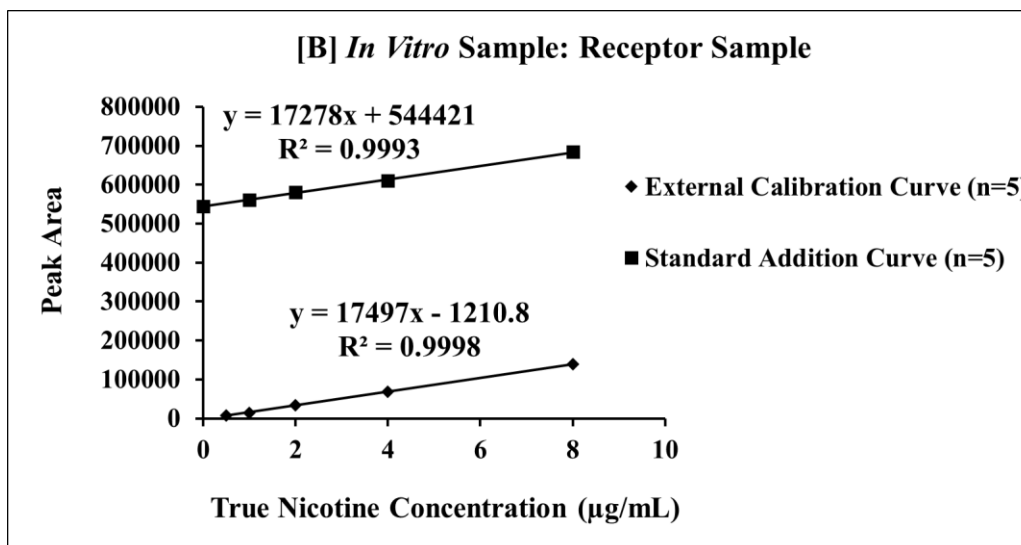
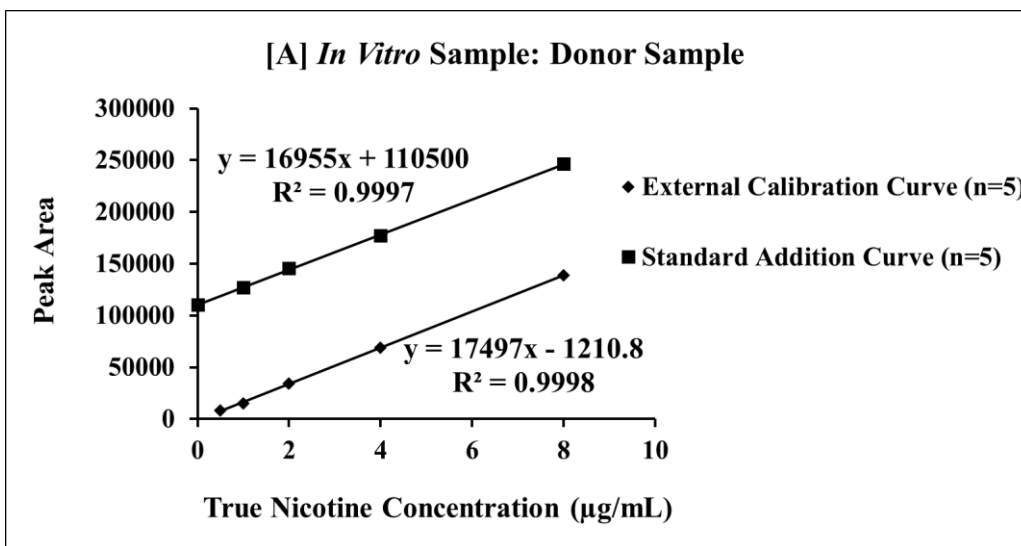


**Figure 2.4:** Comparison of the standard addition and external calibration curves; **[A]** Spiked donor *in vitro* sample obtained at 60 min; **[B]** Spiked receptor *in vitro* sample obtained at 60 min. (Error bar represents one standard deviation; n=5)

### 2.3.3.2 PEAK PURITY TESTING

Peak purity testing on the donor and receptor chamber *in vitro* samples was performed for confirmation of whether or not there was a component present in the sample that coeluted with nicotine and contributed to the measured response. Purity angles and threshold angles obtained by the autothreshold and noise+solvent peak purity testing at 200-300 and 250-270 nm wavelengths scan range for nicotine standards and *in vitro* samples are tabulated in Tables 2.3 and 2.4 respectively. The replicate peak purity data for the donor and receptor samples for snus are shown in Tables A10-A13 of Appendix A. Nicotine peaks from standards at both wavelength scan ranges obtained by the autothreshold and noise+solvent peak purity method were pure as the purity angles were less than the threshold angles. These peak purity results for nicotine standards along with the absence of a peak in the blank chromatogram at the nicotine elution time window suggests that the Hanks' media components were not contributing to any coelution and response.

The purity angles with all *in vitro* samples were larger than the respective threshold angles obtained by the autothreshold method at the 200-300 nm wavelength range suggesting that the nicotine peaks were impure. The impure nicotine peaks could be attributed to the presence of the coeluant in all *in vitro* samples that absorbs in the wavelength range of 200-300 nm. However, when the peak purity testing was performed on the same *in vitro* samples by the autothreshold method at the 250-270 nm wavelength range, the purity angles were smaller than the respective threshold angles in spite of the presence of the coeluant. It was therefore concluded that the coeluant was present in the *in vitro* samples that absorbed UV light in the wavelength range of 200-250 nm and did not absorb at the output wavelength of 260 nm. This indicated that the nicotine peaks were spectrally pure at 250-270 nm even though peaks were chromatographically impure. This conclusion supports the use of 250-270 nm wavelength range for nicotine analysis *in vitro*

samples without any need of chromatographic resolution of the coeluant which did not absorb at the selected wavelength range (250-270 nm)

In contrast, the nicotine peaks with all *in vitro* samples were pure with the noise+solvent peak purity testing (purity angle < threshold angle) irrespective of the wavelength scan range. This indicated the absence of any coeluant. The conclusion from the noise+solvent peak purity testing was in contrast to that of the autothreshold method at the wavelength range of 200-300 nm. In addition, the purity angle line was above the threshold angle line on the purity plots of *in vitro* samples with the noise+solvent method at 200-300 nm indicating that peaks were impure. The noise+solvent peak purity results at 200-300 nm were not in agreement with their respective peak purity plots. Therefore, peak purity results by the autothreshold method were used for further interpretation and that of the noise+solvent method were considered invalid.

Overall, it was concluded from the peak purity testing that the Hanks' media did not contribute to the measured nicotine response. This was evident from the peak purity autothreshold testing results irrespective of the wavelength scan range with nicotine standards. It was confirmed that a substance was coeluting with nicotine that absorbed in the wavelength range of 200-250 nm. Therefore, peak trapping followed by the MS identification was performed to identify the coeluant as well as the experimental source of it.

**Table 2.3:** Peak purity testing on the nicotine standards and *in vitro* samples by autothreshold method\*

Samples	200-300 nm			250-270 nm		
	Purity Angle	Threshold Angle	Interpretation <sup>§</sup>	Purity Angle	Threshold Angle	Interpretation <sup>§</sup>
Nicotine standard (0.5 µg/mL)	3.934	4.825	Pure peak	2.386	2.989	Pure peak
Nicotine standard (32 µg/mL)	0.119	0.290	Pure peak	0.063	0.252	Pure peak
Receptor 1 sample at 60 min <sup>#</sup>	1.393	0.354	Spectrally impure	0.244	0.290	Spectrally pure
Receptor 2 sample at 60 min <sup>#</sup>	1.267	0.389	Spectrally impure	0.253	0.315	Spectrally pure
Donor sample at 60 min <sup>#</sup>	1.120	0.393	Spectrally impure	0.303	0.315	Spectrally pure

\* Each purity angle and threshold angle value represents mean of n=3

<sup>§</sup> Pure peak = chromatographically and spectrally pure peak

<sup>#</sup> All nicotine peaks with *in vitro* samples were chromatographically impure at both 200-300 and 250-270 nm irrespective of its spectrally purity.

**Table 2.4:** Peak purity testing on the nicotine standards and *in vitro* samples by noise+solvent method\*

Samples <sup>§,#</sup>	200-300 nm			250-270 nm		
	Purity Angle	Threshold Angle	Interpretation	Purity Angle	Threshold Angle	Interpretation
Nicotine standard (0.5µg/mL)	5.629	9.665	Pure peak	2.386	5.69	Pure peak
Nicotine standard (32µg/mL)	0.119	5.538	Pure peak	0.063	2.947	Pure peak
Receptor 1 sample at 60 min	1.393	5.609	Pure peak	0.244	2.988	Pure peak
Receptor 2 sample at 60 min	1.267	5.644	Pure peak	0.253	3.014	Pure peak
Donor sample at 60 min	1.120	5.646	Pure peak	0.303	3.013	Pure peak

\* Each purity angle and threshold angle value represents mean of n=3

<sup>§</sup> Pure peak = chromatographically and spectrally pure peak

<sup>#</sup> The peak purity testing by noise+solvent method indicated all nicotine peaks (standards and *in vitro* samples) to be chromatographically and spectrally pure. However, the results were not in agreement with the respective peak purity plots and hence the results were considered invalid.

### 2.3.3.3 PEAK TRAPPING AND IDENTIFICATION BY THE MASS SPECTROMETRIC METHOD

Figures 2.5(A) and 2.5(B) represent mass spectra of the peak trapped samples from Hanks' blank and the nicotine standard in HBSS buffer respectively. The mass spectra of the receptor chamber and beaker samples at 60 min are shown in Figure 2.6(A) and 2.6(B) respectively. The peak at 162.69 m/z corresponded to nicotine. The mass spectra of the receptor *in vitro* sample (Figure 2.6(A)) showed the presence of a peak at 353.8 m/z which was assigned to the coeluant present in the trapped nicotine peak. The coeluant with a m/z of 353.8 present in the apparatus *in vitro* sample might be either from the smokeless tobacco (snus) matrix or the apparatus-assembly. The mass spectra of beaker *in vitro* samples did not show the presence of the 353.8 m/z peak (Figure 2.6(B), which confirmed that the source of coeluant was the apparatus-assembly components and not the smokeless tobacco (snus).

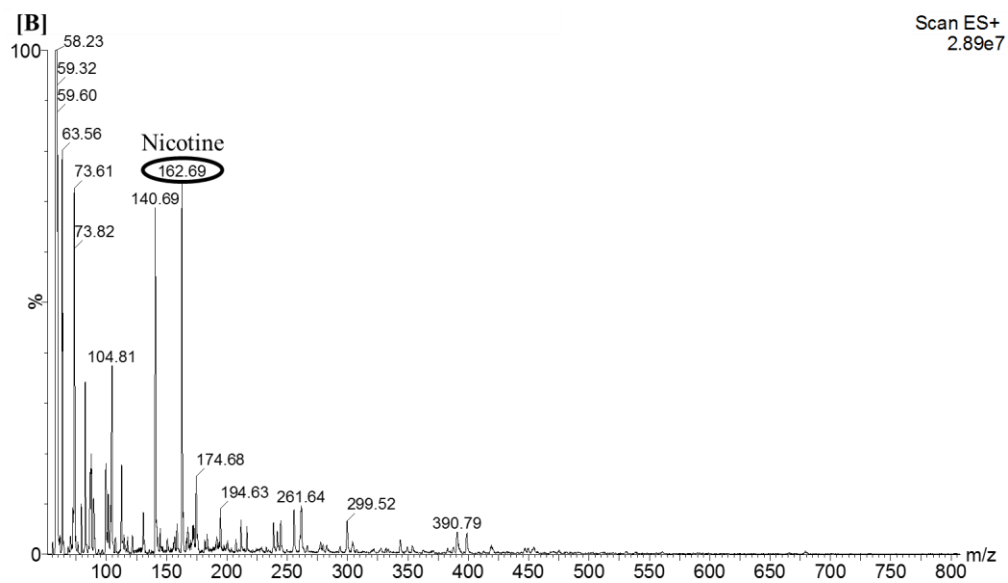
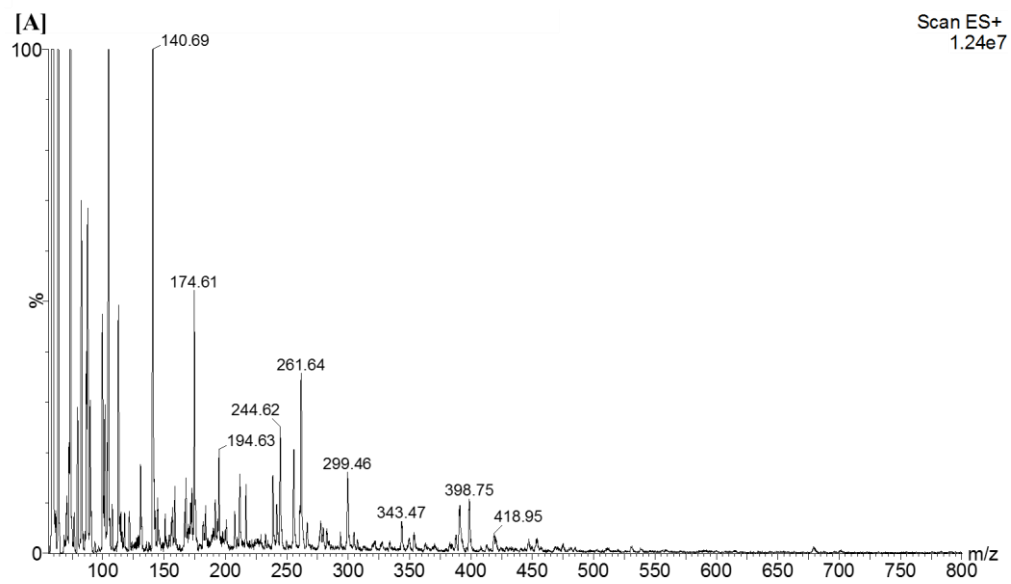


**Figure 2.5:** Mass spectra of peak trapped HBSS blank and external nicotine standard; **[A]** Hanks' blank; **[B]** External nicotine standard (28  $\mu\text{g/mL}$ ).

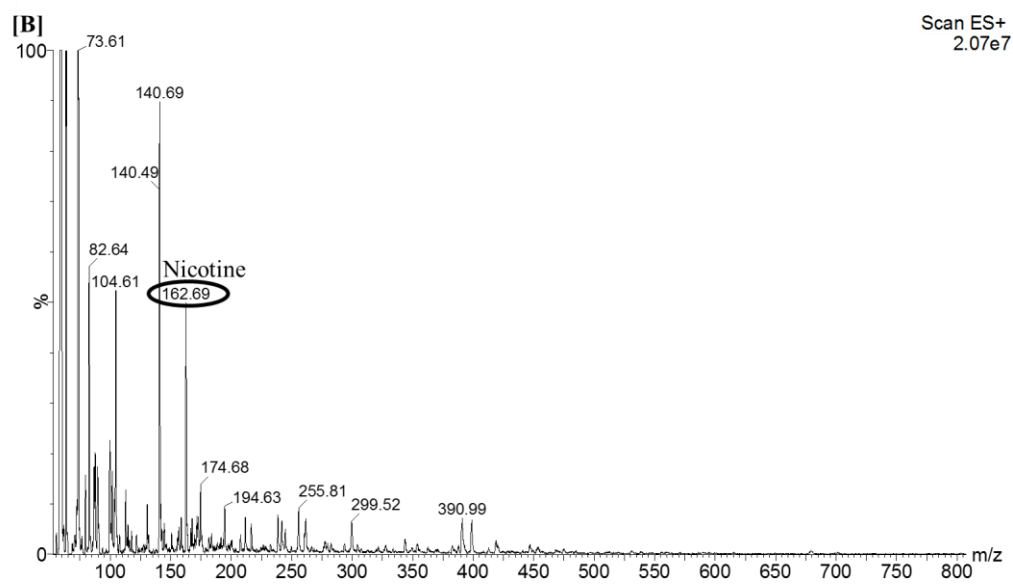
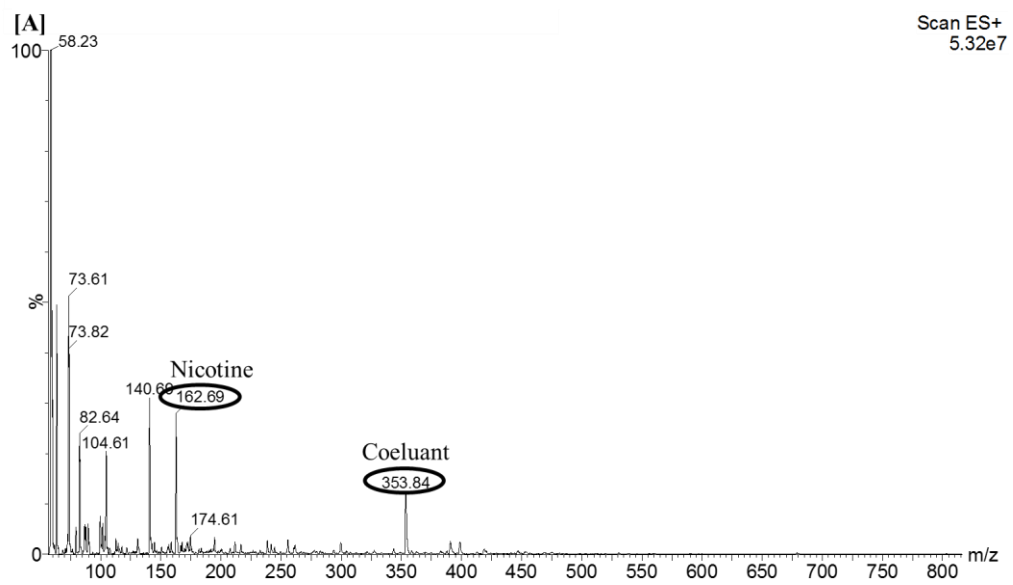


**Figure 2.6:** Mass spectra of peak trapped receptor and beaker *in vitro* sample at 60 min; [A] Receptor *in vitro* sample; [B] Beaker *in vitro* sample.

#### 2.3.4 LEACHING STUDY

The mass spectra of non-circulating Hanks' media and apparatus-assembly recirculating media at 60 min displayed in Figures 2.7(A) and 2.7(B), respectively, were obtained by the direct infusion of samples into the MS without performing peak trapping. The mass spectra of the apparatus-assembly recirculating media yielded  $m/z$  peaks of 358.8, 374.8, 476.7 and 498.6 in addition to 353.7 that were different from that of the non-circulating Hanks' media. Of these,  $m/z$  peaks, 476.7 and 498.8 occurred with low intensity and were also present in the non-peak trapped blank. On studying the mass spectra of the leach study samples of individual apparatus-assembly components in Hanks' media, it was observed that only the neoprene O ring Hanks' media sample showed the presence of  $m/z$  peaks 353.6, 358, 374.6 and 476.7 (Figure 2.8). The neoprene O ring sample was also infused into the MS without performing peak trapping. The peak at 476.7  $m/z$  was present in non-circulating Hanks' blank and hence was not considered a leachable from the neoprene O ring. The  $m/z$  peak at 353.6 in the mass spectra of the neoprene O ring sample (Figure 2.8) which was also present in the peak trapped apparatus *in vitro* sample (Figure 2.6(A)) was considered to be representative of the coeluant. This peak could be due to the leaching of a plasticizer used in the manufacture of neoprene. The mass spectrum (molecular ion with  $m/z$  353.6 or  $353.8 \approx 354$  produced due to protonation in the positive ion mode) for the coeluant was consistent with the molecular weight of one of the most commonly used ester plasticizers, alkyl alkylether diester adipate (molecular weight 353), for the manufacture of rubber (Flick 1993; Stone 2001). Other peaks at 358 and 374.6  $m/z$  were not present in the peak trapped apparatus *in vitro* samples and were not considered representative of the coeluant. It was concluded from the leaching study that the neoprene O ring leached some substance during the experiment and was the source of coeluting substance.



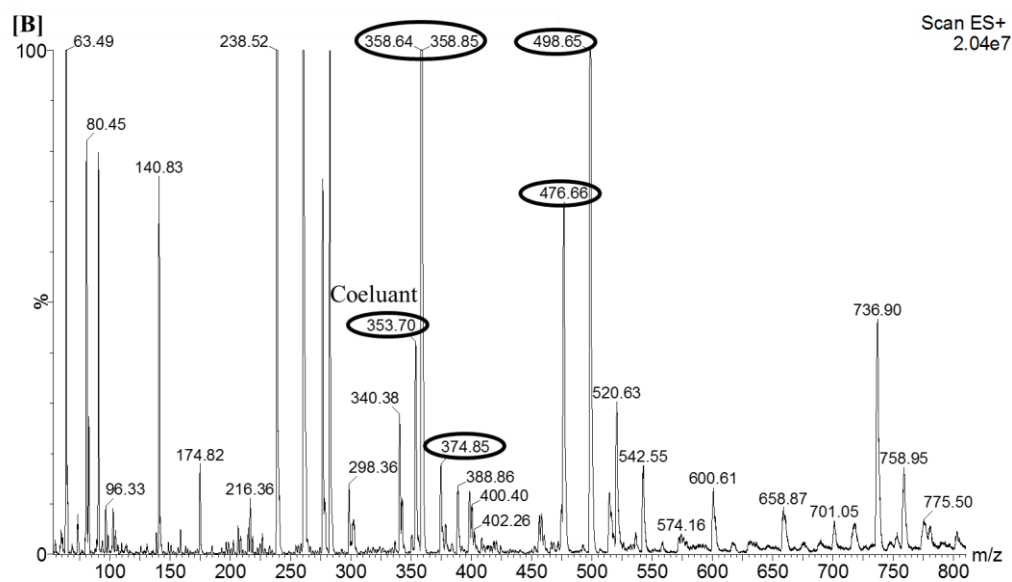
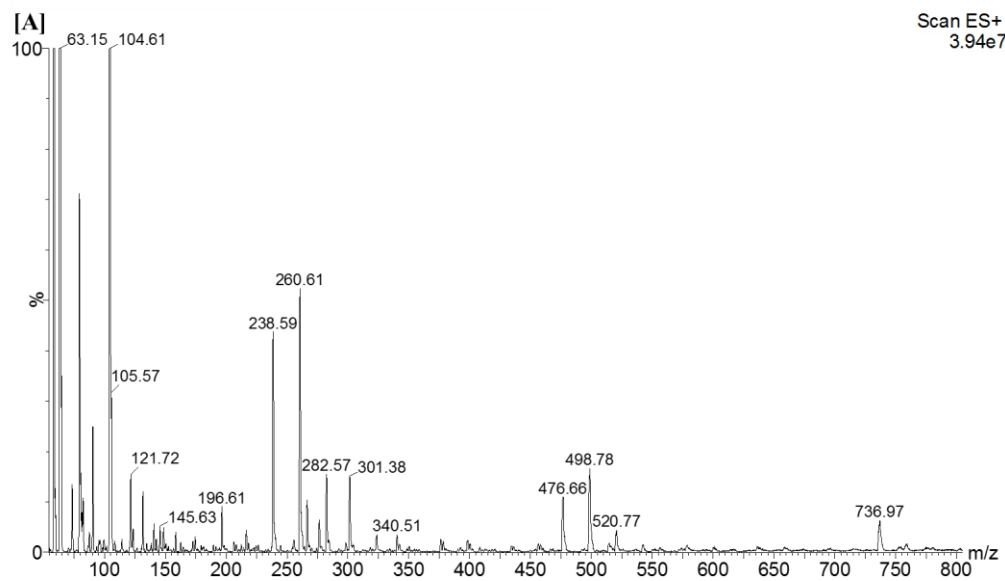


**Figure 2.7:** Mass spectra of non-peak trapped blank and apparatus-assembly components [A] Hanks' media blank; [B] Apparatus-assembly recirculating Hanks' media.

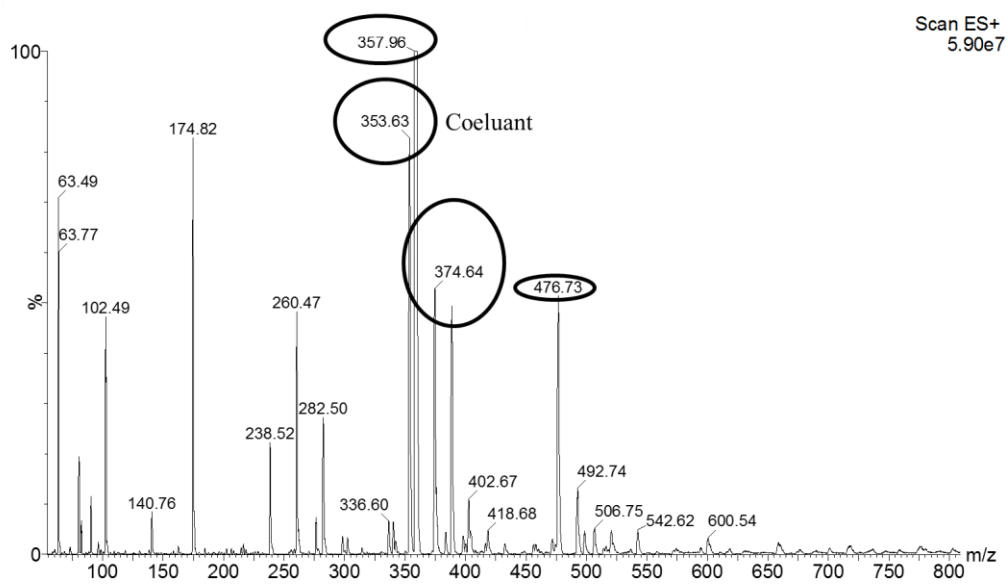


**Figure 2.8:** Mass spectra of non-peak trapped Neoprene O ring in Hanks' media sample.

### 2.3.5 PDA SPECTRUM AND CHROMATOGRAM OF THE LEACH STUDY SAMPLES

The neoprene O ring sample was injected onto the HPLC system for confirmation of whether or not the leachable from the O ring coelutes and absorbs with nicotine. Study of the PDA spectrum of the neoprene O ring in the Hanks' media sample (Figure 2.9(A)) indicated absorbance of the leachable in the wavelength range of 200 to 242 nm; whereas, that of the nicotine standard (Figure 2.9(B)) showed absorbance by nicotine in the wavelength range of 230-278 nm with 260 nm as the wavelength maxima. We observed that nicotine and the leachable from the neoprene O ring shows overlap in their absorbance wavelength (230-240 nm). The chromatogram of the neoprene O ring sample (Figure 2.10) showed a peak at the elution window of 3.8 to 4.5 min which is also the nicotine elution time. The leach study, MS identification, PDA spectrum and chromatogram of the neoprene O ring sample confirmed its role in the leaching and coelution process which resulted in an impure nicotine peak. The peak purity testing on *in vitro* samples demonstrated impure nicotine peaks in the wavelength range of 200-300 nm which could be explained by the overlapping absorbance wavelength of the neoprene O ring leachable and nicotine (230-240 nm). However, the same samples demonstrated an absence of any contribution from the neoprene O ring leachable to the nicotine response on performing the peak purity testing in the wavelength range of 250-270 nm eventhough the peak was chromatographically impure. This was attributed to the absence of the absorption of UV light by theleachable in the wavelength range of 250-270 nm.

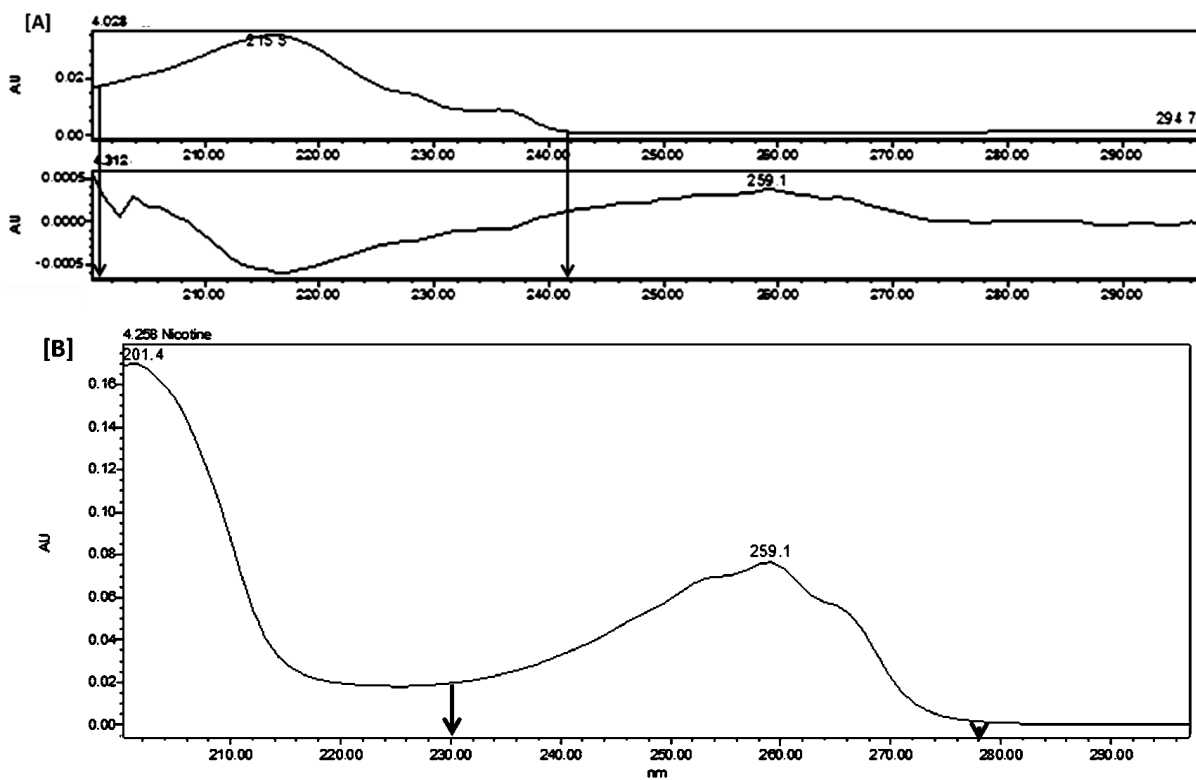


**Figure 2.9:** PDA chromatograms; **[A]** Neoprene O ring in Hanks' media sample; **[B]** Nicotine standard (32  $\mu\text{g/mL}$ ) in Hanks' media.

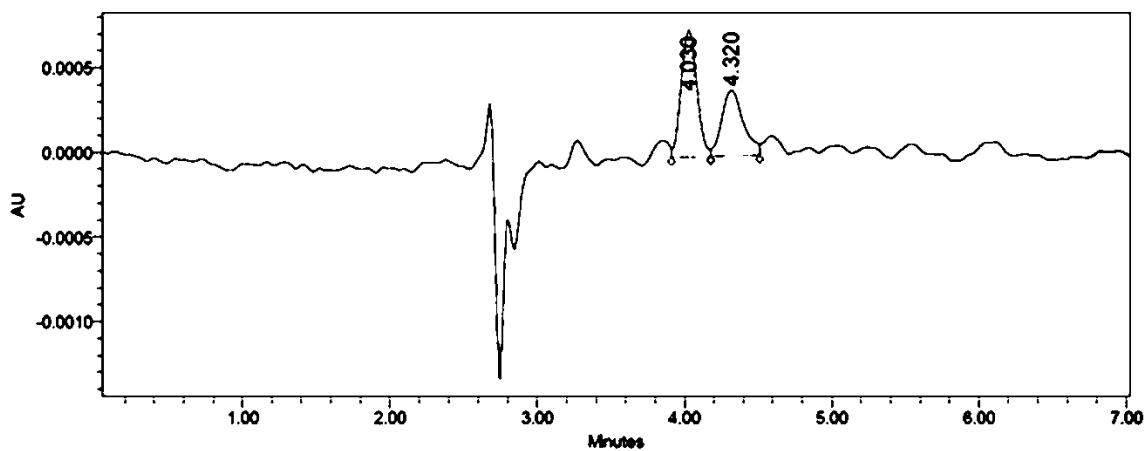


**Figure 2.10:** Chromatogram of neoprene O ring in Hanks' media sample.

## 2.4 CONCLUSIONS

A simple and selective HPLC method for the analysis of nicotine in a Hanks' balanced salts extract of smokeless tobacco (snus) components was presented. The selectivity of the modified HPLC method for nicotine analysis of the *in vitro* samples obtained from a novel *in vitro* release/permeation device for OTPs was investigated. The *in vitro* sample was a matrix containing snus components, excipients and Hanks' salts. The standard addition experiment indicated the absence of a matrix effect; whereas, the peak purity testing and peak trapping with MS suggested the presence of a coeluting substance in the analysis of *in vitro* samples. The contribution to the nicotine response by the coeluant was attributed to the neoprene O ring and was avoided at the wavelength of maximum absorption for nicotine by a change in the wavelength range for *in vitro* sample analysis. This eliminated the contribution to the nicotine response by the coeluant which did not show any absorbance at 260 nm, the wavelength maxima of nicotine. Selectivity was shown without chromatographic resolution of the coeluting substance by selection of an appropriate wavelength range where the coeluant did not absorb UV light. The present validated HPLC method was employed for nicotine analysis in the *in vitro* samples obtained from preliminary, screening and optimization experiments to be reported in Chapters 3, 4 and 5 respectively. The investigation presented provides a strategy to study the selectivity of the analytical method for *in vitro* samples especially when matrix cannot be duplicated in the external standards.

## CHAPTER 3

### **A BIORELEVANT *IN VITRO* RELEASE/PERMEATION SYSTEM FOR ORAL TRANSMUCOSAL PRODUCTS**

Drawn from a manuscript published in Int. J. Pharm. (2012) 430: 104-113

#### **3.1 INTRODUCTION**

The oral transmucosal route is a promising option to circumvent the disadvantages of oral administration, since it is suitable for delivery of drugs with gastric incompatibility and hepatic first pass metabolism (Sudhakar et al. 2006; Madhav et al. 2009; Patel et al. 2011). Oral transmucosal products deliver drug directly into the systemic circulation through the mucosal linings of the oral cavity and bypasses hepatic first pass elimination (Washington et al. 2001; Sudhakar et al. 2006; Madhav et al. 2009). Additionally, the oral transmucosal site is easily accessible and convenient for drug delivery. For these reasons, considerable efforts are in progress for the development of oral transmucosal products (OTPs) for drugs which face challenges for delivery by the oral route (Rathbone et al. 1996; Pfister et al. 2005; Pather et al. 2008).

Predictive drug dissolution/release testing is required as an evaluation tool for cost effective and expedited pharmaceutical product development (Emami 2006; Azarmi et al. 2007). The evidence in the research/review literature and white paper present the need of an improved *in vitro* methodology for characterizing drug dissolution/release/permeation from OTPs (Azarmi et

al. 2007; Brown et al. 2011). A predictive tool is required for the development and evaluation of OTPs that can lead to cost effective product development and shortening of the research phase. Biorelevant dissolution/release/permeation tests when performed under simulated *in vivo* conditions can predict the *in vivo* behavior (drug absorption and plasma concentration time profile) of the product through *in vitro in vivo* relationships (IVIVR) (Polli 2000; Emami 2006; Wang et al. 2009). These biorelevant *in vitro* tests can be used as a quality control and research tool.

Standard/compendial *in vitro* dissolution methods for sublingual and buccal tablets suggests the use of conventional dissolution and disintegration tests with a large volume of media (USP 2009a, b, c, d). These compendial dissolution methods do not allow sufficient simulation of the unique physiological environment of the oral cavity to which OTPs are exposed and therefore may not be good predictors of *in vivo* behavior. However, efforts have been made to address the need for appropriate *in vitro* methods for OTPs either by incorporating small volume dissolution/release/permeation or modification of the apparatus to reflect *in vivo* conditions. These include a system for drug release from bioadhesive buccal tablets using chicken buccal membrane (Mumtaz et al. 1995), a supported liquid membrane system for nicotine release from snuff (Luque-Pérez et al. 1999), a low liquid system for drug release based on ionic current measurement (Frenning et al. 2002), a system for drug release study of dissolve in mouth dosage forms (Hughes 2003), a flow through diffusion cell for drug permeation study using buccal mucosa (Lestari et al. 2009) and a system for sublingual tablets (Rachid et al. 2011). Unfortunately, while these *in vitro* methods offer background for the development of biorelevant *in vitro* testing of OTPs, they do not provide a system that simulates the oral cavity physiological conditions completely and were not validated appropriately using IVIVR. An IVIVR with a slope of unity is sought in order to use *in*

*vitro* data as a surrogate for *in vivo* performance and to make critical research and regulatory decisions.

This research was therefore initiated to design and develop a biorelevant *in vitro* system for characterization of drug release and permeation from OTPs in a more physiologically realistic manner. To fulfill this objective, a novel bidirectional transmucosal apparatus (BTA) was designed and evaluated that allows better simulation of *in vivo* oral cavity conditions (low liquid surroundings, salivary secretion and swallowing rate, agitation, barriers, blood flow rate) . The device also allows adjustment of *in vitro* variables to optimize an IVIVR for OTPs. Snus, a smokeless tobacco product, was selected as a model oral transmucosal product because *in vivo* nicotine pharmacokinetic data were available for comparison. Snus is put between the cheek and gum for nicotine permeation through the buccal and gingival membranes. In the present research, the *in vivo* prediction by novel bidirectional transmucosal apparatus was compared with that of a modified USP IV flow-through apparatus; a widely used device for novel dosage forms; and a commercially available vertical diffusion cell (VDC); an *in vitro* system for semisolid and transdermal products; for its evaluation. The development of this novel system will find application as a quality control and research tool in the development and regulation of smokeless tobacco products in addition to that of the pharmaceutical oral transmucosal products.



## 3.2 MATERIALS AND METHODS

### 3.2.1 MATERIALS

Snus (a type of smokeless tobacco, non mentholated moist portion snus with natural flavor, Nicotine 8.0 mg, 1.0 g pouch) for *in vitro* studies was obtained from Old Virginia Tobacco Co., Richmond, VA, USA. Hanks' Balanced Salt (H-1387) and N-(2-Hydroxyethyl)piperazine-N'-(2-ethanesulfonic acid) (HEPES, 1M) buffer for the preparation of Hank's balanced salt solution (HBSS; pH 7.4) were purchased from Sigma, St. Louis, MO, USA. Sodium hydroxide and hydrochloric acid solution (10 N) for pH adjustment was purchased from Sigma, St. Louis, MO, USA. (-)-Nicotine hydrogen tartrate (working standard) for the assay was also purchased from Sigma, St. Louis, MO, USA. HPLC grade ammonium acetate and glacial acetic acid for the mobile phase preparation were purchased from Fisher Scientific, Fair Lawn, NJ, USA and EMD, Gibbstown, NJ, USA respectively. HPLC grade methanol was purchased from Honeywell Burdick and Jackson, Muskegon, MI, USA. Water was prepared in-house (the Nanopure Diamond™, Barnstead, IO, USA). Polyethersulfone, polypropylene and regenerated cellulose membranes for *in vitro* permeation study were obtained from Pall Life Sciences, Ann Arbor, MI, USA; Sterlitech Corporation, WA, USA; and Thermo Scientific, Rockford, IL, USA respectively. Fluorinated ethylene propylene (FEP) and Tygon® platinized silicon tubing for the *in vitro* set up were purchased from Cole-Parmer, Vernon Hills, IL, USA. Teflon unions and luer fittings for tubing connections were bought from Upchurch Scientific, Oak Harbor, WA, USA. Masterflex L/S 12-channel 8-roller cartridge pump head (Model 7519-25) and variable-speed modular drive (Model 7553-70; 6 to 600 rpm; flow rate range : 0.0006 to 41 mL/min) for circulating media through donor

and receptor chambers of the novel *in vitro* device was purchased from Cole-Parmer, Vernon Hills, IL, USA.

### 3.2.2 DESCRIPTION OF THE SNUS

Snus is a type of moist snuff containing tobacco packed in a porous bag. The snus weighed  $0.98 \pm 0.03$  g (n=6). Each packet of snus contained 8.0 mg of nicotine. The snus was  $3.2$  cm  $\times$   $1.7$  cm  $\times$   $0.43 \pm 0.03$  cm (length  $\times$  width  $\times$  depth, n=6) in size. The other ingredients of snus were water, taste enhance (salt), humectant (propylene glycol), acidity regulators (sodium carbonate), natural and artificial smoke flavors. Figure 3.1 displays a picture of the snus used in this study. The snus is placed under the upper lip or between the cheek and gum for nicotine permeation through the buccal mucosa from one side and the gingival mucosa on the other.

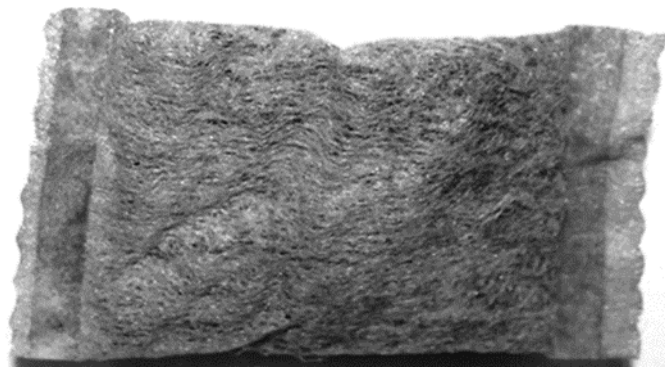


**Figure 3.1:** The smokeless tobacco: Snus

### 3.2.3 MEDIUM FOR RELEASE AND PERMEATION STUDY

A Hanks' Balanced Salt Solution (HBSS) modified by the addition of HEPES buffer was used as a biorelevant release/permeation medium for the present study. HEPES was added to simulate blood pH of 7.4 as it has a pKa of 7.5. The medium was prepared by dissolving 9.8 g of the Hanks' salt mixture in 975 mL of deionized water followed by pH adjustment to  $7.4 \pm 0.1$  with 1 M of sodium hydroxide solution in water. The HEPES solution (25 mL of 1 M) was added into the above medium, mixed well, and vacuum filtered through 0.45  $\mu\text{m}$  nylon filter. The pH of the Hanks' medium was adjusted to  $7.4 \pm 0.05$ , if required, using 1 M sodium hydroxide or 1 M hydrochloric acid solution.

### 3.2.4 APPARATUSES

Nicotine release and permeation studies from a commercially available smokeless tobacco buccal pouch (Snus, 1.0 g) were performed using a Vertical Diffusion Cell (VDC), a Modified USP IV Flow-Through Apparatus (USP IV), and a Novel Bidirectional Transmucosal Apparatus (BTA). Figure 3.2 presents diagrammatic representations of all three apparatuses. The vertical diffusion cell is commercially available from Hanson Research (Chatsworth, CA, USA) and is widely used for the transdermal and semisolid dosage form drug release testing (Hanson 2010). The USP IV flow-through cell is a compendial apparatus and has received wide acceptance for both conventional and novel dosage form testing. The USP IV flow-through apparatus was modified according to (Iyer et al. 2007a) except that the two polycarbonate cells were replaced with conical glass cells (Iyer et al. 2007a). The bidirectional transmucosal apparatus is a novel system designed to better simulate oral cavity conditions and study the effect of physiological

variables on drug release and permeation. The vertical diffusion cell can be used for drug permeation studies, whereas; the modified USP IV flow-through apparatus can be utilized for drug release only. The bidirectional transmucosal apparatus provides the capability of studying drug release and permeation simultaneously. Physiological variables that can be simulated using the bidirectional transmucosal apparatus include low liquid surroundings, saliva secretion and swallowing rate, agitation/chewing movement, bidirectional release and permeation through biorelevant barriers and blood flow rate. In the present study, only low liquid surroundings and bidirectional permeation were simulated to test the suitability of the system.

#### 3.2.4.1 MODIFIED USP IV FLOW THROUGH APPARATUS (USP IV)

The modified USP IV flow through apparatus consisted of two conical glass cells clamped together at their wide ends (Figure. 3.2(A)). The wide ends were provided with O-rings to prevent leaks. Two modified USP IV flow through apparatuses were mounted on a brass stand using cylindrical Teflon fitting at both ends. The inlet and outlet tubing was connected to the bottom and upper Teflon fittings respectively through which the medium was circulated into the glass cell. The length of the modified USP IV flow through apparatus was 19 cm; whereas, the length of the glass cell was 8.5 cm. The lower and upper Teflon fitting was 4.5 and 1.5 cm long respectively. The inlet and outlet diameter of the Teflon fittings was 0.1 cm. The volume of the two glass cells when clamped together along with the Teflon fittings was 7.5 mL, whereas, the bottom and upper connecting tubing had volumes of 3 mL and 0.5 mL respectively.

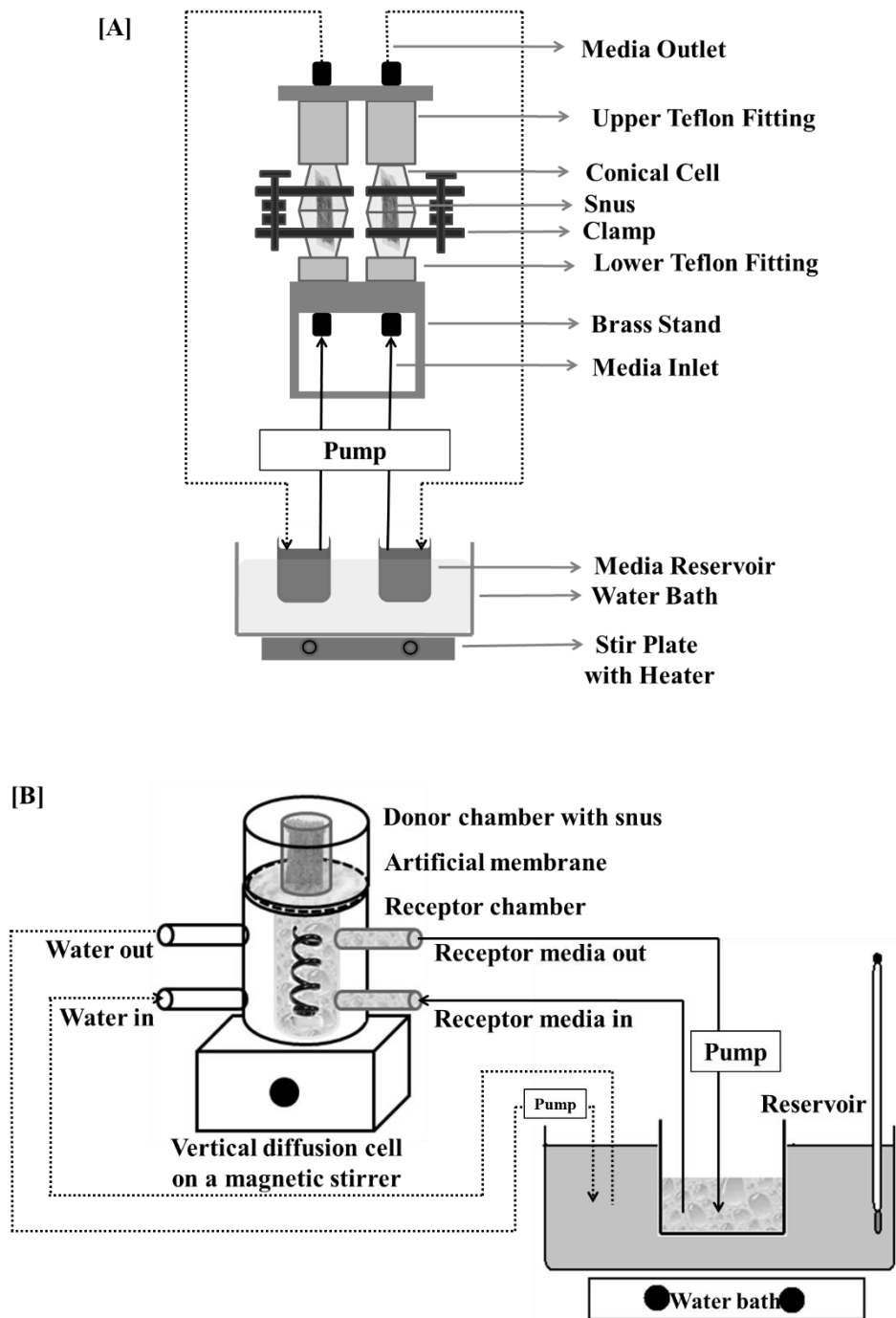


**Figure 3.2:** Experimental set-up with three apparatuses; [A] Modified USP IV flow-through apparatus; [B] vertical diffusion cell; [C] novel bidirectional transmucosal apparatus. Figure 3.2[C] shown on the next page. [Figure not to scale]

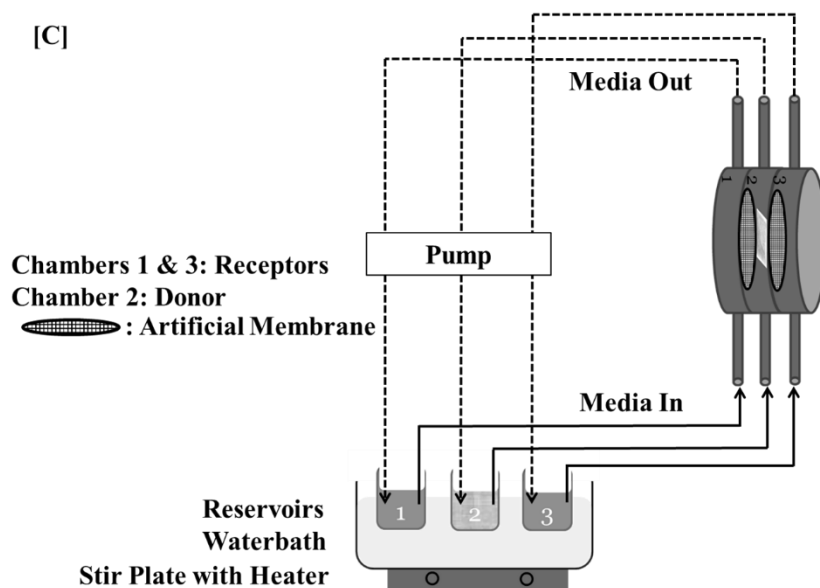


**Figure 3.2:** Experimental set-up with three apparatuses; [A] Modified USP IV flow-through apparatus; [B] vertical diffusion cell; [C] novel bidirectional transmucosal apparatus. Figures 3.2[A] and 3.2 [B] shown on the previous page. [Figure not to scale]

#### 3.2.4.2 VERTICAL DIFFUSION CELL (VDC)

The vertical diffusion cell consisted of a donor (2.5 mL) and receptor (7 mL) chamber (Figure 3.2(B)). The donor and receptor chambers were made of polyether ether ketone (PEEK) and glass respectively. The receptor chamber was enclosed in a water jacket to maintain the temperature of the receptor medium. The receptor chamber had an inlet and outlet port for the circulation of receptor medium from the medium reservoir. The donor chamber was separated from the receptor chamber with an artificial membrane. The membrane area exposed to the receptor media was 1.77 cm<sup>2</sup>. However, the membrane area exposed to the donor medium was 0.79 cm<sup>2</sup>, due to the design of the donor chamber. The media in the receptor chamber was stirred using a spiral helix and magnetic stirrer.

#### 3.2.4.3 NOVEL BIDIRECTIONAL TRANSMUCOSAL APPARATUS (BTA)

In contrast to the vertical diffusion cell, the novel bidirectional transmucosal apparatus consisted of one donor and two receptor chambers. One receptor chamber was present on each side of the donor chamber (Figure 3.2(C)). The presence of two receptor chambers allows study of the bidirectional permeation of nicotine from snus that occurs *in vivo*. When the snus is placed under the upper lip, nicotine from the tobacco permeates through the buccal mucosa from one side and the gingival mucosa on the other. The chambers were separated by an artificial membrane and were stacked together and secured by screws. The artificial membranes represent the buccal and gingival mucosa in the *in vitro* system. The apparatus was made of polymethyl methacrylate (PMMA) and inlets and outlets of all chambers were made of PEEK. The receptor chamber volumes were 7.5 mL and that of the donor chamber was 10 mL based on the height and diameter

of the chamber needed to hold the snus in its proper orientation. The dimensions of the donor chamber were chosen such that it provides low liquid surrounding and simultaneously hold the snus appropriately even after it expands due to the media absorption. The experimentally determined volumes of the receptor and donor chambers were 7.73 and 10.5 mL respectively due to the presence of a thicker neoprene O-ring between the two chambers which adds to the total volume of the chamber. The receptor chambers were 4 cm in diameter and 0.6 cm in height, whereas; the donor chamber was 4 cm in diameter and 0.8 cm in height. The membrane area exposed to the media in each receptor chamber was 14.5 cm<sup>2</sup>. This was different from the theoretical exposure area of 12.6 cm<sup>2</sup> due to the space added between the chamber and O-ring which was 0.3 cm in diameter. Figure 3.3 displays the picture of the BTA constructed with PMMA. The apparatus was fabricated by Custom Design & Fabrication South, LLC (Petersburg, VA).

Saliva secretion/swallowing and blood flow rate can be simulated by adjusting media flow rate in the donor and receptor chambers by the use of appropriate pumps. The effect of chewing or mouth movement can be studied by fabricating flexible walls on the receptors and putting pressure towards the center to agitate the product.



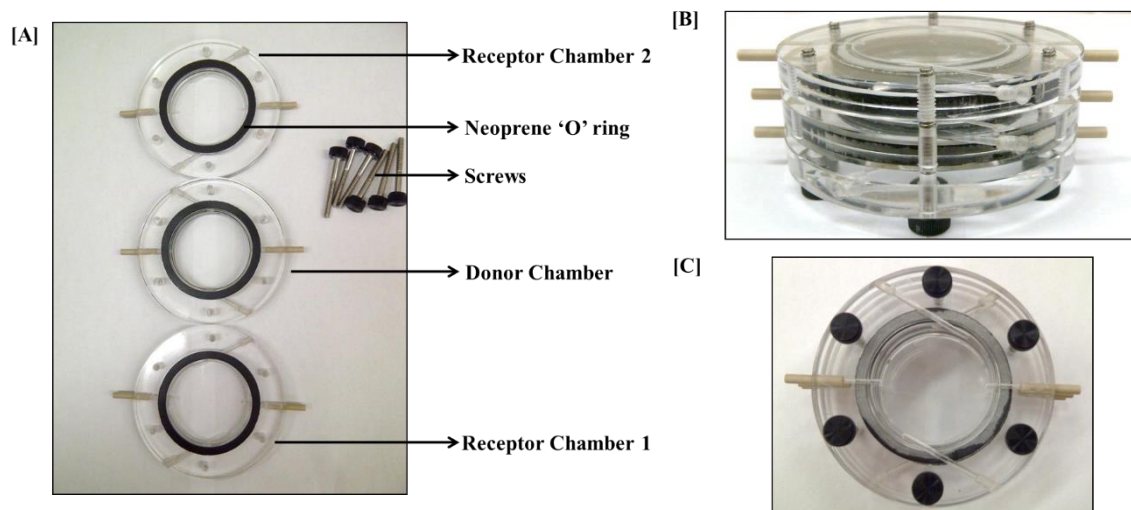


**Figure 3.3:** The novel bidirectional transmucosal apparatus; [A] Donor and receptor chambers; [B] Side view of the apparatus; [C] Top view of the apparatus.

### 3.2.5 *IN VITRO* RELEASE/PERMEATION STUDY

#### 3.2.5.1 EXPERIMENTAL SET-UP/CONDITIONS

A single weighed snus was placed in the donor chamber or glass cell of the apparatuses. With the vertical diffusion cell and bidirectional transmucosal apparatuses, the donor chamber was separated from the receptor chamber by an artificial membrane. The Hanks' medium was re-circulated from the reservoir into the apparatus in a closed loop flow pattern at a flow rate of 1 mL/min using a peristaltic pump, fluorinated ethylene propylene (FEP) and Tygon® platinized silicon tubing. The donor chamber of the vertical diffusion cell contained non-circulating Hanks' medium because it was not possible to circulate donor fluid with this device. The medium reservoirs were 20 mL capacity scintillation glass vials placed in a water bath to maintain temperature at 37 °C. The Hanks' media in the reservoirs were stirred using a magnetic stir bar throughout the experiment. Three separate reservoirs were used for each chamber in the experiment with the bidirectional transmucosal apparatus. A schematic representation of the experimental set up for all apparatuses is shown in Figure. 3.2.

The donor chamber of the vertical diffusion cell contained 1.5 mL of Hanks' medium; whereas, the donor chamber reservoirs of the modified USP IV and bidirectional transmucosal apparatus contained 30 mL including the volumes of tubing and reservoir. The receptor chamber reservoirs of the vertical diffusion cell and bidirectional transmucosal apparatus contained 25 and 20 mL of Hanks' medium respectively which also included the volumes of the tubing and reservoir. Samples (1 mL) were collected from the reservoir at an interval of 2.5 minutes for the initial 10 minutes, 5 minutes for the subsequent 20 minutes and 15 minutes for last 30 minutes (0, 2.5, 5, 7.5, 10, 15, 20, 25, 30, 45 and 60 min) for all experiments and with all apparatuses. These time

points were similar to the plasma sampling time points for an *in vivo* human clinical study that was to be used for IVIVR purposes. In the experiment with the vertical diffusion cell and bidirectional transmucosal apparatus, sampling was performed from receptor chamber reservoirs at the above time intervals and at the last time point from the donor chamber reservoir. The samples were replaced by an equivalent volume of fresh HBSS. The samples were frozen at -20 °C until analysis. The samples were analyzed for nicotine release and permeation using a validated HPLC method reported in Chapter 2. HPLC analysis was performed on a Waters 600E multi-solvent delivery system with a Waters 717 autosampler, Shimadzu solvent degasser DGU-14A and 996 Waters photodiode array detector. Each experiment was performed with replicates of three or five. Cumulative nicotine amounts permeated through both artificial membranes into the receptor chambers of the bidirectional apparatus were added to represent the total permeation achieved at each time point. The method for calculation of the cumulative amount of nicotine permeated and released is tabulated in Table B13 (Appendix B)

### 3.2.5.2 BIORELEVANCE

The presence of snus in the oral cavity stimulates the whole salivary secretion and swallowing rate. These changes will impact the rate and extent of nicotine release and ultimately affecting the overall extent of its permeation. Due to this effect, it was important to simulate the stimulated secretion rate in the donor chamber. The chewing stimulated salivary secretion rate studied in a population with an average age of 25.4 years, was  $0.9 \pm 0.094$  mL/min (Navazesh et al. 1992). Based on this information, it was decided to use 1 mL/min flow rate in the donor chamber of the bidirectional transmucosal and modified USP IV flow-through apparatus. The flow rate in the receptor chambers of the vertical diffusion cell and bidirectional transmucosal apparatus were

both maintained at 1 mL/min. Plasma composition was simulated by use of Hanks' Balanced Salt Solution in the receptor chambers as a biorelevant permeation medium (Iyer et al. 2007b). The same solution was used as a release medium in the donor chamber of the apparatuses as the major inorganic components of saliva and plasma are qualitatively similar (Krebs 1950; Rehak et al. 2000). In addition, employing the same media in the donor and receptor chambers allows the sample analysis of both chambers utilizing the same analytical method.

### 3.2.5.3 BIDIRECTIONAL TRANSMUCOSAL APPARATUS ORIENTATION

The orientation of the vertical diffusion cell and modified USP IV flow-through cell could only be vertical due to the apparatus design. However, the bidirectional transmucosal apparatus could be oriented horizontally and vertically. Therefore, it was necessary to select the orientation of the bidirectional transmucosal apparatus that provided consistent and equivalent permeation in both of the receptor chambers. The effect of horizontal and vertical apparatus orientation on the nicotine permeation was studied using a polyethersulfone membrane (30 KDa MWCO, approximately 3 nm pore size) at a flow rate of 1 mL/min. The samples from the top and bottom receptor chamber's reservoir were collected at 0, 10, 20, 30, 45 and 60 min. The experiment was carried out in triplicate. It is important to mention here, that this set of experiments was performed using the bidirectional transmucosal apparatus made up of PEEK which did not allow for visual examination of air entrapped inside the apparatus during the experiment. Therefore, in order to determine if equivalent permeation occurred during the study, the average of mean ratios of the cumulative amount of nicotine permeated in the bottom and top receptor chambers as a function of time was calculated. Equivalent permeation was expected as both membrane barriers are similar.

The orientation that provided an average ratio of one which indicates equivalent permeation (i.e., the absence of air entrapment) was considered as the optimal orientation.

#### 3.2.5.4 MEMBRANE SELECTION

Three types of membranes were studied for nicotine permeation from snus. Two of them were polymer based, polypropylene (100 nm pore size, 75-110  $\mu\text{m}$  thickness) and polyethersulfone (30 and 300 KDa MWCO; 3 and 30 nm pore size respectively, 220  $\mu\text{m}$  thickness) membranes, whereas; the third membrane was regenerated cellulose membrane (10 KDa MWCO, approximately 2.5 nm pore size, 23  $\mu\text{m}$  thickness). The membranes were studied with both, the vertical diffusion cell and bidirectional transmucosal apparatus to confirm that the results obtained are a function of the membrane and not the apparatus. The polypropylene membrane was studied only with the bidirectional transmucosal apparatus. The effect of pore size on nicotine permeation was studied using the polyethersulfone membranes of 3 and 30 nm pore diameters using only the bidirectional transmucosal apparatus. The criteria for membrane selection were based on consistent nicotine permeation, negligible adsorption of nicotine on the membranes and relatively large extent of permeation. The later was studied by sonication of the membrane in 5 and 10 mL of modified HBSS for 10 min separately for each experiment performed with the vertical diffusion cell and bidirectional transmucosal apparatus respectively. The sonication technique is proved to be an effective method for cleaning membranes and hence the same was used for extracting nicotine adsorbed on membranes in the present study (Kyllonen et al. 2005). The sonicated solution was then analyzed for nicotine adsorption. The cumulative *in vitro* nicotine permeation from snus (1.0 g) obtained with the optimal membrane was compared to the *in vivo* nicotine

absorption from the same snus product. This was done in order to examine the capability of the apparatuses for prediction of *in vivo* performance of oral transmucosal products.

### 3.2.5.5 NICOTINE ADSORPTION STUDY ON ACRYLIC BIDIRECTIONAL TRANSMUCOSAL APPARATUS

The study on adsorption of nicotine on the acrylic bidirectional transmucosal apparatus and assembly components was necessary due to the reported adsorption of nicotine on different materials (Grubner et al. 1980; Caka et al. 1990; Zahlsen et al. 1996; Van Loy et al. 1997; Piade et al. 1999). For this study, a single snus was put in 500 mL of HBSS for 30 minutes under continuous stirring. The resulting nicotine solution was filtered and used for the adsorption study. Sixty eight milliliters of the above nicotine solution from a single glass reservoir at 37 °C temperature was re-circulated at 1 mL/min into the acrylic bidirectional transmucosal apparatus assembly without membranes in place. The nicotine solution in the reservoir was stirred using a magnetic stir bar throughout the experiment. The nicotine solution was sampled from the reservoir at 0, 10, 20, 30, 40, 50 and 60 min and replaced by an equivalent volume of fresh nicotine solution. The adsorption study was performed in triplicate. The samples were analyzed using the validated HPLC method. The percent deviation in the mean nicotine amount at 60 min was calculated relative to the mean nicotine amount at 0 min.

### 3.2.6 *IN VIVO* STUDY

The *in vivo* nicotine absorption from the snus used in this research was obtained from a human clinical study designed and carried out by the Center of Research and Technology, Altria, Richmond, VA, USA. The *in vivo* nicotine pharmacokinetic study was conducted on 18 adult

smokeless tobacco users and mean plasma nicotine concentration time profiles along with their standard deviations were investigated. Snus was put in the oral cavity for 30 minutes after which it was removed during the study (Personal communication). The nicotine level in plasma samples obtained at 0 (Predose), 2.5, 7, 7.5, 10, 15, 20, 25, 30, 45, 60, 90, 120, 180, 240, 300, 600 and 720 min was analyzed by LC-MS/MS (LLOQ 2 ng/mL). The study was approved by an Institutional Review Board.

### 3.2.7 DATA ANALYSIS/PHARMACOKINETIC ASSESSMENT

All calculations for data analysis were performed in Microsoft® Excel 2010. Nicotine concentrations ( $\mu\text{g/mL}$ ) were utilized for calculating the cumulative amount of nicotine released and/or permeated at each time point. The *in vitro* nicotine permeation observed with the vertical diffusion cell, modified USP IV flow-through apparatus and novel bidirectional transmucosal apparatus employing the optimal membrane was related to the *in vivo* nicotine absorption for IVIVR purposes and the slope of the relationship was evaluated. An IVIVR with a slope of unity was targeted, which indicates superimposition of *in vitro* and *in vivo* profiles (Emami 2006).

The observed mean *in vivo* plasma nicotine concentration time profile was deconvolved to its *in vivo* absorption time profile by Wagner-Nelson modeling, assuming an open body one compartment model (Wagner et al. 1964). The area under the curve,  $\text{AUC}_{0-t}$ , was calculated by the trapezoidal rule. The elimination rate constant ( $k_e$ ) was estimated from the terminal slope of the logarithmic plasma nicotine concentration time profile, which was further used for calculating  $\text{AUC}_{0-\infty}$ . All of the above parameters were employed for the determination of the fraction of nicotine absorbed as a function of time by Wagner-Nelson modeling based on Equation 3.1.

$$\frac{A_t}{A_\infty} = \frac{[C_t + (k_e \times AUC_0^t)]}{[k_e \times AUC_0^\infty]} \quad \text{----- Eq 3.1}$$

where,

$\frac{A_t}{A_\infty}$  = fraction amount of drug absorbed at time t

$A_t$  = cumulative amount of drug absorbed at time t

$A_\infty$  = cumulative amount of drug ultimately absorbed of absorbable dose

$C_t$  = plasma drug concentration at time t

$AUC_0^t$  = area under the curve of the plasma concentration time profile between t = 0 and t = t

$AUC_0^\infty$  = area under the curve of the plasma concentration time profile between t = 0 and t =  $\infty$

$k_e$  = Elimination rate constant of the drug obtained from the terminal phase of log plasma concentration time profile

Further, the percent of nicotine (%) absorbed as a function of time (min) was calculated from the fraction of nicotine absorbed ( $\frac{A_t}{A_\infty}$ ) obtained by the Wagner-Nelson modeling and absolute bioavailability (F) (considering 8 mg as the nominal dose, 8 mg is the nominal amount of nicotine present in snus) based on Equation 3.2:

$$\% \text{ Amount of Nicotine Absorbed} = \frac{A_t}{A_\infty} \times 100 \times F \quad \text{----- Eq 3.2}$$

where,  $\frac{A_t}{A_\infty}$  is the fractional amount of nicotine absorbed at time t, and F representing the absolute bioavailability of nicotine from snus. The absolute bioavailability of nicotine from snus was 0.18 [ $F = \frac{(AUC_0^\infty)_{snus}}{(Dose)_{snus}} \times \frac{(Dose)_{IV}}{(AUC_0^\infty)_{IV}}$ ; The  $AUC_{0-\infty, IV}$  and  $Dose_{IV}$  from an intravenous (IV) infusion pharmacokinetic study on 20 healthy adult subject of age 22-43 years was 1596 ng\*min/mL and 1.77 mg respectively (Molander et al. 2001);  $AUC_{0-\infty, snus}$  and  $Dose_{snus}$  was 1283 ng\*min/mL and 8 mg respectively].



The cumulative percent nicotine (% of 8 mg dose) absorption time profile obtained was employed for the *in vitro in vivo* relationship (IVIVR). The percent cumulative *in vitro* nicotine released and/or permeated (% of 8 mg dose; 7.5 to 30 min) was related to the percent cumulative *in vivo* nicotine absorbed (% of 8 mg dose; 7.5 to 30 min) and the IVIVR slope obtained with each apparatus was interpreted.

### **3.3 RESULTS AND DISCUSSION**

#### **3.3.1 VALIDATION OF THE SYSTEM**

##### **3.3.1.1 BIDIRECTIONAL TRANSMUCOSAL APPARATUS ORIENTATION**

Figures 3.4(A) and 3.4(B) represent the cumulative nicotine permeation in the top and bottom receptor chambers when the apparatus was oriented in horizontal and vertical positions respectively. Table 3.1 presents the ratio of the average amount of nicotine permeated in the bottom and top receptor chambers when the BTA was oriented horizontally and vertically. The amounts of nicotine permeated in the bottom and top receptor chambers obtained from replicate experiments at both orientations are displayed in Tables B1 and B2 of Appendix B. The average of the mean ratio of the nicotine permeated in the bottom and top receptor chambers at all-time points with the horizontal and vertical orientation were 2.19 and 1.09 respectively. The ratio of 2.19 with the horizontal apparatus orientation indicates that the permeation was two times higher in the bottom receptor chamber when compared to the top receptor chamber. In the horizontal orientation, total permeation was higher in the bottom chamber due to the initial 10 minutes, where the nicotine permeation was approximately 2.25 times higher than in the top receptor chamber.

Nicotine permeation was comparable after the initial 10 minutes as evident from the parallel slopes of the cumulative nicotine permeation-time profile of the horizontal apparatus orientation in Figure. 3.4(A). This initial difference may be due to entrapment of air in the donor chamber below the top receptor membrane or a higher degree of contact of the lower receptor membrane with the snus in the horizontal orientation. The entrapment of air creates a void space between the membrane of the top receptor chamber and the donor chamber and negatively affects the permeation process. With the vertical orientation, the ratio of 1.09 suggests equivalent permeation in both the receptor chambers of the bidirectional apparatus and the absence of air. Since the extent of nicotine permeation was similar in both receptor chambers in the vertical apparatus orientation; it was decided to conduct future experiments positioning the apparatus vertically. Also, snus placed horizontally in the novel apparatus that is oriented vertically adds biorelevance to the novel system for the reason that the snus is placed horizontally under the upper lip. In addition, the nicotine available for permeation through the gingival and buccal membranes may be the same *in vivo* due to the absence of air at the interface between snus and mucosa. The vertical orientation mimics the availability of nicotine at both membrane-donor media interfaces as indicated by equivalent permeation in both receptors. With respect to the absence of void space and equal availability of nicotine for permeation at both membrane-donor media interfaces; the vertical orientation was considered optimal and is more physiologically relevant.

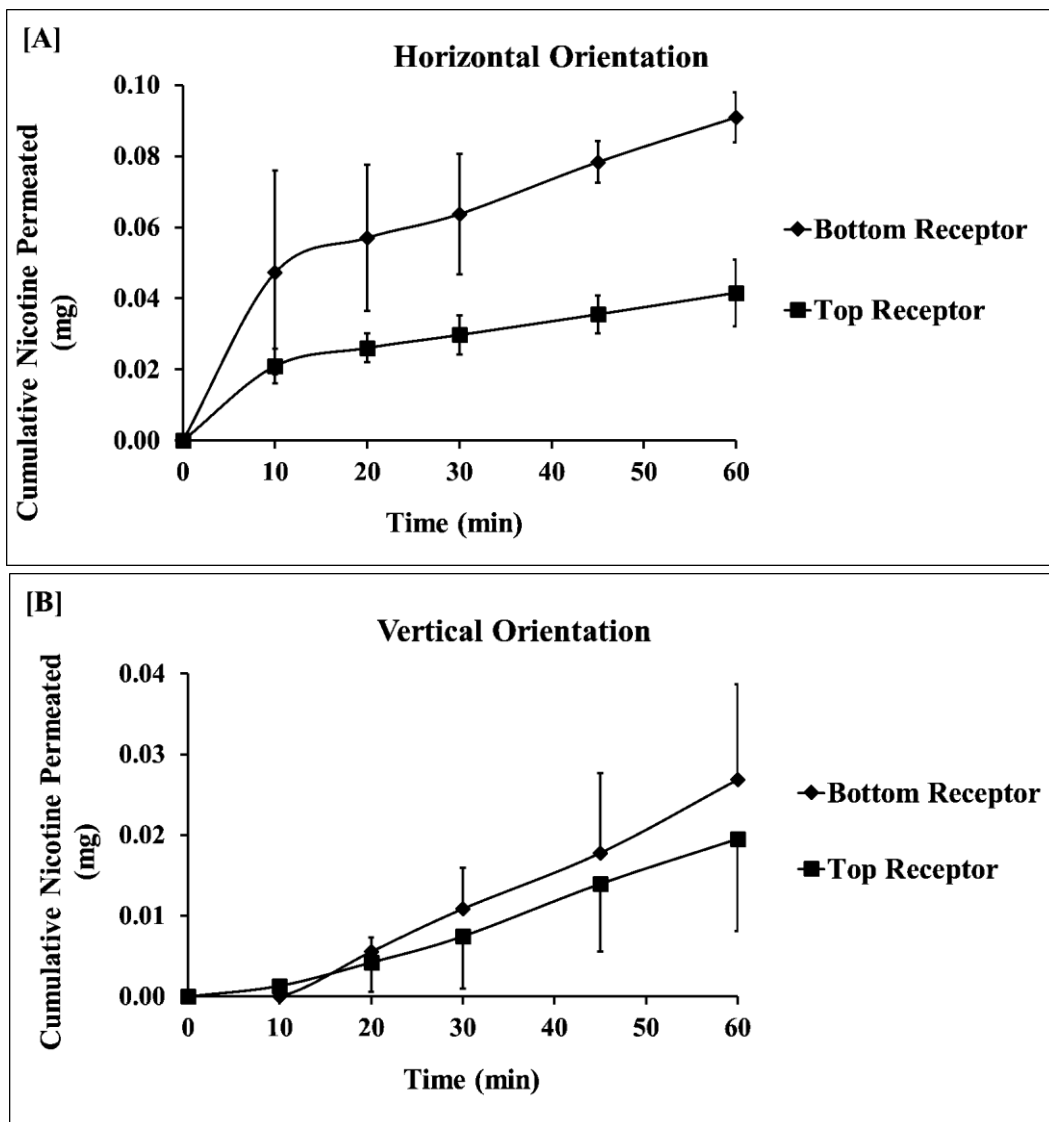


**Figure 3.4:** Effect of apparatus orientation on nicotine permeation in the receptor chambers; **[A]** Horizontal orientation; **[B]** Vertical orientation. (Error bars represents one standard deviation; n=3)

**Table 3.1:** Effect of apparatus orientation on nicotine permeation in receptor chambers (n=3)

	<b>Horizontal</b>	<b>Vertical</b>
<b>Time (min)</b>	<b>Mean ratio of nicotine amount permeated (bottom/top receptor)</b>	
10	2.25	0
20	2.19	1.32
30	2.14	1.46
45	2.20	1.27
60	2.19	1.38
<b>Average ratio</b>	2.19	1.08

### 3.3.1.2 MEMBRANE SELECTION

Membrane selection was affected by the tendency of nicotine to adsorb onto various materials (Grubner et al. 1980; Zahlseu et al. 1996; Van Loy et al. 1997; Piade et al. 1999). Polypropylene (100 nm pore size, 75-110  $\mu\text{m}$  thickness) was first studied for nicotine permeation using the bidirectional transmucosal apparatus. It was found that the nicotine permeation did not occur with this membrane within the lower limit of quantification of the HPLC method. The absence of nicotine permeation can be attributed to the lack of wettability of the polypropylene due to its hydrophobicity. The membrane observed at the end of the experiment was completely dry. Therefore, it was concluded that the polypropylene membrane was not a suitable membrane choice and was not further investigated.

Table 3.2 shows results of nicotine release, cumulative nicotine permeation and nicotine adsorption on membranes studied with the vertical diffusion cell (VDC) and bidirectional transmucosal apparatus (BTA) with both polyethersulfone and regenerated cellulose membranes. The replicate data for nicotine release/permeation obtained from experiments for membrane selection are presented in Table B3-B7 of Appendix B. Figure 3.5(A) and 3.5(B) shows a graphical representation of the effect of the membrane on nicotine permeation with both the VDC and BTA. The cumulative nicotine permeation with the polyethersulfone membrane (3 nm pore size) was highly variable with both the vertical diffusion cell (%RSD<sub>60 min</sub> = 63.88 %) and bidirectional transmucosal apparatus (%RSD<sub>60 min</sub> = 49.64 %). The overall nicotine permeated with the vertical diffusion cell and bidirectional transmucosal apparatus at 60 minutes using the polyethersulfone membrane was only 0.2 and 0.6 % of 8 mg nicotine in the snus respectively which is much less than the 18% nicotine absorbed *in vivo*. However, the bidirectional transmucosal apparatus provided approximately three times greater permeation than the vertical diffusion cell due to the

larger membrane surface area and bidirectional permeation. In addition, an unexpected plateau in the cumulative nicotine permeation with the vertical diffusion cell was observed which could be related to saturation of the small membrane surface. At the end of the permeation study, the membranes were completely brown in color. The analysis of Hanks' media used for sonication of polyethersulfone (3 nm pore size) membranes used in both the apparatuses indicated significant adsorption of nicotine which might have been responsible for the observed low extent of permeation (two tailed t-test at  $\alpha=0.05$ , vertical diffusion cell ( $0.114 \text{ mg/cm}^2$ ):  $t = 13.30$ ,  $df = 4$ ,  $p\text{-value} = 0.0002$ ; bidirectional transmucosal apparatus ( $0.005 \text{ mg/cm}^2$ ):  $t = 6.11$ ,  $df = 2$ ,  $p\text{-value} = 0.0258$ ). Nicotine assayed from the donor chamber accounted for more than 50 % of the nicotine content in the snus (8 mg) which supports the conclusion that the nicotine release is high enough for permeation to occur.

Subsequent studies were conducted using polyethersulfone membranes with a pore size of 30 nm ( $n=3$ ) and the bidirectional apparatus to investigate whether or not the small pore size with the previous study might have been responsible for low permeation. This study demonstrated the complete absence of permeation. As observed previously, membranes were completely brown at the end of the study and the sonication experiment suggested adsorption of nicotine. It is possible that nicotine is adsorbed on the pigment present in tobacco. The pigment might have blocked membrane pores of both types of polyethersulfone membranes and thus provided low nicotine permeation. This study shows that the pore size was not limiting for nicotine permeation. We concluded that the polyethersulfone membrane was not a suitable membrane for nicotine permeation.

Cumulative nicotine permeation with the regenerated cellulose membrane (2.5 nm) was less variable as compared to the polyethersulfone membrane with both the vertical diffusion cell

(%RSD<sub>60 min</sub> = 15.80 %) and the bidirectional transmucosal apparatus (%RSD<sub>60 min</sub> = 14.77). The overall nicotine permeated with the regenerated cellulose membrane was 12.23 and 12.30% of the nicotine content (8 mg) in snus which is close to the 18 % nicotine absorbed *in vivo*. The analysis of regenerated cellulose sonicate samples with both devices again indicated adsorption onto the membrane (two tailed t-test at  $\alpha=0.05$ , vertical diffusion cell (0.005 mg/cm<sup>2</sup>):  $t = 4.42$ ,  $df = 4$ ,  $p$ -value = 0.0115; bidirectional transmucosal apparatus (0.0002 mg/cm<sup>2</sup>):  $t = 3.76$ ,  $df = 4$ ,  $p$ -value = 0.0198) although the regenerated cellulose provided significantly less nicotine adsorption as compared to the polyethersulfone membranes (Equal variance t-test at  $\alpha=0.05$ , vertical diffusion cell:  $t = -12.64$ ,  $df = 8$ ,  $p$ -value < 0.0001; bidirectional transmucosal apparatus:  $t = -5.86$ ,  $df = 2.02$ ,  $p$ -value = 0.0274). Also, the regenerated cellulose membranes observed at the end of the experiment were completely clear. The regenerated cellulose membrane was selected for further study owing to consistent and large extent of nicotine permeation and less nicotine adsorption relative to the polyethersulfone membrane. Nicotine, being a lipophilic molecule, is highly permeable through the oral mucosa. Therefore, the oral mucosa may not be a major barrier to the availability of nicotine in the systemic circulation. Similar nicotine permeation behavior was obtained with the use of regenerated cellulose membrane; whereas, permeation through the polyethersulfone membrane was limited due to adsorption of nicotine.

**Table 3.2:** Nicotine release, cumulative nicotine permeation and nicotine adsorption with polyethersulfone (PES) and regenerated incellulose (RC) membranes

Membrane (pore size)	Apparatus	N	Nicotine release in donor chamber at 60 min (mg) (%RSD) <sup>g</sup>	Adsorption of nicotine on membrane (mg) (%RSD)	Adsorption of nicotine per cm <sup>2</sup> of membrane (mg/cm <sup>2</sup> ) (%RSD)	Percent nicotine adsorption on membrane (%/cm <sup>2</sup> ) <sup>f</sup>	Total nicotine release in donor chamber at 60 min (mg) <sup>a</sup>	Percent nicotine release in donor chamber (%) <sup>f</sup>	Cumulative nicotine permeation at 60 min (mg) (%RSD)	Percent nicotine permeation at 60 min (%) <sup>f</sup>
PES (3 nm)	VDC	5	4.68 ± 0.29 (6.21)	0.09 ± 0.02 <sup>d</sup> (16.82)	0.11 ± 0.02 (16.82)	1.43	4.77	59.59	0.02 ± 0.01 (63.88)	0.21
	BTA	3	5.96 ± 0.71 (11.95)	0.16 ± 0.04 <sup>b,c</sup> (28.35)	0.005 ± 0.002 (28.35)	0.06	6.12	76.46	0.05 ± 0.02 <sup>e</sup> (49.64)	0.58
PES (30 nm)	BTA	3	5.52 ± 0.97 (17.60)	0.24 ± 0.15 <sup>b,c</sup> (60.67)	0.008 ± 0.005 (60.67)	0.10	5.76	72.00	not detected	-
RC (2.5 nm)	VDC	5	3.90 ± 0.53 (13.48)	0.004 ± 0.002 <sup>d</sup> (50.58)	0.005 ± 0.002 (50.58)	0.06	3.90	48.80	0.98 ± 0.16 (15.80)	12.23
	BTA	5	5.86 ± 0.24 (4.02)	0.006 ± 0.004 <sup>b,c</sup> (59.47)	0.0002 ± 0.0001 (59.47)	0.003	5.87	73.33	0.98 ± 0.15 <sup>e</sup> (14.77)	12.30

<sup>a</sup> The total nicotine release in donor chamber represents the sum of nicotine release in donor chamber at 60 min and nicotine adsorbed on the membranes

<sup>b</sup> Values represents the sum of nicotine adsorbed on membranes of both receptors

<sup>c</sup> The total of the surface area of both membranes exposed to donor media was 29 cm<sup>2</sup> in the bidirectional transmucosal apparatus (14.5 cm<sup>2</sup> per membrane)

<sup>d</sup> The total surface area of membrane exposed to donor media was 0.79 cm<sup>2</sup> in the vertical diffusion cell

<sup>e</sup> The nicotine permeation represents the sum of nicotine permeated in both the receptors at 60 min

<sup>f</sup> Values represents the percent of 8 mg

<sup>g</sup> Percent relative standard deviation



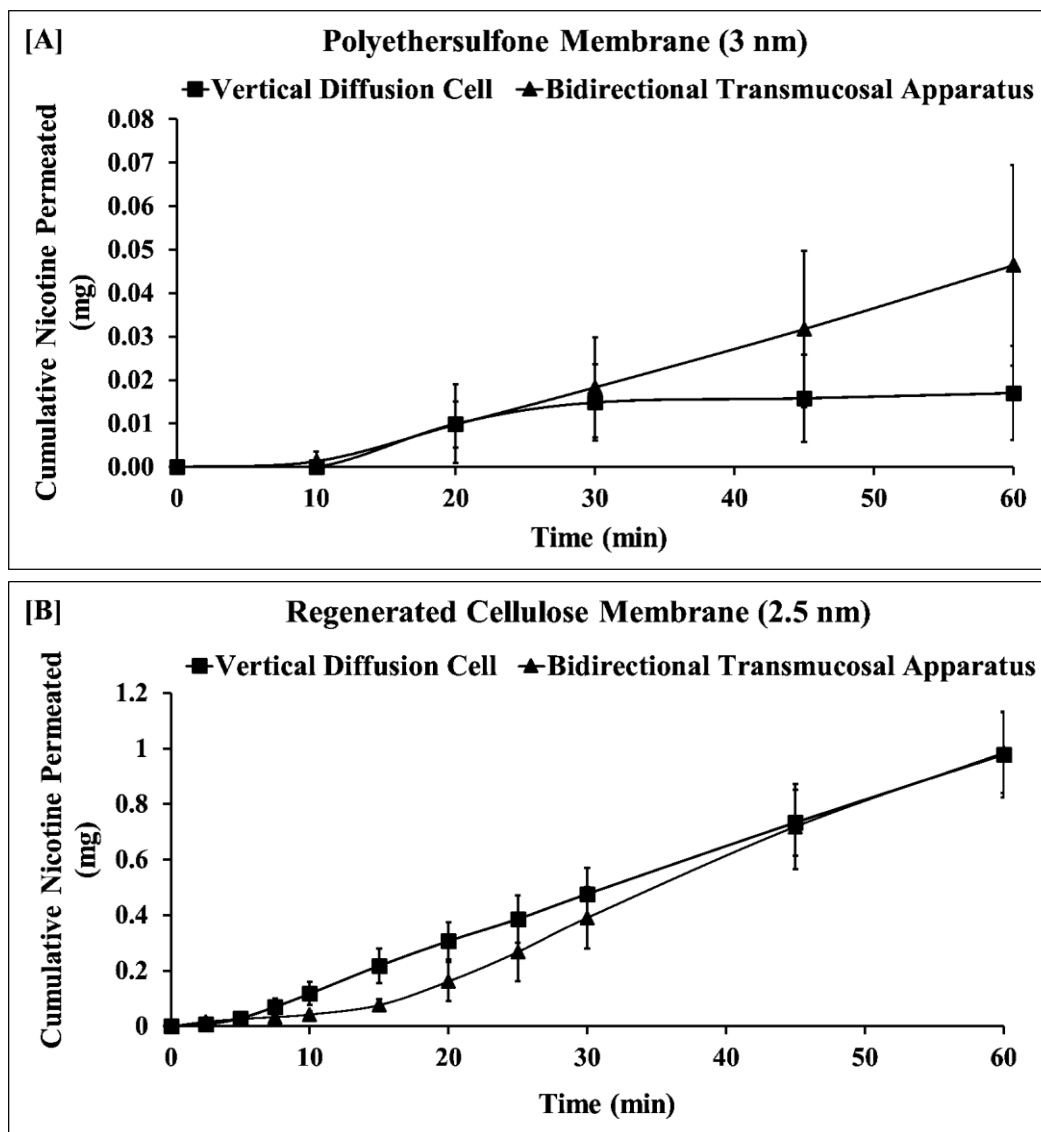


**Figure 3.5:** Effect of membrane type on nicotine permeation with the vertical diffusion cell and bidirectional transmucosal apparatus; **[A]** Polyethersulfone membrane (3 nm); **[B]** Regenerated cellulose membrane (2.5 nm). (Error bars represents one standard deviation; n=5 in all cases except with polyethersulfone membrane and BTA where n=3)

### 3.3.1.3 ADSORPTION OF NICOTINE ON THE ACRYLIC BIDIRECTIONAL TRANSMUCOSAL APPARATUS AND ASSEMBLY COMPONENTS

In addition to the study of nicotine adsorption onto membranes, it was also necessary to examine the adsorption of nicotine onto the acrylic bidirectional transmucosal apparatus and assembly components. The study was not performed with the glass vertical diffusion cell as the glass had shown the least adsorption of nicotine among different materials tested (Grubner et al. 1980). Besides, other assembly components used for these two set ups were similar. The nicotine adsorption study with the acrylic bidirectional transmucosal apparatus set up was conducted by recirculation of nicotine solution of a known concentration and the nicotine time profile obtained from the study is shown in Figure 3.6. The amount of nicotine adsorbed as a function of time obtained from replicate experiments is displayed in Table B8 of Appendix B. The study indicated that approximately 4% of nicotine from the solution was adsorbed at 60 minutes. This deviation was not considered significant and it was concluded that the acrylic bidirectional transmucosal apparatus and assembly components were suitable for further work.

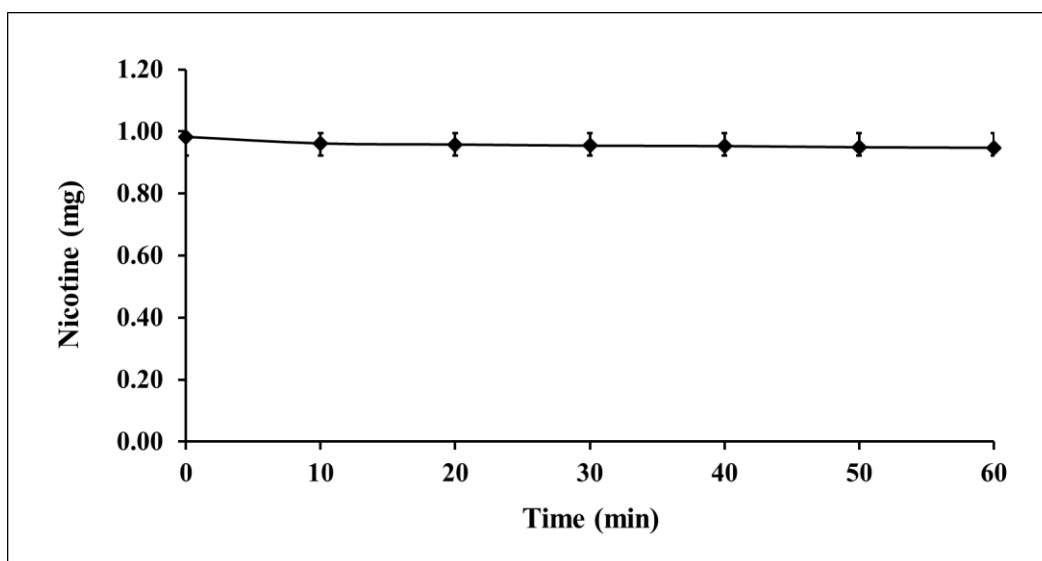


**Figure 3.6:** Nicotine amount time profile for the nicotine adsorption study with the acrylic bidirectional transmucosal apparatus and assembly components. (Error bars represents three standard deviation; n=3)

### 3.3.2 *IN VITRO* RELEASE/PERMEATION STUDY

Figure 3.7 illustrates the mean cumulative nicotine release/permeation time profiles obtained with the modified USP IV flow-through apparatus, vertical diffusion cell and novel bidirectional transmucosal apparatus when the regenerated cellulose membrane was used. The amount of nicotine released/permeated, nicotine release/permeation rate and lag time obtained from all three apparatuses are tabulated in Tables B9-B11 of Appendix B. Nicotine release using the modified UPS IV flow-through apparatus demonstrated a first order release of nicotine [cumulative nicotine release<sub>USP IV</sub> (mg) = 1.7954 \* Ln (time in minutes) – 2.0232, R<sup>2</sup> = 0.957]; whereas, nicotine permeation with the vertical diffusion cell and bidirectional transmucosal apparatus showed zero order permeation of nicotine [cumulative nicotine permeation<sub>VDC</sub> (mg) = 0.0169 \* (time in minutes) – 0.0377, R<sup>2</sup> = 0.997 and cumulative nicotine permeation<sub>BTA</sub> (mg) = 0.0207 \* (time in minutes) – 0.2392, R<sup>2</sup> = 0.998 respectively]. The first order release obtained with the modified USP IV apparatus might be due to depletion of nicotine in the snus as a function of time resulting in the decreased release rate. The cumulative nicotine amount released at 60 minutes accounted 71.21% (5.697 mg ± 0.341, % RSD = 5.99, n=5) of nicotine content in snus (8 mg). In contrast, with the vertical diffusion cell and bidirectional transmucosal apparatus, the donor nicotine concentrations were large relative to the nicotine that permeated in the receptor chambers as shown in Table 3.2; consequently linear permeation was obtained during the 60 minute period.

Table B5 (Appendix B) represents the cumulative amount of nicotine released/permeated as a function of time obtained from replicate experiments with all apparatuses.

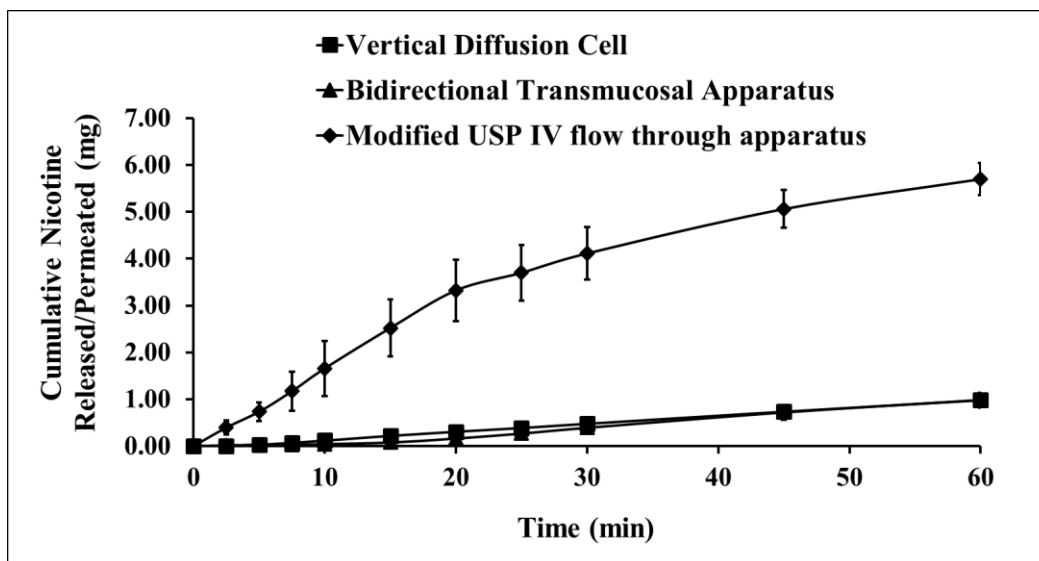


**Figure 3.7:** The mean cumulative nicotine permeation/release time profiles with all three apparatuses; USP IV :  $Y=0.1707*X-0.073$ ,  $R^2=0.99$  (Linear fit : 2.5 to 20 min, No lag time); VDC :  $Y=0.018*X-0.0608$ ,  $R^2=0.99$  (Linear fit : 5 to 30 min, Lag time of 2.5 min); BTA :  $Y=0.021*X-0.2487$ ,  $R^2=0.99$  (Linear fit : 15 to 30 min, Lag time of 11.8 min). (Error bars represent one standard deviation;  $n = 5$ ) [ The line was fitted up to 20 min with the USP IV due to non-linearity after 20 min; The line was fitted up to 30 min for the VDC and BTA as these will be compared to the *in vivo* rate obtained from a study where snus was removed after 30 min] [Slopes of the above fitted lines represent release/permeation rate and are used for comparison with the *in vivo* rates in Chapter 4]

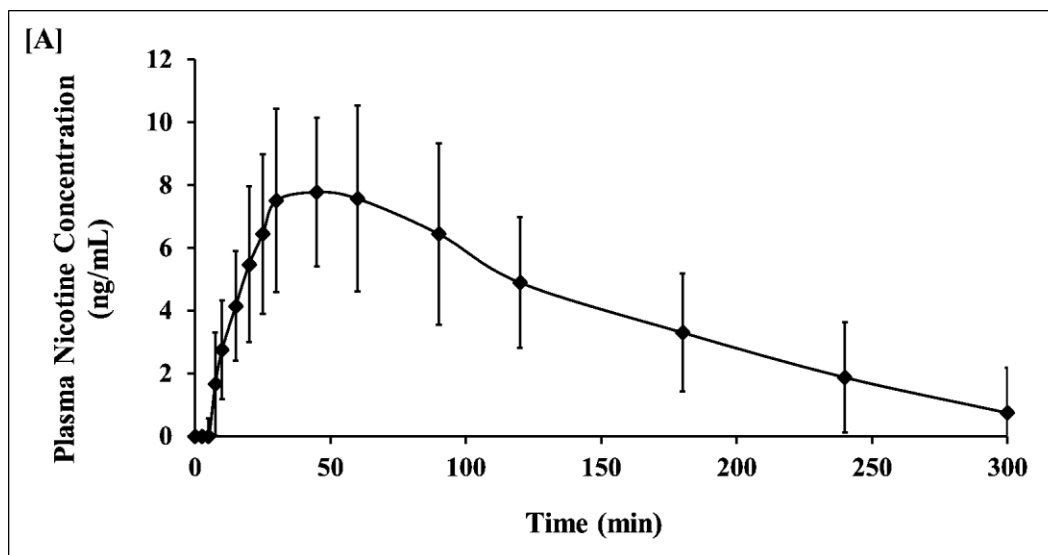
### 3.3.3 IN VIVO STUDY


The mean plasma nicotine concentration time profile obtained from a nicotine pharmacokinetic study carried out on 18 adult smokeless tobacco users by the Center of Research and Technology, Altria, is shown in Figure 3.8(A) and the mean pharmacokinetic parameters are summarized in Table 3.3. The *in vivo* percent nicotine absorption time profile (% of 8 mg – nominal amount of nicotine in snus) obtained after the deconvolution of the mean plasma nicotine concentration time profile and the application of a scaling approach based on absolute bioavailability ( $F = 0.18$ ) is displayed in Figure 3.8(B). The application of the scaling approach was based on the absolute bioavailability  $F$  (Section 3.2.7; Equation 3.2) and provided 18% as the maximum amount of nicotine absorbed as opposed to 100% ( $\frac{A_t}{A_\infty} \times 100$ ) which is usually obtained after modeling of the plasma concentration by the Wagner Nelson approach. The plasma nicotine levels and the amount of nicotine absorbed are summarized in Table B12 (Appendix B).

**Table 3.3:** Mean pharmacokinetic parameters (n=18) after administration of snus 1.0 g (8 mg nicotine)

Pharmacokinetic parameters	Snus 1.0 g
$C_{\max}$ (ng/mL)	7.8
$T_{\max}$ (min)	45
$AUC_{0-300\text{min}}$ (ng*min/ml)	1203.5
$AUC_{0-\infty}$	1283.5
$k_e$ ( $\text{min}^{-1}$ )	0.009
Absolute bioavailability (%)	18
Absorption rate (mg/min)*	0.036

\* The rate was calculated from 7.5 to 30 min of the nicotine absorption time profile [Nicotine absorbed (mg) vs Time (min) plot]




**Deconvolution: Wagner-Nelson Modeling  
Correction based on the absolute bioavailability**

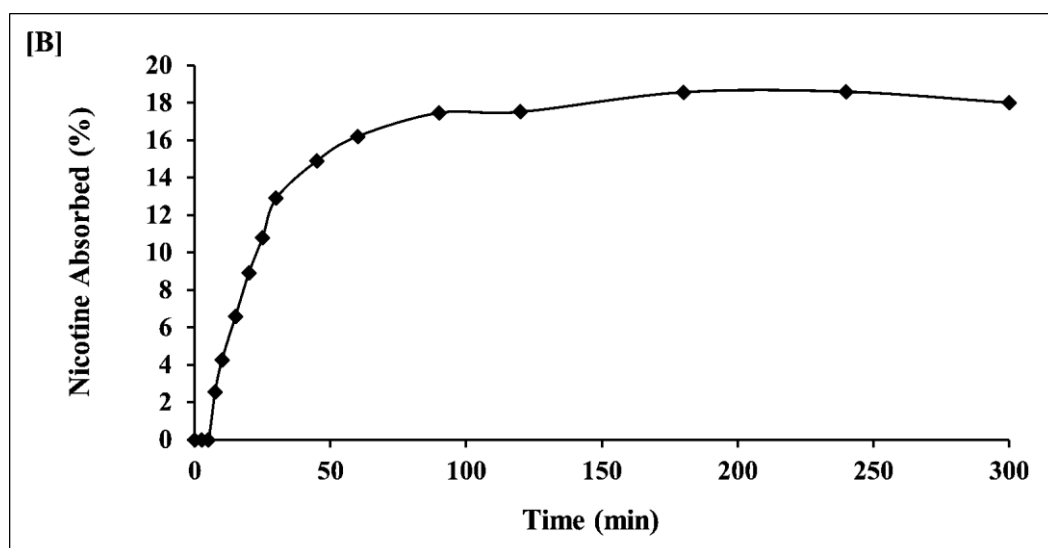


**Figure 3.8:** Deconvolution of plasma nicotine concentration time profile of snus by Wagner-Nelson modeling [A] The mean plasma nicotine concentration time profile of 18 smokeless tobacco users (Error bar represents one standard deviation; n=3); [B] The mean nicotine absorption time profile of 18 smokeless tobacco users.

### 3.3.4 *IN VITRO IN VIVO* RELATIONSHIP (IVIVR)

The percent cumulative nicotine release/permeation obtained in the *in vitro* systems employing regenerated cellulose membranes when related to the cumulative amount absorbed in *in vivo* (Figure 3.8(B)); an *in vitro in vivo* relationship (IVIVR) model was generated and is presented in Figures 3.9 (A), 3.9(B) and 3.9(C). The IVIVR plot was constructed using *in vitro* and *in vivo* data from 7.5 to 30 min. The time frame of 7.5 to 30 min was considered because of the observed lag time of 7.5 min *in vivo* and the removal of snus after 30 min during the clinical study. The IVIVR model obtained for the modified USP IV flow-through apparatus and vertical diffusion cell was linear with  $R^2$  values of 0.99; whereas, the model for the bidirectional transmucosal apparatus showed a relatively poor linear fit  $R^2$  of 0.91. The poor linear fit of the IVIVR model with the bidirectional transmucosal apparatus might be due to relatively slow *in vitro* permeation when compared to rapid *in vivo* absorption during the initial 15 min (IVIVR slope = 2.11) . This may be because of the lower concentration gradient that exists in the bidirectional transmucosal *in vitro* system due to the lower receptor to donor volume ratio of 1.33. In the case of the vertical diffusion cell, the *in vitro* permeation rate was slow relative to the *in vivo* absorption rate regardless of the larger concentration gradient (receptor to donor volume ratio of 16.67). This slow *in vitro* permeation rate is justified by the slope (2.01) of the IVIVR model which is greater than 1 and might be due to the lower membrane surface area available for permeation. In spite of this, the linear model was appropriate to describe the IVIVR achieved with the vertical diffusion cell. The *in vitro* release rate with the modified USP IV apparatus is relatively faster than the *in vivo* absorption as evident from the slope (0.27) of the linear IVIVR model which was due to the absence of a membrane barrier. The details on the *in vitro* nicotine release/permeation rate and *in vivo* nicotine absorption rate are presented in Table B13 (Appendix B).



### 3.3.5 COMPARISON OF THE THREE APPARATUSES

Overall, drug release/permeation testing apparatuses used in the present research provided IVIVR models with a slope either lower or greater than unity. This was evidence of the need of simulating or adjusting physiological oral cavity and *in vitro* variables to incorporate more biorelevance into the *in vitro* system and obtain *in vitro* profiles that represent the *in vivo* behavior of snus. There are limited options available for simulation or adjustment of variables with the USP IV and VDC apparatuses. The bidirectional transmucosal apparatus allows for better simulation oral cavity conditions in comparison to the VDC and USP IV systems. Simulation and adjustment of *in vivo* conditions is very important to achieve better IVIVR for the prediction of the *in vivo* behavior of the drug product because drug dissolution and release kinetics are influenced by these conditions (Dressman et al. 1998; Wang et al. 2009). As represented in Table 3.4, the bidirectional transmucosal apparatus allows adjustment of important oral cavity conditions that can affect drug release/permeation. These *in vivo* conditions include salivary secretion and swallowing rate in the donor chamber, blood flow rate in the receptor chambers and agitation in the donor chamber. In addition, it allows study of bidirectional permeation that occurs *in vivo*. The modified USP IV flow-through apparatus and vertical diffusion cell permits adjustment of only few physiological variables as listed in Table 3.4. The degree of biorelevance achievable with the apparatuses are in the order of modified bidirectional transmucosal apparatus > vertical diffusion cell > USP IV flow-through apparatus.

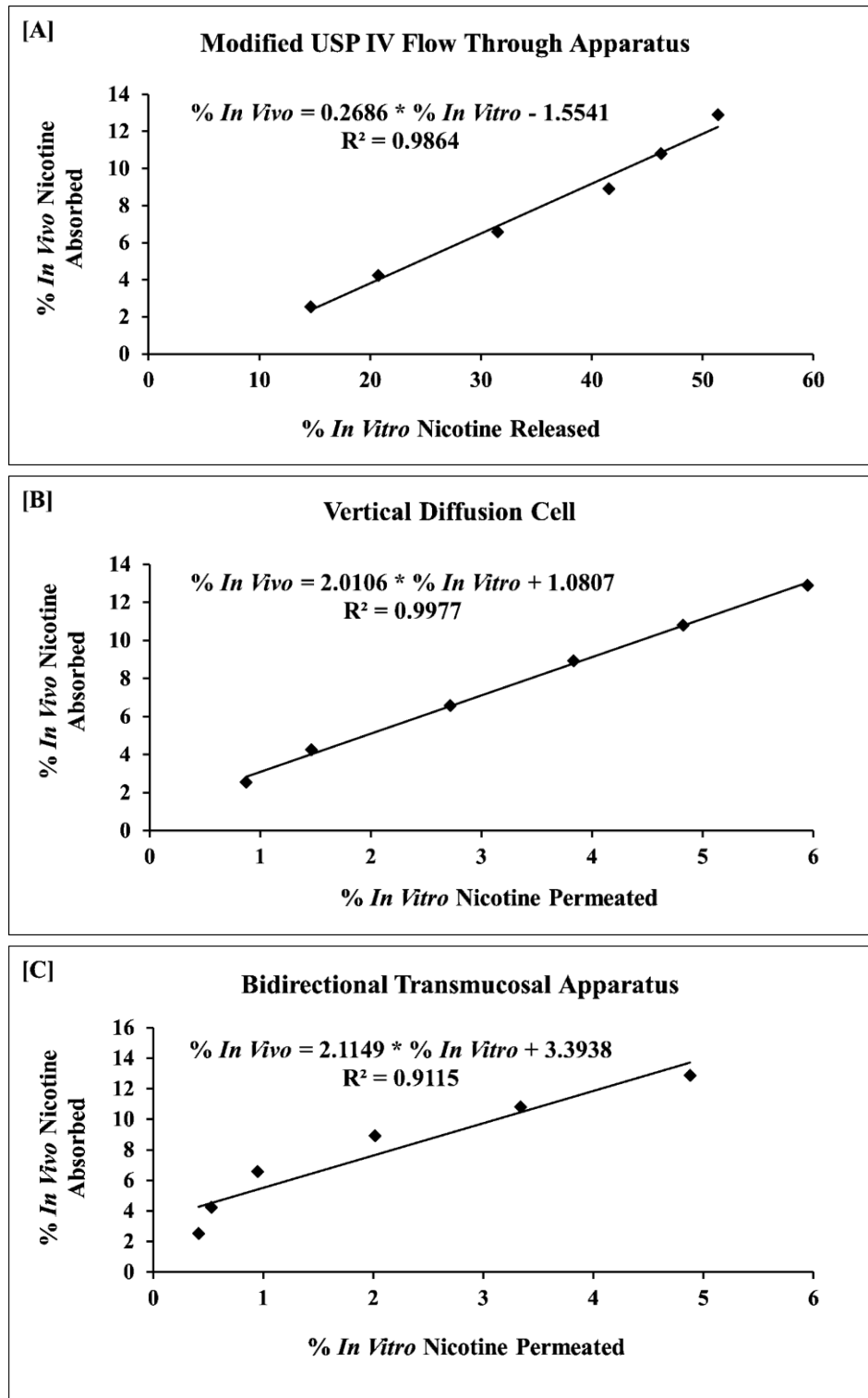


**Figure 3.9:** *In vitro in vivo* relationships (IVIVR from 7.5 to 30 min) for snus with three apparatuses; [A] Modified USP IV flow through apparatus; [B] Vertical diffusion cell; [C] Bidirectional transmucosal apparatus.

**Table 3.4:** Simulation of oral cavity conditions by apparatuses

<b>Apparatus*</b>	<b>Media composition and its physical properties</b>	<b>Salivary secretion and swallowing rate</b>	<b>Agitation</b>	<b>Blood flow rate</b>	<b>Bidirectional biorelevant barriers</b>	<b>Permeation</b>	<b>Release</b>
USP IV	Yes	Yes**	No	No	No	No	Yes
VDC	Yes	No	No	Yes	No	Yes	No
BTA	Yes	Yes	Yes	Yes	Yes	Yes	Yes

\* USP IV (Modified USP IV flow through apparatus); VDC (Vertical Diffusion Cell); BTA (Bidirectional Transmucosal Apparatus)

\*\* The effect of saliva secretion rate on drug release from the product can be studied with the USP IV; however, the effect of saliva swallowing rate on permeation cannot be studied due to the absence of a permeation barrier

### 3.4 CONCLUSIONS

A novel bidirectional transmucosal apparatus was designed and developed, and compared to two commercial devices for biorelevant *in vitro* release and permeation testing of oral transmucosal products. The bidirectional transmucosal system was validated in terms of the orientation of the device, membrane performance and nicotine adsorption on the components. Of the membranes studied, the regenerated cellulose membrane provided consistent permeation and negligible nicotine adsorption. The bidirectional transmucosal apparatus provided linear nicotine permeation profiles with the rate and extent of nicotine permeation similar to the vertical diffusion cell. The modified USP IV and the vertical diffusion cell provided linear relationship between the percent *in vitro* nicotine permeation and *in vivo* nicotine absorption; whereas, the bidirectional transmucosal apparatus demonstrated a poor linear relation. Among three apparatuses studied, the BTA was selected for further optimization of IVIVR for snus since it allowed adjustment of more biorelevant parameters that better simulate the oral cavity. In addition, the work presented here provides a general guide to important steps required for the development and validation of biorelevant systems. The bidirectional transmucosal apparatus is a promising candidate as an evaluation tool for oral transmucosal products. This work demonstrates the potential of the novel bidirectional transmucosal apparatus for predicting the *in vivo* behavior of oral transmucosal products and will be employed further to identify relevant physiological and *in vitro* variables for optimization of the IVIVR for snus. The findings related to screening and identification of biorelevant variables using the bidirectional device are presented in Chapter 4.

## CHAPTER 4

### SCREENING AND SELECTION OF PHYSIOLOGICAL AND *IN VITRO* VARIABLES TO OPTIMIZE THE *IN VITRO IN VIVO* RELATIONSHIP (IVIVR) FOR SMOKELESS TOBACCO (SNUS) USING BIDIRECTIONAL TRANSMUCOSAL APPARATUS

#### 4.1 INTRODUCTION

The evaluation of drug products by dissolution/release/permeation testing during development is an established practice for both quality control and research purposes. Predictive dissolution testing as an evaluation tool through *in vitro in vivo* relationship (IVIVR) can save considerable resources and expedite the development of products (Emami 2006). Oral transmucosal products (OTPs) are currently evaluated using USP compendial and modified *in vitro* dissolution methods which may not be appropriate because these methods do not allow simulation of the unique physiological environment of the oral cavity to which the product is exposed, and hence may not be good predictors of the *in vivo* performance. There is therefore a need for biorelevant *in vitro* methods that facilitate the prediction of *in vivo* behavior of OTPs. This research was initiated to develop a biorelevant *in vitro* system that enables characterization of release and permeation of therapeutic and non-therapeutic substances from OTPs in a more realistic way.

In the previous Chapter (3), we developed a bidirectional transmucosal apparatus (BTA) that allowed simulation of the oral cavity and adjustment of *in vitro* variables for predicting the performance of OTPs. The BTA was tested for its suitability for the evaluation of OTPs using smokeless tobacco (snus) as a model product and by comparing its performance with that of the modified USP IV flow through apparatus and a vertical diffusion cell (VDC). The *in vitro* nicotine release rate obtained with the USP IV (0.171 mg/min) was faster than *in vivo* (0.036 mg/min); whereas, with the BTA (0.021 mg/min) and VDC (0.018 mg/min), *in vitro* nicotine permeation rates were slower. This suggested the need for adjustment of variables with the BTA and VDC to improve predictability of these devices for smokeless tobacco (snus). For this purpose, the BTA was selected because of the availability of more variables for adjustment and simulation in comparison to VDC. In the present research, we investigated the effect of physiological (stimulated saliva pH and stimulated salivary swallowing rate (SSSR)) and *in vitro* (receptor media flow rate, donor media flow rate, receptor media volume, receptor dead volume, media temperature, agitation) variables on nicotine release and permeation from snus using the BTA. It was speculated that a better understanding of the effect of variables on release/permeation characteristics can aid in the selection and application of these variables in optimization of the *in vitro in vivo* relationship (IVIVR) in order to improve predictability. The aim of the present study was to screen for relevant variables that might aid in improving the predictive performance of the BTA. It was important to screen variables to determine their relevance for further optimization experiments which otherwise would require substantial resources and time due to the large number of experiments required for studying significant and insignificant factors. This type of screening strategy is widely followed to select relevant variables for dissolution method development (Qiu et al. 2003).

## 4.2 MATERIALS AND METHODS

### 4.2.1 MATERIALS

Snus (a type of smokeless tobacco, non mentholated moist portion snus with natural flavor, Nicotine 8.0 mg, 1.0 g pouch) for *in vitro* studies was obtained from Old Virginia Tobacco Co., Richmond, VA, USA. Hanks' Balanced Salt (H-1387) and N-(2-Hydroxyethyl)piperazine-N'-(2-ethanesulfonic acid) (HEPES, 1M) buffer for the preparation of Hank's balanced salt solution (pH 7.4) were purchased from Sigma, St. Louis, MO, USA. Potassium phosphate monobasic (anhydrous) and sodium phosphate dibasic (anhydrous) to formulate artificial saliva of pH 6.8, 7.2 and 7.6 was obtained from Sigma, St. Louis, MO, USA. Sodium hydroxide and hydrochloric acid solution (10 N) for pH adjustment was purchased from Sigma, St. Louis, MO, USA. (-)-Nicotine hydrogen tartrate (working standard) for the assay was also purchased from Sigma, St. Louis, MO, USA. HPLC grade ammonium acetate and glacial acetic acid for the mobile phase preparation was purchased from Fisher Scientific, Fair Lawn, NJ, USA and EMD, Gibbstown, NJ, USA respectively. HPLC grade methanol was purchased from Honeywell Burdick and Jackson, Muskegon, MI, USA. Deionized water was obtained in-house (the Nanopure Diamond™, Barnstead, IO, USA). Regenerated cellulose membranes (SnakeSkin Dialysis Tubing, 10K MWCO, 35mm dry diameter (ID) × 10.7m) for *in vitro* permeation studies was obtained from Thermo Scientific, Rockford, IL, USA. Fluorinated ethylene propylene (FEP) and Tygon® platinized silicon tubing for the *in vitro* apparatus were purchased from Cole-Parmer, Vernon Hills, IL, USA. Teflon unions and luer fittings for tubing connections were bought from Upchurch Scientific, Oak Harbor, WA, USA. Masterflex L/S 12-channel 8-roller cartridge pump head (Model 7519-25) and variable-speed modular drive (Model 7553-70; 6 to 600 rpm; flow rate range:

0.0006 to 41 mL/min) for circulating media through the donor chamber was purchased from Cole-Parmer, Vernon Hills, IL, USA. Two variable medium flow mini pumps (Model 3386; flow rate range – 0.4 to 85 mL/min) for circulating media through receptors chambers were purchased from Control Company, Friendswood, TX, USA.

#### 4.2.2 SELECTION OF VARIABLES TO OPTIMIZE IVIVR FOR SMOKELESS TOBACCO

In results reported in Chapter 3, the *in vitro* nicotine permeation rate from snus obtained with the BTA after a lag time of 11.8 min was 0.021 mg/min which was slower than the *in vivo* nicotine absorption rate of 0.036 mg/min after a lag time of 7.5 min by approximately 42%. Similarly, the prediction error in the nicotine permeation rate with the vertical diffusion cell (VDC) was -50%. The *in vitro* nicotine permeation rate with the VDC was 0.018 mg/min after a lag time of 2.5 min. On the contrary, nicotine release with the USP IV flow through apparatus was five times faster than the *in vivo* absorption without any lag time at the rate of 0.171 mg/min. This observation with the USP IV can be attributed to the absence of a permeation barrier. This also indicates that the nicotine release rate cannot be used as a surrogate for the *in vivo* absorption rate and hence the USP IV device was not further evaluated. Of the permeation devices studied, the BTA provided more possibilities for the adjustment and simulation of variables to enhance the permeation rate when compared to the VDC as presented in Table 4.1. The BTA was therefore chosen over VDC in order to improve prediction of the *in vivo* performance of smokeless tobacco. Table 4.1 lists the physiological oral cavity and *in vitro* variables that were considered with the BTA set up in the present study for screening and identifying variables that significantly impact nicotine permeation rate.



**Table 4.1:** Possibilities of the simulation and adjustment of oral cavity physiological and *in vitro* variables with the bidirectional transmucosal apparatus (BTA) and vertical diffusion cell (VDC)

<b>Variables</b>	<b>BTA</b>	<b>VDC</b>
<b>Physiological variables</b>		
Stimulated saliva pH	Yes	Yes
Stimulated saliva secretion and swallowing rate	Yes	No*
<b><i>In vitro</i> variables</b>		
Receptor media flow rate	Yes	Yes
Donor media flow rate	Yes	No*
Receptor media volume	Yes	Yes
Receptor dead volume	Yes	Yes
Receptor and donor media temperature	Yes	No*
Agitation	Yes	No*

\* The donor chamber of VDC was too small for proper placement of snus and circulation of media to simulate secretion and swallowing rate, donor media flow rate and media temperature. In addition, agitation cannot be employed with the VDC attributed to the design of the donor chamber (Refer Figure C1 and C2 of Appendix C)

#### 4.2.2.1 ORAL CAVITY PHYSIOLOGICAL VARIABLES

Table 4.2 demonstrates the anticipated effect of physiological oral cavity variables on the nicotine permeation rate when the bidirectional apparatus is employed. Saliva pH is an important determining factor for nicotine absorption from smokeless tobacco (snus). The proportion of the un-ionized form of nicotine present in smokeless tobacco increases with an increase in saliva pH. The un-ionized form of nicotine permeates through the oral mucosal membrane more readily than the ionized counterpart and leads to faster nicotine absorption (Tomar et al. 1997; Chen et al. 1999). This effect of saliva pH on nicotine permeation cannot be observed in the bidirectional *in vitro* system unless an oral mucosal membrane was employed. However, it can be expected that an increase in saliva pH may enhance the release of nicotine from tobacco in the donor chamber by altering its miscibility/solubility (Nasr et al. 1998). This may result in an increase in the nicotine concentration gradient across donor and receptor chambers as a function of saliva pH and thus possibly increase the permeation rate. This increase in the permeation rate due to the gradient can be explained by Fick's Law of Diffusion (Martin et al. 1983). In a diffusion cell system comprising of donor and receptor compartments of cross sectional area  $S$ , separated by a membrane of thickness  $h$ , the steady state permeation after a lag time ( $dM/dt$ ) can be presented as below in Equation 4.1.

$$\frac{dM}{dt} = \frac{D S K (C_d - C_r)}{h} \text{----- (Eq 4.1)}$$

where,  $M$  is the drug mass permeated (mg) at time  $t$  (min),  $D$  is the diffusion coefficient ( $\text{cm}^2/\text{min}$ ) of drug through the membrane of thickness  $h$  (cm),  $S$  is the surface area of the membrane ( $\text{cm}^2$ ),  $K$  is the partition coefficient of drug between membrane and donor medium,  $C_d$  and  $C_r$  are drug

concentrations in donor and receptor media (mg/mL) respectively. Equation 4.1 can be reduced to Equation 4.2, assuming the sink condition is maintained in the receptor compartment.

$$\frac{dM}{dt} = \frac{D S K C_d}{h} \text{----- (Eq 4.2)}$$

On the basis of Equation 4.2, the mass of drug permeated in unit time ( $dM/dt$ ; permeation rate) is directly proportional to the drug concentration in the donor compartment, membrane surface area, drug diffusion coefficient, drug partition coefficient and is inversely proportional to the membrane thickness. The permeation rate will therefore be altered by factors which affect the above parameters. Hence, it was speculated that saliva pH may increase the permeation rate by enhancing nicotine release and concentration in the donor chamber of the bidirectional apparatus. An increase in the permeation rate, with increasing donor drug concentration has been reported in several studies (Michaels et al. 1975; Lestari et al. 2009).

Another important factor that can impact the bioavailability of drug from OTPs is swallowing the saliva. The product in the mouth stimulates saliva secretion and swallowing which may enhance drug release from the product and drug loss from the oral cavity, respectively (Navazesh et al. 1982; Kapila et al. 1984). The latter can reduce the bioavailability of drug due to pre-systemic metabolism of swallowed drug *in vivo*. A similar effect can be studied in the BTA by simulating stimulated saliva swallowing rate (SSSR) in the donor chamber in an open flow through pattern. The simulation of SSSR was expected to increase the release rate of nicotine from snus followed by the loss of nicotine from the donor chamber. In this set up, the latter may overcome the effect of an increase in release rate on permeation by a decrease in donor nicotine concentration and hence retarding the permeation rate (Equation 4.2).

#### 4.2.2.2 *IN VITRO* VARIABLES

Table 4.2 demonstrates the anticipated effect of *in vitro* variables on the nicotine permeation rate when the bidirectional apparatus is employed. Drug permeated in the receptor chambers through membrane from the donor chamber will appear faster in the reservoir with an increase in the receptor media flow rate; which may truly reflect the permeation process occurring in the receptors. In addition, a larger receptor media flow rate may be able to maintain a sink condition in the receptor compartments by removing permeated drug and resulting in improvement in the permeation rate based on Fick's Law. However, the latter phenomenon may be observed when receptor flows are maintained under open flow through conditions.

Donor media flow rate can also be explored as a potential variable to optimize IVIVR. Because the product is in contact with the donor media, any changes in the flow properties of donor fluid may affect the drug release characteristic from the product. An increase in the donor media flow rate may lead to the faster release of drug from the product due to media turbulence (Cammarn et al. 2000). The donor drug concentration may therefore rise with the donor media flow rate and consequently the permeation would be expected to be faster.

Receptor media volume is another important factor that can alter the permeation rate by an effect on drug concentration gradient across the receptor and donor chambers. Receptor dead volume, defined as the volume of tubing that connects the outlet of the apparatus to the reservoir, may also vary the permeation rate. A decrease in the permeation rate may be observed with an increase in the receptor dead volume in both closed and open flow conditions since drug permeated in the receptor compartments will need a longer time to appear in the reservoir where sampling is performed.

The above *in vitro* variables can also be coupled with media temperature for altering the permeation rate. The temperature rise can reduce the viscosity of donor and receptor media which may result in an increase in the diffusion coefficient of drug. This has been observed in research reported in the literature (Othmer et al. 1953; Hubley et al. 1996). This process is explained by the Stokes-Einstein equation (Edward 1970) displayed in Equation 4.3

$$D = \frac{k_B T}{6 \pi \eta r} \text{----- (Eq 4.3)}$$

where, D is the diffusion coefficient (cm<sup>2</sup>/s), k<sub>B</sub> is the Boltzmann constant (erg/°K), T is the absolute temperature (°K), η is the viscosity of the solvent (g/cm\*s), and r is the radius of the spherical particle (cm). As a consequence, the permeation rate may become faster due to an increase in the diffusion process with elevation in temperature based on the Fick's Law of Diffusion. In addition, the release rate may also increase based on the same reasoning. This can also result in increased donor drug concentration leading to a rise in permeation rate as per the Fick's Law.

Agitation/chewing of product in the mouth may enhance the release of drug which may contribute to the increase in availability of drug for absorption. In the bidirectional *in vitro* system, agitation can be incorporated to escalate the nicotine release rate and increase the concentration in the donor chamber, thus the permeation rate may be increased.

Oral cavity physiological and *in vitro* variables discussed above may alter the *in vitro* permeation rate of nicotine from smokeless tobacco (snus) when the BTA is used; based on the mechanisms explained earlier. The *in vitro* nicotine permeation rate achieved with the bidirectional apparatus in preliminary studies reported in Chapter 3 was not close to that of the *in vivo* absorption rate. Therefore, the above variables were selected to optimize IVIVR using the BTA for smokeless tobacco (snus). In addition, *in vitro* variables may also possess physiological relevance as depicted

in Table 4.2. Details about the simulation and adjustment of physiological and *in vitro* variables in the bidirectional apparatus are mentioned in Section 4.2.3.

**Table 4.2:** Anticipated effect of the increase in levels of oral cavity physiological and *in vitro* variables on the permeation rate of nicotine from smokeless tobacco (snus) using BTA

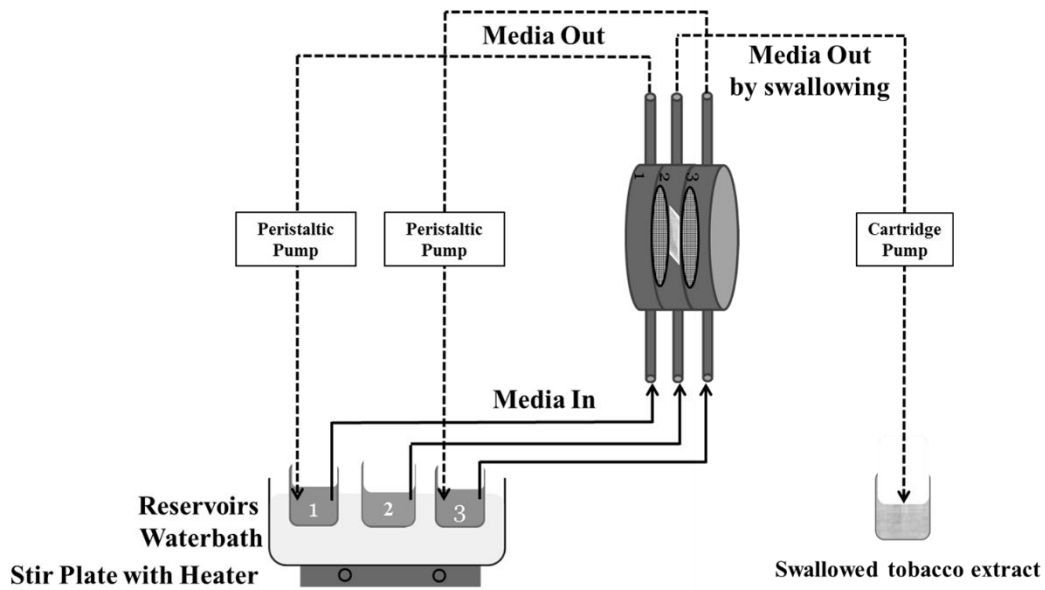
<b>Oral Cavity Physiological Variables</b>	<b>Effect on Permeation Rate</b>	<b>Physiological Relevance</b>
Saliva pH	↑	Effect on the nicotine form (ionized vs unionized) and permeation
Saliva secretion and swallowing rate	↓	Effect on nicotine release and loss due to the secretion and swallowing
<b><i>In Vitro</i> Variables</b>	<b>Effect on Permeation Rate</b>	<b>Physiological Relevance</b>
Receptor media flow rate	↑	Simulation of the effect of blood flow rate which may impact the systemic appearance of nicotine
Donor media flow rate	↑	Simulation of the effect of saliva flow on nicotine release from snus
Receptor media volume	↑	Simulation of the effect of gradient across oral mucosal membrane on nicotine permeation
Receptor dead volume	↓	May simulate the effect of damaged and undamaged oral mucosal membrane on nicotine permeation rate and lag time
Receptor and donor media temperature	↑	Simulation of the effect of body temperature on nicotine release and permeation
Agitation	↑	Simulation of the chewing effect on nicotine release


#### 4.2.3 *IN VITRO* RELEASE AND PERMEATION TESTING

The bidirectional transmucosal apparatus depicted in Figure 3.2(C) of Chapter 3 was used to assess nicotine release and permeation from smokeless tobacco (snus). Snus used in the study is described in Section 3.2.2. The *in vitro* set up employed similar assembly components (Silicon and FEP tubings, luer fitting and unions, reservoirs and regenerated cellulose membrane) and the set up as used previously in preliminary studies (Figure 3.2(C)). Artificial saliva and Hanks' balanced salt solution (HBSS) maintained at required temperature was used as the donor and receptor media respectively. Artificial saliva was circulated through the donor chamber of the BTA by using a cartridge pump (Masterflex L/S). Two separate peristaltic pumps were employed to circulate HBSS through each receptor chamber. The use of three separate pumps was necessary in order to maintain the different flow rates in chambers which was not possible with the single pump used previously. The apparatus was modified as required for simulating variables. In all cases, the media was circulated through all chambers in a closed through pattern except in experiments studying the effect of swallowing rate; where the donor chamber was maintained in an open through arrangement. The required receptor dead volume was simulated by adjusting the lengths of silicon and FEP tubing that connects the outlet of receptor chambers to the media reservoir. The water bath and donor and receptor reservoir media temperatures were maintained at a higher level to achieve the required temperature in the chambers for the temperature study. Temperature studies were performed at large receptor media flow rates to maintain the required temperature in the chamber which provided less time for the media to lose heat during circulation. The chamber temperature was measured with an infra-red (IR) thermometer. The bidirectional *in vitro* system with the modified set up is pictorially represented in Figure 4.1. All experiments were performed in a single sequential pattern in which only one variable was changed at a time and all other



variables were kept constant (Walters 1991). Donor and receptor media were sampled from respective reservoirs to assess nicotine release and permeation. One ml of media was sampled at 0, 2.5, 5, 7.5, 10, 15, 20, 25, 30, 45 and 60 min and was replaced with an equivalent volume of fresh media. The detailed experimental conditions with each of the physiological and *in vitro* variable studies is presented in Table 4.3 and 4.4 respectively. Each experiment was performed either three or five times for statistical analysis. Samples from donor and receptor reservoirs were analyzed for nicotine release and permeation by a validated reverse-phase HPLC method reported in Chapter 2. The HPLC method employed a Waters 600E multisolvent delivery system with a Waters 717 auto-sampler and 996 Waters PDA detector. Nicotine permeated into both receptor chambers of the BTA was added to represent the total permeation achieved at each time point. The method for calculation of the amount of nicotine permeated and released from snus in the BTA is shown in Table C4 of Appendix C



Reservoir 1 & 3: HBSS pH 7.4      Chambers 1 and 3: Receptors       : Artificial Membrane  
 Reservoir 2: Artificial saliva pH 7.2      Chamber 2: Donor

**Figure 4.1:** Bidirectional transmucosal apparatus assembly; donor chamber maintained in an open flow pattern for studying the effects of swallowing on permeation; three separate pumps were employed to maintain different flow rates in donor and receptor chambers. [Figure not to scale]

The effect of saliva pH was studied only on the nicotine release properties by circulating artificial saliva in the donor chamber of BTA; whereas, the HBSS was not circulated in the receptor chambers (the inlets and outlets of receptors were sealed by the use of parafilm). The effect of saliva pH on permeation was anticipated only if there was an effect of pH on nicotine release. Nicotine permeation as a function of saliva pH would be studied only if a significant effect of pH on nicotine release was obtained. Forty microliters of artificial saliva was sampled from the donor reservoir at 0, 2.5, 5, 7.5, 10, 15, 20, 25, 30, 45 and 60 min and was replaced with an equivalent volume of fresh artificial saliva. Artificial saliva samples (15 to 60 min) obtained from the pH studies were diluted twenty five times with the HBSS buffer to perform nicotine analysis within the validated HPLC calibration range as these samples contained high concentration of nicotine. The effect of donor media flow rate on nicotine release in addition to permeation from snus was studied in a separate experiment without circulating receptor media (the inlets and outlets of receptors were sealed by the use of parafilm). The method of sample collection and dilution in the donor media flow rate study was similar to that of the saliva pH release experiments. Artificial saliva (pH 7.2) samples from the donor flow rate study were diluted twenty five times with the HBSS buffer due to the same reason explained above.

**Table 4.3:** Conditions for experiments employing oral cavity physiological variables in the bidirectional transmucosal apparatus\*

Experiment	Levels	N	Donor media (Artificial Saliva)	Receptor media (HBSS buffer)	Donor media flow rate (mL/min)	Receptor media flow rate (mL/min)	Donor dead volume	Receptor dead volume	Donor flow through pattern	Receptor flow through pattern	Agitation	Water bath Temp. (°C)	Reservoir media temp. (°C)	Chamber media temp. (°C)
Stimulated saliva pH (Buffer capacity, $\beta$ mM/L*pH unit)	6.8 (5.5)	3	pH 6.8 $\beta = 5.5$	pH 7.4	1	1	2.67	2.67	Closed	Closed	No	40	37	NM
	7.2 (7.0)	3	pH 7.2 $\beta = 7.0$	pH 7.4	1	1	2.67	2.67	Closed	Closed	No	40	37	NM
	7.6 (9.6)	3	pH 7.6 $\beta = 9.6$	pH 7.4	1	1	2.67	2.67	Closed	Closed	No	40	37	NM
Stimulated saliva swallowing rate (mL/min)	0.32	5	pH 7.2 $\beta = 7.0$	pH 7.4	<b>0.32</b>	6	2.67	2.67	<b>Open</b>	Closed	No	40	37	NM
	1.66	5	pH 7.2 $\beta = 7.0$	pH 7.4	<b>1.66</b>	6	2.67	2.67	<b>Open</b>	Closed	No	40	37	NM
	3	5	pH 7.2 $\beta = 7.0$	pH 7.4	<b>3</b>	6	2.67	2.67	<b>Open</b>	Closed	No	40	37	NM

\* The donor and receptor media volume in all experiments was 25 mL

NM: Not measured

**Table 4.4:** Conditions for experiments employing *in vitro* variables in the bidirectional transmucosal apparatus\*

Experiment	Levels	N	Donor media flow rate (mL/min)	Receptor media flow rate (mL/min)	Donor reservoir media volume	Receptor reservoir media volume	Donor dead volume	Receptor dead volume	Donor flow through pattern	Receptor flow through pattern	Agitation	Water bath temp. (°C)	Reservoir media temp. (°C)	Chamber media temp. (°C)
Receptor media flow rate (mL/min)	1	3	1	<b>1</b>	25	25	2.67	2.67	Closed	Closed	No	40	37	NM
	6	3	1	<b>6</b>	25	25	2.67	2.67	Closed	Closed	No	40	37	NM
	16	3	1	<b>16</b>	25	25	2.67	2.67	Closed	Closed	No	40	37	NM
Donor media flow rate (mL/min)	1.66	5	<b>1.66</b>	6	25	25	2.67	2.67	Closed	Closed	No	40	37	NM
	6	5	<b>6</b>	6	25	25	2.67	2.67	Closed	Closed	No	40	37	NM
	16	5	<b>16</b>	6	25	25	2.67	2.67	Closed	Closed	No	40	37	NM
Receptor to donor media volume ratio	2	3	1	1	25	<b>25</b>	2.67	2.67	Closed	Closed	No	40	37	NM
	4	3	1	1	25	<b>50</b>	2.67	2.67	Closed	Closed	No	40	37	NM
	8	3	1	1	25	<b>100</b>	2.67	2.67	Closed	Closed	No	40	37	NM
Receptor dead volume (mL)	2.67	5	1	1	25	25	2.67	<b>2.67</b>	Closed	Closed	No	40	37	NM
	5.15	5	1	1	25	25	2.67	<b>5.15</b>	Closed	Closed	No	40	37	NM
	10	5	1	1	25	25	2.67	<b>10</b>	Closed	Closed	No	40	37	NM
Receptor and donor media temperature (°C)	25	5	1.66	16	25	25	2.67	2.67	Closed	Closed	No	RT	RT	<b>RT</b>
	37	5	1.66	16	25	25	2.67	2.67	Closed	Closed	No	45-46	40-42	<b>33-37</b>
	45	5	1.66	16	25	25	2.67	2.67	Closed	Closed	No	59-60	50-53	<b>38-45</b>
Agitation	No	5	1	1	25	25	2.67	2.67	Closed	Closed	<b>No</b>	40	37	NM
	Yes	5	1	1	25	25	2.67	2.67	Closed	Closed	<b>1/min</b>	40	37	NM

\* Artificial saliva (pH 7.2,  $\beta$  7.0) and HBSS buffer (pH 7.4) was employed as the donor and receptor media respectively

NM: Not measured; RT: Room temperature

Table 4.3 and 4.4 displays the levels at which all variables were studied. Each variable was explored at three levels to determine the useful optimization range except in the case of agitation. In addition, three levels were studied to identify any non-linearity in release and permeation if existed as a function of the variable studied. The mid-level of stimulated saliva pH (7.2) and secretion rate (1.66 mL/min) were selected for the study because they have been observed as mean values in the normal adult population (Bardow et al. 2000). The lower (L) and upper (U) levels of stimulated pH (L = 6.8, U = 7.6) and secretion rate (L = 0.32 mL/min, U = 3 mL/min) were based on  $\pm 2 \times$  standard deviations (SD) reported for each of the variables in the Bardow, Moe et al. 2000 study. The stimulated salivary secretion and swallowing rate were assumed to be equal based on findings that the swallowing rate is directly influenced by the secretion rate (Kapila et al. 1984). Artificial saliva employed for the study also simulated *in vivo* saliva buffer capacity ( $\beta$ ), in addition to pH as this would be a deciding factor for the resultant pH after the exposure of the saliva to snus during the experiment, as well as *in vivo* use. The mean (7.0 mM/L/pH unit),  $-2 \times$ sd (5.5 mM/L/pH unit) and  $+2 \times$ sd (9.6 mM/L/pH unit) stimulated saliva buffer capacity reported graphically in the Bardow, Moe et al. 2000 study corresponded to the mean (7.2),  $-2 \times$ sd (6.8), and  $+2 \times$ sd (7.6) stimulated saliva pH. Three artificial saliva solutions with different pHs and buffer capacities were prepared using anhydrous monobasic potassium dihydrogen phosphate ( $\text{KH}_2\text{PO}_4$ ) and anhydrous dibasic sodium hydrogen phosphate ( $\text{Na}_2\text{HPO}_4$ ). The amount of  $\text{KH}_2\text{PO}_4$  and  $\text{Na}_2\text{HPO}_4$  required to formulate saliva of specific pH and buffer capacities were experimentally determined and are described below. The required amount of  $\text{KH}_2\text{PO}_4$  and  $\text{Na}_2\text{HPO}_4$  listed in Table 4.5 were dissolved in 1000 mL of deionized water to make artificial saliva of pH 6.8 ( $\beta = 5.5$ ), 7.2 ( $\beta = 7.0$ ) and 7.4 ( $\beta = 9.6$ ). The pH was adjusted using 1 M NaOH or 1 M HCl solution in deionized water when required.

For the preparation of artificial saliva solutions, Van Slyke's Buffer Equation presented in Equation 4.4 was used to calculate the required buffer concentration (represents the total concentration of both  $\text{KH}_2\text{PO}_4$  and  $\text{Na}_2\text{HPO}_4$ ) to obtain the required pH and buffer capacity.

$$\beta = \frac{2.303 * C * K_a * [H^+]}{[K_a + [H^+]]^2} \text{----- (Eq 4.4)}$$

4.4)

where,  $\beta$  is the buffer capacity (mM/L\*pH unit), C is the total buffer concentration (mM/L),  $K_a$  is the acid dissociation constant and  $[H^+]$  is the hydrogen ion concentration. The total buffer concentration required for formulating artificial saliva of specific pH and buffer capacity is presented in Table 4.5. For the experimental determination of the amount of  $\text{KH}_2\text{PO}_4$  and  $\text{Na}_2\text{HPO}_4$  required, a solution containing both salts of equal required total buffer concentrations were made and mixed in different volumes. The mass of each salt was recorded that provided the required pH. The amount of  $\text{KH}_2\text{PO}_4$  and  $\text{Na}_2\text{HPO}_4$  to prepare 1000 mL of artificial saliva of the required pH was calculated based on the volumes and concentration of the salt solution added. This was performed for each stimulated saliva pH and buffer capacity level.

**Table 4.5:** Artificial saliva preparation

pH	Buffer Capacity ( $\beta$ ) (mM/L/pH unit)	Concentration Of Buffer (mM/L)*	$\text{KH}_2\text{PO}_4$ for 1000 mL (g)	$\text{Na}_2\text{HPO}_4$ for 1000 mL (g)
6.8	5.5	11.73	1.0159	0.6055
7.2	7.0	12.16	0.7355	0.9590
7.6	9.6	20.45	0.5566	2.3225

\* Buffer concentration calculated using Van Slyke's Equation;  $H^+$  was calculated from  $\text{pH} = -\log [H^+]$ ; The acid dissociation constant of  $K_a$  of  $\text{H}_2\text{PO}_4^-$  [ $\text{KH}_2\text{PO}_4$ ] is  $6.3 \times 10^{-8}$

Receptor and donor media flow rate ranges incorporated in single sequential experiments for the study of effects on permeation were the usual flow rates employed with the compendial USP IV dissolution apparatus. There was no restriction in the selection of receptor and donor media volumes as nicotine is known to be water miscible in any proportion below 60 °C (Davies et al. 2000). Therefore, the selection of media volume in any range was not expected to affect sink conditions during the study. For permeation studies, 25 mL of artificial saliva was employed in experiments to be performed using the closed flow through pattern, whereas, in experiments using the open flow pattern (i.e., swallowing rate experiments), the donor reservoir was filled with sufficient volume of artificial saliva that would last during the experiment, calculated based on the donor media flow rate. For investigation of the media volume as a variable, 25, 50 and 100 mL of the HBSS was employed in each receptor reservoir that provided a total of 50, 100 and 200 mL of receptor media. For ease of data analysis, these values were presented as the ratio of the total volume of receptor media to that of the donor media (Media volume ratio of 2, 4 and 8). The receptor dead volume levels and agitation frequency were selected based on the practicality of the experiments. Details on the dimensions and types of tubing for the simulation of dead volume is shown in Tables C1, C2 and C3 of Appendix C. Temperature studies were performed at room temperature (25 °C), body temperature (37 °C) and one level higher (45 °C). The highest temperature level that can be selected for nicotine permeation studies with the present bidirectional apparatus was 45 °C which required maintenance of 55 °C in the reservoir. The temperature 55 °C is close to the lower consolute temperature (60 °C, nicotine-water mixture system) of nicotine (Davies et al. 2000) above which, sink condition may not be maintained due to immiscibility of nicotine in water. The water bath and reservoir media were maintained at the temperatures summarized in Table 4.4 to obtain the required chamber temperature.



#### 4.2.4 APPARATUS FOR AGITATION STUDY

An apparatus with flexible walls for the receptor was built for the agitation study. It was built with the same design and dimensions as described in Chapter 3 with minor differences. The receptor chambers of the agitation apparatus were 0.8 cm in height instead of 0.6 cm in the previous design. The outer walls of receptors was a flexible plastic material (Silicone rubber, 0.031" thick, 50 Duro, Translucent) instead of solid polymethyl methacrylate (PMMA). The flexible material was held between the hollow cylindrical receptors and a plate. The receptor, the plastic wall and the plate was stacked and immobilized with the help of screws. Figure 4.2 is the pictorial representation of the components of agitation apparatus (Refer Figure C3 for other views of the apparatus). Agitation can be manually performed by applying pressure on the walls with a beaker of diameter 3 cm smaller than that of flexible walls (4 cm). The effect of agitation was studied at two levels – with and without agitation. Agitation was performed manually at a frequency of 1 agitation/min.

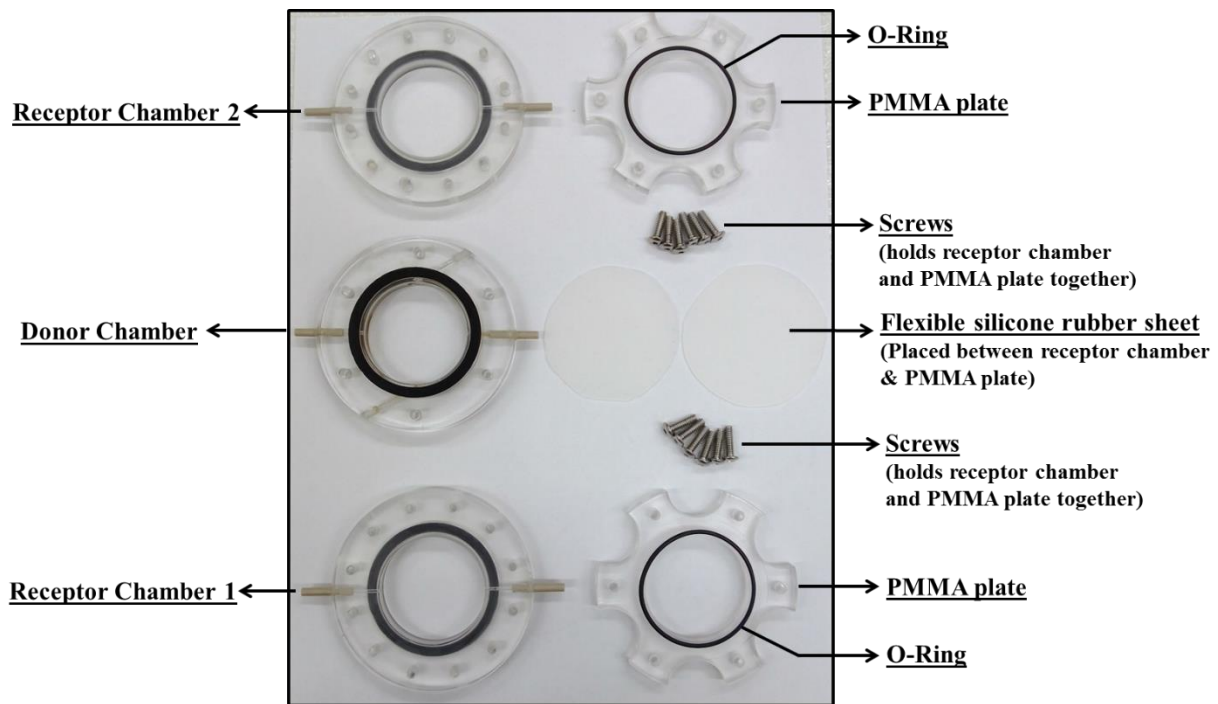


**Figure 4.2:** Components of the bidirectional transmucosal apparatus for agitation study

#### 4.2.5 EFFECT OF SNUS ON SALIVA pH

The effect of snus on saliva pH was studied in a beaker in order to mechanistically understand the results obtained from nicotine release experiments as a function of saliva pH. It can be expected that the buffer components present in snus may change the pH of artificial saliva during an experiment; therefore, the results and interpretation from studies on nicotine release may not be attributed to saliva pH. In order to study the effect of snus on saliva pH, a single smokeless tobacco (snus) pouch was exposed to 2 (volume close to the stimulated saliva volume in oral cavity), 10 (volume of chamber) and 25 (media volume used for *in vitro* nicotine release study) mL of artificial saliva in a glass beaker and was sonicated for 2 min at the room temperature. The volume of 2 mL is very close to the reported 1 mL of the stimulated saliva volume (Lagerlof et al. 1984). Two mL was employed for the study to completely wet the snus. The snus was removed after 2 min and pH was measured using a calibrated pH meter. This experiment was performed at all three levels of artificial saliva pH and buffer capacity in replicates of three. A change in artificial saliva pH was calculated with respect to the pH measured before exposure of saliva to the snus.

#### 4.2.6 DATA ANALYSIS

The steady state nicotine release/permeation rate (rate after lag time) was obtained from the nicotine released/permeated (mg) versus time (min) plot. The nicotine release/permeation rate (mg/min) was obtained from the slope of the line equation fitted to the linear portion of the profile. The lag time (min) was calculated as the X-intercept from the linear fit equation. Nicotine release/permeation rate and lag time was plotted versus the levels of each variable. Statistical analysis of the effect of oral cavity physiological and *in vitro* variables on the nicotine

release/permeation rates and lag time was performed using a one-way analysis of variance (ANOVA) at alpha,  $\alpha = 0.05$ . Equal variance ANOVA was performed when data showed a normal distribution and equal variances. In cases of unequal variances, Welch ANOVA was performed. Post hoc Tukey's Honest Significant Difference (HSD) test was used to compare the effect among the individual levels of variables. A student t-test ( $\alpha = 0.05$ ) was performed to compare the nicotine permeation rate and lag time between experiments with and without agitation. The physiological and *in vitro* variables that show a statistically significant effect on the permeation rate will be selected for further optimization of IVIVR. All statistical analysis were performed in JMP 8.

### **4.3 RESULTS AND DISCUSSION**

#### **4.3.1 EFFECT OF ORAL CAVITY PHYSIOLOGICAL VARIABLES ON NICOTINE RELEASE/PERMEATION**

A comparison of the nicotine release profiles and release rates obtained at three saliva pHs is displayed in Figures 4.3(A) and 4.3(B) respectively. The amount of nicotine released over time and the release rates obtained at three saliva pH levels are shown in Table C5-C7 of Appendix C. A significant effect of saliva pH on nicotine release was not obtained (Table 4.6). A possible reason for the above observation can be attributed to the buffer components present in snus. The buffer components of snus may result in saliva-snus mixture of higher buffer capacity in comparison to the artificial saliva. The higher buffer capacity may be required to maintain the pH that allows a greater extent of nicotine permeation at faster rate when snus is placed in the oral cavity. The pH of snus therefore may dominate the saliva pH. A similar effect can be expected across all three levels of artificial saliva pH. Therefore, the resultant pH after exposure of snus to saliva may be

similar in all three cases. This may justify the similarity in the nicotine release profiles obtained at all pH levels. In order to confirm the above speculation, the effect of snus on saliva pH was studied in a beaker set up described in section 4.2.5. The change in pH observed at three levels of saliva pH and buffer capacity due to snus is presented in Table C8 of Appendix C and illustrated graphically in Figure 4.4. The change in pH at 10 and 25 mL was closer to zero when compared to 2 mL in all cases of artificial saliva pH 6.8 ( $\beta = 5.5$ ), 7.2 ( $\beta = 7.0$ ) and 7.6 ( $\beta = 9.6$ ). This indicates that the buffer components present in snus are diluted at larger volumes which reduces the buffer capacity and the resultant pH is closer to the pH of saliva. During the use of smokeless tobacco as well as in an *in vitro* system, pH due to the buffer components present in snus dominates at smaller volumes of saliva. This observation agrees with that reported in the literature (Ciolino et al. 2001). Buffers are added to smokeless tobacco to maintain higher pH for transformation of nicotine to the unionized form for greater permeation. The pH of 8.1 obtained after exposure of snus to 10 mL of water and sonication for 2 min supports the above statement. In the BTA, the donor chamber volume is 10 mL and in this apparatus pH will be closer to saliva pH as confirmed from the beaker study. However, at 10 mL, the resultant pH range of saliva across three levels was too narrow to produce any substantial increase in the solubility/miscibility of nicotine in the donor chamber. Therefore, a significant effect of saliva pH on the nicotine release was not obtained.

The amount of nicotine permeated (mg) versus time (min) data and a plot at the physiological range of stimulated saliva swallowing rate (SSSR) is shown in Tables C9-C11 of Appendix C and Figure 4.5(A) respectively. There was a significant effect of swallowing on the nicotine permeation rate (Table 4.6 and Figure 4.5(B)). The permeation rate at 0.32 mL/min was significantly faster than at 1.66 and 3 mL/min (Tukey's post hoc test). There was a decrease in the nicotine permeation rate with an increase in swallowing. Because of swallowing, nicotine released

in the donor chamber was removed. The nicotine removal rate from the donor chamber was faster with the increase in swallowing which resulted in a reduction in donor nicotine concentration ( $C_d$ ). As a consequence, there was a decrease in the nicotine permeation rate according to Fick's Law (Section 4.2.2.1, Equation 4.2). The stimulated saliva swallowing rate is a potential variable that can be used to optimize IVIVR for smokeless tobacco (snus) due to its impact on the nicotine permeation rate.

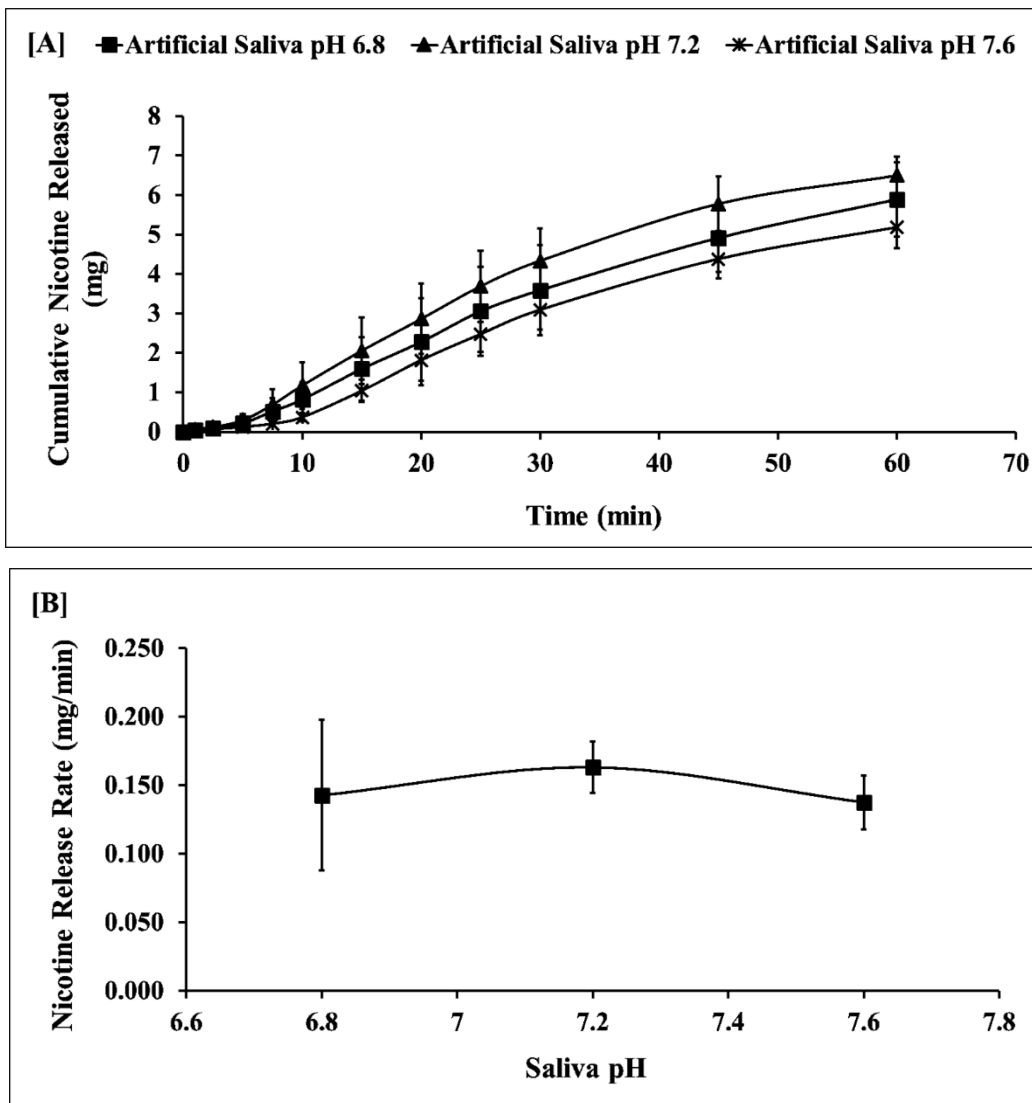


**Figure 4.3:** The mean cumulative nicotine release at three saliva pH levels; **[A]** The mean cumulative nicotine release time profile at three saliva pH levels; the line was fitted to the linear portion of the profile;  $Y=0.1428*X-0.5483$ ,  $R^2=0.99$  (Saliva pH 6.8);  $Y=0.1631*X-0.4547$ ,  $R^2=0.99$  (Saliva pH 7.2);  $Y=0.1376-0.9906$ ,  $R^2=0.99$  (Saliva pH 7.6); **[B]** The mean release rates at three saliva pH levels. (Error bars represent one standard deviation;  $n=3$ )

**Table 4.6:** Nicotine release/permeation rate from snus as a function of physiological variables

	Level	N	Release/Permeation Rate (mg/min)			Statistical Test	Statistical Results
			Mean	SD	%RSD		
Artificial saliva	pH 6.8 ( $\beta$ 5.5)	3	0.14	0.06	38.45	Unequal variance ANOVA	F(2,4)=1.15; p-value=0.409; Not significant
	pH 7.2 ( $\beta$ 7.0)	3	0.16	0.02	11.51		
	pH 7.6 ( $\beta$ 9.6)	3	0.14	0.02	14.22		
Stimulated saliva swallowing rate (SSSR) (mL/min)	0.32	5	0.03*	0.01	20.91	Equal variance ANOVA	F(2,12)=8.92; p-value=0.006; Significant
	1.66	5	0.017	0.004	21.06		
	3	5	0.016	0.003	20.41		

\* Nicotine permeation rate was significantly faster at 0.32 mL/min compared to 1.66 and 3 mL/min

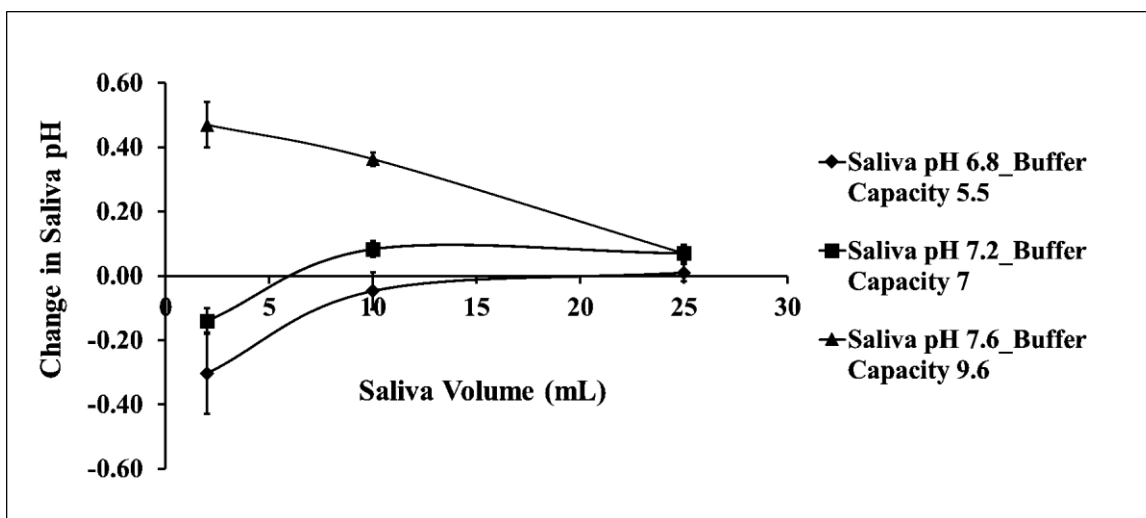


**Figure 4.4:** Effect of snus on saliva pH at different volumes of saliva.



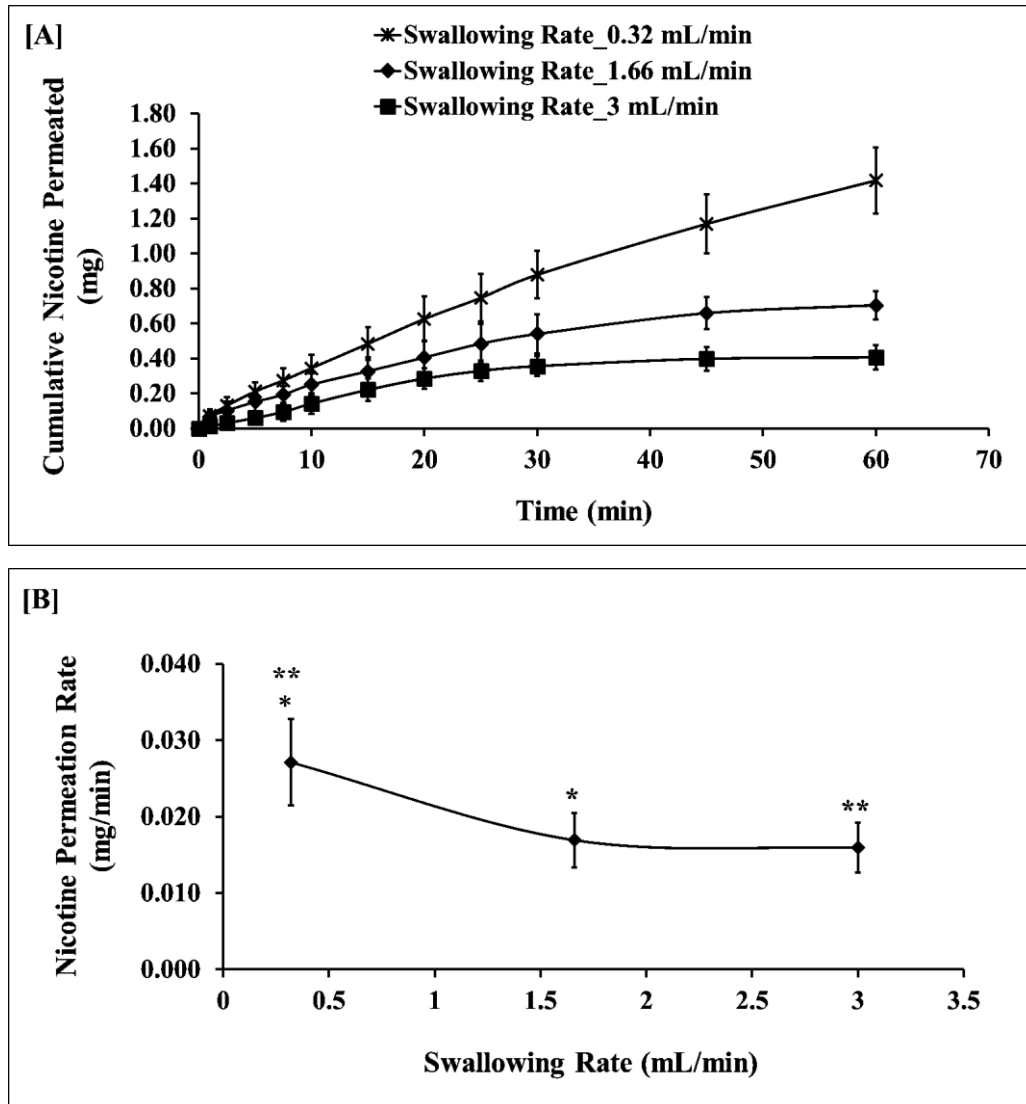


**Figure 4.5:** The mean cumulative nicotine permeation at three stimulated saliva swallowing rate; **[A]** The mean cumulative nicotine permeation time profile at three stimulated saliva swallowing rate levels; the line was fitted to the linear portion of the profile;  $Y=0.0271 \cdot X+0.0717$ ,  $R^2=0.99$  (Swallowing rate 0.32 mL/min);  $Y=0.0169 \cdot X+0.068$ ,  $R^2=0.99$  (Swallowing rate 1.66 mL/min);  $Y=0.015-0.0117$ ,  $R^2=0.99$  (Swallowing rate 3 mL/min); **[B]** The mean permeation rates at three stimulated saliva swallowing rate levels; \* & \*\* the permeation rate at 0.32 mL/min was significantly faster than at 1.66 and 3 mL/min. (Error bars represent one standard deviation; n=5)

#### 4.3.2 EFFECT OF *IN VITRO* VARIABLES ON NICOTINE RELEASE/PERMEATION

The release/permeation rates obtained from experiments utilizing the *in vitro* variables are tabulated in Table 4.7. The mean *in vitro* nicotine permeation profiles obtained from experiments with receptor media flow rates are shown in Figure 4.6(A). The amount of nicotine permeated over time in replicate studies of receptor media flow rate at all levels is represented in Tables C12-C14 of Appendix C. The receptor flow rate did not produce a significant effect on nicotine permeation rate (Table 4.7). However, there was a significant effect of the receptor media flow rate on nicotine permeation lag time (Figure 4.6(B)). An increase in the receptor media flow rate led to the faster appearance of permeated nicotine from the receptors to media reservoirs and hence reduced the permeation lag time. However, the decrease in permeation lag time saturated at higher receptor media flow rates. This nonlinearity in the permeation lag time can be related to the larger effect of lower receptor media flow rate and smaller effect of higher receptor media flow rates on permeation lag time at the receptor dead volume of 2.67 mL.

The *in vitro* permeation profiles, release profiles and release rates as a function of donor media flow rate are shown in Figures 4.7(A), 4.7(B) and 4.7(C) respectively. The amount of nicotine permeated and released over time as a function of the donor media flow rate are shown in Tables C15-C17 and C18-C20 of Appendix C respectively. The effect of donor media flow rate on nicotine release was studied separately without circulation of the receptor media. The nicotine release rate at the donor media flow rate of 1.66 mL/min was significantly slower than that obtained with 6 and 16 mL/min (Figure 4.7(C)). An increase in the donor media flow rate resulted in the faster release rate; however a similar effect on permeation (Table 4.7) was not obtained as anticipated. In spite of the increase in release rate, nicotine released in the donor chamber remained for a shorter time in the donor chamber with an increase in donor media flow rate, regardless of

the flow pattern (closed vs open). In addition, there might be a decrease in nicotine concentration in the donor chamber due to dilution with the increase in donor media flow rate. The former and latter explanations provide a rationale for the absence of an effect of donor media flow rate on nicotine permeation.

The *in vitro* nicotine permeation profiles obtained as a function of receptor to donor media volume ratio are displayed in Figure 4.8. The amount of nicotine permeated in individual experiments at all levels of media volume are presented in Tables C21-C23 of Appendix C respectively. A significant effect of receptor media volume on permeation rate (Table 4.7) was not observed. This is likely because the media volume was altered by increasing the volume in the reservoir without any change in the volume of the chambers. The size of the chambers of the apparatus remained the same at all levels of media volume. Because of this, the nicotine concentration gradient across donor and receptor compartments remained the same and the effect of volume on permeation rate was not obtained as expected. This explains the absence of an effect of media volume on permeation. The effect of donor in place of receptor media volume on the concentration gradient across the chambers of BTA could be considered for the optimization of IVIVR.

**Table 4.7:** Nicotine release/permeation rate from snus as a function of *in vitro* variables

	Level	N	Release/Permeation Rate (mg/min)			Statistical Test	Statistical Results
			Mean	SD	%RSD		
Receptor media flow rate (mL/min)	1	3	0.022	0.001	3.38	Equal variance ANOVA	F(2,6)=0.70; p-value=0.533; Not significant
	6	3	0.021	0.002	11.98		
	16	3	0.022	0.0002	0.78		
Donor media flow rate (mL/min)**	1.66	5	0.024	0.001	4.25	Equal variance ANOVA	F(2,12)=3.21; p-value=0.077; Not significant
	6	5	0.027	0.002	8.18		
	16	5	0.027	0.003	9.36		
Donor media flow rate (mL/min)*	1.66	5	0.123	0.020	16.46	Unequal variance ANOVA	F(2,7)=90.91; p-value<0.05; Significant
	6	5	0.274	0.072	26.32		
	16	5	0.334	0.027	8.13		
Receptor to donor media volume ratio	2	3	0.026	0.001	5.51	Equal variance ANOVA	F(2,6)=2.66; p-value=0.149; Not significant
	4	3	0.022	0.002	8.48		
	8	3	0.025	0.003	11.49		
Receptor dead volume (mL)#	2.67	5	0.040	0.004	10.26	Equal variance ANOVA	F(2,12)=5.34; p-value<0.05; Significant
	5.15	5	0.030	0.007	24.45		
	10	5	0.032	0.004	13.10		
Receptor and donor media temperature (°C)^	25	5	0.022	0.002	11.30	Unequal variance ANOVA	F(2,7)=75.07; p-value<0.05; Significant
	37	5	0.038	0.002	5.46		
	45	5	0.045	0.005	11.08		
Agitation\$	No	5	0.036	0.005	13.50	Equal variance t- test	t=2.62;df=8;p- value<0.05; Significant
	Yes	5	0.027	0.006	22.94		

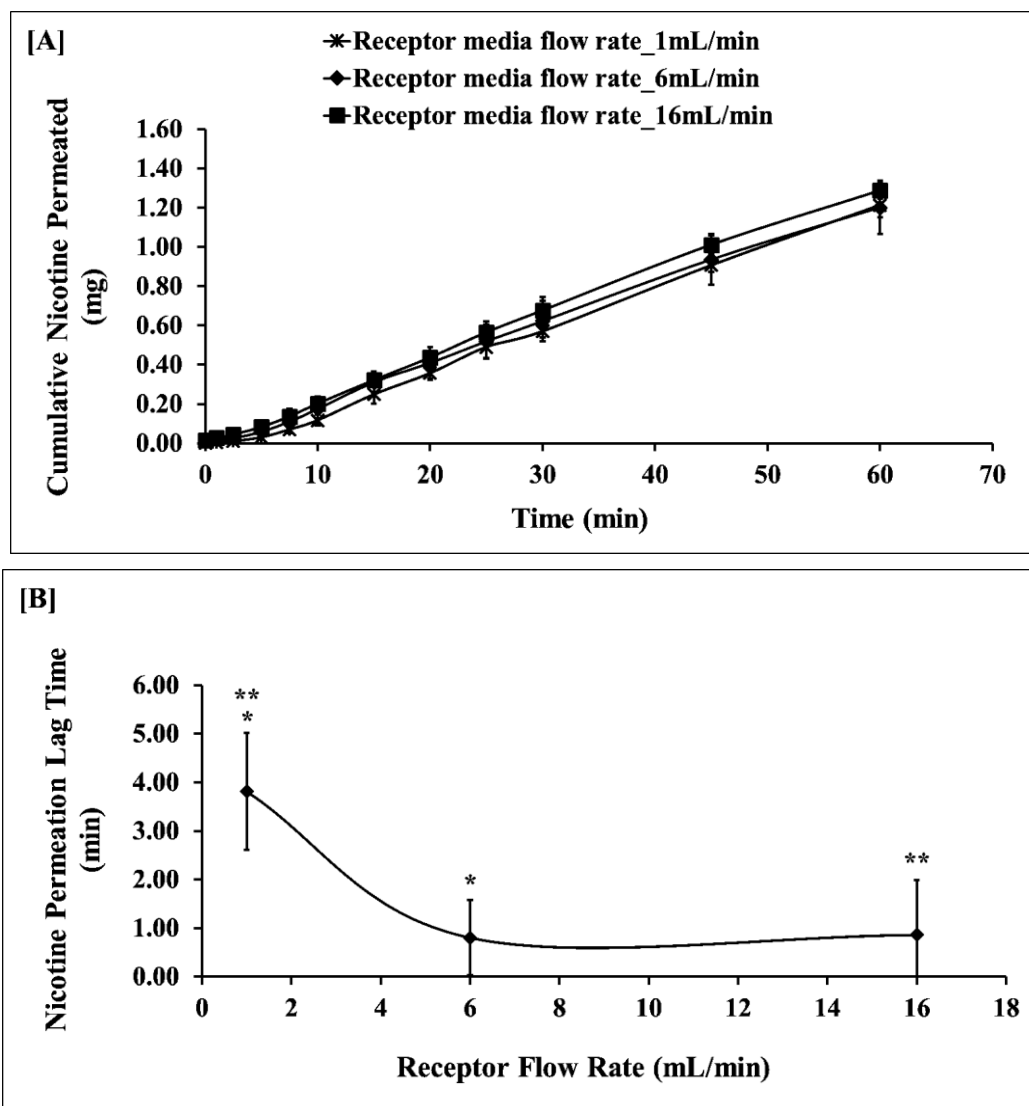
\*\* Data represents nicotine permeation rate.

\* Data represents nicotine release rate. Nicotine release rate was significantly slower at 1.66 mL/min donor media flow rate compared to 6 and 16 mL/min

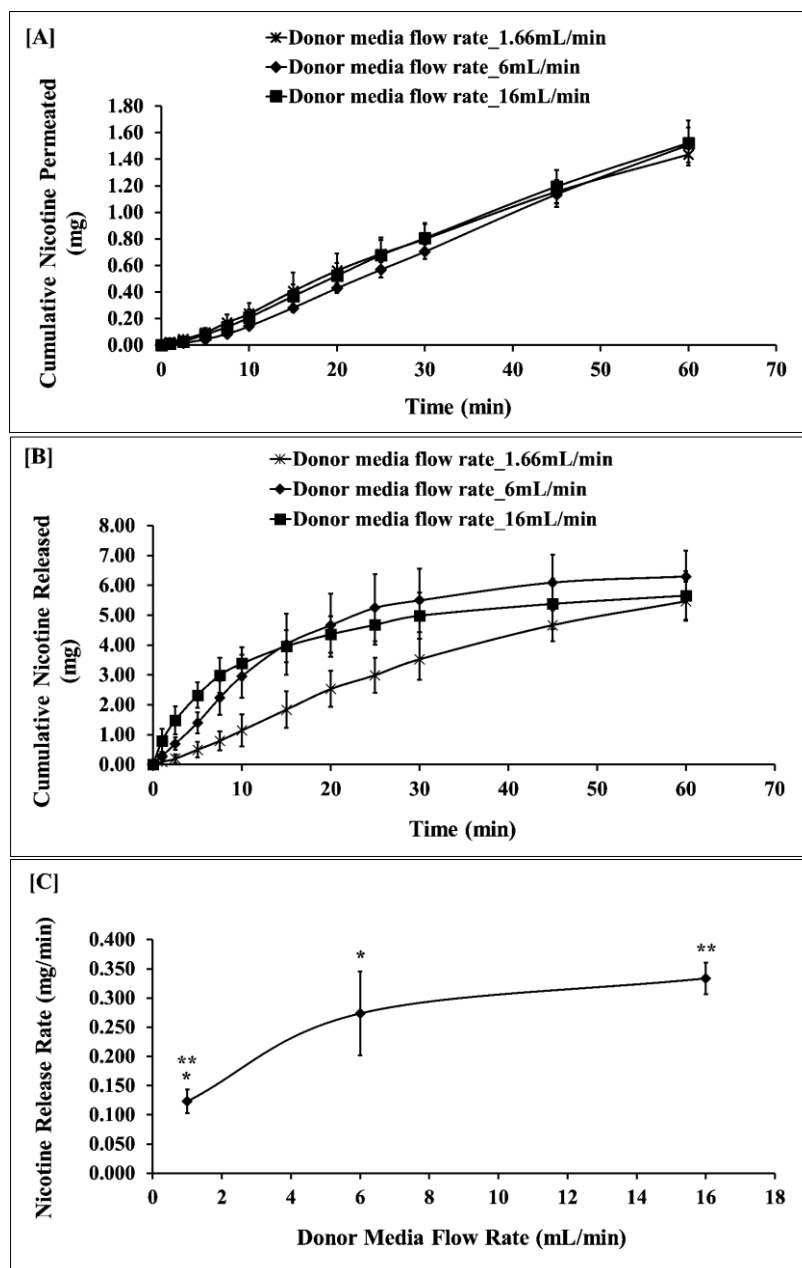
# Nicotine permeation rate was significantly faster at 2.67 mL compared to 5.15 mL

^ Nicotine permeation rate was significantly different from one another

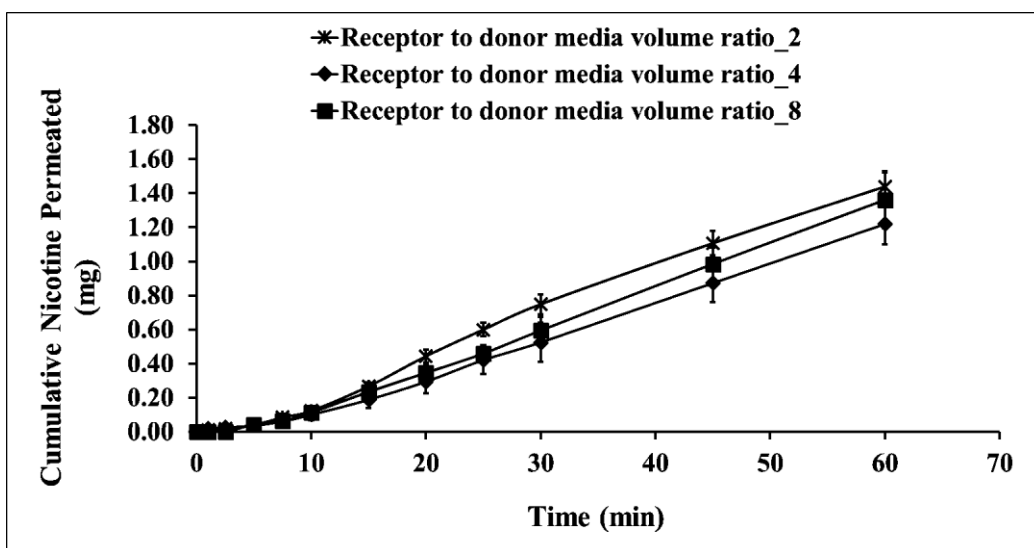
\$ Nicotine permeation rate was significantly faster “without agitation” compared to that “with agitation”



**Figure 4.6:** The mean cumulative nicotine permeation at three receptor media flow rates; **[A]** The mean cumulative nicotine permeation time profile at three receptor media flow rate levels; the line was fitted to the linear portion of the profile;  $Y=0.0219*X-0.083$ ,  $R^2=0.99$  (Receptor media flow rate 1 mL/min);  $Y=0.0208*X-0.0159$ ,  $R^2=0.99$  (Receptor media flow rate 6 mL/min);  $Y=0.0221-0.0073$ ,  $R^2=0.99$  (Receptor media flow rate 16 mL/min); **[B]** The mean permeation lag time at three receptor media flow rate levels; \* & \*\* the permeation lag time at 1 mL/min was significantly longer than at 6 and 16 mL/min. (Error bars represent one standard deviation; n=3)



**Figure 4.7:** The mean cumulative nicotine permeation at three donor media flow rates; **[A]** The mean cumulative nicotine permeation time profile at three donor media flow rate levels; the line was fitted to the linear portion of the profile;  $Y=0.0242*X+0.0378$ ,  $R^2=0.99$  (Donor media flow rate 1.66 mL/min);  $Y=0.0273*X-0.115$ ,  $R^2=0.99$  (Donor media flow rate 6 mL/min);  $Y=0.0268-0.0346$ ,  $R^2=0.99$  (Donor media flow rate 16 mL/min); **[B]** The mean cumulative nicotine release time profile at three donor media flow rate levels; the line was fitted to the linear portion of the profile;  $Y=0.1231*X-0.075$ ,  $R^2=0.99$  (Donor media flow rate 1.66 mL/min);  $Y=0.2737*X+0.0625$ ,  $R^2=0.99$  (Donor media flow rate 6 mL/min);  $Y=0.3337+0.5612$ ,  $R^2=0.99$  (Donor media flow rate 16 mL/min); **[C]** The mean release rates at three donor media flow rate levels; \* & \*\* the release lag time at 1.66 mL/min was significantly shorter than at 6 and 16 mL/min. (Error bars represent one standard deviation; n=5)



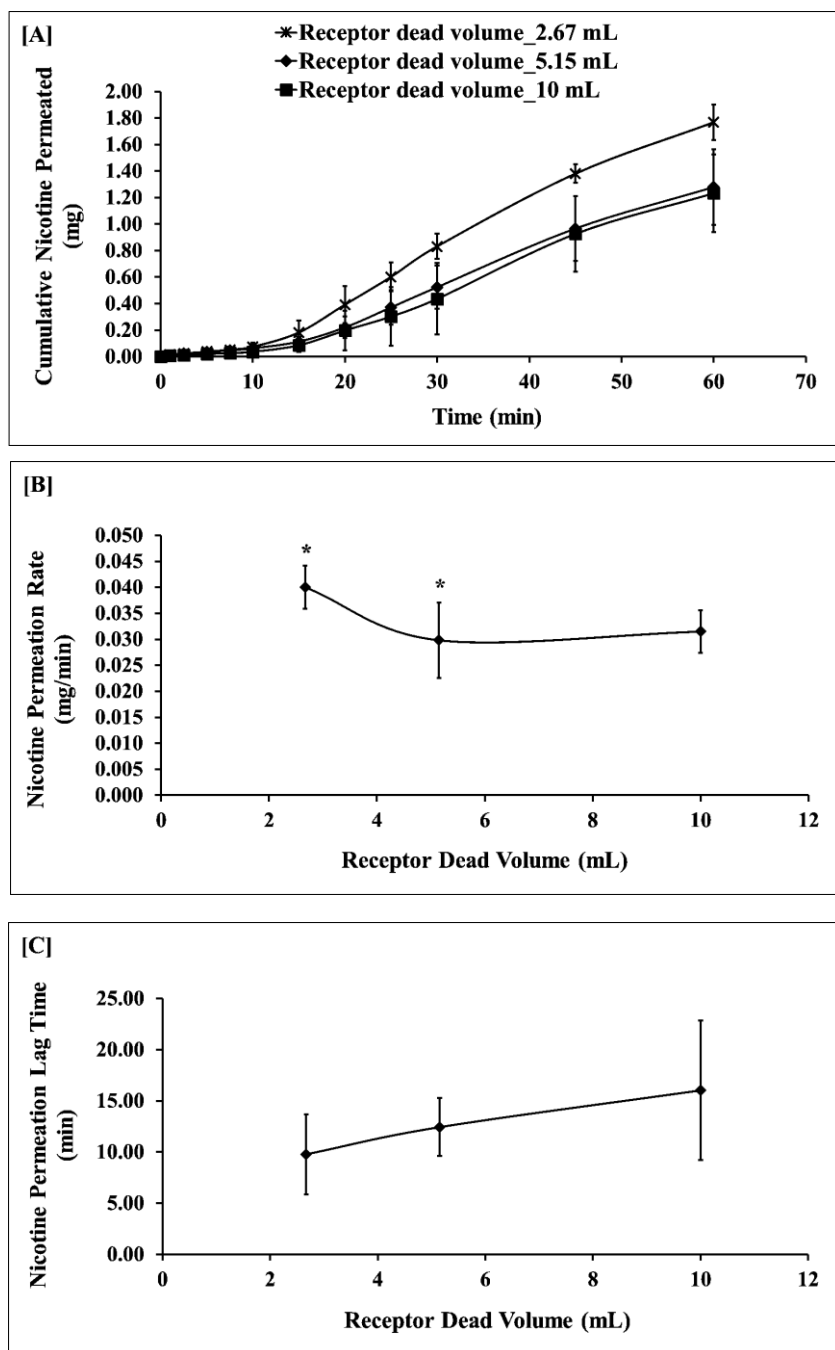
**Figure 4.8:** The mean cumulative nicotine permeation time profile at three receptor to donor media volume ratios; the line was fitted to the linear portion of the profile;  $Y=0.0265*X-0.1012$ ,  $R^2=0.99$  (Media volume ratio 2);  $Y=0.0223*X-0.133$ ,  $R^2=0.99$  (Media volume ratio 4);  $Y=0.0249*X-0.1414$ ,  $R^2=0.99$  (Media volume ratio 8). (Error bars represent one standard deviation;  $n=3$ )

Table 4.7 summarizes the mean nicotine permeation rate data at receptor dead volumes of 2.67, 5.15 and 10 mL. Figures 4.9(A), 4.9(B) and 4.9(C) illustrate the nicotine permeation time profiles, permeation rate and lag time plots obtained with these receptor dead volumes respectively. The nicotine permeation rate was significantly faster with a receptor dead volume of 2.67 mL in comparison to that obtained with 5.15 mL. This can be attributed to the late appearance of permeated nicotine into the reservoir at large dead volumes. However, the permeation rate at 2.67 and 5.15 mL was not significantly different from that obtained with 10 mL of dead volume which might be due to large variability in the permeation rate (Table 4.7). The variability in permeation increased with an increase in the dead volume (Table 4.7). The apparent increase in nicotine permeation lag time with dead volume was not significant due to high variability. The apparent increase in permeation lag time was attributed to a longer time needed for permeated nicotine to reach the reservoir at large dead volumes. The nicotine permeation with each replicate at all levels of dead volume is presented in Tables C24-C26 of Appendix C.

The amount of nicotine permeated, permeation rates and lag time observed as a function of media temperature is displayed in Tables C27-C29 of Appendix C. The nicotine permeation time profile and permeation rate and lag time versus temperature is presented in Figures 4.10(A), 4.10(B) and 4.10(C) respectively. The nicotine permeation rates (Table 4.7 and Figure 4.10(B)) were significantly different from one another. Also, the nicotine permeation lag time at 45 °C was significantly shorter than at 25 °C (Figure 4.10(C)). The temperature increase might have resulted in an increase in the diffusion coefficient of nicotine leading to its faster release from snus, increased donor nicotine concentration and consequently faster permeation. This can be explained by the Stokes-Einstein theory and Fick's Law of Diffusion (Section 4.2.2.1 and 4.2.2.2) (Othmer et al. 1953; Edward 1970; Martin et al. 1983; Hubley et al. 1996).



The amount of nicotine permeated from snus over time as a function of agitation is summarized in Tables C30-C31 of Appendix C. Figures 4.11(A), 4.11(B) and 4.11(C) illustrate the nicotine permeation time profiles, nicotine permeation rate and lag time obtained with and without agitation. The nicotine permeation rate was significantly slower with agitation than without agitation. The nicotine permeation lag time, however, was significantly longer without agitation. The change in permeation rates was opposite to what was expected. The explanation of this result can be related to the manner in which the snus was agitated. The application of pressure towards the center of the apparatus with a beaker resulted in the movement of media in the top of the donor and receptor chambers towards their respective outlets; whereas the media in the bottom of the chambers moved toward the reservoirs through the inlet tubing. The latter effect is undesirable and results did not represent the true permeation rate and lag time. Because of the above unwanted effect, in the presence of agitation, nicotine released from snus was removed from the donor chamber through inlets and outlets reducing the concentration gradient across the chambers which decreased the permeation rate. The nicotine permeation rates and lag times obtained with agitation were not true representations, since media from the bottom of the chamber reached the reservoir before the media from the top of the chamber. This event cannot be avoided with the present BTA apparatus with flexible walls. An appropriate modification was required in the set up to avoid the above undesirable event and study the agitation effect suitably. An assembly that only agitates the product in the donor chamber without reducing the chamber volumes instead of agitation incorporated through the application of pressure on the receptor chambers should be sought. Automation can also be employed to agitate the product to avoid variability that may result from manual agitation.



**Figure 4.9:** The mean cumulative nicotine permeation at three receptor dead volumes; **[A]** The mean cumulative nicotine permeation time profile at three receptor dead volumes; the line was fitted to the linear portion of the profile;  $Y=0.04*X-0.4025$ ,  $R^2=0.99$  (Receptor dead volume 2.67 mL);  $Y=0.0298*X-0.3732$ ,  $R^2=0.99$  (Receptor dead volume 5.15 mL);  $Y=0.0315X-0.4955$ ,  $R^2=0.99$  (Receptor dead volume 10 mL/min); **[B]** The mean permeation rates at three receptor dead volume levels; \* the permeation rate at 2.67 mL was significantly faster than at 5.15 mL of dead volume; **[C]** The mean permeation lag time at three receptor dead volumes. (Error bars represent one standard deviation; n=5)

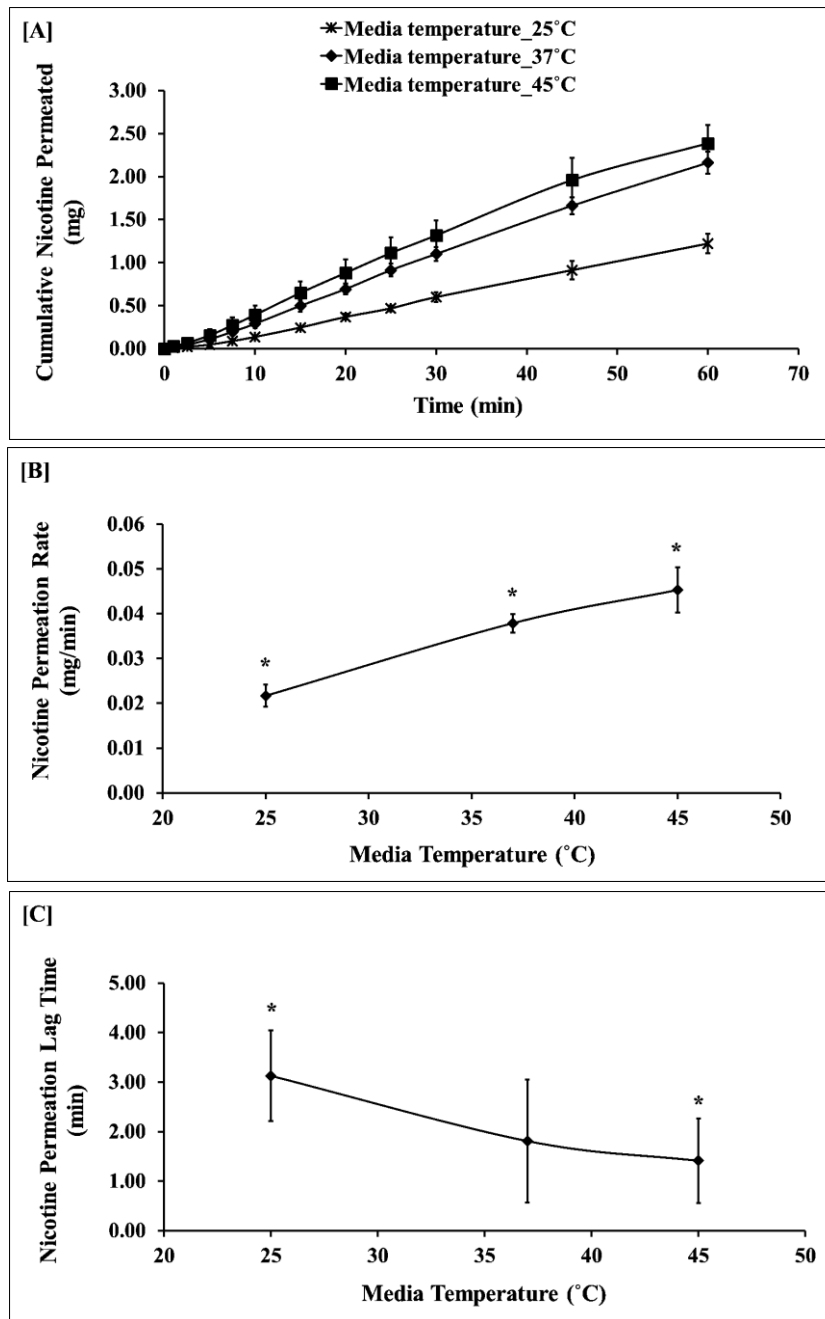


**Figure 4.10:** The mean cumulative nicotine permeation at three media temperatures; **[A]** The mean cumulative nicotine permeation time profile at three media temperature levels; the line was fitted to the linear portion of the profile;  $Y=0.0217*X-0.0693$ ,  $R^2=0.99$  (Media temperature 25 °C);  $Y=0.0379*X-0.0683$ ,  $R^2=0.99$  (Media temperature 37 °C);  $Y=0.0453*X-0.0491$ ,  $R^2=0.99$  (Media temperature 45 °C); **[B]** The mean permeation rates at three media temperatures; \* indicates the permeation rates were significantly different from one another; **[C]** The mean permeation lag time at three media temperature levels; \* the permeation lag time was significantly longer at 25 °C than at 45 °C temperature. (Error bars represent one standard deviation; n=5)

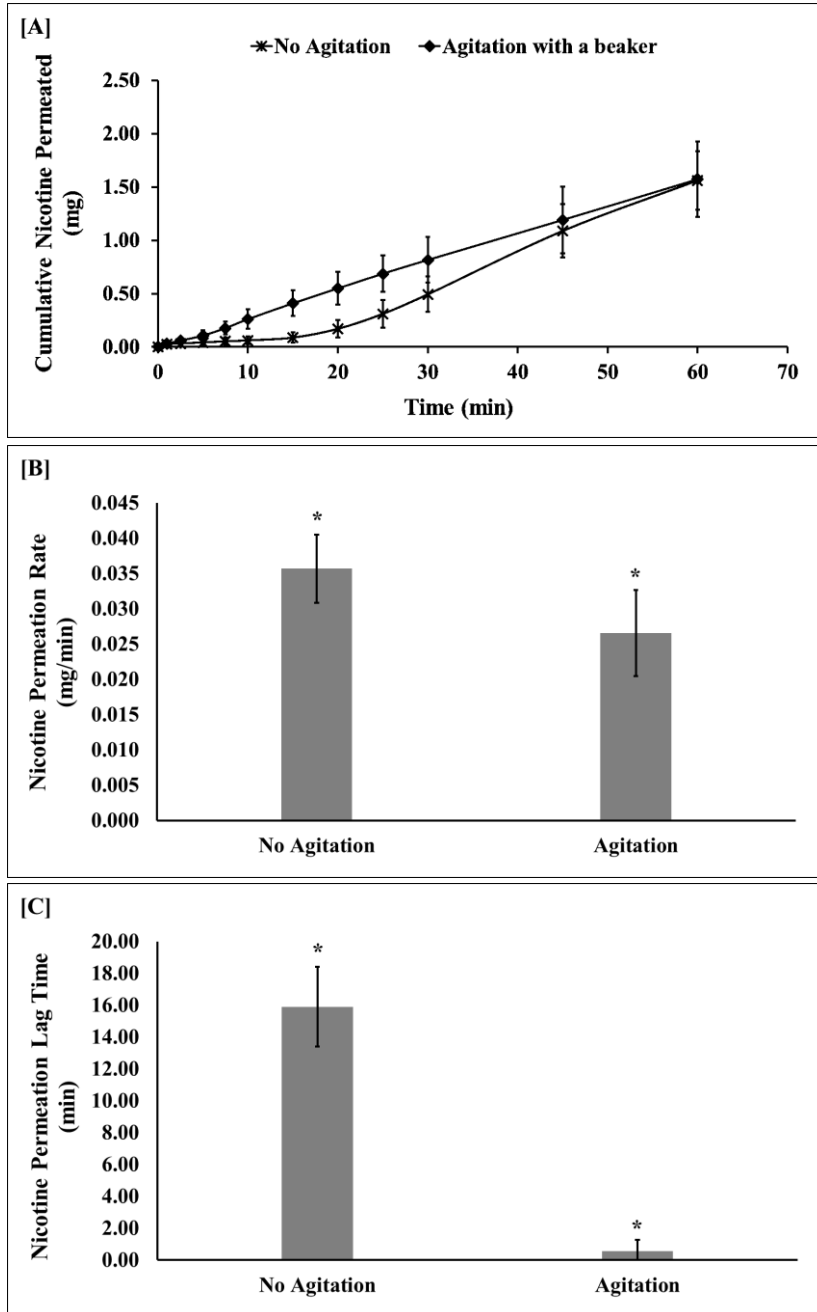


**Figure 4.11:** The mean cumulative nicotine permeation as a function of agitation; **[A]** The mean cumulative nicotine permeation time profile with and without agitation; the line was fitted to the linear portion of the profile;  $Y=0.0357*X-0.5592$ ,  $R^2=0.99$  (Without Agitation);  $Y=0.0266*X-0.0012$ ,  $R^2=0.99$  (With Agitation); **[B]** The mean permeation rates with and without agitation; \* the permeation rates significantly different from one another; **[C]** The mean permeation lag time with and without agitation; \* the permeation lag time was significantly longer without agitation in comparison to with agitation. (Error bars represent one standard deviation; n=5)

Among the eight variables studied, the SSSR, media temperature, receptor dead volume and agitation showed significant effects on nicotine permeation rate. However, SSSR and media temperature was selected for further optimization of the BTA. The receptor dead volume of 2.67 mL (minimum possible with the apparatus) was selected for further optimization using SSSR and temperature as variables. The receptor dead volume was not selected because the temperature effect can be studied only at large receptor media flow rate which is expected to overcome the effect of large dead volume. In addition, the receptor dead volume lacked physiological relevance. The receptor dead volume could be related to the degree of damage to oral mucosal membrane due to the use of smokeless tobacco products. Due to the lack of relevant literature on the degree of damage to the oral mucosal membrane caused by the use of smokeless tobacco products, the range of dead volume was selected in the present study keeping in view the practicality of performing experiments. This range of dead volume could not be considered physiologically relevant. Agitation was not selected because of the issues discussed above. The incorporation of agitation resulted in the decrease of permeation rate which was highly variable (Table 4.7). This will not only introduce significant variability but also lead in a direction opposite to the need of increasing permeation rate due to the removal of nicotine from the donor chamber. However, agitation can be studied and incorporated on a case by case basis. In addition, information on chewing/agitation frequency was lacking in the literature. The agitation frequency of 1/min may not be physiologically relevant. Therefore, the SSSR and media temperature were selected for further work over the receptor dead volume and agitation.

#### 4.4 CONCLUSIONS

From this study it was concluded that the bidirectional transmucosal apparatus allows simulation and adjustment of oral cavity physiological and *in vitro* variables for the prediction of the *in vivo* performance of OTPs. A total of eight variables, two oral cavity physiological and six *in vitro* variables were investigated in an independent manner to study their effect on nicotine permeation using the BTA. Of all the variables studied, stimulated saliva swallowing rate (SSSR), media temperature, receptor dead volume and agitation showed a significant impact on nicotine permeation rate which provided evidence of the possibility for optimization of IVIVR in a realistic manner. Due to the lack of physiological relevance with receptor dead volume and issues related to agitation because of the apparatus design, SSSR and media temperature were chosen for further optimization of IVIVR for snus. The work presented in this chapter demonstrates the potential for optimization and adjustment of variables for improving the predictability of an *in vitro* system. Factorial experiments integrating the SSSR and media temperature as relevant variables using the BTA were performed for the optimization of the prediction of *in vivo* behavior of smokeless tobacco (snus). The results of this optimization study are reported in Chapter 5.

## CHAPTER 5

### OPTIMIZATION OF THE *IN VITRO IN VIVO* RELATIONSHIP (IVIVR) FOR SMOKELESS TOBACCO (SNUS) EMPLOYING STIMULATED SALIVA SWALLOWING RATE (SSSR) AND MEDIA TEMPERATURE AS VARIABLES

#### 5.1 INTRODUCTION

Biorelevant dissolution/release/permeation testing can serve as an *in vitro* surrogate for the *in vivo* performance of a product. The *in vitro* system can be an accurate predictive tool when it simulates the relevant physiological environment closely (Fotaki et al. 2010) and can lead to selection of an appropriate drug candidate along with successful formulation development. (Wang et al. 2009). With the goal of the development of a tool that can accurately predict *the in vivo* behavior of oral transmucosal products (OTPs); an *in vitro* device, the bidirectional transmucosal apparatus (BTA), that simulates relevant oral cavity physiological variables and allows adjustment of *in vitro* variables, was designed and fabricated (Chapter 3). The BTA was selected over the USP IV and VDC because of its higher potential for simulation and adjustment of variables. The screening experiments reported in Chapter 4 indicated stimulated salivary swallowing rate (SSSR) and media temperature as the most relevant variables which showed a significant effect on the *in vitro* nicotine permeation rate (Chapter 4).

Multivariate optimization using an experimental design is a useful strategy to establish optimal conditions of multiple variables to achieve a desired response (i.e., a minimum, a maximum or a target). Various experimental designs utilized for the multivariate optimization include but are not limited to the multi factorial design, Plackett-Burman design, central composite design (CCD) and Box-Behnken (BB) design (Khuri et al. 2010). The multivariate optimization strategy is widely utilized for the formulation, dissolution and analytical method development (Lundstedt et al. 1998; Kincl et al. 2005; Ferreira et al. 2007; Gomez-Gaete et al. 2013; Zhou et al. 2013). Optimization helps in acquiring relevant useful information from a smaller number of experiments and assists in the development phase in a cost effective manner. In addition, a multivariate optimization method allows the development of models for a better understanding of the relationship between multiple factors and response mechanistically and statistically. Furthermore, the multivariate optimization design allows study of interaction between multiple variables and provides accurate information as compared to univariate studies which analyzes the effect of only a single variable. The information provided by univariate studies will not be as reliable due to a significant interaction between variables or factors under the study (Ferreira et al. 2007). The present study was therefore aimed at the optimization of IVIVR for snus using the BTA by employing an experimental design (multi factorial design – 3 level 2 factor ( $3^2$ ) design) involving SSSR and media temperature as relevant variables, each at three levels. The optimized IVIVR is defined as the relationship between the cumulative amount absorbed *in vivo* (mg) and the cumulative amount permeated *in vitro* (mg) at the same time with a slope of unity. An IVIVR with a slope of unity indicates closeness of the *in vitro* permeation and the *in vivo* absorption rate or time course. Response surface methodology was utilized to determine the best condition of



SSSR and media temperature that predicts the *in vivo* permeation rate of nicotine from snus accurately.

## 5.2 MATERIALS AND METHODS

### 5.2.1 MATERIALS

Snus (a type of smokeless tobacco, Nicotine 8.0 mg, 1.0 g pouch) for *in vitro* studies was purchased from Old Virginia Tobacco Co., Richmond, VA, USA. Hanks' Balanced Salt (H-1387) and N-(2-hydroxyethyl)piperazine-N'-(2-ethanesulfonic acid) (HEPES, 1M) buffer for the preparation of Hank's balanced salt solution (HBSS, pH 7.4) were purchased from Sigma, St. Louis, MO, USA. Potassium phosphate monobasic (anhydrous) and sodium phosphate dibasic (anhydrous) to formulate artificial saliva of pH 7.2 was procured from Sigma, St. Louis, MO, USA. Sodium hydroxide and hydrochloric acid solution (10 N) for pH adjustment was obtained from Sigma, St. Louis, MO, USA. (-)-Nicotine hydrogen tartrate for the assay was also purchased from Sigma, St. Louis, MO, USA. HPLC grade ammonium acetate and glacial acetic acid for the mobile phase preparation was obtained from Fisher Scientific, Fair Lawn, NJ, USA and EMD, Gibbstown, NJ, USA respectively. HPLC grade methanol was purchased from Honeywell Burdick and Jackson, Muskegon, MI, USA. Water was obtained in-house (the Nanopure Diamond™, Barnstead, IO, USA). Regenerated cellulose membranes for *in vitro* permeation studies was purchased from Thermo Scientific, Rockford, IL, USA. Fluorinated ethylene propylene (FEP) and Tygon® platinized silicon tubing for the *in vitro* apparatus were purchased from Cole-Parmer, Vernon Hills, IL, USA. Teflon unions and luer fittings for tubing connections were bought from Upchurch Scientific, Oak Harbor, WA, USA. Masterflex L/S 12-channel 8-roller cartridge pump

head (Model 7519-25) and variable-speed modular drive (Model 7553-70; 6 to 600 rpm; flow rate range : 0.0006 to 41 mL/min) for circulating media through the donor chamber was purchased from Cole-Parmer, Vernon Hills, IL, USA. Two variable medium flow mini pumps (Model 3386; flow rate range – 0.4 to 85 mL/min) for circulating media through the receptors chambers were purchased from Control Company, Friendswood, TX, USA.

### 5.2.2 EXPERIMENTAL DESIGN

Optimization of the IVIVR for snus was conducted by a multifactorial design experiment. A  $3^2$  design involving two factors (SSSR and media temperature) each at 3 levels (Table 5.1), was employed to estimate a second-order response surface of the *in vitro* nicotine permeation rate, ratio of *in vitro* to *in vivo* rates and *in vitro* nicotine release. Each experiment was performed four times. The factorial experiments will allow study of the effect of interaction between factors on the response and nonlinearity in the response as a function of the independent variables. Table 5.2 lists the nine experiments at the combinations of different levels of the two variables conducted with the multifactorial ( $3^2$ ) design.

### 5.2.3 *IN VITRO* RELEASE AND PERMEATION TESTING

The bidirectional transmucosal apparatus represented schematically in Figure 4.1 (Chapter 4) was employed to perform multifactorial experiments and study nicotine release and permeation from snus to optimize IVIVR. The assembly components, pumps and experimental method previously used (Chapter 3) were also employed in the present study. Snus used in the study is described in Section 3.2.2 (Chapter 3). Artificial saliva (pH 7.2,  $\beta$  7.0 mM/L/pH unit) and Hanks'

balanced salt solution (HBSS, pH 7.4,  $\beta$  14.21 mM/L/pH unit) was maintained at the required temperature and were used as the donor and receptor media respectively. Artificial saliva was circulated through the donor chamber of the BTA in an open flow through pattern by using a cartridge pump. Two separate peristaltic pumps were employed to circulate HBSS through each receptor chamber which was maintained in a closed flow through arrangement. Table 5.2 presents the detailed experimental conditions for the factorial design. The required chamber temperature was obtained by maintaining the water bath and donor and receptor reservoir media at higher temperatures. One ml of HBSS was sampled at 0, 2.5, 5, 7.5, 10, 15, 20, 25 and 30 min from receptor reservoirs to assess nicotine permeation. Forty microliters of artificial saliva was sampled at similar time points from the reservoir collecting swallowed tobacco extract (Figure 4.1) and diluted twenty five times with HBSS buffer to measure the amount of nicotine swallowed. The sampled media was replaced with an equivalent volume of fresh media. Each experiment was performed in replicates of four. A validated reverse-phase HPLC method (Chapter 2) was employed to assess nicotine release and permeation in *in vitro* samples. Nicotine permeated into both receptor chambers of the BTA was added to represent the total permeation achieved at each time point. The total volume circulated through the donor chamber was measured by collecting media from the chamber and reservoir containing simulated swallowed tobacco extract. This volume was useful to calculate the amount of nicotine released in the donor chamber. The method for the calculation of the amount of nicotine permeated, released and swallowed are shown in Tables D0, D10 and D22 of Appendix D respectively.

**Table 5.1:** A  $3^2$  full multifactorial design for the optimization of IVIVR for snus using the bidirectional transmucosal apparatus

<b>Factors (X)</b>	<b>Levels</b>		
	<b>1</b>	<b>2</b>	<b>3</b>
Stimulated saliva swallowing rate (mL/min) ( $X_1$ )	0.32	1.66	3
Media temperature ( $^{\circ}\text{C}$ ) ( $X_2$ )	25	37	45
<b>Responses (Y)</b>	<b>Aim</b>		
<i>In vitro</i> nicotine permeation rate ( $Y_1$ )	To study the effect of factors and their interaction on the permeation of nicotine and optimization of IVIVR		
Ratio of <i>in vitro</i> nicotine permeation to <i>in vivo</i> nicotine absorption rates ( $Y_2$ )	To study the effect of factors and their interaction on the ratio of rates and optimization of IVIVR		
<i>In vitro</i> nicotine release at 10 min ( $Y_3$ )	To study the effect of factors and their interaction on the release of nicotine from snus		

**Table 5.2:** Experimental conditions for 3<sup>2</sup> factorial design

Expt No.	SSSR (mL/min)	Temperature (°C)	N	Donor media (Artificial Saliva)	Receptor media (HBSS)	Receptor media flow rate (mL/min)	Donor reservoir media volume	Receptor reservoir media volume	Donor and Receptor dead volume	Donor flow through pattern	Receptor flow through pattern	Agitation	Water bath temp. (°C)	Reservoir media temp. (°C)	Chamber media temp. (°C)
1	0.32	25	4	pH 7.2 $\beta = 7.0$	pH 7.4	16	50	25	2.67	Open	Closed	No	RT	RT	RT
2	0.32	37	4	pH 7.2 $\beta = 7.0$	pH 7.4	16	50	25	2.67	Open	Closed	No	45-46	40-42	33-37
3	0.32	45	4	pH 7.2 $\beta = 7.0$	pH 7.4	16	50	25	2.67	Open	Closed	No	59-60	50-53	38-45
4	1.66	25	4	pH 7.2 $\beta = 7.0$	pH 7.4	16	120	25	2.67	Open	Closed	No	RT	RT	RT
5	1.66	37	4	pH 7.2 $\beta = 7.0$	pH 7.4	16	120	25	2.67	Open	Closed	No	45-46	40-42	33-37
6	1.66	45	4	pH 7.2 $\beta = 7.0$	pH 7.4	16	120	25	2.67	Open	Closed	No	59-60	50-53	38-45
7	3	25	4	pH 7.2 $\beta = 7.0$	pH 7.4	16	150	25	2.67	Open	Closed	No	RT	RT	RT
8	3	37	4	pH 7.2 $\beta = 7.0$	pH 7.4	16	150	25	2.67	Open	Closed	No	45-46	40-42	33-37
9	3	45	4	pH 7.2 $\beta = 7.0$	pH 7.4	16	150	25	2.67	Open	Closed	No	59-60	50-53	38-45

RT: Room Temperature

#### 5.2.4 DATA ANALYSIS

Data analysis was performed on three responses; the *in vitro* nicotine permeation rate, the ratio of *in vitro* nicotine permeation to *in vivo* nicotine absorption rate and the amount of nicotine released at 10 min. The *in vitro* nicotine permeation rate and ratio of rates were analyzed to optimize the IVIVR for snus. The ratio of rates was utilized to aid in the interpretation. A ratio of rates of one would indicate comparable *in vitro* permeation and *in vivo* absorption profiles. The *in vitro* nicotine permeation rate (mg/min) was obtained from the slope of the nicotine permeation time profile from 7.5 to 30 min. This time frame was selected to obtain the permeation rate since a lag time of 7.5 min was observed *in vivo* for nicotine absorption. All experiments were performed for 30 min as the snus was removed after half an hour during the clinical study. Ratios also represented rates obtained between 7.5 and 30 min. The amount of nicotine released at 10 min was analyzed to study the effect of the chosen variables (SSSR and media temperature) on release properties of nicotine. The amount of nicotine released at 10 min was interpreted rather than the release rate because of the unexpected troughs observed in the release profile over time (Figure 5.6). Nicotine release at 10 min was differentiable and the range observed can be explained as a function of swallowing rate and media temperature.

A second-order statistical model comprised of interaction and quadratic terms obtained by multiple linear regression was used to define the relationship between the factors (SSSR and media temperature) and each response (permeation rate, ratio of rates and amount of nicotine release at 10 min). Equation 5.1 represents the second-order model that was used to fit the response data obtained from the 3<sup>2</sup> factorial experiment (Table 5.1).

$$Y = b_0 + b_1X_1 + b_2X_2 + b_{12}(X_1 - \bar{X}_1)(X_2 - \bar{X}_2) + b_{11}(X_1 - \bar{X}_1)^2 + b_{22}(X_2 - \bar{X}_2)^2 \quad (\text{Eq 5.1})$$

where,  $Y$  was the observed response (*in vitro* nicotine permeation rate or the ratio of *in vitro* nicotine permeation to *in vivo* nicotine absorption rates or the amount of nicotine released at 10 min);  $b_0$  was the  $Y$  intercept;  $b_1$  and  $b_2$  were coefficients of the effects of variables  $X_1$  and  $X_2$  respectively;  $b_{12}$  was the coefficient of the effect of interaction between  $X_1$  and  $X_2$ ;  $b_{11}$  and  $b_{22}$  were coefficients explaining the nonlinearity in  $Y$  as a function of  $X_1$  and  $X_2$  respectively. The terms  $(X_1 - \bar{X}_1)$  and  $(X_2 - \bar{X}_2)$  are mean-centered variables; where,  $(\bar{X}_1)$  and  $(\bar{X}_2)$  represented the mean of SSSR and media temperature respectively. Both the SSSR and media temperature were mean-centered because of the absence of zero point in their levels and to facilitate an appropriate interpretation of the intercept (Wainer 2000). Two-way analysis of variance (ANOVA) was performed to identify the statistically significant effects and interactions. A lack of fit test was also performed to test the adequacy of the model. The plot of residuals versus predicted value was also studied to confirm the absence of any trend and to test the suitability of the model. The statistical analysis was performed in JMP Pro 10 at  $\alpha = 0.05$ .

Analysis of the response surface explained by the second-order model was performed to choose the best combination of SSSR and media temperature to obtain the IVIVR and ratio of *in vitro* to *in vivo* rate for snus as close to 1 as possible. The model was validated by performing an experiment at the optimal conditions of SSSR and media temperature.

### 5.3 RESULTS AND DISCUSSION

#### 5.3.1 EFFECT OF SSSR AND MEDIA TEMPERATURE ON *IN VITRO* NICOTINE PERMEATION RATE

The average *in vitro* nicotine permeation rates resulted from the combined effects of SSSR and media temperature are summarized in Table 5.3. The mean cumulative *in vitro* nicotine permeation time profiles obtained from the 3<sup>2</sup> factorial design experiments are displayed in Figure 5.1. The amount of nicotine permeated as a function of time and the permeation rate obtained from each replicate experiment at all combinations of the SSSR and media temperature are presented in Tables D1-D9 of Appendix D. The mean *in vitro* nicotine permeation rate varied from 0.008 to 0.044 mg/min indicating the possibility for optimization of IVIVR by varying the level of SSSR and media temperature. The slowest permeation was obtained at the low and high level of media temperature and SSSR respectively. Whereas, the fastest permeation was observed at the high and low level of media temperature and SSSR, respectively. This influence of variables on the permeation rate was defined by a second-order model (Equation 5.2) which was obtained by multiple regression analysis on the results presented in Table 5.3. The statistical validation of the estimated model for the *in vitro* nicotine permeation rate is shown in Table 5.4.

$$Y_1 = 0.0079 - 0.0086X_1 + 0.0006X_2 - 0.0004(X_1 - 1.66)(X_2 - 35.67) + 0.0025(X_1 - 1.66)^2 + 0.00002(X_2 - 35.67)^2 \quad \text{----- (Eq 5.2)}$$



**Table 5.3:** *In vitro* nicotine permeation rate and the ratio of *in vitro* nicotine permeation to the *in vivo* nicotine absorption rate obtained from the 3<sup>2</sup> factorial experiment

SSSR (mL/min)	Media Temperature (°C)	N	<i>In Vitro</i> Nicotine Permeation Rate (mg/min)			Ratio of <i>In Vitro</i> Nicotine Permeation to <i>In Vivo</i> Absorption Rate*		
			Mean	SD	%RSD	Mean	SD	%RSD
0.32	25	4	0.022	0.005	23.104	0.60	0.14	23.10
0.32	37	4	0.033	0.002	7.627	0.90	0.07	7.63
0.32	45	4	0.044	0.003	6.323	1.22	0.08	6.32
1.66	25	4	0.012	0.002	13.301	0.33	0.04	13.30
1.66	37	4	0.016	0.001	7.763	0.44	0.03	7.76
1.66	45	4	0.023	0.002	8.707	0.63	0.05	8.71
3	25	4	0.008	0.001	14.565	0.22	0.03	14.56
3	37	4	0.010	0.001	6.350	0.29	0.02	6.35
3	45	4	0.011	0.001	6.079	0.31	0.02	6.08

\* *In vivo* nicotine absorption rate = 0.036 mg/min (Chapter 3)

**Table 5.4:** Statistical validation of the second-order model for the *in vitro* nicotine permeation rate (ANOVA)

Model term	Coefficient	Std error	t-ratio	p-value	95% confidence interval	Model significance and adequacy
$b_0$	0.008	0.002	3.43	0.0018*	(0.003, 0.013)	<b>R<sup>2</sup></b>
$b_1$	-0.0086	0.0004	-23.47	<.0001*	(-0.0093, -0.0078)	0.96
$b_2$	0.00060	0.00005	12.02	<.0001*	(0.0005, 0.0007)	<b>ANOVA</b>
$b_{12}$	-0.00040	0.00004	-7.85	<.0001*	(-0.0004, -0.0003)	F(5,30)=158.23
$b_{11}$	0.0025	0.0005	5.28	<.0001*	(0.0015, 0.0035)	p-value<0.0001*
$b_{22}$	0.000020	0.000009	1.72	0.0965	(-0.000003, 0.00003)	<b>Lack of Fit</b>
						F(3,27)=1.42
						p-value = 0.2575

\* p-value < 0.05; statistically significant

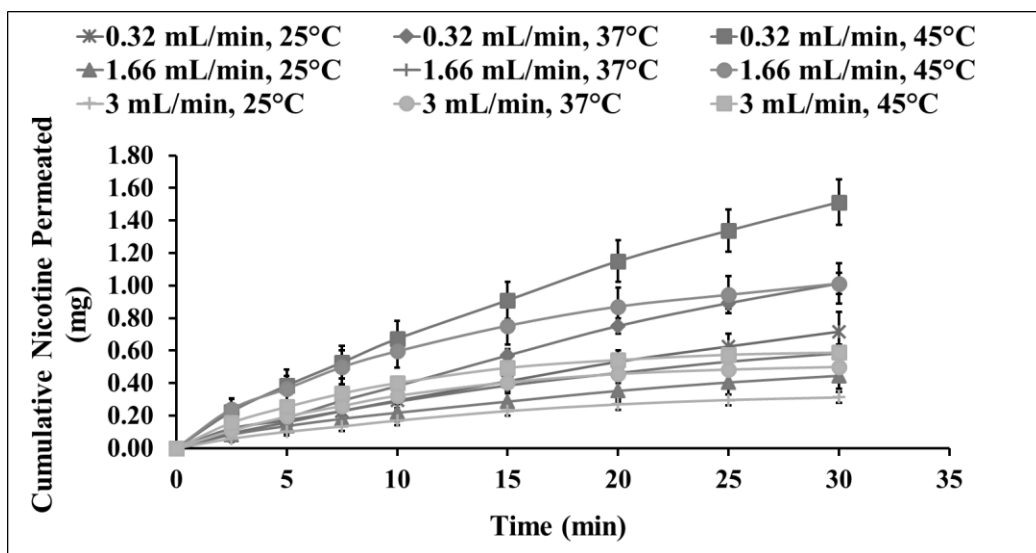


**Figure 5.1:** The mean cumulative nicotine permeation time profile as a function of SSSR (mL/min) and media temperature (°C). (Error bars represent one standard deviation; n=4)

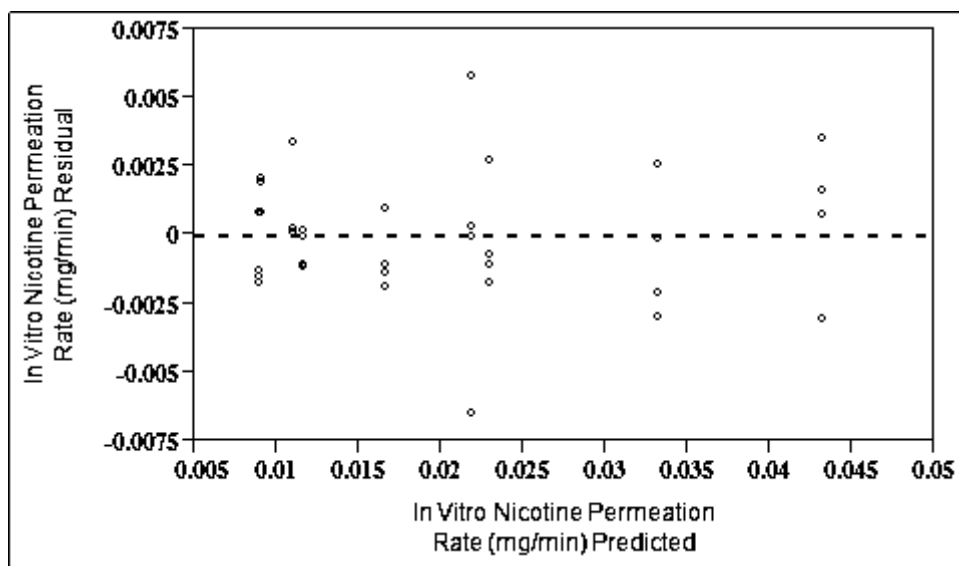


**Figure 5.2:** The residual (predicted permeation rate – observed permeation rate) versus predicted *in vitro* nicotine permeation plot for the validation of the second-order model built to define the relationship between *in vitro* nicotine permeation rate (mg/min) and SSSR (mL/min) along with media temperature (°C).

The coefficients and p-values in Table 5.4 indicated a significant effect of both the SSSR and media temperature on the *in vitro* nicotine permeation rate. In addition, there was a significant interaction suggesting that the effect of SSSR on the permeation rate depended on the level of media temperature and vice versa. Also, a significant quadratic effect of the SSSR on the permeation rate was observed. A low p-value [ $F(5,30)=158.23$ ;  $p\text{-value}<0.0001$ ] obtained on performing an F-test showed the statistical significance of the regression model for the *in vitro* permeation rate. The goodness of fit of the model was further confirmed by a high coefficient of determination [ $R^2 = 0.96$ ] and a lack of fit test [ $F(3,27)=1.42$ ;  $p\text{-value}>0.05$ ] which was not significant. The residual (predicted – observed) versus predicted nicotine permeation rate plot obtained with the model is shown in Figure 5.2. The residual plot suggested the absence of any pattern and hence any heteroscedasticity and validated the use of the model for the prediction. All of the above goodness of fit tests established adequacy of the second-order regression model for the *in vitro* nicotine permeation rate obtained by employing the SSSR and media temperature in the bidirectional apparatus. The SSSR decreased the nicotine permeation rate indicating a negative effect. In contrast, the media temperature showed a positive effect on the nicotine permeation rate suggesting that the rate can be increased by an increase in the media temperature. The effect of SSSR on the *in vitro* permeation rate was greater than the media temperature.

The response surface plot displayed in Figure 5.3 represents the *in vitro* nicotine permeation rate as a function of the SSSR and media temperature three dimensionally. It was concluded from the response surface that an increase in the media temperature resulted in an increase in the nicotine permeation rate. This observation was attributed to an increase in the diffusion coefficient of nicotine causing its faster release from snus and consequently enhanced the donor nicotine concentration which caused the permeation of nicotine into the receptors of the BTA to occur at a faster rate. This was a theoretical explanation based on the Stokes-Einstein

theory and Fick's Law (Section 4.2.2.1 and 4.2.2.2) (Othmer et al. 1953; Edward 1970; Martin et al. 1983; Hubley et al. 1996).

There was a significant decrease in the permeation rate as a function of SSSR and this decrease was significantly non-linear with an increase in the SSSR. An increase in the swallowing rate caused the removal of released nicotine from the donor chamber at a faster rate. As a consequence, the donor nicotine concentration reduced leading to a decrease in the nicotine gradient across the donor chamber and receptors. The resultant effect of the above phenomenon was a decrease in nicotine permeation rate. This explanation of the reduction in the nicotine permeation rate with an increase in the SSSR was based on Fick's Law of Diffusion (Section 4.2.2.1, Equation 4.2). However, there was significant non-linearity in the *in vitro* nicotine permeation rate as a function of SSSR. The above quadratic effect was because of saturation of the nicotine removal process from the donor chamber with the increase in SSSR. The removal rate was a function of the amount of nicotine present in snus over time in addition to the SSSR. The amount of nicotine in snus decreased with an increase in the removal rate. A large difference between the amount of nicotine in snus at the swallowing rate of 1.66 and 3 mL/min over time may not be present. Therefore, a smaller decrease in the nicotine gradient across the donor and receptor chambers, with an increase in SSSR from 1.66 to 3 mL/min, might have existed which would explain the observed nonlinearity in the permeation rate.

There was a significant negative effect for the interaction between the SSSR and media temperature on the *in vitro* nicotine permeation rate. The effect of the decrease in nicotine gradient across the BTA chambers due to simulated swallowing was predominant over the increased gradient as a function of temperature. Therefore, the overall interaction effect was negative, indicating that the effect of swallowing on the permeation rate was predominant.

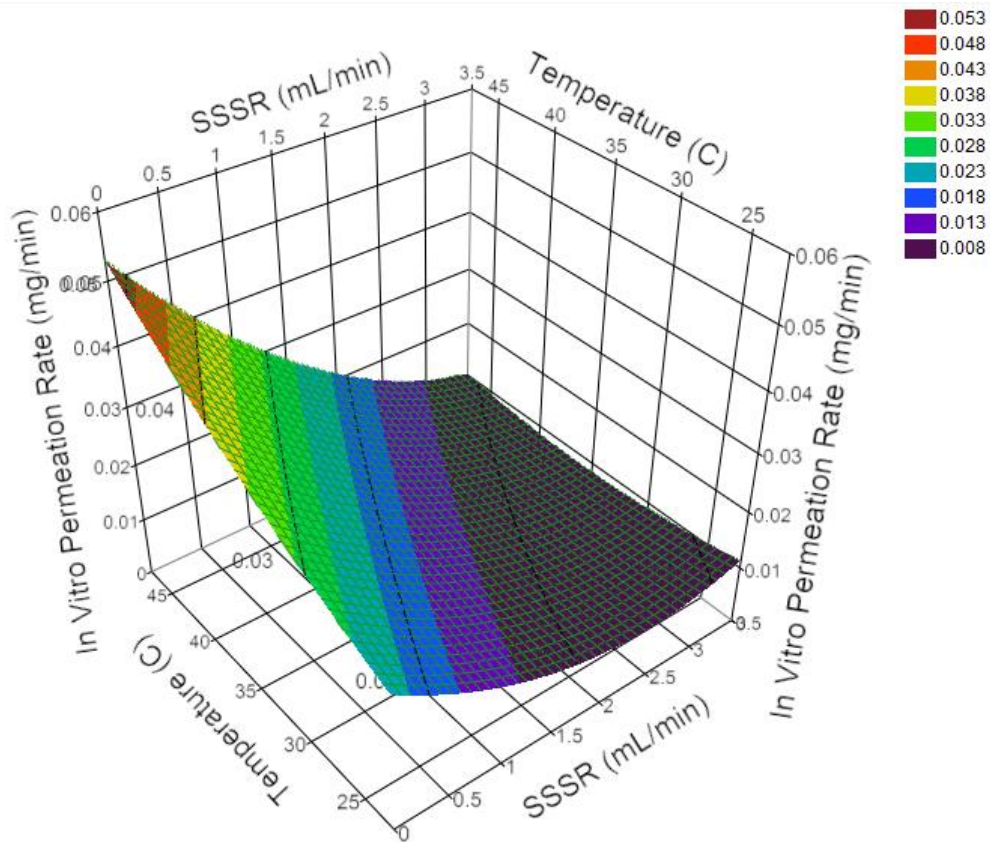


**Figure 5.3:** Three dimensional response surface plot for the *in vitro* nicotine permeation rate as a function of SSSR (mL/min) and media temperature (°C). [The color band representing the *in vitro* nicotine permeation rate of 0.038 mg/min constitutes the combination of SSSR and media temperature that will provide the *in vitro* nicotine permeation rate close to that of the *in vivo* nicotine absorption rate]

### 5.3.2 EFFECT OF SSSR AND MEDIA TEMPERATURE ON THE RATIO OF *IN VITRO* NICOTINE PERMEATION TO *IN VIVO* NICOTINE ABSORPTION RATE

The average ratio of *in vitro* nicotine permeation to *in vivo* nicotine absorption rates that resulted as a function of the joint effects of SSSR and media temperature are tabulated in Table 5.3. The individual ratio of rates obtained as a function of SSSR and media temperature are presented in Tables D1-D9 of Appendix D. The mean ratio of rates varied from 0.22 to 1.22. This observed range suggested the potential for obtaining the ratio of *in vitro* to *in vivo* rate (1/slope of IVIVR) close to one by altering the level of SSSR and media temperature. The ratio of one was desired to obtain comparable *in vitro* nicotine permeation and an *in vivo* nicotine absorption time course for the optimization of IVIVR for snus. The ratio of rates was chosen as a response for easy visualization of the response surface and optimization of the IVIVR. Multiple regression analysis was conducted to describe the effect of the variables SSSR and media temperature on the ratio of rates. A second-order quadratic model employed to fit the ratios is presented in Equation 5.3. Statistical validation of the estimated model for the ratio of rates is shown in Table 5.5.

$$Y_2 = 0.219 - 0.237X_1 + 0.017X_2 - 0.010(X_1 - 1.66)(X_2 - 35.67) \\ + 0.068(X_1 - 1.66)^2 + 0.0004(X_2 - 35.67)^2 \quad \text{-----} \quad (\text{Eq 5.3})$$

**Table 5.5:** Statistical validation of the second-order model for the ratio of *in vitro* nicotine permeation to the *in vivo* nicotine absorption rate (ANOVA)

Model term	Coefficient	Std error	t-ratio	p-value	95% confidence interval	Model significance and adequacy
$b_0$	0.22	0.06	3.42	0.0018*	(0.09, 0.35)	<b>R<sup>2</sup></b> 0.96
$b_1$	-0.24	0.01	-23.52	<.0001*	(-0.26, -0.22)	
$b_2$	0.017	0.001	12.02	<.0001*	(0.014, 0.020)	<b>ANOVA</b> F(5,30)=158.71 p-value<0.0001*
$b_{12}$	-0.010	0.001	-7.85	<.0001*	(-0.012, -0.007)	
$b_{11}$	0.068	0.013	5.29	<.0001*	(0.042, 0.096)	<b>Lack of Fit</b> F(3,27)=1.37 p-value = 0.2739
$b_{22}$	0.0004	0.0003	1.73	0.0947	(-0.00008, 0.00092)	

\* p-value < 0.05; statistically significant

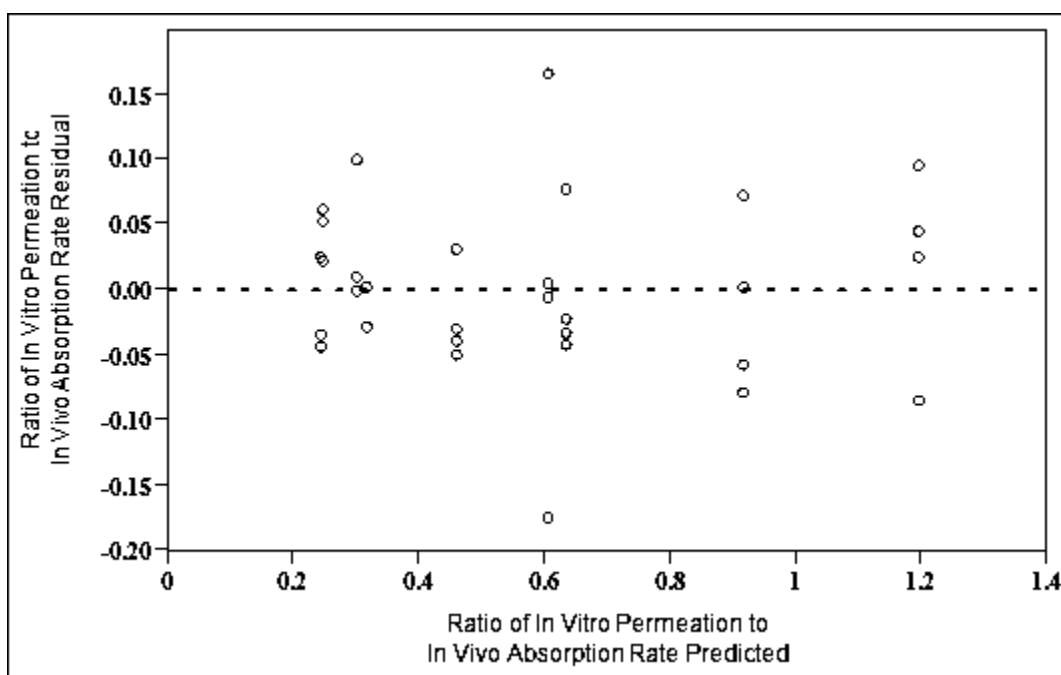


**Figure 5.4:** The residual (predicted ratio of rates – observed ratio of rates) versus predicted ratio of rates plot for the validation of the second-order model built to define the relationship between ratio of rates and SSSR (mL/min) and media temperature (°C).

The coefficients and p-values presented in Table 5.5 represent the effect of both SSSR and media temperature on the ratio of *in vitro* nicotine permeation to *in vivo* nicotine absorption rate. The estimated second-order model was significant [F(5,30)=158.71; p-value<0.0001; Table 5.5] and adequate for the prediction of the ratio of *in vitro* to *in vivo* rate (inverse of IVIVR slope) as evident from high coefficient of determination [ $R^2 = 0.96$ ], non-significant lack of fit [F(3,27)=1.37; p-value>0.05] and the absence of any trend on the residual plot (Figure 5.4). There was a significant decrease in the ratio with an increase of SSSR as suggested by the negative sign for the coefficient of SSSR (Table 5.5). The media temperature positively affected the ratio, indicating an increase in the ratio with increasing temperature. Also, there was a significant influence of interaction between SSSR and media temperature on the ratio of rates. In addition, a significant quadratic influence of the SSSR on the ratio of rates was observed. A three dimensional response surface plot for the ratio of rates illustrated in Figure 5.5 is similar to the one obtained for the *in vitro* nicotine permeation rate (Figure 5.3). The ratio of rates is the *in vitro* nicotine permeation rate obtained at each level of the SSSR and media temperature divided by the *in vivo* nicotine absorption rate of 0.036 mg/min. Therefore, the effect of SSSR and media temperature on both the ratio and permeation rate are qualitatively similar. Hence, the reasoning for the significant effect of SSSR and media temperature; and the quadratic term of SSSR on the permeation rate presented in Section 5.3.1 explains similar effects on the ratio mechanistically.



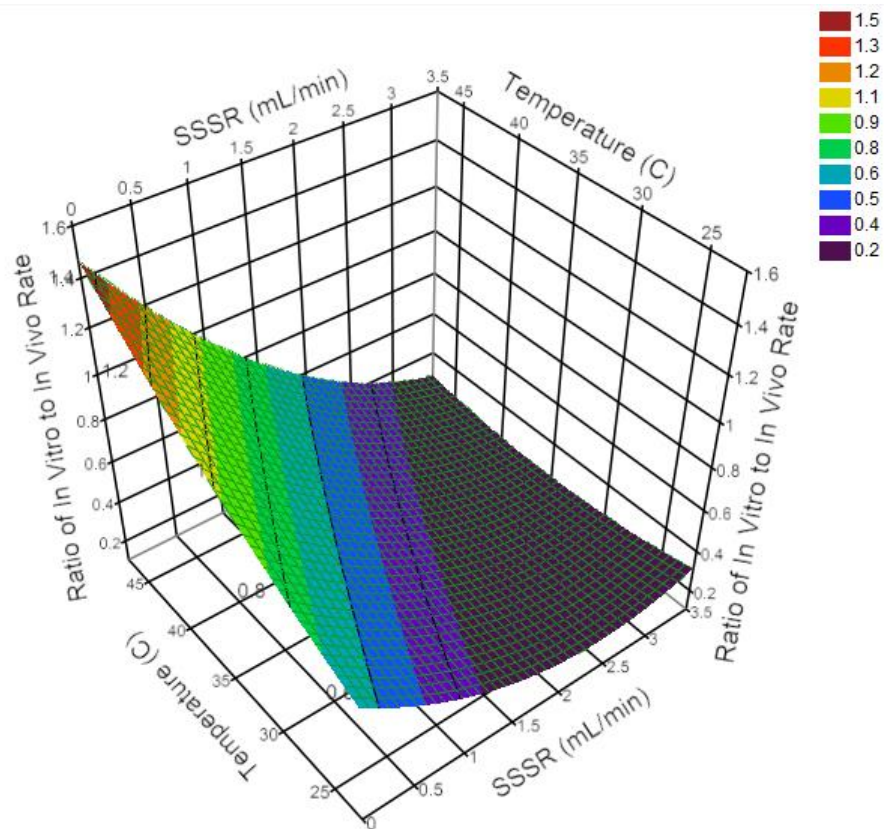


**Figure 5.5:** Three dimensional response surface plot for the ratio of *in vitro* nicotine permeation to *in vivo* nicotine absorption rate as a function of SSSR (mL/min) and media temperature (°C). [The color band representing the ratio of rates of 1 constitutes a combination of SSSR and media temperature that will provide IVIVR with a slope close to one. The IVIVR with a slope of unity indicates a comparable *in vitro* and *in vivo* nicotine time course]

### 5.3.3 EFFECT OF SSSR AND MEDIA TEMPERATURE ON NICOTINE RELEASE AT 10 MIN FROM SNUS

For the purpose of studying the effect of SSSR and media temperature on the release properties of nicotine from snus, the nicotine release at 10 min was considered as a response. On the basis of the mean cumulative nicotine release time profiles presented in Figure 5.6, the release at 10 min was chosen over the release rate because of the absence of a smooth release profile over time. The presence of troughs in the release profiles might be due to errors in sampling and dilution of samples and variability in the *in vitro* behavior of snus. It might also be possible that variability in the media flow rate and hence the media volume could introduce errors in the calculation of the amount of nicotine released and release rate. Nicotine release at 10 min was distinguishable across the range of SSSR and media temperature studied. In addition, the release of nicotine in experiments at the SSSR of 3 mL/min saturated within initial five minutes (which represents the first two sampling points) and therefore it was not possible to calculate release rates. Furthermore, the study of nicotine release at 10 min as a function of SSSR and media temperature should provide a fair approximation of the effect of these factors on the release properties of nicotine from snus.

The mean *in vitro* nicotine released at 10 min as a function of the combined effects of SSSR and media temperature are displayed in Table 5.6. The method of calculation of nicotine release at 10 min is presented in detail in tabular form (Table D10 of Appendix D). The amount of nicotine released as a function of time obtained from replicate experiments at all combinations of the SSSR and media temperature are presented in Tables D11-D19 of Appendix D. The mean *in vitro* nicotine release at 10 min varied from 1.07 to 6.61 mg at low and high levels of SSSR and media temperature respectively. This indicated the influence of SSSR and media temperature on the release of nicotine from snus which could impact permeation by altering the nicotine concentration

gradient across the donor and receptor chambers of the BTA. The effect of SSSR and media temperature on nicotine release at 10 min was explained by second-order model presented in Equation 5.4.

$$Y_3 = -1.22 + 1.55X_1 + 0.09X_2 - 0.008(X_1 - 1.66)(X_2 - 35.67) - 0.45(X_1 - 1.66)^2 + 0.003(X_2 - 35.67)^2 \quad \text{----- (Eq 5.4)}$$

The validation of the estimated model is summarized in Table 5.7. The estimated model was significant and adequately described the influence of SSSR and media temperature on nicotine release at 10 min (Table 5.7). The residual plot illustrated in Figure 5.7 also indicated the validity of the model on the basis of the absence of heteroscedasticity.

There was a significant positive influence of both the SSSR and media temperature on *in vitro* nicotine release at 10 min which suggested an increase in the release of nicotine from snus with increasing SSSR and media temperature (Table 5.7). In contrast to the *in vitro* permeation rate, there was not a significant influence of interaction between SSSR and media temperature which indicated that the release behavior of nicotine from snus was independent to that of the media temperature and vice versa. This is because the release of nicotine represented the process occurring in the donor chamber as opposed to the permeation process that occurred across the donor and receptor compartments. The nicotine concentration gradient across the donor and receptor chambers defined the permeation rate which was affected positively and negatively by the media temperature and SSSR, respectively (Table 5.4). In contrast, the increase in the release of nicotine as a function of SSSR at media temperatures of 25, 37 and 45 °C followed similar increasing trend (Figure 5.8) which justified the absence of interaction between SSSR and

temperature on the nicotine release. In addition, the nonlinearity in the *in vitro* release as a function of both SSSR and temperature was not significant. This could be attributed to the maintenance of sink condition for nicotine, i.e., the media volume was sufficient to solubilize the amount of nicotine released with increasing SSSR and temperature. The effect of SSSR on *in vitro* nicotine release was greater than that of media temperature (Table 5.7). The response surface plot in Figure 5.9 represents the effect of SSSR and media temperature on *in vitro* nicotine release at 10 min. The increase in *in vitro* nicotine release from snus as a function of temperature could be attributed to the increase in the diffusion of nicotine from snus which might be due to the reduction in artificial saliva viscosity with the increase in temperature (Section 4.2.2.1 and 4.2.2.2). An increase in nicotine release with increasing saliva swallowing rate (which is also saliva secretion rate/flow rate) might be because of the faster release of nicotine from snus due to media turbulence. The degree of turbulence of the dissolution media was found to be associated with the media flow rate/velocity (Cammarn et al. 2000).

The effect of SSSR and media temperature on the release of nicotine from snus demonstrates the range of the nicotine concentration gradient that could exist across the donor and receptor chambers of the BTA. The positive effect of media temperature on the release could also produce a similar effect on the permeation due to the simultaneous effect of an increase in diffusion as a function of temperature. However, the positive effect of simulated swallowing rate (saliva secretion/flow rate) on nicotine release did not result into a similar effect on permeation (Section 5.3.1). This was attributed to the removal of nicotine from the donor chamber by the simulation of swallowing in an open flow through pattern which resulted in a decrease in nicotine concentration gradient with increasing swallowing rate.

**Table 5.6:** Cumulative *in vitro* nicotine release at 10 min obtained from the 3<sup>2</sup> factorial experiments

SSSR (mL/min)	Media Temperature (°C)	N	<i>In Vitro</i> Nicotine Release at 10 min (mg)		
			Mean	SD	%RSD
0.32	25	4	1.07	0.55	51.29
0.32	37	4	1.43	0.49	34.13
0.32	45	4	2.98	0.59	19.85
1.66	25	4	3.99	2.02	50.64
1.66	37	4	4.23	0.65	15.37
1.66	45	4	5.90	1.01	17.15
3	25	4	5.03	0.73	14.54
3	37	4	6.61	1.95	29.43
3	45	4	6.28	0.93	14.83

**Table 5.7:** Statistical validation of the second-order model for *in vitro* nicotine release at 10 min (ANOVA)

Model term	Coefficient	Std error	t-ratio	p-value	95% confidence interval	Model significance and adequacy
$b_0$	-1.22	1.11	-1.10	0.2819	(-3.49, 1.05)	<b>R<sup>2</sup></b> 0.76
$b_1$	1.55	0.18	8.81	<.0001*	(1.19, 1.91)	
$b_2$	0.09	0.03	3.56	0.0012*	(0.04, 0.14)	<b>ANOVA</b> F(5,30)=18.95 p-value<0.0001*
$b_{12}$	-0.01	0.02	-0.39	0.7013	(-0.05, 0.04)	
$b_{11}$	-0.45	0.23	-1.98	0.0568	(-0.91, 0.01)	<b>Lack of Fit</b> F(3,27)=1.29 p-value = 0.2963
$b_{22}$	0.003	0.004	0.70	0.4903	(-0.006, 0.012)	

\* p-value < 0.05; statistically significant

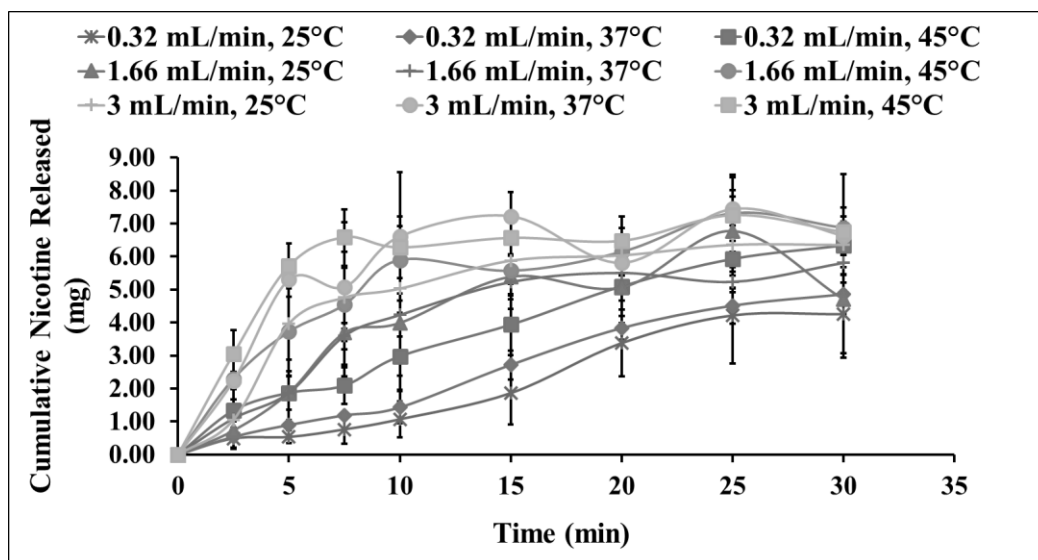


**Figure 5.6:** The mean cumulative *in vitro* nicotine release time profile as a function of SSSR (mL/min) and media temperature (°C). (Error bars represent one standard deviation; n=4)

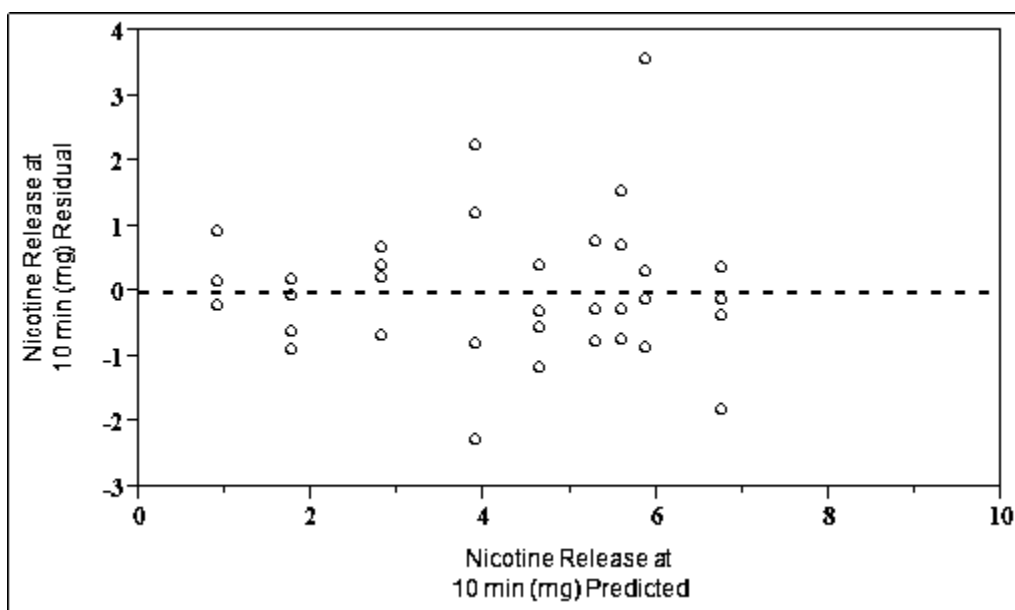


**Figure 5.7:** Residual nicotine release (predicted nicotine release – observed nicotine release) versus predicted nicotine release at 10 min for the validation of the second-order model built to define the relationship between the release of nicotine at 10 min and SSSR (mL/min) and media temperature (°C).

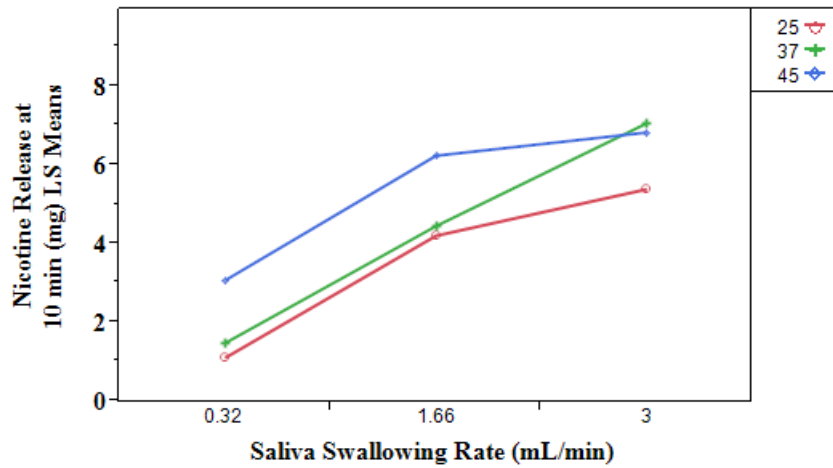


**Figure 5.8:** Interaction plot for the effect of SSSR (mL/min) and media temperature (°C) on the release of nicotine at 10 min

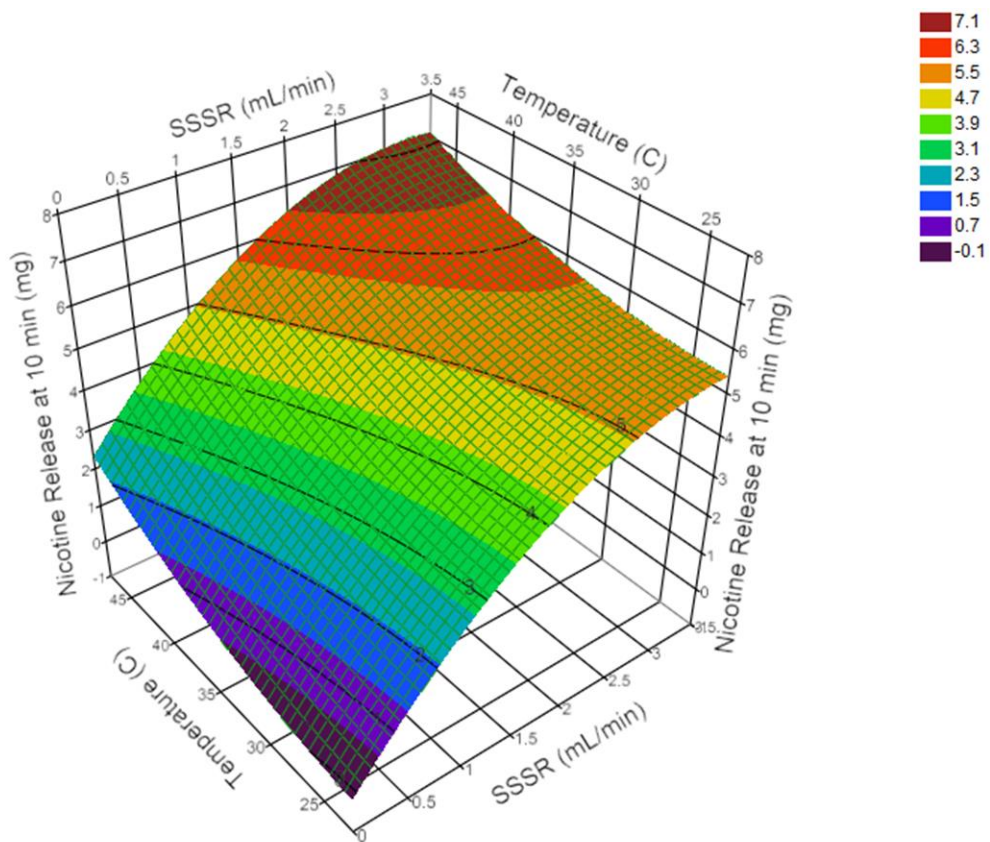


**Figure 5.9:** Three dimensional response surface plot for *in vitro* nicotine release at 10 min as a function of SSSR (mL/min) and media temperature (°C).

#### 5.3.4 OPTIMIZATION OF IVIVR FOR SNUS

The goal of the present optimization study was to determine the best levels of SSSR and media temperature that provide an *in vitro* nicotine permeation profile comparable to *in vivo* nicotine absorption profile. In other words, an IVIVR with a slope of unity was desired for smokeless tobacco (snus) to employ an *in vitro* nicotine permeation profile as the surrogate for the *in vivo* nicotine absorption profile. Figure 5.10 demonstrates the contour plot for the ratio of *in vitro* nicotine permeation to *in vivo* nicotine absorption rate at different levels of the SSSR and media temperature. The white zone in the contour plot represents the desirable area for various combinations of the SSSR and media temperature that provided ratio of rates in the range of 0.9 to 1.1. The point at the intersection of black lines represent the SSSR of 0.55 mL/min and media temperature of 43 °C that was expected to provide the ratio of *in vitro* to *in vivo* rate of 1.01 or the IVIVR slope of 0.99. For the purpose of validation of the optimization model, an *in vitro* experiment was performed at the optimal condition of SSSR (0.55 mL/min) and media temperature (43 °C) and replicated, n=4.

The mean cumulative nicotine permeated (mg), the *in vitro* nicotine permeation rate (mg/min) and the ratio of *in vitro* nicotine permeation to *in vivo* nicotine absorption rates were obtained at the optimal conditions of SSSR (0.55 mL/min) and media temperature (43 °C) using bidirectional apparatus and are tabulated in Table 5.8. The *in vitro* nicotine permeation results obtained with each replicate experiment are presented in Table D20 of Appendix D. Figure 5.11 illustrates the *in vitro* nicotine permeation profile at the SSSR of 0.55 mL/min and media temperature of 43 °C. The mean *in vitro* nicotine permeation rate of 0.039 mg/min was obtained at the optimal levels which was very close to the *in vivo* rate of 0.036 mg/min, as indicated by the ratio of *in vitro* to *in vivo* rates of 1.09 (Table 5.8). The slope resulted from the IVIVR constructed



using the *in vitro* permeation profile obtained at optimal levels of SSSR (0.55 mL/min) and media temperature (43 °C) shown graphically in Figure 5.12 was 0.92. These results indicated that the bidirectional transmucosal apparatus at the optimal levels of SSSR and media temperature predicted the *in vivo* behavior of snus accurately.

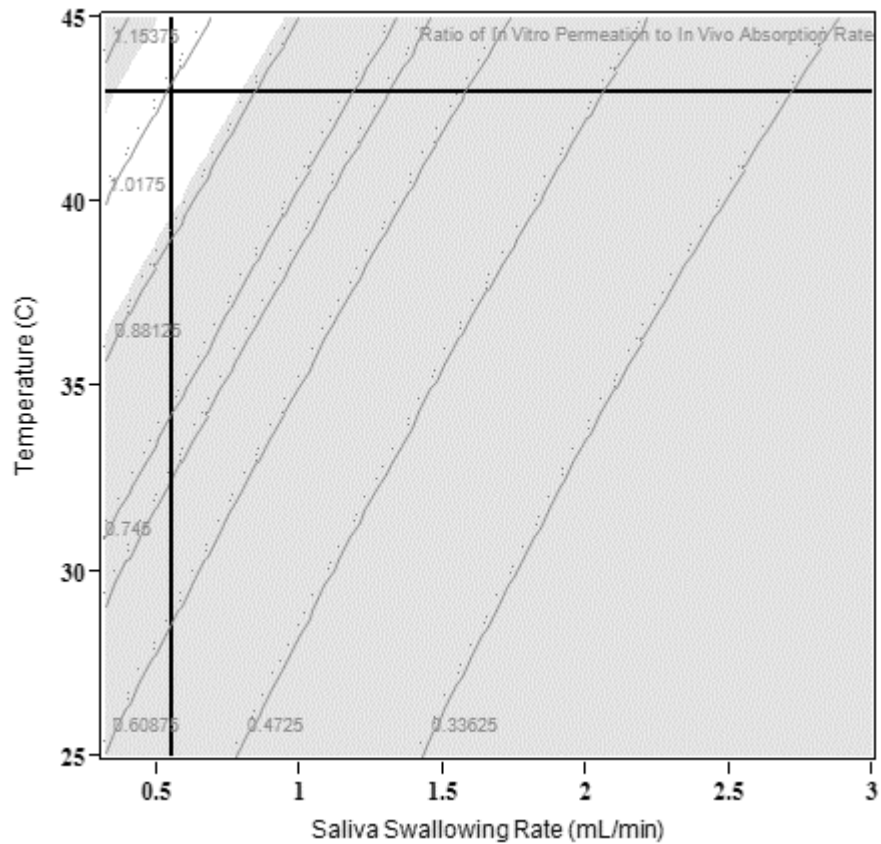


**Figure 5.10:** Contour plot of the ratio of *in vitro* nicotine permeation to *in vivo* nicotine absorption rate as a function of SSSR (mL/min) and media temperature (°C). [White zone is the desirable area representing various combinations of the SSSR and temperature that provide a ratio in the range of 0.9 to 1.1. The point at the intersection of black lines represents the SSSR of 0.55 mL/min and media temperature of 43 °C that was expected to provide the ratio of *in vitro* to *in vivo* rate of 1.01 or IVIVR slope of 0.99]

**Table 5.8:** Cumulative amount of nicotine permeated (mg), *in vitro* nicotine permeation rate (mg/min) and the ratio of *in vitro* nicotine permeation to *in vivo* nicotine absorption rates from snus at the optimal levels for SSSR 0.55 mL/min and media temperature 43 °C

<b>Time (min)</b>	<b>Mean</b>	<b>SD</b>	<b>%RSD</b>
0	0	0	-
2.5	0.25	0.06	24.32
5	0.36	0.07	20.09
7.5	0.50	0.09	17.15
10	0.64	0.07	10.57
15	0.85	0.11	13.37
20	1.06	0.14	12.94
25	1.23	0.13	10.96
30	1.39	0.17	11.91
<b>Permeation rate (mg/min)*</b>	0.039	0.005	12.33
<b>Ratio of rates**</b>	1.09	0.13	12.33

\* Permeation rate was calculated from the amount of nicotine permeated from 7.5 to 30 min

\*\* Ratio of rates is the ratio of *in vitro* nicotine permeation to the *in vivo* nicotine absorption rate (0.036 mg/min)

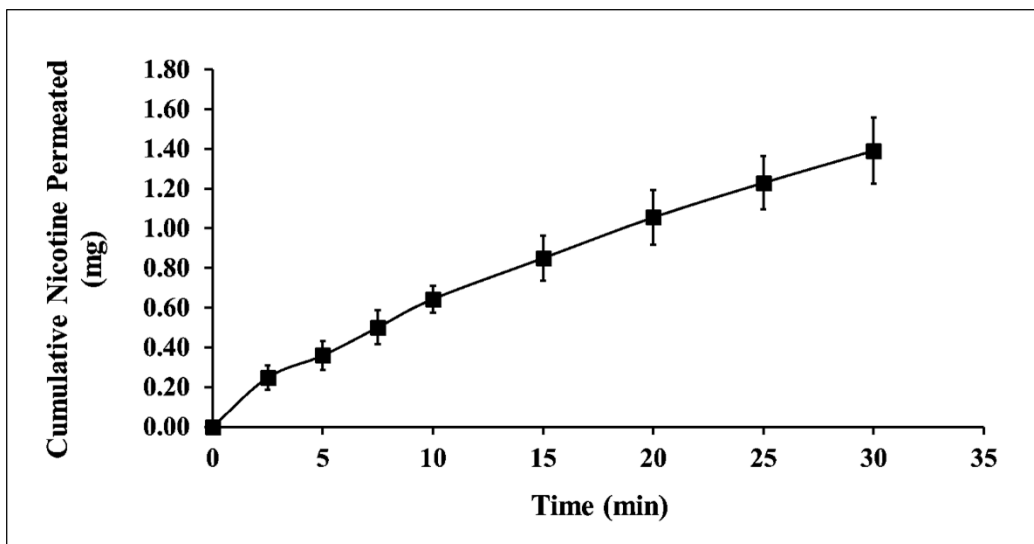


**Figure 5.11:** The mean cumulative *in vitro* nicotine permeation time profile at optimal levels of SSSR (0.55 mL/min) and media temperature (43 °C). (Error bars represent one standard deviation; n=4)

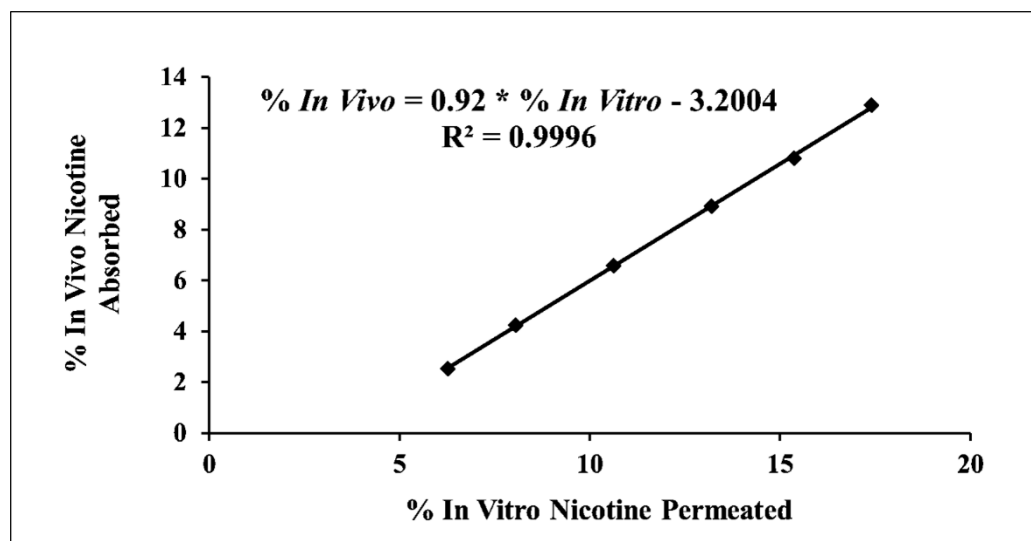


**Figure 5.12:** The *in vitro in vivo* relationship (IVIVR) plot for snus at optimal levels of SSSR (0.55 mL/min) and media temperature (43 °C) using the BTA.

## 5.4 CONCLUSIONS

An accurate prediction of the *in vivo* performance of smokeless tobacco (snus) was successfully performed employing the bidirectional transmucosal apparatus and relevant physiological (SSSR) and *in vitro* (media temperature) variables. A 3<sup>2</sup> factorial experimental design and response surface analysis allowed determination of the optimal levels of SSSR and media temperature that resulted in an IVIVR for snus with a slope of unity and with comparable *in vitro* and *in vivo* time courses. The *in vitro* nicotine permeation profile obtained at the optimal *in vitro* levels for the BTA thus can be employed as a surrogate for the *in vivo* performance for snus. The findings from Chapter 4 and the present chapter demonstrated that the BTA facilitated accurate prediction of the *in vivo* behavior of smokeless tobacco, a type of OTP, by allowing simulation of the oral cavity and adjustment of *in vitro* variables. These findings and conclusions establish the biorelevancy of the bidirectional transmucosal apparatus which can be utilized as a quality control and research tool for oral transmucosal products. To further extend application of the BTA for a different type of OTP, a study was performed on a dissolvable tobacco product called “Stonewall”. Determinations obtained from this study are presented in Chapter 6.

## CHAPTER 6

### APPLICATION OF THE BIORELEVANT BIDIRECTIONAL TRANSMUCOSAL APPARATUS FOR THE PREDICTION OF THE *IN VIVO* PERFORMANCE OF DISSOLVABLE COMPRESSED TOBACCO

#### 6.1 INTRODUCTION

The biorelevant *in vitro* system plays a key role in the research and development phase of therapeutic and non-therapeutic products and can be valuable in accurately predicting the *in vivo* behavior of these products (Wang et al. 2009; Fotaki et al. 2010). Biorelevant testing, a predictive tool, can serve as a validated surrogate for human studies, leading to fewer clinical studies and a reduction in cost along with expediting the drug development process (Emami 2006). Oral transmucosal products (OTPs) due to benefits such as quick onset of drug action and avoidance of presystemic elimination, may be preferred for systemic drug delivery. Because of these advantages, many pharmaceutical and non-pharmaceutical oral transmucosal products are commercially available and many are under development (Pather et al. 2008). OTPs are available in tablets, patches, films, sprays, lozenges, and chewing gum formulations for sublingual, buccal, gingival, or local drug delivery in the oral cavity. Since this is becoming a common route for delivery, development of a biorelevant *in vitro* system for OTPs can more effectively support such

product development at minimal cost and time. To fulfill this need, a biorelevant bidirectional transmucosal apparatus (BTA) that enables characterization of drug release and permeation from OTPs in a more realistic way was developed and validated using smokeless tobacco (snus) as a model product (Chapter 3, 4 and 5). It would be beneficial if the BTA could be employed for all types of OTPs to predict the *in vivo* performance. A single biorelevant system for all types of OTPs will prevent unnecessary replication of *in vitro* systems. Therefore, the goal of the present research was to study the application of the biorelevant BTA for a different type of OTP. A dissolvable compressed tobacco tablet (Stonewall – A Star Scientific Product, Glen Allen, Virginia) was selected for the above purpose. Dissolvable tobacco, like snus, is also placed between the cheek and gum for nicotine permeation through buccal and gingival mucosal membranes. Unlike snus, disintegration might be the rate limiting step for nicotine release from compressed tobacco attributed to the hardness of the compact; consequently, permeation may be affected. The donor media flow rate through turbulence may enhance disintegration of the Stonewall tablet and thus increase the release of nicotine (Cammarn et al. 2000), whereas, the media temperature may increase the diffusion of nicotine across the donor and receptor compartments by reducing the viscosity of the media (Section 4.2.2.2) (Othmer et al. 1953; Edward 1970; Hubley et al. 1996). Therefore, the donor media flow rate and media temperature which may influence disintegration and diffusion respectively were employed in the BTA with a target to develop an *in vitro in vivo* relationship (IVIVR) with a slope of unity for compressed tobacco.

## 6.2 MATERIALS AND METHODS

### 6.2.1 MATERIALS

Stonewall (a type of compressed smokeless tobacco, Nicotine 4.0 mg, 0.48 g tablet) for *in vitro* studies was purchased online at [www.rakuten.com](http://www.rakuten.com). Hanks' Balanced Salt (H-1387) and N-(2-hydroxyethyl)piperazine-N'-(2-ethanesulfonic acid) (HEPES, 1M) buffer for the preparation of Hank's balanced salt solution (pH 7.4) were purchased from Sigma, St. Louis, MO, USA. Potassium phosphate monobasic (anhydrous) and sodium phosphate dibasic (anhydrous) to formulate artificial saliva of pH 7.2 was obtained from Sigma, St. Louis, MO, USA. Sodium hydroxide and hydrochloric acid solution (10 N) for pH adjustment was purchased from Sigma, St. Louis, MO, USA. (-)-Nicotine hydrogen tartrate (working standard) for the assay was also purchased from Sigma, St. Louis, MO, USA. HPLC grade ammonium acetate and glacial acetic acid for the mobile phase preparation was purchased from Fisher Scientific, Fair Lawn, NJ, USA and EMD, Gibbstown, NJ, USA respectively. HPLC grade methanol was purchased from Honeywell Burdick and Jackson, Muskegon, MI, USA. High purity water was prepared in-house (the Nanopure Diamond™, Barnstead, IO, USA). Regenerated cellulose membranes (SnakeSkin Dialysis Tubing, 10K MWCO, 35mm dry diameter (ID) × 10.7m) for *in vitro* permeation studies was obtained from Thermo Scientific, Rockford, IL, USA. Fluorinated ethylene propylene (FEP) and Tygon® platinized silicon tubing for the *in vitro* apparatus were purchased from Cole-Parmer, Vernon Hills, IL, USA. Teflon unions and luer fittings for tubing connections were bought from Upchurch Scientific, Oak Harbor, WA, USA. Masterflex L/S 12-channel 8-roller cartridge pump head (Model 7519-25) and variable-speed modular drive (Model 7553-70; 6 to 600 rpm; flow rate range – 0.0006 to 41 mL/min) for circulating media through the donor chamber was purchased

from Cole-Parmer, Vernon Hills, IL, USA. Two variable medium flow mini pumps (Model 3386; flow rate range – 0.4 to 85 mL/min) for circulating media through receptor chambers were purchased from Control Company, Friendswood, TX, USA.

## 6.2.2 DESCRIPTION OF STONEWALL

Stonewall is a type of commercial smokeless tobacco compressed into a tablet. The tablet weighed  $0.47 \pm 0.01$  g (n=3). Each Stonewall tablet contained 3.40 mg of nicotine (Stepanov et al. 2012). The tablet dimensions were 1.4 cm × 0.9 cm × 0.55 cm (length × width × depth). The Stonewall tablet also contained a binder/granulating agent, a sweetener, flavorants, coloring agents, a filler/diluent, a lubricant and buffers that facilitated the granulation and compression of powdered/extracted/cured tobacco (Williams 2004). Figure 6.1 represents a picture of Stonewall used for this study. The Stonewall is placed between cheek and gum for nicotine permeation from tobacco which permeates through buccal and gingival membrane.



**Figure 6.1:** Compressed dissolvable tobacco: Stonewall



### 6.2.3 SELECTION OF VARIABLES FOR OPTIMIZATION OF IVIVR FOR STONEWALL

Nicotine release from Stonewall may be limited by disintegration of the tobacco compact. The compressed tobacco is relatively hard in comparison to the loose tobacco in snus. The hardness of the tablet may result in a decrease in nicotine release by increasing disintegration time (Jacob et al. 1968). A similar effect can be anticipated on the release of nicotine from Stonewall (tobacco compact) in the donor chamber of the BTA. As a consequence, the permeation of nicotine into the receptors of the BTA may also be limited by disintegration and slower nicotine release rate. Accordingly, *in vitro* variables that were anticipated to circumvent the effect of the hardness of Stonewall and hence nicotine release were considered for optimization. The donor media flow rate was considered because of its expected enhancement of disintegration of Stonewall and nicotine release by media turbulence (Cammarn et al. 2000). Media temperature was found to be a relevant variable that significantly increased nicotine permeation from snus in the BTA (Section 4.2.2.2 and 4.3.2). Therefore, the donor media flow rate and media temperature were employed for better prediction of the *in vivo* performance of Stonewall using the BTA. Donor media flow rates, ranging from the physiological saliva secretion rate (1.66 mL/min; (Bardow et al. 2000)) to a large *in vitro* flow rate (16 mL/min) were considered for optimization. The large donor media flow rate may enhance the disintegration of compressed tobacco through turbulence and hence permeation of nicotine into the receptor chambers of BTA. Whereas, the media temperature, ranging from 37 °C (body temperature) to 45 °C (a level higher) was employed to accurately predict the *in vivo* behavior of Stonewall. The reason for the selection of 45 °C for nicotine permeation studies with the bidirectional apparatus was explained in detail in Section 4.2.3 of Chapter 4.

#### 6.2.4 *IN VITRO* RELEASE AND PERMEATION TESTING

The bidirectional transmucosal apparatus presented in Figure 3.2(C) of Chapter 3 was used to study nicotine release and permeation from compressed tobacco (Stonewall). The *in vitro* set up consisted of similar assembly components (Silicon and FEP tubings, luer fitting and unions, reservoirs and regenerated cellulose membrane) that were employed in the previous studies (Chapter 3, 4 and 5). A single tablet of Stonewall was placed in the donor chamber which was separated from the receptors using the regenerated cellulose membrane. Twenty five mL of artificial saliva (pH 7.2,  $\beta = 7.0$ ) and Hanks' balanced salt solution (HBSS, pH 7.4) maintained at the required temperature was circulated in a closed through pattern through the donor and receptor chambers respectively using three separate pumps. The donor and receptor dead volumes were both 2.67 mL. Forty microliters and one milliliter of media was sampled from the donor and receptor reservoirs respectively at 0, 1, 5, 10, 15, 20, 25, 30, 45 and 60 min, to assess nicotine release and permeation. The sampled media was replaced with an equivalent volume of fresh media. Samples obtained from the donor reservoir were immediately subjected to centrifugation (Thomas<sup>®</sup> mini centrifuge; 6000 rpm) for 1 min in 1.5 mL capacity polypropylene micro centrifuge tubes (Biohit) to remove undissolved tobacco particles, the supernatant was used for analysis. The supernatant of donor media samples was diluted ten times with the HBBS buffer to perform nicotine analysis using the validated HPLC calibration range as these samples were expected to be concentrated with nicotine. The types of experiments performed are presented in Table 6.1. The cumulative amount of nicotine released and permeated was calculated. Nicotine concentrations that permeated into both receptor chambers of the BTA were added to represent the total cumulative permeation achieved at each time point. The method for calculation of the amount of nicotine permeated and released from Stonewall is presented in Table E0 and E9 of Appendix E respectively.

**Table 6.1:** Experiments to optimize IVIVR for Stonewall using the BTA

<b>Expt.</b>	<b>N</b>	<b>Donor media flow rate (mL/min)</b>	<b>Receptor media flow rate (mL/min)</b>	<b>Chamber Temp. Required (°C)</b>	<b>Water bath Temp. (°C)</b>	<b>Reservoir media temp. (°C)</b>	<b>Chamber media temp. (°C)</b>
1	5	<i>1.66</i>	16	<i>37</i>	45-46	40-42	33-37
2	3	<i>16</i>	16	<i>37</i>	45-46	40-42	33-37
3	5	<i>16</i>	16	<i>45</i>	59-60	50-53	38-45

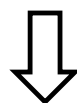
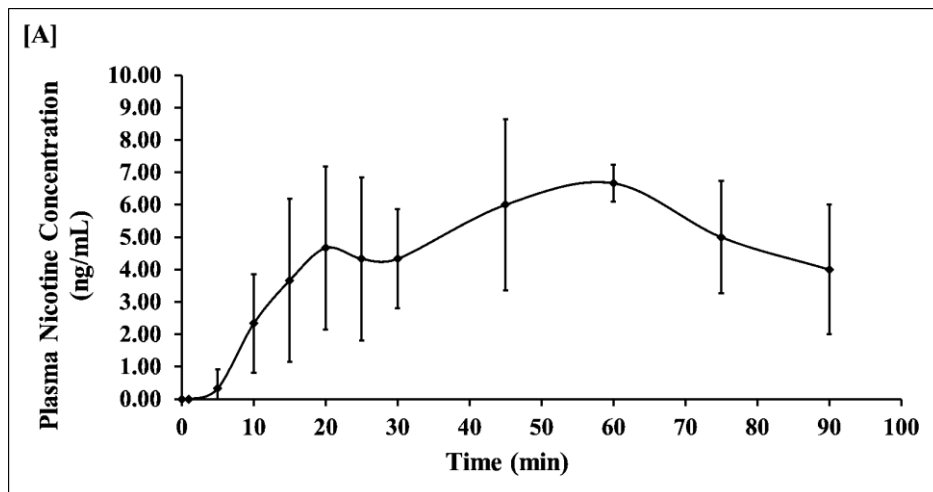
## 6.2.5 *IN VIVO* STUDY AND PHARMACOKINETIC ASSESSMENT OF STONEWALL

The plasma nicotine concentration time profile for Stonewall was obtained from a human clinical study reported in the literature (Kotlyar et al. 2007). The study was approved by an Institutional Review Board. The *in vivo* study was conducted on 10 adult smokeless tobacco users. The product was removed from the mouth after 30 min and the mouth was rinsed with water. The nicotine levels for each subject were kindly provided by Michael Kotlyar, Ph.D., the author of the above research paper. Of the 10 subjects enrolled in the study, 7 subjects showed nicotine levels below LLOQ or at the LLOQ (2 ng/mL) of the analytical method (Gas Chromatography with nitrogen phosphorous detection) in predose and postdose samples, whereas, the remaining three subjects showed nicotine levels above LLOQ in predose and postdose samples. Therefore, only the nicotine levels of three subjects who showed nicotine levels above LLOQ after baseline correction were considered for the IVIVR analysis. The baseline corrected mean plasma nicotine concentration time profile for the three subjects was deconvolved to the absorption time profile by Wagner-Nelson modeling assuming that nicotine followed one compartment kinetics (The method of deconvolution presented in detail in Section 3.2.7 of Chapter 3) (Wagner et al. 1964). All pharmacokinetic calculations were performed in Microsoft Excel 2013. Briefly, the area under the curve,  $AUC_{0-90 \text{ min}}$  [414.83 (ng/mL)\*min], was calculated by the trapezoidal method. The elimination rate constant ( $k_e$ ;  $0.004 \text{ min}^{-1}$ ) from an intravenous (IV) infusion pharmacokinetic study on 20 healthy adults reported in the literature was used to calculate  $AUC_{0-\infty}$  [1414.83 (ng/mL)\*min] for Stonewall (Molander et al. 2001). The cumulative amount of nicotine (mg) absorbed as a function of time (min) was calculated from the fraction of nicotine absorbed ( $\frac{A_t}{A_\infty}$ ) obtained by the Wagner-Nelson modeling and absolute bioavailability (F) (considering 4 mg as

the nominal dose, 4 mg is the nominal amount of nicotine present in Stonewall) based on the Equation below:

$$A_t = \frac{(\text{Cumulative \% nicotine absorbed} \times F \times 4)}{100} \quad \text{----- Eq. 6.1}$$

where,  $A_t$  is the cumulative amount of nicotine absorbed at time  $t$  (mg);  $F$  is the absolute bioavailability of nicotine from Stonewall; 4 mg refers to the nominal amount of nicotine present in Stonewall. The absolute bioavailability of nicotine from Stonewall was 0.39 [The  $AUC_{0-\infty, IV}$  and Dose  $_{IV}$  was 1596 ng\*min/mL and 1.77 mg respectively (Molander et al. 2001)]. Figure 6.2 displays the mean nicotine concentration and absorption time profile for Stonewall obtained from three subjects. The cumulative percent nicotine (% of 4 mg) absorption time profile can be related to the cumulative percent nicotine (% of 4 mg) permeation time profile obtained using the BTA for IVIVR. The nicotine absorption data shown in Figure 6.2(B) from 5 to 20 min was used to calculate *in vivo* absorption rate (0.083 mg/min) which was compared to the *in vitro* nicotine permeation rate. The time frame of 5 to 20 min was considered because of the lag time of 1 min and the unusual flat profile observed from 20 to 30 min.



**Deconvolution: Wagner-Nelson Modeling  
Correction based on the absolute bioavailability**

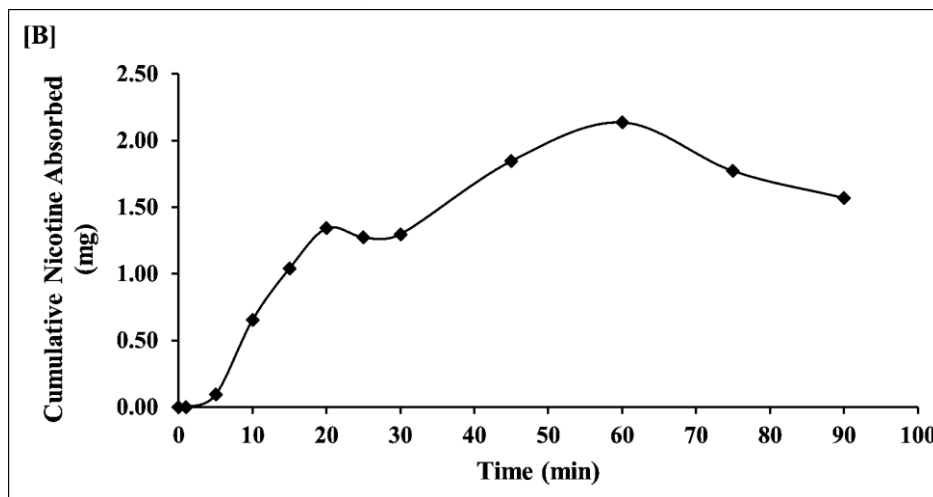


**Figure 6.2:** Deconvolution of plasma nicotine concentration time profile for Stonewall by Wagner-Nelson modeling [A] The mean plasma nicotine concentration time profile for three subjects (Error bars represent one standard deviation; n=3); [B] The mean nicotine absorption time profile for three subjects.

## 6.2.6 SAMPLE ANALYSIS

The samples obtained from *in vitro* experiments on Stonewall using the BTA were analyzed for nicotine release and permeation using the validated HPLC method reported in Chapter 2. HPLC analysis was performed using Waters 600E multisolvent delivery system with a Waters 717 autosampler and 996 Waters photodiode array (PDA) detector. Like snus, *in vitro* nicotine samples of Stonewall also contained tobacco components and excipients in addition to nicotine. External standards of nicotine prepared in HBSS (pH 7.4) were used for the analysis as it was not possible to prepare standards with the matrix containing tobacco and excipients present in Stonewall. The HPLC method for nicotine analysis in samples obtained from *in vitro* studies of snus was appropriately validated qualitatively and quantitatively (Chapter 3). However, the matrix present in snus and Stonewall differed substantially, which required selectivity testing of the HPLC method for *in vitro* samples from Stonewall. Therefore, standard addition and peak purity experiments were performed to test the selectivity of the HPLC method in the presence of Stonewall matrix.

The standard addition method described in Chapter 2 was employed for the assessment of matrix effect in the *in vitro* samples of Stonewall. Both the donor and receptor chamber *in vitro* samples at 60 min were tested for the selectivity of nicotine analysis. Briefly, nine hundred fifty microliters of the *in vitro* sample (Receptor sample – undiluted; donor sample – 25 times diluted before spiking) of Stonewall was spiked with 10, 20, 40, 80, 160, 320 and 640 µg/mL of nicotine in HBSS buffer separately. The spiking was performed in replicates of three. The spiked samples and external nicotine standards were analyzed at 250 – 270 nm wavelength range with 260 nm as the output wavelength. The peak area responses for spiked (donor and receptor chamber spiked samples) and external nicotine standards obtained, were plotted against true nicotine

concentrations. The slopes of standard addition and external calibration curves were statistically compared (Student t-test at  $\alpha=0.05$ ).

Peak purity testing using the Waters 996 PDA detector and Empower software was performed on the donor and receptor chamber samples obtained at 60 min from the *in vitro* experiment for the assessment of interference. The donor sample was diluted twenty five fold with HBBS buffer before injection and peak purity analysis. The dilution of donor sample was performed to represent the real situation where the donor sample is diluted for quantification within the calibration range. The testing was performed using the autothreshold method in a similar manner as described in Chapter 2. Each donor and receptor sample was injected in triplicate for peak purity analysis along with lower (0.5  $\mu\text{g/mL}$ ) and higher (32  $\mu\text{g/mL}$ ) nicotine external standards. Purity and threshold angles (Refer Chapter 2) at the nicotine retention time for each sample were obtained and compared.

Other selectivity tests reported in Chapter 2 were not studied for Stonewall, as the above methods were tested at 250 – 270 nm; a selective wavelength range for nicotine analysis with 260 nm as its wavelength maxima. The use of 250 - 270 nm wavelength range avoided the contribution of a leachable substance from the neoprene O ring; which was also employed in the present BTA set up for preventing leaks; to the nicotine response that absorbed in the wavelength range of 200 – 242 nm.

#### 6.2.7 DATA ANALYSIS

The nicotine release/permeation rate (mg/min) (rate after lag time) was calculated from the slope of the linear portion of the nicotine release/permeation (mg)-time (min) profile. The lag time (min) for release and permeation was calculated from the X-intercept of the fitted line. The rates



obtained were compared to study the effect of donor media flow rate and media temperature on the release and permeation of nicotine from Stonewall when BTA is employed. Appropriate statistical analysis (Student t-test at  $\alpha = 0.05$ ) was performed to compare the release/permeation rates obtained as a function of donor media flow rate and media temperature. All statistical analysis was performed using JMP Pro 10. The *in vitro* nicotine permeation rate for Stonewall obtained at each of the experimental conditions was compared to the *in vivo* nicotine absorption rate and a ratio was calculated. A ratio of *in vitro* to *in vivo* rates( which is also the inverse of the IVIVR slope; *in vivo* absorption; Y versus *in vitro* permeation; X); of one was desired in order to use the *in vitro* profile as a surrogate for the *in vivo* behavior of the product.

## **6.3 RESULTS AND DISCUSSION**

### **6.3.1 SAMPLE ANALYSIS**

The comparisons of the mean standard addition curve with the external calibration curve obtained with the spiked donor and receptor samples are illustrated in Figures 6.3(A) and 6.3(B) respectively. The individual peak areas of the external standards and spiked donor and receptor samples obtained from replicate analysis are presented in Tables E1-E2 of Appendix E. The slopes of both; standard addition and external calibration curves; for the donor and receptor spiked samples were not significantly different (Equal variance t-test at  $\alpha=0.05$ ; donor *in vitro* spiked sample:  $t = -1.38$ ,  $df = 4$ ,  $p\text{-value} = 0.2384$ ; receptor *in vitro* spiked sample:  $t = -1.82$ ,  $df = 4$ ,  $p\text{-value} = 0.1429$ ). This result suggested the absence of a matrix effect or proportional error in the analysis of nicotine in the *in vitro* samples of Stonewall.

Table 6.2 tabulates the purity and threshold angles obtained by the autothreshold peak purity testing method at 250-270 nm for nicotine external standards and the *in vitro* donor and receptor samples. The replicate peak purity data for the donor and receptor Stonewall samples are shown in Tables E3 and E4 of Appendix E respectively. The peak purity results in Table 6.2 suggest that the nicotine peaks from standards were spectrally and chromatographically pure (purity angles < threshold angles). Whereas, the nicotine peaks from *in vitro* donor and receptor samples were considered only spectrally pure (purity angles < threshold angles) since the coelution of the leachable from the neoprene O ring was possible. The peak purity analysis confirmed the absence of interference during the analysis of nicotine *in vitro* samples of Stonewall based on the spectral purity of the peaks.

It was concluded from the standard addition method and peak purity testing that the HPLC method reported in Chapter 2 is selective for the analysis of nicotine in the *in vitro* samples of Stonewall obtained from experiments performed in the bidirectional transmucosal apparatus.

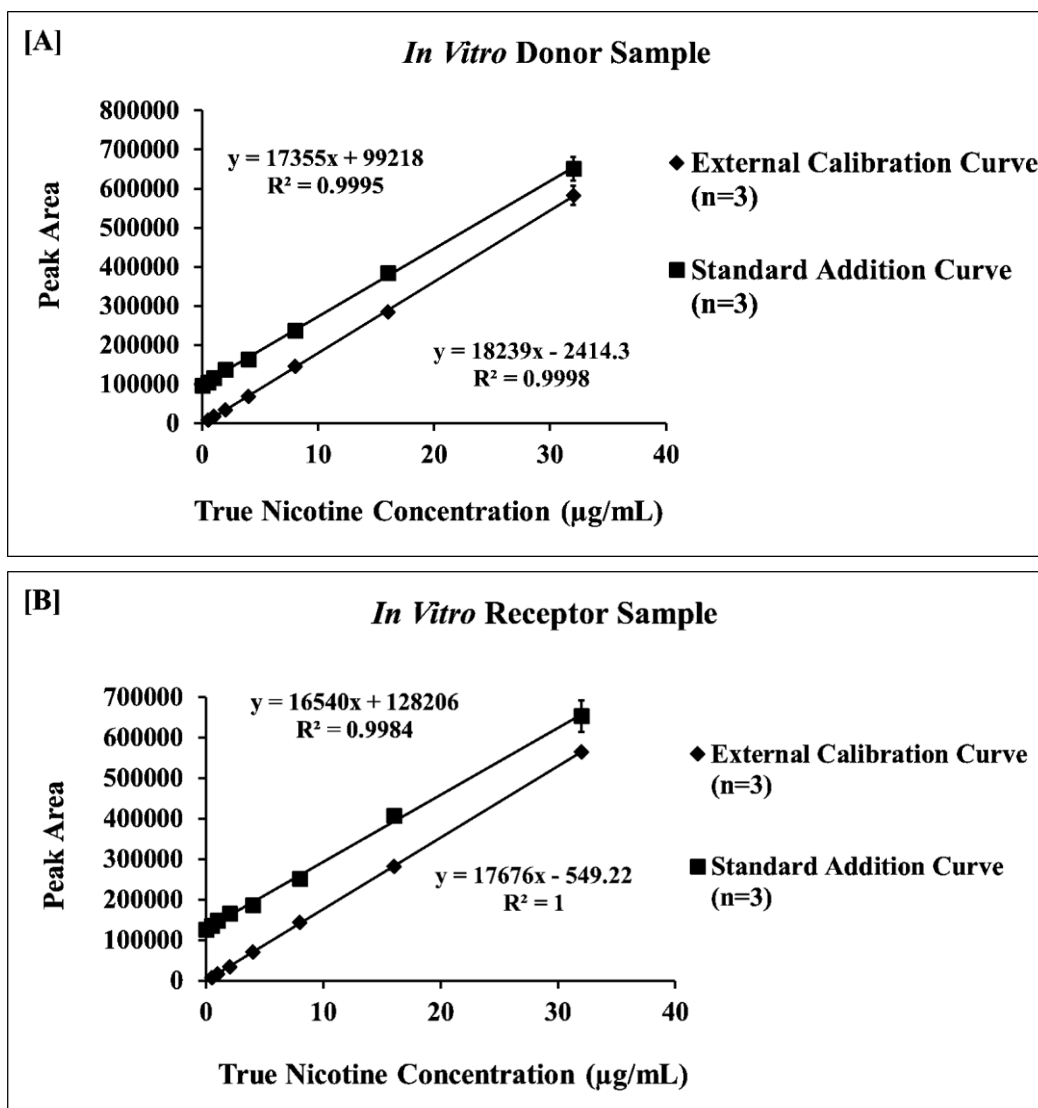


**Figure 6.3:** Comparison of the standard addition and external calibration curves [A] Spiked donor *in vitro* sample; [B] Spiked receptor *in vitro* sample. (Error bars represent one standard deviation;  $n=3$ )

**Table 6.2:** Peak purity testing on the nicotine standards and *in vitro* samples using the autothreshold method\*

<b>Donor <i>In Vitro</i> Sample**</b>			
	Purity Angle	Threshold Angle	Interpretation***
Nicotine standard (0.5 µg/mL)	2.144	8.657	Pure peak
Nicotine standard (32 µg/mL)	0.067	0.381	Pure peak
Donor sample at 60 min	0.695	0.931	Spectrally pure
<b>Receptor <i>In Vitro</i> Sample**</b>			
	Purity Angle	Threshold Angle	Interpretation***
Nicotine standard (0.5 µg/mL)	1.642	4.258	Pure peak
Nicotine standard (32 µg/mL)	0.054	0.285	Pure peak
Receptor sample at 60 min	0.408	0.487	Spectrally pure

\* Each purity angle and threshold angle value represents a mean of n=3

\*\* Peak purity analysis was performed at the wavelength range of 250-270 nm

\*\*\* Pure peak = Chromatographically and spectrally pure peak

### 6.3.2 EFFECT OF DONOR MEDIA FLOW RATE AND MEDIA TEMPERATURE ON NICOTINE RELEASE/PERMEATION FROM STONEWALL

The mean nicotine permeation profiles, permeation rates and the ratio of *in vitro* to *in vivo* rates obtained at different donor media flow rates (1.66 and 16 mL/min) and media temperatures (37 and 45 °C) are presented in Figure 6.4, Table 6.3 and Table 6.4 respectively. The mean nicotine release profiles and release rates are shown in Figure 6.5 and Table 6.5 respectively. The amount of nicotine permeated/released as a function of time and the permeation/release rates obtained from each replicate experiment are shown in Tables E5-E13 of Appendix E. The nicotine permeation rate was significantly faster at 16 mL/min (37°C) than 1.66 mL/min (37°C) of donor media flow rate (Table 6.3). The increase in donor media flow rate may have resulted into an increase in media turbulence in the donor chamber of the BTA. The increase in media flow rate and turbulence has been found to accelerate the disintegration of tablets (Cammarn et al. 2000; Gao 2009). Therefore, the disintegration time of Stonewall possibly would decrease with the increase in donor media flow rate. In consequence, the release rate of nicotine from Stonewall significantly increased with an increase in the donor media flow rate (Table 6.5 and Figure 6.5) and thus enhancing the nicotine concentration in the donor chamber. The resultant effect of the above phenomenon would be increase in the gradient across the donor and receptor chambers of the BTA leading to significantly faster permeation based on the Fick's Law (Section 4.2.2.1 of Chapter 4). The study of the donor media flow rate on the *in vitro* behavior of Stonewall also indicated that disintegration might be the rate limiting step in the release and permeation of nicotine. The *in vitro* permeation rates at both 1.66 and 16 mL/min when media temperature was maintained at 37°C were slower than the *in vivo* nicotine absorption rate (0.083 mg/min) indicated by the ratio of rates of less than one (0.04 and 0.10 respectively; Table 6.4). The above results

suggest a need for increasing the *in vitro* nicotine permeation rate for accurate prediction of the *in vivo* performance of Stonewall. Therefore, media temperature was employed for enhancing the permeation rate of nicotine as it was found to be an important variable in the optimization of IVIVR for snus (Chapter 4).

The permeation of nicotine significantly increased as a function of the media temperature (Table 6.3). The above result could be attributed to a reduction in media viscosity and increase in the diffusion coefficient of nicotine when the media temperature was increased based on Stokes-Einstein theory (Section 4.2.2.2 of Chapter 4). The increasing diffusion coefficient resulted into an increase in the permeation rate of nicotine from the donor to receptor chambers of the BTA (Fick's law of diffusion, Section 4.2.2.2 or Chapter 4). A similar effect involving media temperature was not observed on the nicotine release rate from Stonewall. The nicotine release rate at temperatures of 37 and 45°C were not significantly different (Table 6.5). This observation may be either due to the huge variability in the release rate at 37 and 45°C or the absence of an effect of temperature on disintegration of Stonewall which may have been the rate limiting step in the release of nicotine. The nicotine permeation rate (0.012 mg/min) obtained by increasing the media temperature to 45°C was not comparable to the *in vivo* nicotine absorption rate (0.083 mg/min) as suggested by the ratio of *in vitro* to *in vivo* rates of less than one (0.14; Table 6.4). The results obtained from the above studies suggests the need for adjustment of other variables in order to better predict the *in vivo* behavior of Stonewall using the BTA.

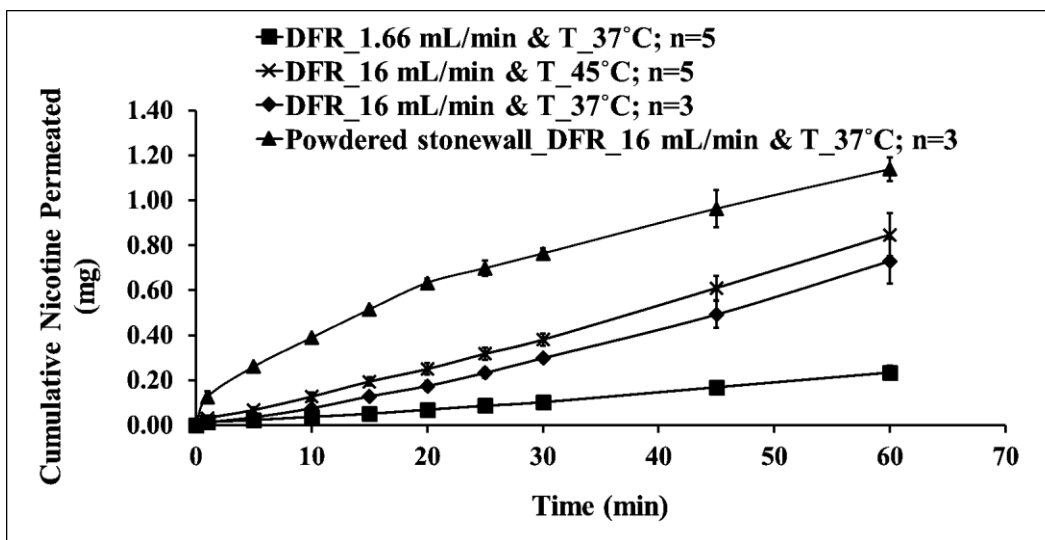


**Figure 6.4:** The mean cumulative nicotine permeation time profile for Stonewall at different donor media flow rates (DFR; mL/min) and media temperatures (T; °C); the line was fitted to the linear portion of the profile from 5 to 20 min;  $Y=0.003*X+0.0074$ ,  $R^2=0.99$  (DFR\_1.66 mL/min & T\_37°C);  $Y=0.0094*X-0.014$ ,  $R^2=0.99$  (DFR\_16 mL/min & T\_37°C);  $Y=0.0122*X+0.0069$ ,  $R^2=0.99$  (DFR\_16 mL/min & T\_45°C);  $Y=0.0249*X+0.1389$ ,  $R^2=0.99$  (Powdered Stonewall\_DFR\_16 mL/min & T\_37°C). (Error bars represent one standard deviation)

**Table 6.3:** Nicotine permeation rate from Stonewall as a function of donor media flow rate and media temperature

Donor media flow rate (mL/min)	Media temperature (°C)	N	Permeation Rate** (mg/min)			Statistical Test	Statistical Results
			Mean	SD	%RSD		
1.66	37	5	0.003*	0.001	18.50	*t(6) =7.51; p-value=0.0003; Significant	
16	37	3	0.009* <sup>\$</sup> #	0.002	18.50	Equal variance t-test at $\alpha=0.05$ \$t(6)=3.59; p-value=0.0115; Significant	
16	45	5	0.012 <sup>\$</sup>	0.001	7.60	#t(4)=16.85; p-value<0.0001 Significant	
16 <sup>^</sup>	37 <sup>^</sup>	3	0.025 <sup>#</sup>	0.001	2.04		

\*\* The rate was calculated from the linear portion of the permeation profile from 5 to 20 min

<sup>^</sup> Stonewall was crushed in a mortar and pestle to a uniform particle size for *in vitro* release and permeation studies

**Table 6.4:** The ratio of *in vitro* nicotine permeation to the *in vivo* absorption rate\* from Stonewall as a function of donor media flow rate and media temperature

Donor media flow rate (mL/min)	Media temperature (°C)	N	Ratio of <i>In Vitro</i> Nicotine Permeation to <i>In Vivo</i> Nicotine Absorption Rate* <sup>\$</sup>		
			Mean	SD	%RSD
1.66	37	5	0.04	0.01	18.5
16	37	3	0.10	0.02	18.5
16	45	5	0.14	0.01	7.6
16 <sup>^</sup>	37 <sup>^</sup>	3	0.30	0.01	2.0

\* *In vitro* nicotine permeation and *in vivo* nicotine absorption rates were calculated from the permeation and absorption profiles from 5 to 20 min respectively

<sup>\$</sup> *In vivo* nicotine absorption rate was 0.083 mg/min

<sup>^</sup> Stonewall was crushed in a mortar and pestle to a uniform particle size for *in vitro* release and permeation studies



It was concluded from the donor media flow rate and temperature studies, that disintegration could be the rate limiting step for the release and permeation of nicotine from Stonewall. A similar effect could also be anticipated *in vivo* for Stonewall. The rate limiting step of disintegration for Stonewall could justify the observation of nicotine levels being below LLOQ in seven subjects out of ten enrolled in the study. In these seven subjects, the nicotine release could be slower due to the rate limiting step of disintegration of stonewall. In addition, swallowing of the saliva containing released nicotine from Stonewall might have led to loss of nicotine that would have been available for oral transmucosal absorption. The above explanations possibly justify the nicotine levels observed to be below LLOQ in most of the subjects in the clinical study. Three subjects that showed measurable nicotine levels might have crushed or otherwise agitated the Stonewall tablet instead leaving it placed between the cheek and gum. This crushing of Stonewall could lead to faster release and permeation of nicotine *in vivo* due to the instant disintegration. In order to confirm this reasoning, an *in vitro* experiment was performed using crushed Stonewall in the biorelevant BTA. A single tablet of Stonewall was crushed using a mortar and pestle and the Stonewall powder was placed in the donor chamber of the BTA. The experiment was performed in triplicate at the conditions mentioned in Section 6.2.4 at 16 mL/min of donor media flow rate and 37°C temperature. The nicotine permeation and release profiles obtained from crushed Stonewall are illustrated in Figures 6.4 and 6.5 respectively. The permeation and release of nicotine from powdered Stonewall was significantly faster in comparison to compact Stonewall (Tables 6.3 and 6.5). This significant effect on the nicotine permeation and release rate can be related to the absence of a disintegration step when powdered Stonewall was used. The faster release of nicotine with the powdered Stonewall led to a larger gradient across the BTA chambers and therefore resulted into faster permeation as per Fick's Law (Section 4.2.2.2 of Chapter 4). However, the

release of nicotine from powdered Stonewall was not complete (1.88 and 2.60 mg at 10 and 60 min respectively) which could be due to the entrapment of nicotine in granules that existed after crushing. In addition, the *in vitro* nicotine permeation rate obtained with powdered Stonewall was slower than the *in vivo* absorption rate of nicotine in the clinical study which suggests that perhaps another relevant variable should be incorporated into the BTA that might explain the measurable levels of nicotine observed for of the three subjects and predict the *in vivo* behavior of Stonewall. Agitation and a larger range of donor media flow rate along with high media temperature might be incorporated in the BTA system in an attempt to predict the *in vivo* performance of Stonewall in three subjects considered for IVIVR. Agitation would require modification of the BTA system as discussed in Section 4.3.2 of Chapter 4. In addition, a mesh type holder that can retain the Stonewall tablet in the center of the donor chamber of the BTA along with a stir bar for agitation could be incorporated. This would allow exposure of the disintegrated tablet uniformly to the artificial membranes. It was observed that Stonewall and disintegrated Stonewall tablet remained at the bottom of the donor chamber throughout the experiment which did not allow for uniform exposure of tablet particles to membranes. This could be one of the reasons for slower *in vitro* permeation of nicotine from Stonewall than *in vivo* absorption observed in three subjects. However, it is important to highlight that three subjects considered for IVIVR could be considered outliers as majority of the subjects showed immeasurable nicotine levels. Therefore, efforts for predicting the *in vivo* behavior of Stonewall in outliers may not be very useful.

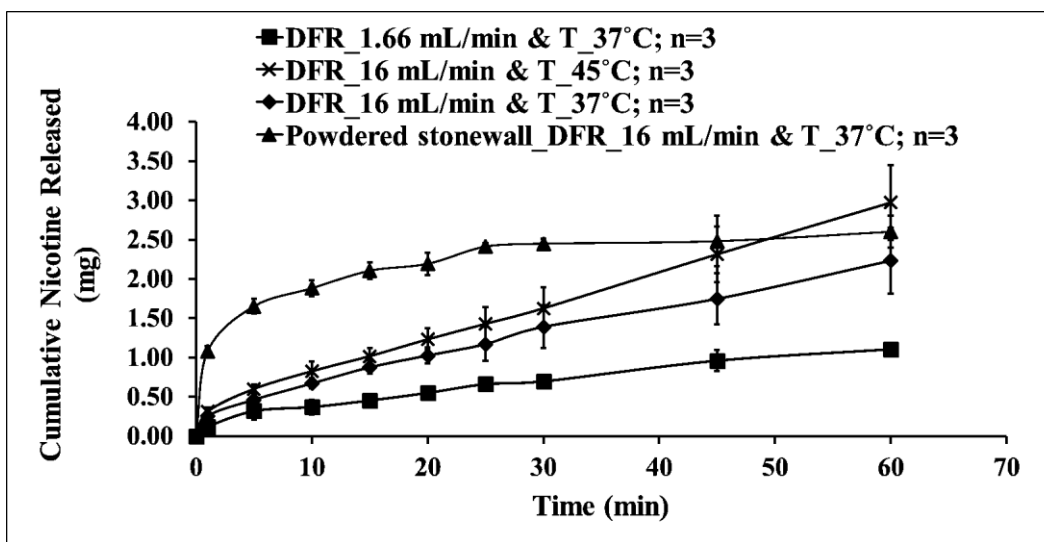


**Figure 6.5:** The mean cumulative nicotine release time profile for Stonewall at different donor media flow rates (DFR; mL/min) and media temperatures (T; °C); the line was fitted to the linear portion of the profile from 1 to 60 min except in the case of powdered Stonewall where fitting was performed in the range of 1 to 10 min;  $Y=0.0161*X+0.206$ ,  $R^2=0.97$  (DFR\_1.66 mL/min & T\_37°C);  $Y=0.0325*X+0.332$ ,  $R^2=0.99$  (DFR\_16 mL/min & T\_37°C);  $Y=0.0438*X+0.3442$ ,  $R^2=0.99$  (DFR\_16 mL/min & T\_45°C);  $Y=0.0871*X+1.0755$ ,  $R^2=0.99$  (Powdered Stonewall\_DFR\_16 mL/min & T\_37°C). (Error bars represent one standard deviation; n=3)

**Table 6.5:** Nicotine release rate from Stonewall as a function of donor media flow rate and media temperature

Donor media flow rate (mL/min)	Media temperature (°C)	N	Release Rate** (mg/min)			Statistical Test	Statistical Results
			Mean	SD	%RSD		
1.66	37	3	0.016*	0.001	2.85	*t(4) =3.68; p-value=0.0213; Significant	
16	37	3	0.032*\$#	0.008	23.37	Equal variance t-test at $\alpha=0.05$ \$t(4)=1.87; p-value=0.1353; Not significant	
16	45	3	0.044\$	0.007	16.91	#t(4)=5.01; p-value=0.0074 Significant	
16 <sup>^</sup>	37 <sup>^</sup>	3	0.087#	0.017	19.88		

\*\* The rate was calculated from the linear portion of the release profile from 1 to 60 min

<sup>^</sup> Stonewall was crushed in a mortar and pestle to a uniform particle size for *in vitro* release and permeation studies. The rate was calculated from the linear portion of the release profile from 1 to 10 min

### 6.3.3 RELATIONSHIP BETWEEN NICOTINE RELEASE AND PERMEATION RATE

A significant increase in the permeation rate of nicotine from Stonewall in the BTA was obtained as a function of donor media flow rate (1.66 vs 6 mL/min) and media temperature (37 vs 45 °C). A similar effect on the nicotine release rate was observed at the same levels of donor media flow rates (1.66 vs 6 mL/min) at media temperature of 37 °C. An increase in the permeation of nicotine with increasing donor media flow rate was attributed to an increase in the nicotine release rate under similar experimental conditions (Section 6.3.2). The increase in nicotine release rate might increase the nicotine gradient across the BTA chambers which could lead to a faster permeation rate. For the confirmation of this, the nicotine permeation rate (mg/min) was related to the nicotine release rate (mg/min) obtained at donor media flow rate and media temperature conditions as presented in Figure 6.6. The nicotine release and permeation rate for Stonewall in the BTA showed a significant linear relationship ( $F(1,10) = 115.41$ ,  $p\text{-value} < 0.05$ ,  $\alpha=0.05$ ,  $R^2=0.92$ ). The significant linear relationship between release and permeation rate confirmed that the nicotine gradient across the donor and receptor chambers of BTA increased with an increase in the release rate, leading to faster permeation of nicotine. In addition, it was concluded that the *in vitro* behavior of Stonewall in the BTA follows Fick's Law of Diffusion.

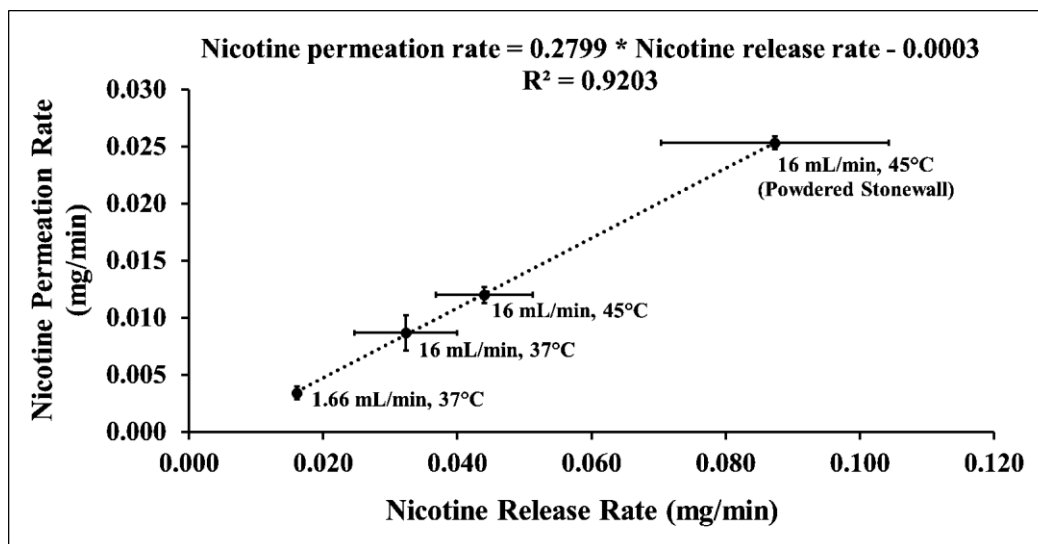


**Figure 6.6:** The relationship between nicotine release rate and permeation rate from Stonewall in the bidirectional transmucosal apparatus; each point on the graph represents mean value; whereas, the line equation was obtained by fitting individual values. (Error bars represent one standard deviation)

## 6.4 CONCLUSIONS

The present study was carried out in order to study application of the bidirectional transmucosal apparatus for predicting the *in vivo* behavior of Stonewall, a dissolvable compressed tobacco product. Stonewall has characteristics that are different from snus, the product that was employed for the development and evaluation of the BTA. The donor media flow rate and media temperature were selected for optimization of the IVIVR for Stonewall which were found to be relevant variables for snus. Both the donor media flow and media temperature showed a significant effect on the permeation of nicotine from Stonewall; however, the *in vitro* nicotine permeation was slower than the *in vivo* nicotine absorption at all conditions studied. Therefore, an optimal IVIVR for Stonewall was not obtained as opposed to snus for which reliable clinical data were available. Additionally, the *in vivo* data of Stonewall considered for IVIVR were obtained from outliers of the clinical study as only these subjects showed measurable nicotine. Further, the disintegration of compressed tobacco might be considered to be a rate limiting step for nicotine permeation in the BTA system as well as absorption *in vivo*. The present research on Stonewall suggests the need for incorporation and adjustment of additional variables and appropriate modification of the BTA for better prediction of the *in vivo* performance in outliers. Variables such as agitation may enhance nicotine permeation and optimize prediction of the *in vivo* performance of Stonewall using the BTA. However, the applicability of the prediction of the *in vivo* behavior in outliers should be considered before efforts are made to modify BTA. The research presented in this chapter establishes the potential for prediction of the *in vivo* behavior of compressed OTPs like Stonewall using a biorelevant BTA through IVIVR when reliable clinical data are available.

## CHAPTER 7

### SUMMARY AND GENERAL CONCLUSIONS

The role of dissolution/release/permeation in *in vitro* testing has been expanded from traditional quality control application to research and development of pharmaceutical and non-pharmaceutical products. Biorelevant *in vitro* testing is needed as an inexpensive resource to address questions related to the *in vivo* performance of products. Therapeutic and non-therapeutic oral transmucosal products (OTPs) are currently evaluated by standard/compendial *in vitro* methods which are not adequate predictors of the *in vivo* performance of these products. Therefore, the goal of the current investigation was to address the limitations of the standard *in vitro* methods employed for the testing of OTPs. This research involved the development and validation of a novel biorelevant *in vitro* system, the bidirectional transmucosal apparatus (BTA), for accurate prediction of the *in vivo* behavior of OTP. To reach this objective, a combination of apparatus design, relevant oral cavity physiological variables and *in vitro* variables were investigated. Validation of the *in vitro* device for its role as an accurate *in vivo* predictor of OTPs was performed using snus (a type of commercial smokeless tobacco) as a product. Snus was selected due to the availability of the *in vivo* data for nicotine to evaluate the predictability of the BTA.



An HPLC method was developed and validated for the analysis of *in vitro* samples obtained from the research investigation. Particular focus was on testing the selectivity of the HPLC method for the analysis of nicotine in the *in vitro* samples in the presence of tobacco components and snus excipients. The analysis was performed using external standards for nicotine and demonstrating the selectivity of the method for nicotine analysis by the standard addition method, peak purity testing and peak trapping and mass spectrometry identification. A contribution to the nicotine response from a leachable component of the Neoprene O ring was avoided by choosing a more selective wavelength range for nicotine. This part of the research provided a strategy for testing the selectivity of an analytical method, a critical step for *in vitro* studies, especially when matched matrix is not available.

The designing of the *in vitro* system, the bidirectional transmucosal apparatus (BTA), a first approach for the incorporation of biorelevance for OTPs, has been described. The BTA allowed simulation of saliva secretion and swallowing rate, bidirectional permeation barriers, chewing effect and blood flow rate which may be significant physiological factors that affect drug release and permeation from OTPs. This design also allowed the adjustment of the *in vitro* variables (media flow rate, media volume, media temperature) for accurate prediction of the *in vivo* behavior of OTPs. The BTA was validated for apparatus orientation, membrane selection for permeation and lack of nicotine adsorption onto the apparatus. The commercially available modified USP IV flow through apparatus and the vertical diffusion cell commonly used for semi-solid and transdermal products were employed to test the suitability of the BTA for OTPs by direct comparison. The BTA was selected for further testing of its biorelevancy for snus despite of a lack of optimal IVIVR (IVIVR slope of unity) on a first attempt with all three apparatuses. The selection

of the BTA was based on its greater number of possibilities for simulation and adjustment of variables for optimization of IVIVR which were not feasible with the USP IV and VDC.

The novel BTA was further explored to study the effect of oral cavity physiological and *in vitro* variables on nicotine release and permeation. This was crucial to identify relevant parameter that would allow accurate prediction of the *in vivo* behavior of snus. Pre-screening of all possible variables indicated saliva secretion and swallowing rate (SSSR), media temperature, receptor dead volume and agitation as critical parameters that can be optimized to obtain *in vitro* nicotine profiles as a surrogate for the *in vivo* behavior of snus. However, only SSSR and media temperature was further employed because of the lack of physiological relevance with dead volume and experimental issues related to agitation because of the apparatus design. The effect of SSSR and media temperature on nicotine permeation could be explained mechanistically by diffusion theory. The optimal *in vitro* levels of SSSR and media temperature determined by multifactorial experimental design were 0.55 mL/min and 43 °C. These levels successfully provided comparable *in vitro* and *in vivo* profiles as indicated by an IVIVR slope of 0.92. The results of this part of the research provided good evidence for a biorelevant device through combining apparatus design with carefully selected variables. The BTA proved to be a valid predictor for snus.

In an attempt to test the broad applicability of the BTA device for other OTPs, Stonewall, a dissolvable compressed tobacco that behaved completely differently than snus *in vivo*, was tested. Though an optimized IVIVR for Stonewall was not obtained with the BTA device, results of this investigation indicated the possibility of having comparable *in vitro* and *in vivo* profiles of Stonewall by adjusting *in vitro* variables. The lack of a good IVIVR was attributed to the lack of reliable clinical data for Stonewall. The clinical data of Stonewall were not reliable since only 3 out of 10 subjects showed measurable nicotine levels which may be either due to an inappropriate study or inconsistent *in vivo* behavior of Stonewall. However, if reliable clinical data were

available and optimal IVIVR is not obtained, an appropriate modification of the apparatus to incorporate agitation and include an assembly to hold the Stonewall tablet in order to provide the required hydrodynamics for accurate prediction could be considered.

The novel BTA device offers a superior platform for the evaluation of OTPs. The incorporation of simulated chewing, mixing of the media within the chambers, an assembly to hold in place a tablet type of OTPs and water jackets for accurate temperature maintenance are some options that can be explored to broaden the applicability of the BTA. The BTA system provides a foundation for building an *in vitro* device capable of incorporating modifications for all types of OTPs. Automation of the BTA can be carried out to facilitate ease of operation and to provide more reproducible results. Application of the BTA for setting clinically relevant specifications and prediction of the *in vivo* performance of bioadhesive OTPs and orally disintegrating OTPs should be further explored. The evaluation of BTA as a discriminatory tool for OTPs of different drug strengths or drug release mechanisms is also suggested.

In conclusion, the current research shows the potential for use of the novel bidirectional transmucosal *in vitro* device for the development of OTPs. The device is also promising as an accurate *in vivo* predictor for quality control and research of OTPs. It is the expectation that the novel BTA device will be investigated for further advancement and improvement in broadening its applicability for different OTPs. The bidirectional transmucosal apparatus is potentially applicable to the development and regulation of pharmaceutical OTPs as well as tobacco oral transmucosal products that have been studied here.

## REFERENCES

- Abdelbary, G., Eouani, C., Prinderre, P., et al. (2005). Determination of the in vitro disintegration profile of rapidly disintegrating tablets and correlation with oral disintegration. *International Journal of Pharmaceutics*, 292(1), 29-41.
- Arce, L., Rios, A. & Valcarcel, M. (1998). Determination of anti-carcinogenic polyphenols present in green tea using capillary electrophoresis coupled to a flow injection system. *Journal of Chromatography A*, 827(1), 113-120.
- Azarmi, S., Roa, W. & Löbenberg, R. (2007). Current perspectives in dissolution testing of conventional and novel dosage forms. *International Journal of Pharmaceutics*, 328(1), 12-21.
- Bardow, A., Moe, D., Nyvad, B., et al. (2000). The buffer capacity and buffer systems of human whole saliva measured without loss of CO<sub>2</sub>. *Archives of Oral Biology*, 45(1), 1-12.
- Basilicata, P., Miraglia, N., Pieri, M., et al. (2005). Application of the standard addition approach for the quantification of urinary benzene. *Journal of Chromatography B*, 818(2), 293-299.
- Benowitz, N., Jacob III, P. & Savanapridi, C. (1987). Determinants of nicotine intake while chewing nicotine polacrilex gum. *Clinical Pharmacology and Therapeutics*, 41, 467-473.
- Brown, C. K., Friedel, H. D., Barker, A. R., et al. (2011). FIP/AAPS Joint Workshop Report: Dissolution/In Vitro Release Testing of Novel/Special Dosage Forms. *AAPS PharmSciTech*, 1-13.
- Bryant, D. K., Kingswood, M. D. & Belenguer, A. (1996). Determination of liquid chromatographic peak purity by electrospray ionization mass spectrometry. *Journal of Chromatography A*, 721(1), 41-51.
- Caka, F. M., Eatough, D. J., Lewis, E. A., et al. (1990). An intercomparison of sampling techniques for nicotine in indoor environments. *Environmental Science and Technology*, 24(8), 1196-1203.
- Cammarn, S. R. & Sakr, A. (2000). Predicting dissolution via hydrodynamics: salicylic acid tablets in flow through cell dissolution. *International Journal of Pharmaceutics*, 201(2), 199-209.

- Cappendijk, S. L., Pirvan, D. F., Miller, G. L., et al. (2010). In vivo nicotine exposure in the zebra finch: a promising innovative animal model to use in neurodegenerative disorders related research. *Pharmacology, Biochemistry and Behavior*, 96(2), 152-159.
- Chen, L. L., Chetty, D. J. & Chien, Y. W. (1999). A mechanistic analysis to characterize oramucosal permeation properties. *International Journal of Pharmaceutics*, 184(1), 63-72.
- Chidambaram, N. & Burgess, D. J. (1999). A novel in vitro release method for submicron sized dispersed systems. *AAPS PharmSci*, 1(3), E11.
- Ciolino, L. A., McCauley, H. A., Fraser, D. B., et al. (2001). The relative buffering capacities of saliva and moist snuff: implications for nicotine absorption. *Journal of Analytical Toxicology*, 25(1), 15-25.
- Crist, G. B. (2009). Trends in small-volume dissolution apparatus for low-dose compounds. *Dissolution Technologies*, 16, 19-22.
- Darwish, M., Hamed, E. & Messina, J. (2010). Fentanyl buccal tablet for the treatment of breakthrough pain: pharmacokinetics of buccal mucosa delivery and clinical efficacy. *Perspectives in Medicinal Chemistry*, 4, 11-21.
- Davies, N. S. & Gillard, R. D. (2000). The solubility loop of nicotine: water. *Transition Metal Chemistry*, 25(6), 628-629.
- Delvadia, P. R., Barr, W. H. & Karnes, H. T. (2012). A biorelevant in vitro release/permeation system for oral transmucosal dosage forms. *International Journal of Pharmaceutics*, 430(1-2), 104-113.
- Dezani, A. B., Pereira, T. M., Caffaro, A. M., et al. (2013). Determination of lamivudine and zidovudine permeability using a different ex vivo method in Franz cells. *Journal of Pharmacological and Toxicological methods*, 67, 194-202.
- Dixit, R. & Puthli, S. (2009). Oral strip technology: Overview and future potential. *Journal of Controlled Release*, 139(2), 94-107.
- Dressman, J. B., Amidon, G. L., Reppas, C., et al. (1998). Dissolution testing as a prognostic tool for oral drug absorption: immediate release dosage forms. *Pharmaceutical Research*, 15(1), 11-22.
- Dressman, J. B. & Reppas, C. (2000). In vitro–in vivo correlations for lipophilic, poorly water-soluble drugs. *European Journal of Pharmaceutical Sciences*, 11, S73-S80.
- Duchêne, D. & Ponchel, G. (1997). Bioadhesion of solid oral dosage forms, why and how? *European Journal of Pharmaceutics and Biopharmaceutics*, 44(1), 15-23.

- Dunge, A., Sharda, N., Singh, B., et al. (2005). Validated specific HPLC method for determination of zidovudine during stability studies. *Journal of Pharmaceutical and Biomedical Analysis*, 37(5), 1109-1114.
- Edward, J. T. (1970). Molecular volumes and the Stokes-Einstein equation. *Journal of Chemical Education*, 47(4), 261.
- Ellison, S. L. & Thompson, M. (2008). Standard additions: myth and reality. *Analyst*, 133(8), 992-997.
- Emami, J. (2006). In vitro-in vivo correlation: from theory to applications. *Journal of Pharmacy and Pharmaceutical Sciences*, 9(2), 169-189.
- Fang, J. B., Robertson, V. K., Rawat, A., et al. (2010). Development and application of a biorelevant dissolution method using USP apparatus 4 in early phase formulation development. *Molecular Pharmaceutics*, 7(5), 1466-1477.
- Ferreira, S. L., Bruns, R. E., Ferreira, H. S., et al. (2007). Box-Behnken design: an alternative for the optimization of analytical methods. *Analytica Chimica Acta*, 597(2), 179-186.
- Flick, E. (1993). Plasticizers and esters. In: *Plastic Additives, An Industrial Guide*. New Jersey, USA, Second edition, Noyes Publication, New Jersey, USA, 534-661.
- Fotaki, N. & Vertzoni, M. (2010). Biorelevant dissolution methods and their applications in in vitro-in vivo correlations for oral formulations. *The Open Drug Delivery Journal*, 4, 2-13.
- Frenning, G., Ek, R. & Stromme, M. (2002). A new method for characterizing the release of drugs from tablets in low liquid surroundings. *Journal of Pharmaceutical Sciences*, 91(3), 776-784.
- Fu, J., Li, L., Yang, X., et al. (2011). Application of standard addition for the determination of carboxypeptidase activity in *Actinomucor elegans* bran koji. *Applied Biochemistry and Microbiology*, 47(5), 556-562.
- Gao, Z. (2009). In Vitro Dissolution Testing with Flow-Through Method: A Technical Note. *AAPS PharmSciTech*, 10(4), 1401-1405.
- Gillespie, W. R. (1997). Convolution-based approaches for in vivo-in vitro correlation modeling. *Advances in Experimental Medicine and Biology*, 423, 53-65.
- Gomez-Gaete, C., Bustos, G. L., Godoy, R. R., et al. (2013). Successful factorial design for the optimization of methylprednisolone encapsulation in biodegradable nanoparticles. *Drug Development and Industrial Pharmacy*, 39(2), 310-320.

- Grubner, O., First, M. W. & Huber, G. L. (1980). Gas chromatographic determination of nicotine in gases and liquids with suppression of adsorption effects. *Analytical Chemistry*, 52(11), 1755-1758.
- Guhmann, M., Thommes, M., Gerber, F., et al. (2013). Design of Biorelevant Test Setups for the Prediction of Diclofenac In Vivo Features After Oral Administration. *Pharmaceutical Research*, 1-19.
- Hanson, R. (2010). A Primer on Release-Rate Testing of Semisolids. *Dissolution Technologies*, 17(4), 3.
- Harvey, D. T. (2002). External Standards or Standard Addition? Selecting and Validating a Method of Standardization. *Journal of Chemical Education*, 79(5), 613.
- Horacio, N. & Anthony, J. (2008). Revised USP system suitability parameters. In IPC-USP 7<sup>th</sup> Annual Scientific Meeting, February 6-7, Hyderabad, India. <http://www.usp.org/pdf/EN/meetings/asMeetingIndia/revisedUSPSystemSuitabilityParameters.pdf> (Last accessed on 12/23/2011).
- Hubley, M. J., Locke, B. R. & Moerland, T. S. (1996). The effects of temperature, pH, and magnesium on the diffusion coefficient of ATP in solutions of physiological ionic strength. *Biochimica et Biophysica Acta*, 1291(2), 115-121.
- Hughes, L. (2003). Tightening up buccal testing. *Manufacturing Chemist*, 74(6), 28-30.
- Hughes, L. & Gehris, A. (2002). A new method of characterizing the buccal dissolution of drugs. Rohm and Haas Research Laboratory Spring House, Philadelphia. [http://www.rohmhaas.com/ionexchange/pharmaceuticals/Formulations\\_doc/buccal\\_dissolution.pdf](http://www.rohmhaas.com/ionexchange/pharmaceuticals/Formulations_doc/buccal_dissolution.pdf). (Last accessed on 06/11/2013).
- Hukkanen, J., Jacob III, P. & Benowitz, N. (2005). Metabolism and disposition kinetics of nicotine. *Pharmacological Reviews*, 57(1), 79-115.
- International Conference on Harmonization (ICH) of Technical Requirements for registration of Pharmaceuticals for Human Use, (2005). Topic Q2 (R1): Validation of Analytical Procedures: Text and Methodology, Geneva.
- Iyer, S. S., Barr, W. H., Dance, M. E., et al. (2007a). A 'biorelevant' system to investigate in vitro drug released from a naltrexone implant. *International Journal of Pharmaceutics*, 340(1-2), 104-118.
- Iyer, S. S., Barr, W. H. & Karnes, H. T. (2007b). Characterization of a potential medium for 'biorelevant' in vitro release testing of a naltrexone implant, employing a validated stability-indicating HPLC method. *Journal of Pharmaceutical and Biomedical Analysis*, 43(3), 845-853.

- Jacob, J. T. & Plein, E. M. (1968). Factors affecting the dissolution rate of medicaments from tablets II. Effect of binder concentration, tablet hardness, and storage conditions on the dissolution rate of phenobarbital from tablets. *Journal of Pharmaceutical Sciences*, 57(5), 802-805.
- Jantratid, E., Janssen, N., Reppas, C., et al. (2008). Dissolution media simulating conditions in the proximal human gastrointestinal tract: an update. *Pharmaceutical Research*, 25(7), 1663-1676.
- Jenner, P., Gorrod, J. W., & Beckett, A. H. (1973). The absorption of nicotine-1'-N-oxide and its reduction in the gastro-intestinal tract in man. *Xenobiotica*, 3(6), 341-349.
- Kapila, Y. V., Dodds, W. J., Helm, J. F., et al. (1984). Relationship between swallow rate and salivary flow. *Digestive Diseases and Sciences*, 29(6), 528-533.
- Karnes, H. T., Shiu, G. & Shah, V. P. (1991). Validation of bioanalytical methods. *Pharmaceutical Research*, 8(4), 421-426.
- Karnes, H. T. (2004). Validation and control of bioanalytical methods in clinical drug development. In: Figg, W. D. & McLeod, H. L. (Eds.), *Handbook of Anticancer Pharmacokinetics and Pharmacodynamics*, Humana Press Inc., New Jersey, USA, 91-110.
- Khuri, A. I. & Mukhopadhyay, S. (2010). Response surface methodology. *Wiley Interdisciplinary Reviews: Computational Statistics*, 2(2), 128-149.
- Kincl, M., Turk, S. & Vrečer, F. (2005). Application of experimental design methodology in development and optimization of drug release method. *International Journal of Pharmaceutics*, 291(1), 39-49.
- Klein, S., Rudolph, M. W., Skalsky, B., et al. (2008). Use of the BioDis to generate a physiologically relevant IVIVC. *Journal of Controlled Release*, 130(3), 216-219.
- Kotlyar, M., Mendoza-Baumgart, M. I., Li, Z. Z., et al. (2007). Nicotine pharmacokinetics and subjective effects of three potential reduced exposure products, moist snuff and nicotine lozenge. *Tobacco Control*, 16(2), 138-142.
- Krebs, H. A. (1950). Chemical composition of blood plasma and serum. *Annual Review of Biochemistry*, 19, 409-430.
- Krull, I. & Swartz, M. (2001). Determining specificity in a regulated environment. *LC GC North America*, 19(6), 604-615.
- Kvist, C., Andersson, S. B., Fors, S., et al. (1999). Apparatus for studying in vitro drug release from medicated chewing gums. *International Journal of Pharmaceutics*, 189(1), 57-65.



- Kyllonen, H., Pirkonen, P. & Nystrom, M. (2005). Membrane filtration enhanced by ultrasound: a review. *Desalination*, 181(1-3), 319-335.
- Lagerlof, F. & Dawes, C. (1984). The volume of saliva in the mouth before and after swallowing. *Journal of Dental Research*, 63(5), 618.
- Lestari, M. L., Nicolazzo, J. A. & Finnin, B. C. (2009). A novel flow through diffusion cell for assessing drug transport across the buccal mucosa in vitro. *Journal of Pharmaceutical Sciences*, 98(12), 4577-4588.
- Lundstedt, T., Seifert, E., Abramo, L., et al. (1998). Experimental design and optimization. *Chemometrics and Intelligent Laboratory Systems*, 42(1), 3-40.
- Lunell, E. & Lunell, M. (2005). Steady-state nicotine plasma levels following use of four different types of Swedish snus compared with 2-mg Nicorette chewing gum: a crossover study. *Nicotine and Tobacco Research*, 7(3), 397-403.
- Luque-Pérez, E., Ríos, A., Valcárcel, M., et al. (1999). Analysis of solid samples using supported liquid membranes: a method for the evaluation of the release of nicotine from Swedish snuff. *Analytica Chimica Acta*, 387(2), 155-164.
- Madhav, N. V., Shakya, A. K., Shakya, P., et al. (2009). Orotransmucosal drug delivery systems: a review. *Journal of Control Release*, 140(1), 2-11.
- Marques, M. R., Loebenberg, R. & Almukainzi, M. (2011). Simulated biological fluids with possible application in dissolution testing. *Dissolution Technologies*, 18(3), 15-28.
- Martin, G. C., Brown, J. P., Eifler, C. W. et al. (1999). Oral leukoplakia status six weeks after cessation of smokeless tobacco use. *The Journal of the American Dental Association*, 130, 945-954.
- Martin, A., Swarbrick, J. & Cammarata, A. (1983). Diffusion and dissolution. In: *Physical Pharmacy, Physical Chemical Principles in the Pharmaceutical Sciences*. Lea & Febiger, Philadelphia. USA, 399-444.
- Michaels, A., Chandrasekaran, S. & Shaw, J. (1975). Drug permeation through human skin: Theory and in vitro experimental measurement. *AIChE Journal*, 21(5), 985-996.
- Molander, L., Hansson, A. & Lunell, E. (2001). Pharmacokinetics of nicotine in healthy elderly people. *Clinical Pharmacology and Therapeutics*, 69(1), 57-65.
- Morjaria, Y., Irwin, W. J., Barnett, P. X., et al. (2004). In vitro release of nicotine from chewing gum formulations. *Dissolution Technologies*, 11(2), 12-15.

- Mumtaz, A. M. & Ch'ng, H. S. (1995). Design of a dissolution apparatus suitable for in situ release study of triamcinolone acetonide from bioadhesive buccal tablets. *International Journal of Pharmaceutics*, 121(2), 129-139.
- Nasr, M. M., Reepmeyer, J. C. & Tang, Y. (1998). In vitro study of nicotine release from smokeless tobacco. *Journal of AOAC International*, 81(3), 540-543.
- Navazesh, M. & Christensen, C. M. (1982). A comparison of whole mouth resting and stimulated salivary measurement procedures. *Journal of Dental Research*, 61(10), 1158-1162.
- Navazesh, M., Mulligan, R., Kipnis, V., et al. (1992). Comparison of whole saliva flow rates and mucin concentrations in healthy Caucasian young and aged adults. *Journal of Dental Research*, 71(6), 1275.
- Nicolazzo, J. A. & Finnin, B. C. (2008). In vivo and in vitro models for assessing drug absorption across the buccal mucosa. *Drug Absorption Studies*, Springer: 89-111.
- Official monograph, (2009a). Ergoloid mesylate sublingual tablets. The United States Pharmacopeia 32 – The National Formulary 27, vol. 2. United States Pharmacopeial Convention Inc., Rockville, USA, pp. 2274–2275.
- Official monograph, (2009b). Ergotamine tartrate sublingual tablets. The United States Pharmacopeia 32 – The National Formulary 27, vol. 2. United States Pharmacopeial Convention Inc., Rockville, USA, pp. 2280–2281.
- Official monograph, (2009c). Isosorbide dinitrate sublingual tablets. The United States Pharmacopeia 32 – The National Formulary 27, vol. 2. United States Pharmacopeial Convention Inc., Rockville, USA, p. 2716.
- Official monograph, (2009d). Nitroglycerine sublingual tablets. The United States Pharmacopeia 32 – The National Formulary 27, vol. 2. United States Pharmacopeial Convention Inc., Rockville, USA, pp. 3097–3098.
- Othmer, D. F. & Thakar, M. S. (1953). Correlating diffusion coefficient in liquids. *Industrial & Engineering Chemistry*, 45(3), 589-593.
- Patel, V. F., Liu, F. & Brown, M. B. (2011). Advances in oral transmucosal drug delivery. *Journal of Controlled Release*, 153(2), 106-116.
- Patel, V. F., Liu, F. & Brown, M. B. (2012). Modelling the oral cavity: In vitro and in vivo evaluations of buccal drug delivery systems. *Journal of Controlled Release*.
- Pather, S. I., Rathbone, M. J. & Senel, S. (2008). Current status and the future of buccal drug delivery systems. *Expert Opinion on Drug Delivery*, 5(5), 531-542.

- Pfister, W. & Ghosh, T. (2005). Intraoral delivery systems - An overview, current status, and future trends. In: Pfister, W., Ghosh, T. (Eds.), *Drug Delivery to the Oral Cavity-Molecules to Market*. CRC Press, Boca Raton, USA, 1-40.
- Piade, J. J., Sandrine D'André s, a. & Sanders, E. B. (1999). Sorption phenomena of nicotine and ethenylpyridine vapors on different materials in a test chamber. *Environmental Science and Technology*, 33(12), 2046-2052.
- Polli, J. E. (2000). IVIVR versus IVIVC. *Dissolution Technologies*, 7(3), 6-9.
- Qiu, Y., Garren, J., Samara, E., et al. (2003). Once-a-day controlled-release dosage form of divalproex sodium II: development of a predictive in vitro drug release method. *Journal of Pharmaceutial Sciences*, 92(11), 2317-2325.
- Rachid, O., Rawas-Qalaji, M., Simons, F. E., et al. (2011). Dissolution testing of sublingual tablets: a novel in vitro method. *AAPS PharmSciTech*, 12(2), 544-552.
- Rathbone, M. J., Ponchel, G. & Ghazali, F. (1996). Systemic oral mucosal drug delivery and delivery systems. In: Rathbone, M. J. (Ed.), *Oral Mucosal Drug Delivery*. Marcek Dekker Inc., New York, USA, 241-284.
- Rehak, N. N., Cecco, S. A. & Csako, G. (2000). Biochemical composition and electrolyte balance of "unstimulated" whole human saliva. *Clinical Chemistry and Laboratory Medicine*, 38(4), 335-343.
- Ribeiro, I. A. & Ribeiro, M. H. L. (2008). Naringin and naringenin determination and control in grapefruit juice by a validated HPLC method. *Food Control*, 19(4), 432-438.
- Rosing, H., Man, W., Doyle, E., et al. (2000). Bioanalytical liquid chromatographic method validation. A review of current practices and procedures. *Journal of Liquid Chromatography and Related Technologies*, 23(3), 329-354.
- Seidlitz, A., Nagel, S., Semmling, B., et al. (2013). In vitro dissolution testing of drug-eluting stents. *Current Pharmaceutical Biotechnology*, 14(1), 67-75.
- Shah, V. P. (2001). Dissolution: A Quality Control Test vs A Bioequivalence Test. *Dissolution Technologies*, 8(4), 1-2.
- Sistla, R., Tata, V., Kashyap, Y., et al. (2005). Development and validation of a reversed-phase HPLC method for the determination of ezetimibe in pharmaceutical dosage forms. *Journal of Pharmaceutical and Biomedical Analysis*, 39(3-4), 517-522.
- Sohi, H., Ahuja, A., Ahmad, F. J., et al. (2010). Critical evaluation of permeation enhancers for oral mucosal drug delivery. *Drug Development and Industrial Pharmacy*, 36(3), 254-282.

- Stead, L. F., Perera, R., Bullen, C., et al. (2008). Nicotine replacement therapy for smoking cessation. *Cochrane Database of Systematic Reviews*, 1(1), 1-160.
- Stepanov, I., Biener, L., Knezevich, A., et al. (2012). Monitoring tobacco-specific N-nitrosamines and nicotine in novel Marlboro and Camel smokeless tobacco products: findings from Round 1 of the New Product Watch. *Nicotine and Tobacco Research*, 14(3), 274-281.
- Stone, C. R. (2001). Ester plasticizers and processing additives. In: Dick, J. S. (Ed.), *Rubber Technology, Compounding and Testing for Performance*. Hanser Gardner Publications Inc., Ohio, USA, 344-379.
- Stüber, M. & Reemtsma, T. (2004). Evaluation of three calibration methods to compensate matrix effects in environmental analysis with LC-ESI-MS. *Analytical and Bioanalytical Chemistry*, 378(4), 910-916.
- Sudhakar, Y., Kuotsu, K. & Bandyopadhyay, A. (2006). Buccal bioadhesive drug delivery--a promising option for orally less efficient drugs. *Journal of Controlled Release*, 114(1), 15-40.
- Svensson C. K. (1987). Clinical pharmacokinetics of nicotine. *Clinical pharmacokinetics*, 12, 30-40.
- Tambwekar, K. R., Kakariya, R. B. & Garg, S. (2003). A validated high performance liquid chromatographic method for analysis of nicotine in pure form and from formulations. *Journal of Pharmaceutical and Biomedical Analysis*, 32(3), 441-450.
- The United States Pharmacopeia 32 – The National Formulary 27 (Volume 1) (2009e). *Validation of Compendial Procedures <1225>*; United States Pharmacopeial Convention Inc.: Rockville, USA, pp 733–736.
- The United States Pharmacopeia 32 – The National Formulary 27 (Volume 1) (2009f). *Chromatography <621>*. United States Pharmacopeial Convention Inc.: Rockville, USA, 2009, pp. 227–238.
- Tomar, S. L. & Henningfield, J. E. (1997). Review of the evidence that pH is a determinant of nicotine dosage from oral use of smokeless tobacco. *Tobacco Control*, 6(3), 219-225.
- US Food and Drug Administration, Center for Drug Evaluation and Research, US Department of Health and Human Services. (1994). *Reviewer Guidance: Validation of chromatographic methods*. Rockville, USA.
- US Food and Drug Administration, Center for Drug Evaluation and Research, US Department of Health and Human Services. (2001). *Guidance for industry: Bioanalytical method validation*. Rockville, USA.

- Van Loy, M. D., Lee, V. C., Gundel, L. A., et al. (1997). Dynamic behavior of semivolatile organic compounds in indoor air. 1. Nicotine in a stainless steel chamber. *Environmental Science & Technology*, 31(9), 2554-2561.
- Vertzoni, M., Dressman, J., Butler, J., et al. (2005). Simulation of fasting gastric conditions and its importance for the in vivo dissolution of lipophilic compounds. *European Journal of Pharmaceutics and Biopharmaceutics*, 60(3), 413-417.
- Wagner, J. G. & Nelson, E. (1964). Kinetic Analysis of Blood Levels and Urinary Excretion in the Absorptive Phase after Single Doses of Drug. *Journal of Pharmaceutical Sciences*, 53, 1392-1403.
- Wainer, H. (2000). The centercept: An estimable and meaningful regression parameter. *Psychological Science*, 11(5), 434-436.
- Walters, F. H., Parker, L. R., Morgan, S. L. & Deming, S. N. (1991). Chapter 2 - Systems theory and response surfaces. In: *Sequential Simplex Optimization: A Technique for Improving Quality and Productivity in Research, Development, and Manufacturing*, CRC Press, Boca Raton, USA, 30-64.
- Wang, Q., Fotaki, N. & Mao, Y. (2009). Biorelevant dissolution: Methodology and application in drug development. *Dissolution Technologies*, 16(3), 6-12.
- Washington, N., Washington, C. & Wilson, C. (2001). Drug delivery to the oral cavity or mouth. In: Washington, N., Washington, C., Wilson, C. (Eds.), *Physiological Pharmaceutics: Barriers to Drug Absorption*. CRC Press, Boca Raton, USA, 37-55.
- Waters 996 Photodiode Detector (2002a): Peak Purity I. What is Peak Purity Analysis? <http://www.forumsci.co.il/HPLC/wpp16.pdf>. (Last accessed on 01/30/2012).
- Waters 996 Photodiode Detector (2002b): Peak Purity II. Peak Purity Plot. <http://www.forumsci.co.il/HPLC/wpp17.pdf>. (Last accessed on 01/30/2012).
- Waters 996 Photodiode Detector (2002c): Peak Purity III. Interpretation of peak purity plots. <http://www.forumsci.co.il/HPLC/wpp18.pdf>. (Last accessed on 01/30/2012).
- Williams, J. R. (2004). Smokeless tobacco product, United States Patent – 6,834,654, 1-14.
- Zahlsen, K., Nilsen, T. & Nilsen, O. G. (1996). Interindividual differences in hair uptake of air nicotine and significance of cigarette counting for estimation of environmental tobacco smoke exposure. *Pharmacology and Toxicology*, 79(4), 183-190.
- Zhang, H., Zhang, J. & Streisand, J. B. (2002). Oral mucosal drug delivery. *Clinical Pharmacokinetics*, 41(9), 661-680.

Zhou, Y. Z., Alany, R. G., Chuang, V., et al. (2013). Optimization of PLGA nanoparticles formulation containing L-DOPA by applying the central composite design. *Drug Development and Industrial Pharmacy*, 39(2), 321-330.

## **APPENDICES**

**APPENDIX A**

**METHOD VALIDATION RESULTS FOR THE HPLC METHOD REPORTED IN  
CHAPTER 2**



**Table A1:** Peak areas for nicotine in external standards prepared in HBSS (Method validation\_Linearity and LOQ)

Nominal Nicotine Conc. ( $\mu\text{g/mL}$ )	1	2	3	4	5	Mean
0.5	7652	7783	7299	8007	7740	7696
1	15910	16150	16139	16717	15189	16021
2	34931	35443	34117	34217	34857	34713
4	69541	69124	67668	68601	69918	68970
8	142856	139237	142109	141045	140928	141235
16	283954	281943	282226	285911	287112	284229
32	576884	575243	574751	576241	576394	575903

**Table A2:** Calculated concentrations for nicotine in external standards prepared in HBSS buffer (Method validation\_Linearity and LOQ)

Nominal Nicotine Conc. ( $\mu\text{g/mL}$ )	1	2	3	4	5	Mean	SD	%RSD	%DFN	% Recovery
0.5	0.51	0.52	0.49	0.53	0.52	0.52	0.01	2.78	3.20	103.20
1	0.97	0.99	0.99	1.02	0.93	0.98	0.03	3.14	-2.02	97.98
2	2.03	2.06	1.99	1.99	2.03	2.02	0.03	1.51	1.06	101.06
4	3.96	3.94	3.86	3.91	3.98	3.93	0.05	1.24	-1.75	98.25
8	8.05	7.84	8.00	7.95	7.94	7.96	0.08	0.96	-0.55	99.45
16	15.91	15.80	15.81	16.02	16.08	15.92	0.13	0.79	-0.48	99.52
32	32.23	32.14	32.11	32.19	32.20	32.17	0.05	0.15	0.54	100.54

**Table A3:** Nicotine concentration at all QC levels for HPLC method validation (Intraday accuracy and precision)

<b>Nominal Nicotine Conc. (µg/mL)</b>	<b>1</b>	<b>2</b>	<b>3</b>	<b>4</b>	<b>5</b>	<b>6</b>	<b>Mean</b>	<b>SD</b>	<b>%RSD</b>	<b>% Recovery</b>
1.5	1.44	1.55	1.52	1.59	1.54	1.53	1.53	0.05	3.26	101.80
5	4.82	5.02	5.00	4.77	4.98	4.96	4.93	0.11	2.15	98.50
28	28.11	27.92	27.93	27.89	27.92	27.89	27.94	0.08	0.29	99.80
64 (25x dilution)	62.33	65.38	62.76	64.69	62.18	65.36	63.78	1.52	2.39	99.66
64 (10x dilution)	63.98	64.58	61.96	64.39	63.26	62.82	63.50	1.01	1.59	99.21

**Table A4:** Nicotine concentration at all QC levels for HPLC method validation (Interday accuracy and precision)

<b>Nominal Nicotine Conc. (µg/mL)</b>	<b>1.5</b>	<b>5</b>	<b>28</b>	<b>64 (25x dilution)</b>	<b>64 (10x dilution)</b>
<b>Day1</b>					
1	1.44	4.82	28.11	62.33	63.98
2	1.55	5.02	27.92	65.38	64.58
3	1.52	5.00	27.93	62.76	61.96
4	1.59	4.77	27.89	64.69	64.39
5	1.54	4.98	27.92	62.18	63.26
6	1.53	4.96	27.89	65.36	62.82
<b>Day2</b>					
1	1.52	4.71	29.38	64.80	62.58
2	1.53	4.77	29.66	64.65	62.19
3	1.50	4.834	29.53	62.18	62.32
<b>Day3</b>					
1	1.51	4.86	28.32	65.67	63.58
2	1.52	4.74	28.35	62.75	64.42
3	1.64	4.76	28.27	62.51	63.75
<b>Mean</b>	1.53	4.85	28.43	63.77	63.32
<b>SD</b>	0.05	0.11	0.68	1.42	0.93
<b>%RSD</b>	3.18	2.30	2.40	2.23	1.47
<b>% Recovery</b>	102.13	97.04	101.54	99.64	98.94

**Table A5:** System suitability parameters for nicotine

Parameter	1	2	3	4	5	Mean	SD	%RSD
<b>Nicotine Standard</b>								
Resolution	11.7	11.8	11.7	11.7	9.8	11.3	0.9	7.8
Tailing factor	1.8	1.8	2.3	1.2	1.5	1.7	0.4	25.1
Theoretical plates	5849.0	5854.6	5849.0	5846.2	5846.2	5849.0	3.5	0.1
Retention time (min)	4.15	4.15	4.15	4.15	4.15	4.15	0.001	0.030
<b>Nicotine <i>in vitro</i> sample</b>								
Resolution	4.6	5.4	5.4	4.9	4.4	4.9	0.5	9.2
Tailing factor	1.4	1.4	1.3	2.0	1.3	1.5	0.3	18.8
Theoretical plates	4795.7	6509.6	6497.8	4765.1	4762.9	5466.2	947.2	17.3
Retention time (min)	4.38	4.38	4.37	4.37	4.37	4.37	0.01	0.14

**Table A6:** Short term stability data for nicotine in HBSS buffer

Quality Control	Conc. at zero day	Conc. after 2 months	Concentration at zero day			Concentration after 2 months				
			Mean	SD	%RSD	Mean	SD	%RSD	% Recovery	
LQC (1.5 µg/mL)	1	1.61	1.55	1.62	0.02	1.33	1.53	0.04	2.61	94.13
	2	1.65	1.51							
	3	1.62	1.55							
	4	1.59	1.50							
	5	1.65	1.59							
	6	1.62	1.48							
HQC (28 µg/mL)	1	27.99	27.92	27.92	0.12	0.44	28.09	0.16	0.57	100.63
	2	27.76	27.86							
	3	27.77	28.15							
	4	27.93	28.19							
	5	28.01	28.24							
	6	28.03	28.19							

**Table A7:** Freeze-thaw stability data for nicotine in HBSS buffer

Quality Control	Conc. at zero day	Conc. after 3 freeze thaw cycles	Concentration at zero day			Concentration after 3 freeze thaw cycles				
			Mean	SD	%RSD	Mean	SD	%RSD	% Recovery	
LQC (1.5 µg/mL)	1	1.61	1.55	1.62	0.02	1.33	1.54	0.06	4.12	95.00
	2	1.65	1.52							
	3	1.62	1.66							
	4	1.59	1.48							
	5	1.65	1.51							
	6	1.62	1.54							
HQC (28 µg/mL)	1	27.99	28.95	27.92	0.12	0.44	29.13	0.28	0.97	104.34
	2	27.76	28.90							
	3	27.77	28.82							
	4	27.93	29.52							
	5	28.01	29.38							
	6	28.03	29.19							

**Table A8:** Peak areas for nicotine analysis of the external standards and spiked *in vitro* donor samples of snus

<b>Nicotine external standards</b>								
<b>Nicotine concentration (µg/mL)</b>	<b>1</b>	<b>2</b>	<b>3</b>	<b>4</b>	<b>5</b>	<b>Mean</b>	<b>SD</b>	<b>%RSD</b>
0.5	8505	8282	8598	8002	8354	8348	229.8	2.8
1	15420	15342	14716	14286	15606	15074	553.2	3.7
2	34230	34452	34410	34506	33386	34197	465.0	1.4
4	68398	70403	68136	68566	68283	68757	933.6	1.4
8	137863	140936	140110	137897	137050	138771	1660.8	1.2
16	280444	278840	277126	279095	277488	278599	1333.4	0.5
32	558558	558690	557697	556238	557485	557734	986.7	0.2
<b>Spiked donor <i>in vitro</i> sample</b>								
<b>Nicotine concentration (µg/mL)</b>	<b>1</b>	<b>2</b>	<b>3</b>	<b>4</b>	<b>5</b>	<b>Mean</b>	<b>SD</b>	<b>%RSD</b>
0	110576	110359	110513	110634	110412	110499	113.5	0.1
1	127216	127030	126655	127073	127079	127011	210.7	0.2
2	146691	145339	145472	145409	146088	145800	580.9	0.4
4	178421	177706	177386	176528	175032	177015	1300.1	0.7
8	245327	247120	245987	247056	247017	246501	806.2	0.3

**Table A9:** Peak areas for nicotine analysis of the external standards and spiked *in vitro* receptor compartment samples for snus

<b>Nicotine external standards</b>								
<b>Nicotine concentration (µg/mL)</b>	<b>1</b>	<b>2</b>	<b>3</b>	<b>4</b>	<b>5</b>	<b>Mean</b>	<b>SD</b>	<b>%RSD</b>
0.5	8505	8282	8598	8002	8354	8348	229.8	2.8
1	15420	15342	14716	14286	15606	15074	553.2	3.7
2	34230	34452	34410	34506	33386	34197	465.0	1.4
4	68398	70403	68136	68566	68283	68757	933.6	1.4
8	137863	140936	140110	137897	137050	138771	1660.8	1.2
16	280444	278840	277126	279095	277488	278599	1333.4	0.5
32	558558	558690	557697	556238	557485	557734	986.7	0.2
<b>Spiked receptor <i>in vitro</i> sample</b>								
<b>Nicotine concentration (µg/mL)</b>	<b>1</b>	<b>2</b>	<b>3</b>	<b>4</b>	<b>5</b>	<b>Mean</b>	<b>SD</b>	<b>%RSD</b>
0	545652	544346	544863	544971	545013	544969	465.8	0.1
1	562153	560715	561702	562671	560558	561560	911.6	0.2
2	580736	581048	579745	579330	579601	580092	753.5	0.1
4	611788	612098	609016	609862	612271	611007	1472.5	0.2
8	683816	683496	684845	684474	681604	683647	1259.4	0.2

**Table A10:** Peak purity testing on the nicotine standards and *in vitro* donor and receptor compartment samples for snus by the autothreshold method at 200-300 nm\*

		Purity Angle* <sup>§</sup>			Threshold Angle* <sup>§</sup>		
		Mean	SD	%RSD	Mean	SD	%RSD
<b>Nicotine standard (0.5 µg/mL)</b>	<b>1</b>	3.502			3.871		
	<b>2</b>	3.682	3.934	0.599	15.217	4.825	0.942
	<b>3</b>	4.617			5.755		19.528
<b>Nicotine standard (32 µg/mL)</b>	<b>1</b>	0.112			0.263		
	<b>2</b>	0.122	0.119	0.006	5.112	0.290	0.028
	<b>3</b>	0.123			0.319		9.699
<b>Receptor 1 sample at 60 min</b>	<b>1</b>	1.211			0.402		
	<b>2</b>	1.983	1.393	0.523	37.566	0.354	0.043
	<b>3</b>	0.985			0.319		12.094
<b>Receptor 2 sample at 60 min</b>	<b>1</b>	1.467			0.347		
	<b>2</b>	0.997	1.267	0.243	19.161	0.389	0.054
	<b>3</b>	1.338			0.371		13.842
<b>Donor sample at 60 min</b>	<b>1</b>	1.173			0.473		
	<b>2</b>	1.052	1.120	0.062	5.516	0.393	0.079
	<b>3</b>	1.134			0.316		19.964

\* Peak purity analysis was performed at the wavelength range of 200-300 nm

<sup>§</sup> Purity angle if less than threshold angle indicates pure peak (i.e. absence of coeluant)



**Table A11:** Peak purity testing on the nicotine standards and *in vitro* donor and receptor samples for snus by the autothreshold method at 250-270 nm\*

		Purity Angle* <sup>§</sup>			Threshold Angle* <sup>§</sup>				
		Mean	SD	%RSD	Mean	SD	%RSD		
<b>Nicotine standard (0.5 µg/mL)</b>	<b>1</b>	1.780			2.703				
	<b>2</b>	2.296	2.386	0.655	27.461	3.197	2.989	0.256	8.571
	<b>3</b>	3.081			3.068				
<b>Nicotine standard (32 µg/mL)</b>	<b>1</b>	0.066			0.232				
	<b>2</b>	0.064	0.063	0.003	4.824	0.247	0.252	0.022	8.888
	<b>3</b>	0.060			0.276				
<b>Receptor 1 sample at 60 min</b>	<b>1</b>	0.258			0.321				
	<b>2</b>	0.235	0.244	0.013	5.131	0.282	0.290	0.028	9.766
	<b>3</b>	0.238			0.266				
<b>Receptor 2 sample at 60 min</b>	<b>1</b>	0.211			0.282				
	<b>2</b>	0.293	0.253	0.041	16.220	0.356	0.315	0.038	11.905
	<b>3</b>	0.255			0.308				
<b>Donor sample at 60 min</b>	<b>1</b>	0.339			0.357				
	<b>2</b>	0.315	0.303	0.044	14.479	0.321	0.315	0.045	14.198
	<b>3</b>	0.254			0.268				

\* Peak purity analysis was performed at the wavelength range of 250-270nm

<sup>§</sup> Purity angle if less than threshold angle indicates pure peak (i.e. absence of coeluant)

**Table A12:** Peak purity testing on nicotine standards and *in vitro* donor and receptor samples for snus by the noise+solvent method at 200-300 nm<sup>\*#</sup>

		Purity Angle <sup>*\$</sup>				Threshold Angle <sup>*\$</sup>			
		Mean	SD	%RSD	Mean	SD	%RSD		
<b>Nicotine standard (0.5 µg/mL)</b>	<b>1</b>	3.502			9.132				
	<b>2</b>	3.682	5.629	3.529	62.693	10.11	9.665	0.495	
	<b>3</b>	9.702			9.754			5.121	
<b>Nicotine standard (32 µg/mL)</b>	<b>1</b>	0.112			5.511				
	<b>2</b>	0.122	0.119	0.006	5.112	5.535	5.538	0.028	
	<b>3</b>	0.123			5.567			0.507	
<b>Receptor 1 sample at 60 min</b>	<b>1</b>	1.211			5.656				
	<b>2</b>	1.983	1.393	0.523	37.566	5.597	5.609	0.042	
	<b>3</b>	0.985			5.574			0.754	
<b>Receptor 2 sample at 60 min</b>	<b>1</b>	1.467			5.602				
	<b>2</b>	0.997	1.267	0.243	19.161	5.705	5.644	0.054	
	<b>3</b>	1.338			5.626			0.955	
<b>Donor sample at 60 min</b>	<b>1</b>	1.173			5.726				
	<b>2</b>	1.052	1.120	0.062	5.516	5.644	5.646	0.079	
	<b>3</b>	1.134			5.569			1.391	

\* Peak purity analysis was performed at the wavelength range of 200-300 nm

# Solvent angle for lowest nicotine standard (0.5 µg/mL) at 200-300 nm was 5.436

\$ Purity angle if less than threshold angle indicates pure peak (i.e. absence of coeluant)

**Table A13:** Peak purity testing on nicotine standards and *in vitro* donor and receptor samples for snus by the noise+solvent method at 250-270 nm<sup>\*#</sup>

		Purity Angle <sup>*\$</sup>				Threshold Angle <sup>*\$</sup>			
		Mean	SD	%RSD	Mean	SD	%RSD		
<b>Nicotine standard (0.5 µg/mL)</b>	<b>1</b>	1.78			5.404				
	<b>2</b>	2.296	2.386	0.655	27.461	5.898	5.690	0.256	
	<b>3</b>	3.081			5.769			4.503	
<b>Nicotine standard (32 µg/mL)</b>	<b>1</b>	0.066			2.927				
	<b>2</b>	0.064	0.063	0.003	4.824	2.943	2.947	0.022	
	<b>3</b>	0.06			2.971			0.756	
<b>Receptor 1 sample at 60 min</b>	<b>1</b>	0.258			3.019				
	<b>2</b>	0.235	0.244	0.013	5.131	2.98	2.988	0.028	
	<b>3</b>	0.238			2.964			0.947	
<b>Receptor 2 sample at 60 min</b>	<b>1</b>	0.211			2.98				
	<b>2</b>	0.293	0.253	0.041	16.220	3.055	3.014	0.038	
	<b>3</b>	0.255			3.006			1.264	
<b>Donor sample at 60 min</b>	<b>1</b>	0.339			3.055				
	<b>2</b>	0.315	0.303	0.044	14.479	3.019	3.013	0.045	
	<b>3</b>	0.254			2.965			1.503	

\* Peak purity analysis was performed at the wavelength range of 250-270 nm

# Solvent angle for lowest nicotine standard (0.5 µg/mL) at 250-270 nm was 2.881

\$ Purity angle if less than threshold angle indicates pure peak (i.e. absence of coeluant)

## **APPENDIX B**

### **DATA ON VALIDATION OF THE NOVEL BIDIRECTIONAL TRANSMUCOSAL APPARATUS DESIGNED FOR OTPs REPORTED IN CHAPTER 3**

**Table B1:** Amount of nicotine permeated (mg) from snus in the bottom and top receptor chambers of the BTA in the horizontal orientation

Time (min)	Bottom Receptor						Top Receptor						Mean Ratio (Bottom/Top)
	1	2	3	Mean	SD	%RSD	1	2	3	Mean	SD	%RSD	
0	0.00	0.00	0.00	0.00	0.00	-	0.00	0.00	0.00	0.00	0.00	-	-
10	0.04	0.02	0.08	0.05	0.03	60.71	0.02	0.02	0.03	0.02	0.00	23.13	2.25
20	0.06	0.04	0.08	0.06	0.02	36.12	0.02	0.03	0.03	0.03	0.00	15.57	2.19
30	0.06	0.05	0.08	0.06	0.02	26.63	0.02	0.03	0.03	0.03	0.01	18.44	2.14
45	0.08	0.07	0.08	0.08	0.01	7.51	0.03	0.04	0.04	0.04	0.01	15.05	2.20
60	0.09	0.10	0.09	0.09	0.01	7.65	0.03	0.05	0.04	0.04	0.01	22.47	2.19
<b>Average of the Mean Ratio</b>													<b>2.19</b>

**Table B2:** Amount of nicotine permeated (mg) from snus in the bottom and top receptor compartments of the BTA in the vertical orientation

Time (min)	Bottom Receptor						Top Receptor						Mean Ratio (Bottom/Top)
	1	2	3	Mean	SD	%RSD	1	2	3	Mean	SD	%RSD	
0	0.00	0.00	0.00	0.00	0.00	-	0.00	0.00	0.00	0.00	0.00	-	-
10	0.00	0.00	0.00	0.00	0.00	-	0.00	0.00	0.00	0.00	0.00	173.21	0.00
20	0.00	0.01	0.01	0.01	0.00	31.72	0.00	0.01	0.01	0.00	0.00	86.87	1.32
30	0.01	0.01	0.01	0.01	0.01	46.88	0.00	0.01	0.01	0.01	0.01	86.73	1.46
45	0.01	0.02	0.03	0.02	0.01	55.51	0.00	0.02	0.02	0.01	0.01	60.16	1.27
60	0.01	0.03	0.04	0.03	0.01	43.89	0.01	0.03	0.03	0.02	0.01	58.62	1.38
<b>Average of the Mean Ratio</b>													<b>1.08</b>

**Table B3:** Amount of nicotine permeated/released (mg) from snus [Polyethersulfone membrane (3 nm); Vertical diffusion cell]

<b>Time (min)</b>	<b>1</b>	<b>2</b>	<b>3</b>	<b>4</b>	<b>5</b>	<b>Mean</b>	<b>SD</b>	<b>%RSD</b>
0	0	0	0	0	0	0	0	-
10	0	0	0	0	0	0	0	-
20	0	0.016	0.016	0.000	0.017	0.010	0.009	91.357
30	0.015	0.019	0.018	0.000	0.023	0.015	0.009	58.814
45	0.018	0.020	0.014	0.000	0.027	0.016	0.010	63.713
60	0.017	0.019	0.018	0.000	0.030	0.017	0.011	63.876
<b>Nicotine release at 60 min (mg)</b>	4.763	5.144	4.439	4.470	4.569	4.677	0.290	6.206
<b>Adsorption of nicotine on membrane (mg)</b>	0.081	0.115	0.077	0.083	0.096	0.090	0.015	16.817

**Table B4:** Amount of nicotine permeated/released (mg) from snus [Polyethersulfone membrane (3 nm); Bidirectional transmucosal apparatus]

<b>Time (min)</b>	<b>1</b>	<b>2</b>	<b>3</b>	<b>Mean</b>	<b>SD</b>	<b>%RSD</b>
0	0	0	0	0	0	-
10	0.000	0.004	0.000	0.001	0.002	173.205
20	0.004	0.011	0.014	0.010	0.005	54.064
30	0.005	0.024	0.026	0.018	0.011	62.518
45	0.011	0.040	0.044	0.032	0.018	56.640
60	0.020	0.058	0.062	0.046	0.023	49.641
<b>Nicotine release at 60 min (mg)</b>	6.648	5.225	6.008	5.960	0.712	11.952
<b>Adsorption of nicotine on membrane of receptor 1 (mg)</b>	0.059	0.094	0.061	0.071	0.020	27.792
<b>Adsorption of nicotine on membrane of receptor 1 (mg)</b>	0.058	0.110	0.088	0.085	0.026	30.864

**Table B5:** Amount of nicotine permeated/released (mg) from snus [Polyethersulfone membrane (30 nm); Bidirectional transmucosal apparatus]

Time (min)	1	2	3	Mean	SD	%RSD
0						
10						
20						
30						
45						
60						
<b>Nicotine release at 60 min (mg)</b>	5.129	6.625	4.804	5.519	0.971	17.599
<b>Adsorption of nicotine on membrane of receptor 1 (mg)</b>	0.163	0.045	0.049	0.085	0.067	78.236
<b>Adsorption of nicotine on membrane of receptor 1 (mg)</b>	0.246	0.090	0.132	0.156	0.081	51.693

No Permeation achieved

**Table B6:** Amount of nicotine permeated/released (mg) from snus [Regenerated cellulose membrane (2.5 nm); Vertical diffusion cell]

Time (min)	1	2	3	4	5	Mean	SD	%RSD
0	0	0	0	0	0	0	0	-
2.5	0.016	0.000	0.000	0.000	0.000	0.003	0.007	223.607
5	0.058	0.023	0.033	0.013	0.015	0.028	0.018	64.426
7.5	0.104	0.056	0.101	0.044	0.044	0.070	0.030	43.541
10	0.169	0.105	0.152	0.080	0.079	0.117	0.041	35.358
15	0.290	0.212	0.271	0.154	0.160	0.217	0.062	28.624
20	0.376	0.313	0.366	0.234	0.244	0.307	0.066	21.628
25	0.480	0.406	0.447	0.297	0.299	0.386	0.084	21.900
30	0.578	0.506	0.544	0.372	0.381	0.476	0.094	19.840
45	0.864	0.797	0.792	0.607	0.607	0.733	0.119	16.213
60	1.155	1.071	1.030	0.803	0.830	0.978	0.155	15.803
<b>Nicotine release at 60 min (mg)</b>	4.550	4.050	4.152	3.226	3.522	3.900	0.526	13.476
<b>Adsorption of nicotine on membrane (mg)</b>	0.003	0.007	0.004	0.002	0.003	0.004	0.002	50.582

**Table B7:** Amount of nicotine permeated/released (mg) from snus [Regenerated cellulose membrane (2.5 nm); Bidirectional transmucosal apparatus]

<b>Time (min)</b>	<b>1</b>	<b>2</b>	<b>3</b>	<b>4</b>	<b>5</b>	<b>Mean</b>	<b>SD</b>	<b>%RSD</b>
0	0	0	0	0	0	0	0	-
2.5	0.018	0.006	0.034	0.006	0.015	0.016	0.012	73.043
5	0.030	0.017	0.040	0.017	0.029	0.026	0.010	37.204
7.5	0.042	0.026	0.043	0.021	0.033	0.033	0.010	29.119
10	0.053	0.038	0.050	0.027	0.042	0.042	0.010	24.771
15	0.094	0.077	0.071	0.041	0.095	0.076	0.022	28.813
20	0.180	0.178	0.112	0.076	0.260	0.161	0.071	43.846
25	0.262	0.324	0.192	0.147	0.411	0.267	0.105	39.149
30	0.369	0.440	0.319	0.270	0.553	0.390	0.111	28.352
45	0.679	0.793	0.590	0.583	0.948	0.719	0.154	21.418
60	0.912	1.087	0.858	0.877	1.188	0.984	0.145	14.767
<b>Nicotine release at 60 min (mg)</b>	5.524	5.870	5.784	5.952	6.168	5.860	0.235	4.016
<b>Adsorption of nicotine on membrane of receptor 1 (mg)</b>	0.000	0.004	0.004	0.005	0.000	0.003	0.002	92.196
<b>Adsorption of nicotine on membrane of receptor 3 (mg)</b>	0.006	0.004	0.004	0.004	0.000	0.004	0.002	59.603



**Table B8:** Amount of nicotine adsorbed (mg) on the bidirectional transmucosal apparatus

<b>Time (min)</b>	<b>1</b>	<b>2</b>	<b>3</b>	<b>Mean</b>	<b>SD</b>	<b>%RSD</b>	<b>%DFN*</b>
0	0.983	0.978	0.988	0.983	0.005	0.553	0.000
10	0.956	0.959	0.970	0.962	0.007	0.735	-2.162
20	0.954	0.956	0.964	0.958	0.005	0.536	-2.527
30	0.951	0.951	0.961	0.954	0.006	0.645	-2.905
45	0.945	0.960	0.954	0.953	0.007	0.770	-3.036
50	0.944	0.947	0.957	0.949	0.007	0.704	-3.413
60	0.940	0.946	0.957	0.948	0.009	0.910	-3.582

\* % Deviation from nominal (%DFN) was calculated from the mean nominal value of nicotine at zero min

**Table B9:** Amount of nicotine released (mg) from snus in the modified USP IV flow through apparatus

<b>Time (min)</b>	<b>1</b>	<b>2</b>	<b>3</b>	<b>4</b>	<b>5</b>	<b>Mean</b>	<b>SD</b>	<b>%RSD</b>
0	0	0	0	0	0	0	0	-
2.5	0.22	0.33	0.57	0.52	0.34	0.40	0.15	36.73
5	0.92	0.86	0.59	0.83	0.47	0.73	0.20	26.69
7.5	1.70	1.32	0.79	1.33	0.71	1.17	0.41	35.28
10	2.47	1.82	1.17	1.83	1.01	1.66	0.59	35.34
15	3.32	2.63	2.11	2.78	1.76	2.52	0.60	23.95
20	3.92	3.22	3.24	3.92	2.32	3.32	0.66	19.88
25	4.33	4.05	3.29	3.94	2.89	3.70	0.59	16.02
30	4.85	4.30	3.78	4.25	3.38	4.11	0.56	13.60
45	5.45	5.23	4.74	5.34	4.52	5.06	0.40	7.95
60	5.97	5.86	5.30	6.00	5.36	5.70	0.34	5.99
<b>Release rate (mg/min)*</b>	0.213	0.166	0.159	0.196	0.119	0.171	0.036	21.316
<b>Lag time (min)**</b>	0.18	0.00	1.11	0.49	0.75	0.51	0.44	87.44

\* Release rate was calculated from 2.5 to 20 min of the nicotine release-time profile because of non-linearity after 20 min

\*\* Lag time was calculated from 2.5 to 30 min of the nicotine permeation-time profile

**Table B10:** Amount of nicotine permeated (mg) from snus in the vertical diffusion cell

<b>Time (min)</b>	<b>1</b>	<b>2</b>	<b>3</b>	<b>4</b>	<b>5</b>	<b>Mean</b>	<b>SD</b>	<b>%RSD</b>
0	0	0	0	0	0	0	0	-
2.5	0.02	0.00	0.00	0.00	0.00	0.00	0.01	223.61
5	0.06	0.02	0.03	0.01	0.01	0.03	0.02	64.43
7.5	0.10	0.06	0.10	0.04	0.04	0.07	0.03	43.54
10	0.17	0.11	0.15	0.08	0.08	0.12	0.04	35.36
15	0.29	0.21	0.27	0.15	0.16	0.22	0.06	28.62
20	0.38	0.31	0.37	0.23	0.24	0.31	0.07	21.63
25	0.48	0.41	0.45	0.30	0.30	0.39	0.08	21.90
30	0.58	0.51	0.54	0.37	0.38	0.48	0.09	19.84
45	0.86	0.80	0.79	0.61	0.61	0.73	0.12	16.21
60	1.16	1.07	1.03	0.80	0.83	0.98	0.15	15.80
<b>Permeation rate (mg/min)*</b>	0.021	0.020	0.020	0.015	0.015	0.018	0.003	17.245
<b>Lag time (min)**</b>	2.03	4.30	2.53	4.28	4.28	3.49	1.12	32.01

\* Permeation rate was calculated from 5 to 30 min of the nicotine permeation-time profile because of lag time of 3.5 min and the removal of snus after 30 min in vivo for comparison of in vitro and in vivo rates

\*\* Lag time was calculated from 5 to 30 min of the nicotine permeation-time profile

**Table B11:** Amount of nicotine permeated (mg) from snus in the bidirectional transmucosal apparatus

<b>Time (min)</b>	<b>1</b>	<b>2</b>	<b>3</b>	<b>4</b>	<b>5</b>	<b>Mean</b>	<b>SD</b>	<b>%RSD</b>
0	0	0	0	0	0	0	0	-
2.5	0.02	0.01	0.03	0.01	0.02	0.02	0.01	73.04
5	0.03	0.02	0.04	0.02	0.03	0.03	0.01	37.20
7.5	0.04	0.03	0.04	0.02	0.03	0.03	0.01	29.12
10	0.05	0.04	0.05	0.03	0.04	0.04	0.01	24.77
15	0.09	0.08	0.07	0.04	0.10	0.08	0.02	28.81
20	0.18	0.18	0.11	0.08	0.26	0.16	0.07	43.85
25	0.26	0.32	0.19	0.15	0.41	0.27	0.10	39.15
30	0.37	0.44	0.32	0.27	0.55	0.39	0.11	28.35
45	0.68	0.79	0.59	0.58	0.95	0.72	0.15	21.42
60	0.91	1.09	0.86	0.88	1.19	0.98	0.15	14.77
<b>Permeation rate (mg/min)*</b>	0.018	0.025	0.017	0.015	0.031	0.021	0.006	30.754
<b>Lag time (min)**</b>	10.02	12.16	11.95	13.70	11.70	11.91	1.31	11.02

\* Permeation rate was calculated from 15 to 30 min of nicotine permeation-time profile because of the lag time of 11.9 min and the removal of snus after 30 min in vivo

\*\* Lag time was calculated from 15 to 30 min of the nicotine permeation-time profile

**Table B12:** Average plasma nicotine levels (ng/mL) for snus (Pouch 1.0g; Nicotine 8 mg) obtained from a clinical study on 18 smokeless tobacco users conducted by the Center of Research and Technology, Altria\*

Time (min)	N	Mean Plasma Conc. (ng/mL)	SD	CV (%)	SEM	Median	Minimum	Maximum	Amount of nicotine absorbed (%)**	Amount of nicotine absorbed (mg)**
0	18	0	0	0	0	0	0	-		
2.5	18	0	0	.	0	0	0	0	0	0
5	18	0.133	0.565	424.264	0.133	0	0	2.398	0	0
7.5	18	1.667	1.646	98.748	0.388	2.139	0	4.942	2.54	0.20
10	18	2.752	1.578	57.359	0.372	2.969	0	5.908	4.25	0.34
15	18	4.148	1.746	42.086	0.411	4.11	0	7.560	6.59	0.53
20	17	5.476	2.484	45.358	0.602	4.783	0	10.183	8.93	0.71
25	18	6.447	2.542	39.427	0.599	5.756	2.340	11.703	10.81	0.86
30	18	7.51	2.914	38.802	0.687	6.845	2.846	12.940	12.89	1.03
45	18	7.775	2.37	30.479	0.559	7.137	3.740	12.758	14.90	1.19
60	18	7.57	2.956	39.049	0.697	6.591	3.884	14.737	16.21	1.30
90	18	6.445	2.888	44.809	0.681	5.873	2.924	13.499	17.46	1.40
120	18	4.895	2.086	42.619	0.492	4.162	2.175	9.287	17.51	1.40
180	18	3.303	1.879	56.88	0.443	2.913	0	6.649	18.57	1.49
240	18	1.873	1.759	93.901	0.415	2.045	0	4.606	18.59	1.49
300	18	0.746	1.44	192.871	0.339	0	0	3.629	18.00	1.44
600	18	0	0	.	0	0	0	0		
720	18	0	0	.	0	0	0	0		

\* Values below limit of quantification of 2 ng/mL were reported as zero; \*\* Amount of nicotine absorbed by Wagner Nelson Modeling (Refer Table B15)

**Table B13:** Method for calculation of the amount of nicotine permeated and released from snus in the BTA \*\*, VDC and USP IV respectively

	Time (min) (A)	Dilution corrected concentration (mcg/mL) (B)*	Amount of nicotine in the volume of receptor or donor media (V mL)*** (mcg) [BxV] (C)	Amount of nicotine in the volume of receptor or donor media sampled (1 mL) [Cx1/V] (mcg) (D)	Amount of nicotine lost at each time point due to sampling (mcg) (E)	Cumulative amount of nicotine permeated or released [C+E] (mcg) (F)	Cumulative amount of nicotine permeated or released [H/1000] (mg) (G) <sup>§</sup>
1	0	0	0	0	0	0	0
2	A2	B2	C2=B2xV	D2=(C2x1)/V	E2=0	F2=C2+E2	G2=F2/1000
3	A3	B3	C3=B3xV	D3=(C3x1)/V	E3=Sum of D1 to D2	F3=C3+E3	G3=F3/1000
4	A4	B4	C4=B4xV	D4=(C4x1)/V	E4=Sum of D1 to D3	F4=C4+E4	G4=F4/1000
5	A5	B5	C5=B5xV	D5=(C5x1)/V	E5=Sum of D1 to D4	F5=C5+E5	G5=F5/1000
6	A6	B6	C6=B6xV	D6=(C6x1)/V	E6=Sum of D1 to D5	F6=C6+E6	G6=F6/1000
7	A7	B7	C7=B7xV	D7=(C7x1)/V	E7=Sum of D1 to D6	F7=C7+E7	G7=F7/1000
8	A8	B8	C8=B8xV	D8=(C8x1)/V	E8=Sum of D1 to D7	F8=C8+E8	G8=F8/1000
9	A9	B9	C9=B9xV	D9=(C9x1)/V	E9=Sum of D1 to D8	F9=C9+E9	G9=F9/1000
10	A10	B10	C10=C10xV	D10=(D10x1)/V	E10=Sum of D1 to D9	F10=C10+E10	G10=G10/1000
* Dilution corrected concentration = Concentration (mcg/mL) x Dilution factor							
** Amount permeated in both receptors calculated by the above method are added to obtain the total amount of nicotine permeated in case of BTA							
*** V = 25 mL for VDC; 20 mL for BTA (Receptor media volume) & V = 30 mL for USP IV (Donor media volume)							
§ Nicotine release was measured for USP IV and permeation was measured for VDC and BTA							

**Table B14:** Wagner Nelson Modeling and deconvolution of plasma drug concentrations to drug absorption time profiles for snus

Time (min) (A)	Mean Plasma Conc. [C <sub>pt</sub> ] (ng/mL) (B)	AUC <sub>0-t</sub> [(ng/mL)*min] (C)	Cumulative AUC <sub>0-t</sub> [(ng/mL)*min] (D)	[K <sub>e</sub> × Cumulative AUC <sub>0-t</sub> ] (ng/mL) (E)*	[C <sub>pt</sub> +(K <sub>e</sub> × Cumulative AUC <sub>0-t</sub> )] (ng/mL) (F)	% of total absorbed [C <sub>pt</sub> +(K <sub>e</sub> × Cumulative AUC <sub>0-t</sub> )]/[K <sub>e</sub> × AUC <sub>0-∞</sub> ] (G)**	Amount of nicotine absorbed (%) (H)***
A0	B0=C <sub>p</sub> 0	C0=0	D0=0	E0=0	F0=0	G0=0	H0=0
A1	B1=C <sub>p</sub> 1	C1=(A1-A0)(B1+B0)/2	D1=D0+C1	E1=K <sub>e</sub> ×D1	F1=B1+E1	G1=F1/( K <sub>e</sub> ×Z)	H1=G1×f
A2	B2=C <sub>p</sub> 2	C2=(A2-A1)(B2+B1)/2	D2=D1+C2	E2=K <sub>e</sub> ×D2	F2=B2+E2	G2=F2/( K <sub>e</sub> ×Z)	H2=G2×f
A3	B3=C <sub>p</sub> 3	C3=(A3-A2)(B3+B2)/2	D3=D2+C3	E3=K <sub>e</sub> ×D3	F3=B3+E3	G3=F3/( K <sub>e</sub> ×Z)	H3=G3×f
A4	B4=C <sub>p</sub> 4	C4=(A4-A3)(B4+B3)/2	D4=D3+C4	E4=K <sub>e</sub> ×D4	F4=B4+E4	G4=F4/( K <sub>e</sub> ×Z)	H4=G4×f
A5	B5=C <sub>p</sub> 5	C5=(A5-A4)(B5+B4)/2	D5=D4+C5	E5=K <sub>e</sub> ×D5	F5=B5+E5	G5=F5/( K <sub>e</sub> ×Z)	H5=G5×f
A6	B6=C <sub>p</sub> 6	C6=(A6-A5)(B6+B5)/2	D6=D5+C6	E6=K <sub>e</sub> ×D6	F6=B6+E6	G6=F6/( K <sub>e</sub> ×Z)	H6=G6×f
A7	B7=C <sub>p</sub> 7	C7=(A7-A6)(B7+B6)/2	D7=D6+C7	E7=K <sub>e</sub> ×D7	F7=B7+E7	G7=F7/( K <sub>e</sub> ×Z)	H7=G7×f
A8	B8=C <sub>p</sub> 8	C8=(A8-A7)(B8+B7)/2	D8=D7+C8	E8=K <sub>e</sub> ×D8	F8=B8+E8	G8=F8/( K <sub>e</sub> ×Z)	H8=G8×f
A9	B9=C <sub>p</sub> 9	C9=(A9-A8)(B9+B8)/2	D9=D8+C9	E9=K <sub>e</sub> ×D9	F9=B9+E9	G9=F9/( K <sub>e</sub> ×Z)	H9=G9×f
A10	B10=C <sub>p</sub> 10	C10=(A10-A9)(B10+B9)/2	D10=D9+C10	E10=K <sub>e</sub> ×D10	F10=B10+E10	G10=F10/( K <sub>e</sub> ×Z)	H10=G10×f

\* K<sub>e</sub> = The elimination rate constant is obtained from the slope of terminal phase of log plasma concentration time profile for the drug product

\*\* AUC<sub>0-∞</sub> = Z = (sum of C0 to C10) + (B10/K<sub>e</sub>)

\*\*\* “f” refers to the absolute availability of drug based on IV study

**Table B15:** Deconvolution of the plasma nicotine concentration to nicotine absorption time profiles using Wagner Nelson Modeling for snus (Pouch 1.0 g, Nicotine 8 mg) (Refer modeling method in Table B14)

Time (min) (A)	Mean Plasma Conc. [C <sub>pt</sub> ] (ng/mL) (B)	AUC <sub>0-t</sub> [(ng/mL)*min] (C)	Cumulative AUC <sub>0-t</sub> [(ng/mL)*min] (D)	[K <sub>e</sub> × Cumulative AUC <sub>0-t</sub> ] (ng/mL) (E)	[C <sub>pt</sub> +(K <sub>e</sub> × Cumulative AUC <sub>0-t</sub> )] (ng/mL) (F)	% of total absorbed [C <sub>pt</sub> +(K <sub>e</sub> × Cumulative AUC <sub>0-t</sub> )/[K <sub>e</sub> × AUC <sub>0-∞</sub> ] (G)	Amount of nicotine absorbed (%) G × f (H)*	Amount of nicotine absorbed (mg) (H×8)/10 0 (I)**
0	0	0	0	0	0	0		
2.5	0	0	0	0	0	0	0	0
5	0	0	0	0	0	0	0	0
7.5	1.667	2.08	2.08	0.02	1.69	14.10	2.54	0.20
10	2.752	5.52	7.61	0.07	2.82	23.60	4.25	0.34
15	4.148	17.25	24.86	0.23	4.38	36.61	6.59	0.53
20	5.476	24.06	48.92	0.46	5.93	49.59	8.93	0.71
25	6.447	29.81	78.73	0.73	7.18	60.03	10.81	0.86
30	7.51	34.89	113.62	1.06	8.57	71.64	12.89	1.03
45	7.775	114.64	228.26	2.13	9.90	82.78	14.90	1.19
60	7.57	115.09	343.34	3.20	10.77	90.04	16.21	1.30
90	6.445	210.23	553.57	5.16	11.60	97.01	17.46	1.40
120	4.895	170.10	723.67	6.74	11.64	97.31	17.51	1.40
180	3.303	245.94	969.61	9.04	12.34	103.16	18.57	1.49
240	1.873	155.28	1124.89	10.48	12.36	103.30	18.59	1.49
300	0.746	78.57	1203.46	11.22	11.96	100.00	18.00	1.44

\* f = 0.18 (Absolute bioavailability based on IV study; Refer Section 3.2.7 of Chapter 3); \*\* “8” refers to the amount of nicotine present in snus

## **APPENDIX C**

### **REPLICATE AND MEAN DATA ON SCREENING OF VARIABLES FOR THE OPTIMIZATION OF IVIVR FOR SNUS REPORTED IN CHAPTER 4**



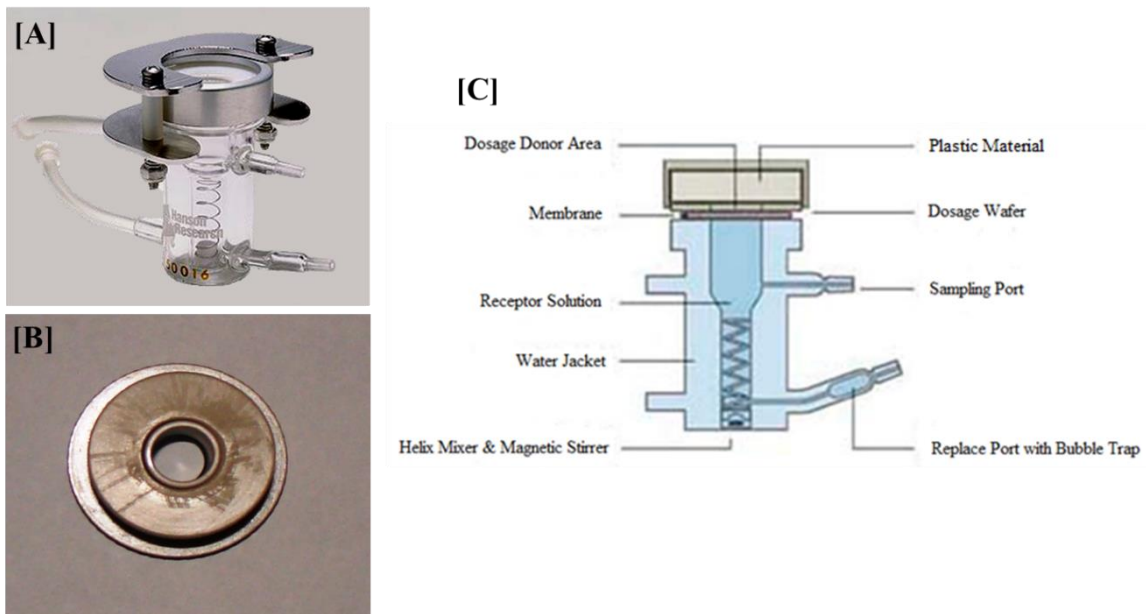


**Figure C1:** [A] Vertical Diffusion Cell (VDC) made of glass with a stainless steel clipper (<http://www.hansonresearch.com/>); [B] Donor chamber of the VDC make of PEEK; [C] Details on the VDC (<http://www.hansonresearch.com/>)

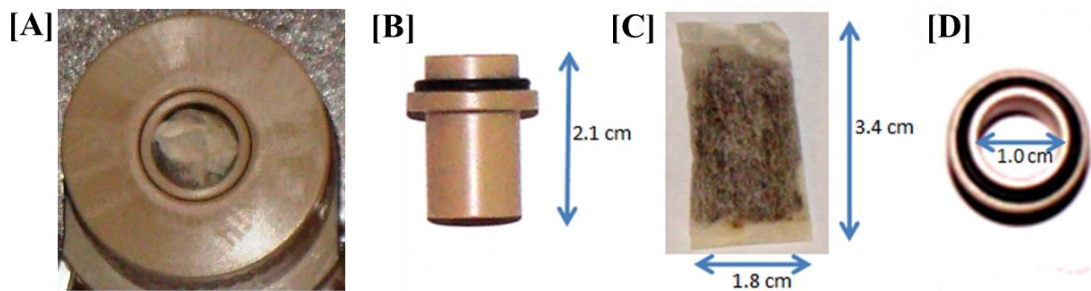


**Figure C2:** [A] The donor chamber of VDC with snus; [B] Side view of the donor chamber of VDC; [C] Dimensions of snus; [D] Top view of the donor chamber of VDC

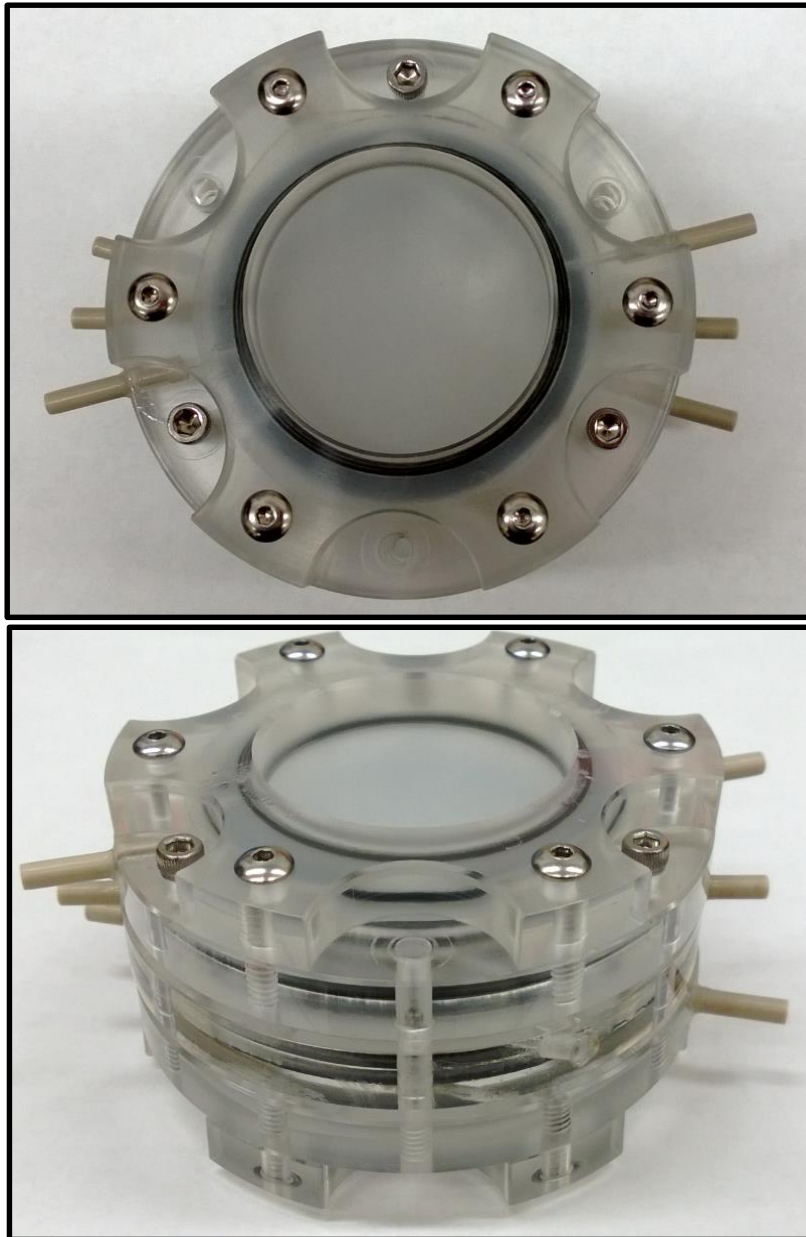


**Figure C3:** The bidirectional transmucosal apparatus for agitation study [A] Top view of the apparatus; [B] Side view of the apparatus.

**Table C1:** Dimensions and types of outlet tubing for the simulation of dead volume in receptor chambers of BTA

<b>Dead Volume of Receptor Chambers (<u>2.67mL</u>)</b>	<b>Tubing type</b>	<b>Tubing Diameter (inch)</b>	<b>Tubing Diameter (inch)</b>	<b>Tubing Diameter (cm)</b>	<b>Tubing radius (cm)</b>	<b>Length (cm)</b>	<b>Volume (cm<sup>3</sup>)</b>
Tubing from BTA outlet to peristaltic pump tubing	FEP	1/16	0.063	0.159	0.079	30	0.59
Peristaltic pump tubing	Silicon	3/32	0.094	0.238	0.119	12	0.53
Peristaltic pump tubing to connector tubing	Silicon	1/8	0.125	0.318	0.159	12	0.95
Connector tubing to reservoir	FEP	1/16	0.063	0.159	0.079	30	0.59
<b>Total Dead Volume (cm<sup>3</sup> or mL)</b>							<b>2.67</b>
<b>Dead Volume of Receptor Chambers (<u>5.15mL</u>)</b>	<b>Tubing type</b>	<b>Tubing Diameter (inch)</b>	<b>Tubing Diameter (inch)</b>	<b>Tubing Diameter (cm)</b>	<b>Tubing radius (cm)</b>	<b>Length (cm)</b>	<b>Volume (cm<sup>3</sup>)</b>
Tubing from BTA outlet to peristaltic pump tubing	FEP	1/16	0.063	0.159	0.079	79	1.56
Peristaltic pump tubing	Silicon	3/32	0.094	0.238	0.119	12	0.53
Peristaltic pump tubing to connector tubing	Silicon	1/8	0.125	0.318	0.159	19	1.50
Connector tubing to reservoir	FEP	1/16	0.063	0.159	0.079	79	1.56
<b>Total Dead Volume (cm<sup>3</sup> or mL)</b>							<b>5.15</b>
<b>Dead Volume of Receptor Chambers (<u>10mL</u>)</b>	<b>Tubing type</b>	<b>Tubing Diameter (inch)</b>	<b>Tubing Diameter (inch)</b>	<b>Tubing Diameter (cm)</b>	<b>Tubing radius (cm)</b>	<b>Length (cm)</b>	<b>Volume (cm<sup>3</sup>)</b>
Tubing from BTA outlet to peristaltic pump tubing	FEP	1/16	0.063	0.159	0.079	93	1.84
Peristaltic pump tubing	Silicon	3/32	0.094	0.238	0.119	12	0.53
Peristaltic pump tubing to connector tubing	Silicon	1/8	0.125	0.318	0.159	73	5.78
Connector tubing to reservoir	FEP	1/16	0.063	0.159	0.079	93	1.84
<b>Total Dead Volume (cm<sup>3</sup> or mL)</b>							<b>9.99</b>

Dead volume is defined as the volume of tubings that connects the outlet of apparatus to the reservoir

Volume was calculated by  $V = \pi * r^2 * L$  (cm<sup>3</sup> or mL) (V is volume, r is tubing radius in cm, L is tubing length in cm)

**Table C2:** Dimensions and types of outlet tubing for the simulation of dead volume in donor chamber of BTA

<b>Dead Volume of Donor Chamber in all Cases (2.67mL)</b>	<b>Tubing type</b>	<b>Tubing Diameter (inch)</b>	<b>Tubing Diameter (inch)</b>	<b>Tubing Diameter (cm)</b>	<b>Tubing radius (cm)</b>	<b>Length (cm)</b>	<b>Volume (cm<sup>3</sup>)</b>
Tubing from BTA outlet to cartridge pump tubing	FEP	1/16	0.063	0.159	0.079	30	0.59
Cartridge pump tubing	Silicon	1/8	0.125	0.318	0.159	19	1.50
Cartridge pump tubing to reservoir	FEP	1/16	0.063	0.159	0.079	30	0.59
<b>Total Dead Volume (cm<sup>3</sup> or mL)</b>							<b>2.68</b>

Dead volume is defined as the volume of tubings that connects the outlet of apparatus to the reservoir

Volume was calculated by  $V = \pi * r^2 * L$  (cm<sup>3</sup> or mL) (V is volume, r is tubing radius in cm, L is tubing length in cm)

**Table C3:** Dimensions and type of inlet tubings in the donor and receptors chambers of BTA

<b>Volume of Inlet Tubing in all Cases</b>	<b>Tubing type</b>	<b>Tubing Diameter (inch)</b>	<b>Tubing Diameter (inch)</b>	<b>Tubing Diameter (cm)</b>	<b>Tubing radius (cm)</b>	<b>Length (cm)</b>	<b>Volume (cm<sup>3</sup>)</b>
Tubing from the reservoir to BTA inlet	FEP	1/16	0.063	0.159	0.079	30	<b>0.59</b>

Volume was calculated by  $V = \pi * r^2 * L$  (cm<sup>3</sup> or mL) (V is volume, r is tubing radius in cm, L is tubing length in cm)

**Table C4:** Method for calculation of the amount of nicotine permeated and released from snus in the BTA

	Time (min) (A)	Dilution corrected concentration (mcg/mL) (B)*	Amount of nicotine in the volume of receptor or donor media (25 mL) (mcg) [Bx25] (C)	Amount of nicotine in the volume of receptor or donor media sampled (1 mL) [Cx1/25] (mcg) (D)	Amount of nicotine lost at each time point due to sampling (mcg) (E)	Cumulative amount of nicotine permeated or released [C+E] (mcg) (F)	Cumulative amount of nicotine permeated or released [H/1000] (mg) (G) <sup>#, \$, ^</sup>
1	0	0	0	0	0	0	0
2	A2	B2	C2=B2x25	D2=(C2x1)/25	E2=0	F2=C2+E2	G2=F2/1000
3	A3	B3	C3=B3x25	D3=(C3x1)/25	E3=Sum of D1 to D2	F3=C3+E3	G3=F3/1000
4	A4	B4	C4=B4x25	D4=(C4x1)/25	E4=Sum of D1 to D3	F4=C4+E4	G4=F4/1000
5	A5	B5	C5=B5x25	D5=(C5x1)/25	E5=Sum of D1 to D4	F5=C5+E5	G5=F5/1000
6	A6	B6	C6=B6x25	D6=(C6x1)/25	E6=Sum of D1 to D5	F6=C6+E6	G6=F6/1000
7	A7	B7	C7=B7x25	D7=(C7x1)/25	E7=Sum of D1 to D6	F7=C7+E7	G7=F7/1000
8	A8	B8	C8=B8x25	D8=(C8x1)/25	E8=Sum of D1 to D7	F8=C8+E8	G8=F8/1000
9	A9	B9	C9=B9x25	D9=(C9x1)/25	E9=Sum of D1 to D8	F9=C9+E9	G9=F9/1000
10	A10	B10	C10=C10x25	D10=(D10x1)/25	E10=Sum of D1 to D9	F10=C10+E10	G10=G10/1000
* Dilution corrected concentration = Concentration (mcg/mL) x Dilution factor							
# Amount permeated in both receptors calculated by the above method are added to obtain the total amount of nicotine permeated							
\$ Nicotine release was measured as a function of saliva pH and donor media flow rate and permeation was measured as a function of all variables except saliva pH							
^ Nicotine release as a function of saliva pH and donor media flow rate was measured separately (i.e. without flowing media in the receptors of BTA)							

**Table C5:** Amount of nicotine released (mg) from snus as a function of saliva pH 6.8( $\beta = 5.5$ )

<b>Time (min)</b>	<b>1</b>	<b>2</b>	<b>3</b>	<b>Mean</b>	<b>SD</b>	<b>%RSD</b>
0	0	0	0	0	0	-
2.5	0.15	0.05	0.08	0.09	0.05	55.47
5	0.36	0.15	0.14	0.22	0.13	57.90
7.5	0.90	0.37	0.30	0.52	0.33	63.16
10	1.33	0.54	0.59	0.82	0.44	53.87
15	2.50	1.01	1.27	1.59	0.80	50.02
20	3.48	1.32	2.04	2.28	1.10	48.42
25	4.26	2.01	2.90	3.06	1.13	37.07
30	4.78	2.51	3.47	3.59	1.14	31.74
45	5.69	3.98	5.08	4.91	0.87	17.65
60	6.57	4.81	6.29	5.89	0.94	15.98
<b>Release rate (mg/min)</b>	0.199	0.089	0.140	0.143	0.055	38.451
<b>Lag time (min)</b>	2.99	3.66	5.16	3.94	1.11	28.16

**Table C6:** Amount of nicotine released (mg) from snus as a function of saliva pH 7.2( $\beta = 7.0$ )

<b>Time (min)</b>	<b>1</b>	<b>2</b>	<b>3</b>	<b>Mean</b>	<b>SD</b>	<b>%RSD</b>
0	0	0	0	0	0	-
2.5	0.07	0.11	0.17	0.12	0.05	40.42
5	0.13	0.42	0.33	0.30	0.15	50.75
7.5	0.26	1.06	0.75	0.69	0.40	58.19
10	0.56	1.74	1.23	1.17	0.59	50.62
15	1.19	2.86	2.11	2.06	0.84	40.69
20	1.90	3.66	3.03	2.86	0.89	31.18
25	2.70	4.47	3.90	3.69	0.90	24.43
30	3.42	5.04	4.54	4.33	0.83	19.10
45	5.19	6.54	5.61	5.78	0.69	11.99
60	6.26	7.04	6.18	6.49	0.47	7.30
<b>Release rate (mg/min)</b>	0.142	0.172	0.176	0.163	0.019	11.507
<b>Lag time (min)</b>	6.10	2.81	0.11	3.00	3.00	99.94

**Table C7:** Amount of nicotine released (mg) from snus as a function of saliva pH 7.6( $\beta = 9.6$ )

<b>Time (min)</b>	<b>1</b>	<b>2</b>	<b>3</b>	<b>Mean</b>	<b>SD</b>	<b>%RSD</b>
0	0	0	0	0	0	-
2.5	0.06	0.05	0.09	0.07	0.02	31.88
5	0.12	0.10	0.16	0.13	0.03	23.39
7.5	0.16	0.20	0.27	0.21	0.05	25.23
10	0.25	0.42	0.44	0.37	0.10	27.75
15	0.72	1.26	1.15	1.04	0.29	27.43
20	1.29	2.33	1.83	1.82	0.52	28.53
25	1.96	2.78	2.70	2.48	0.45	18.33
30	2.51	3.44	3.33	3.09	0.51	16.35
45	3.81	4.75	4.58	4.38	0.50	11.39
60	4.57	5.50	5.49	5.19	0.54	10.34
<b>Release rate (mg/min)</b>	0.151	0.115	0.146	0.138	0.020	14.215
<b>Lag time (min)</b>	6.47	8.30	7.09	7.29	0.93	12.77

**Table C8:** Effect of snus on saliva pH

<b>Saliva pH (<math>\beta</math>)</b>	<b>Saliva Volume (mL)</b>	<b>Sonication Time (min)</b>	<b>Initial pH</b>	<b>Change in pH (Observed – Initial)</b>				
				<b>1</b>	<b>2</b>	<b>3</b>	<b>Mean</b>	<b>SD</b>
6.8 (5.5)	2	2	6.88	-0.16	-0.4	-0.35	-0.30	0.13
	10	2		-0.08	-0.08	0.02	-0.05	0.06
	25	2		0	-0.01	0.04	0.01	0.03
7.2 (7.0)	2	2	7.2	-0.18	-0.1	-0.14	-0.14	0.04
	10	2		0.08	0.06	0.11	0.08	0.03
	25	2		0.06	0.07	0.08	0.07	0.01
7.6 (9.6)	2	2	7.58	0.58	0.44	0.5	0.47	0.07
	10	2		0.34	0.37	0.38	0.36	0.02
	25	2		0.04	0.08	0.09	0.07	0.03

**Table C9:** Amount of nicotine permeated (mg) from snus as a function of SSSR (0.32mL/min)

<b>Time (min)</b>	<b>1</b>	<b>2</b>	<b>3</b>	<b>4</b>	<b>5</b>	<b>Mean</b>	<b>SD</b>	<b>%RSD</b>
0	0	0	0	0	0	0	0	0
2.5	0.08	0.18	0.09	0.18	0.12	0.13	0.05	37.06
5	0.13	0.24	0.24	0.25	0.19	0.21	0.05	24.72
7.5	0.17	0.32	0.34	0.30	0.25	0.27	0.07	24.97
10	0.23	0.40	0.42	0.34	0.34	0.34	0.08	21.85
15	0.37	0.53	0.61	0.43	0.49	0.48	0.09	19.21
20	0.49	0.65	0.82	0.53	0.64	0.63	0.13	20.47
25	0.58	0.77	0.93	0.65	0.79	0.75	0.14	18.26
30	0.73	0.88	1.04	0.76	0.98	0.88	0.14	15.56
45	0.97	1.16	1.34	1.04	1.33	1.17	0.17	14.30
60	1.20	1.41	1.63	1.27	1.58	1.42	0.19	13.42
<b>Permeation rate (mg/min)</b>	0.024	0.026	0.035	0.021	0.031	0.027	0.006	20.911
<b>Lag time (min)</b>	0	0	0	0	0	0	0	-

**Table C10:** Amount of nicotine permeated (mg) from snus as a function of SSSR (1.66mL/min)

<b>Time (min)</b>	<b>1</b>	<b>2</b>	<b>3</b>	<b>4</b>	<b>Mean</b>	<b>SD</b>	<b>%RSD</b>
0	0	0	0	0	0	0	0
2.5	0.15	0.06	0.14	0.06	0.10	0.05	48.57
5	0.21	0.10	0.18	0.11	0.15	0.05	34.43
7.5	0.26	0.16	0.20	0.15	0.19	0.05	25.78
10	0.33	0.21	0.27	0.19	0.25	0.07	26.16
15	0.43	0.25	0.34	0.28	0.33	0.08	24.41
20	0.53	0.30	0.42	0.37	0.41	0.10	23.76
25	0.62	0.36	0.49	0.47	0.48	0.11	22.77
30	0.68	0.41	0.54	0.53	0.54	0.11	20.86
45	0.77	0.54	0.65	0.67	0.66	0.09	13.98
60	0.79	0.60	0.69	0.73	0.70	0.08	11.41
<b>Permeation rate (mg/min)</b>	0.021	0.013	0.016	0.018	0.017	0.004	21.063
<b>Lag time (min)</b>	0	0	0	0	0	0	-



**Table C11:** Amount of nicotine permeated (mg) from snus as a function of SSSR (3mL/min)

<b>Time (min)</b>	<b>1</b>	<b>2</b>	<b>3</b>	<b>4</b>	<b>Mean</b>	<b>SD</b>	<b>%RSD</b>
0	0	0	0	0	0	0	0
2.5	0.06	0.03	0.01	0.02	0.03	0.02	61.77
5	0.11	0.06	0.03	0.03	0.06	0.04	61.65
7.5	0.17	0.09	0.06	0.06	0.09	0.05	56.22
10	0.23	0.14	0.11	0.09	0.14	0.06	42.18
15	0.31	0.22	0.19	0.17	0.22	0.06	28.75
20	0.36	0.29	0.26	0.22	0.28	0.06	20.73
25	0.40	0.35	0.29	0.27	0.33	0.06	18.14
30	0.42	0.38	0.32	0.30	0.36	0.06	16.12
45	0.47	0.44	0.35	0.33	0.40	0.07	17.00
60	0.48	0.45	0.35	0.34	0.41	0.07	17.11
<b>Permeation rate (mg/min)</b>	0.021	0.015	0.016	0.013	0.016	0.003	20.408
<b>Lag time (min)</b>	0	0.74	3.15	2.62	1.63	1.50	92.08

**Table C12:** Amount of nicotine permeated (mg) from snus as a function of receptor media flow rate (1 mL/min)

<b>Time (min)</b>	<b>1</b>	<b>2</b>	<b>3</b>	<b>Mean</b>	<b>SD</b>	<b>%RSD</b>
0	0	0	0	0	0	-
2.5	0.01	0.01	0.01	0.01	0.00	16.77
5	0.03	0.04	0.03	0.03	0.00	15.48
7.5	0.06	0.09	0.06	0.07	0.02	27.97
10	0.10	0.15	0.10	0.12	0.03	23.84
15	0.22	0.30	0.23	0.25	0.05	18.69
20	0.32	0.38	0.37	0.36	0.03	9.63
25	0.43	0.54	0.51	0.49	0.06	12.01
30	0.54	0.60	0.58	0.57	0.03	5.42
45	0.87	0.93	0.92	0.91	0.03	3.66
60	1.15	1.27	1.23	1.21	0.06	5.18
<b>Permeation rate (mg/min)</b>	0.021	0.022	0.022	0.022	0.001	3.376
<b>Lag time (min)</b>	4.72	2.45	4.27	3.81	1.20	31.58

**Table C13:** Amount of nicotine permeated (mg) from snus as a function of receptor media flow rate (6 mL/min)

<b>Time (min)</b>	<b>1</b>	<b>2</b>	<b>3</b>	<b>Mean</b>	<b>SD</b>	<b>%RSD</b>
0	0	0	0	0	0	-
2.5	0.02	0.03	0.03	0.03	0.01	24.27
5	0.06	0.07	0.05	0.06	0.01	12.00
7.5	0.12	0.11	0.10	0.11	0.01	5.92
10	0.19	0.17	0.16	0.17	0.02	9.44
15	0.37	0.27	0.29	0.31	0.05	16.91
20	0.50	0.34	0.39	0.41	0.08	19.51
25	0.61	0.44	0.51	0.52	0.09	16.60
30	0.74	0.54	0.58	0.62	0.10	16.73
45	1.09	0.87	0.86	0.94	0.13	13.90
60	1.36	1.12	1.12	1.20	0.14	11.36
<b>Permeation rate (mg/min)</b>	0.024	0.019	0.019	0.021	0.002	11.984
<b>Lag time (min)</b>	0.25	1.69	0.46	0.80	0.78	97.02

**Table C14:** Amount of nicotine permeated (mg) from snus as a function of receptor media flow rate (16 mL/min)

<b>Time (min)</b>	<b>1</b>	<b>2</b>	<b>3</b>	<b>Mean</b>	<b>SD</b>	<b>%RSD</b>
0	0	0	0	0	0	-
2.5	0.07	0.04	0.03	0.04	0.02	43.64
5	0.12	0.06	0.07	0.08	0.03	33.49
7.5	0.18	0.10	0.13	0.14	0.04	26.92
10	0.24	0.18	0.19	0.20	0.03	16.81
15	0.36	0.29	0.32	0.32	0.04	11.39
20	0.48	0.38	0.45	0.44	0.05	11.63
25	0.62	0.51	0.57	0.57	0.05	9.53
30	0.74	0.61	0.68	0.68	0.07	9.84
45	1.05	0.96	1.03	1.01	0.05	4.71
60	1.34	1.25	1.27	1.29	0.04	3.32
<b>Permeation rate (mg/min)</b>	0.022	0.022	0.022	0.022	0.000	0.784
<b>Lag time (min)</b>	0.00	2.14	0.44	0.86	1.13	131.66

**Table C15:** Amount of nicotine permeated (mg) from snus as a function of donor media flow rate (1.66 mL/min)

<b>Time (min)</b>	<b>1</b>	<b>2</b>	<b>3</b>	<b>4</b>	<b>5</b>	<b>Mean</b>	<b>SD</b>	<b>%RSD</b>
0	0	0	0	0	0	0	0	-
2.5	0.02	0.04	0.03	0.06	0.07	0.04	0.02	43.61
5	0.05	0.09	0.08	0.10	0.15	0.09	0.03	37.22
7.5	0.08	0.19	0.17	0.18	0.24	0.17	0.06	35.13
10	0.11	0.24	0.24	0.25	0.34	0.24	0.08	34.28
15	0.18	0.46	0.37	0.55	0.47	0.41	0.14	34.68
20	0.35	0.59	0.54	0.69	0.63	0.56	0.13	23.08
25	0.51	0.70	0.65	0.85	0.72	0.69	0.12	17.94
30	0.63	0.83	0.79	0.95	0.80	0.80	0.11	14.18
45	1.01	1.21	1.14	1.24	1.18	1.16	0.09	7.70
60	1.31	1.52	1.42	1.49	1.44	1.44	0.08	5.80
<b>Permeation rate (mg/min)</b>	0.025	0.025	0.024	0.025	0.023	0.024	0.001	4.253
<b>Lag time (min)</b>	5.22	0.00	0.00	0.00	0.00	1.04	2.34	223.61

**Table C16:** Amount of nicotine permeated (mg) from snus as a function of donor media flow rate (6 mL/min)

<b>Time (min)</b>	<b>1</b>	<b>2</b>	<b>3</b>	<b>4</b>	<b>5</b>	<b>Mean</b>	<b>SD</b>	<b>%RSD</b>
0	0	0	0	0	0	0	0	-
2.5	0.01	0.02	0.02	0.02	0.02	0.02	0.00	22.22
5	0.03	0.04	0.06	0.04	0.05	0.04	0.01	25.92
7.5	0.07	0.08	0.12	0.08	0.09	0.09	0.02	21.36
10	0.13	0.14	0.17	0.13	0.13	0.14	0.02	13.34
15	0.24	0.28	0.31	0.26	0.30	0.28	0.03	10.57
20	0.39	0.40	0.48	0.44	0.43	0.43	0.04	8.53
25	0.49	0.54	0.65	0.58	0.59	0.57	0.06	10.32
30	0.62	0.68	0.76	0.74	0.72	0.70	0.05	7.72
45	1.06	1.02	1.26	1.17	1.18	1.14	0.10	8.52
60	1.31	1.44	1.63	1.59	1.57	1.51	0.13	8.78
<b>Permeation rate (mg/min)</b>	0.024	0.026	0.029	0.029	0.028	0.027	0.002	8.181
<b>Lag time (min)</b>	4.39	4.03	3.63	4.78	4.28	4.22	0.43	10.12

**Table C17:** Amount of nicotine permeated (mg) from snus as a function of donor media flow rate (16 mL/min)

<b>Time (min)</b>	<b>1</b>	<b>2</b>	<b>3</b>	<b>4</b>	<b>5</b>	<b>Mean</b>	<b>SD</b>	<b>%RSD</b>
0	0	0	0	0	0	0	0	-
2.5	0.02	0.03	0.03	0.02	0.05	0.03	0.01	42.70
5	0.04	0.09	0.09	0.06	0.11	0.08	0.03	32.33
7.5	0.09	0.20	0.14	0.11	0.15	0.14	0.04	29.24
10	0.14	0.29	0.22	0.17	0.23	0.21	0.06	28.58
15	0.26	0.47	0.44	0.32	0.36	0.37	0.09	23.52
20	0.39	0.64	0.58	0.52	0.49	0.52	0.10	18.35
25	0.53	0.84	0.73	0.64	0.65	0.68	0.12	17.10
30	0.64	0.93	0.87	0.77	0.82	0.81	0.11	13.95
45	1.00	1.25	1.33	1.17	1.23	1.19	0.12	10.26
60	1.28	1.62	1.73	1.45	1.53	1.52	0.17	11.06
<b>Permeation rate (mg/min)</b>	0.023	0.027	0.030	0.026	0.027	0.027	0.003	9.359
<b>Lag time (min)</b>	3.34	0.00	1.66	2.11	1.15	1.65	1.23	74.48

**Table C18:** Amount of nicotine released (mg) from snus as a function of donor media flow rate (1.66 mL/min)

<b>Time (min)</b>	<b>1</b>	<b>2</b>	<b>3</b>	<b>4</b>	<b>5</b>	<b>Mean</b>	<b>SD</b>	<b>%RSD</b>
0	0	0	0	0	0	0	0	-
2.5	0.45	0.10	0.13	0.10	0.21	0.20	0.15	75.06
5	0.94	0.27	0.32	0.44	0.52	0.50	0.27	53.35
7.5	1.30	0.53	0.52	0.72	0.89	0.79	0.32	41.03
10	2.04	0.83	0.77	0.85	1.21	1.14	0.53	46.71
15	2.80	1.52	1.29	1.53	2.06	1.84	0.61	33.06
20	3.49	2.30	1.85	2.41	2.59	2.53	0.60	23.88
25	3.97	2.81	2.44	2.68	3.05	2.99	0.59	19.72
30	4.63	3.44	2.77	3.22	3.56	3.52	0.69	19.48
45	5.49	4.36	4.21	4.33	4.94	4.67	0.54	11.50
60	6.32	5.43	4.68	5.03	5.86	5.47	0.65	11.90
<b>Release rate (mg/min)</b>	0.155	0.123	0.099	0.115	0.124	0.123	0.020	16.459
<b>Lag time (min)</b>	0	2.17	1.51	1.27	1.51	1.29	0.80	61.61

**Table C19:** Amount of nicotine released (mg) from snus as a function of donor media flow rate (6 mL/min)

<b>Time (min)</b>	<b>1</b>	<b>2</b>	<b>3</b>	<b>4</b>	<b>5</b>	<b>Mean</b>	<b>SD</b>	<b>%RSD</b>
0	0	0	0	0	0	0	0	-
2.5	0.68	0.83	0.74	0.35	0.88	0.70	0.21	29.60
5	1.23	1.57	1.74	0.85	1.59	1.40	0.36	25.55
7.5	1.78	2.62	2.83	1.49	2.44	2.23	0.57	25.55
10	2.25	3.36	3.81	2.16	3.19	2.96	0.72	24.33
15	2.96	5.19	4.91	3.07	4.00	4.03	1.02	25.41
20	3.48	5.84	5.53	3.70	4.78	4.66	1.06	22.71
25	4.04	6.26	6.27	4.08	5.58	5.25	1.12	21.34
30	4.35	6.61	6.29	4.39	5.84	5.50	1.07	19.38
45	5.42	7.26	6.60	4.93	6.25	6.09	0.93	15.23
60	5.73	7.22	6.89	5.11	6.53	6.30	0.87	13.75
<b>Release rate (mg/min)</b>	0.194	0.349	0.347	0.217	0.261	0.274	0.072	26.323
<b>Lag time (min)</b>	0	0.21	0	0.64	0	0.17	0.28	163.35

**Table C20:** Amount of nicotine released (mg) from snus as a function of donor media flow rate (16 mL/min)

<b>Time (min)</b>	<b>1</b>	<b>2</b>	<b>3</b>	<b>4</b>	<b>5</b>	<b>Mean</b>	<b>SD</b>	<b>%RSD</b>
0	0	0	0	0	0	0	0	-
2.5	1.46	0.89	1.34	1.53	2.20	1.48	0.47	31.74
5	2.35	1.79	2.10	2.41	2.95	2.32	0.43	18.54
7.5	2.96	2.31	2.72	3.02	3.92	2.99	0.59	19.81
10	3.72	2.56	3.26	3.39	3.99	3.38	0.54	16.06
15	3.87	3.16	3.91	4.28	4.58	3.96	0.53	13.44
20	4.38	3.37	4.37	4.67	5.01	4.36	0.61	14.04
25	4.68	3.62	4.64	5.01	5.44	4.68	0.67	14.41
30	4.83	3.74	5.17	5.50	5.68	4.98	0.77	15.44
45	5.23	4.03	5.52	5.91	6.21	5.38	0.84	15.67
60	5.54	4.33	5.88	6.18	6.37	5.66	0.81	14.28
<b>Release rate (mg/min)</b>	0.331	0.304	0.313	0.352	0.369	0.334	0.027	8.131
<b>Lag time (min)</b>	0	0	0	0	0	0	0	-

**Table C21:** Amount of nicotine permeated (mg) from snus as a function of receptor to donor media volume ratio (2)

<b>Time (min)</b>	<b>1</b>	<b>2</b>	<b>3</b>	<b>Mean</b>	<b>SD</b>	<b>%RSD</b>
0	0	0	0	0	0	-
2.5	0.03	0.01	0.01	0.02	0.01	65.37
5	0.06	0.03	0.04	0.04	0.02	38.15
7.5	0.11	0.06	0.08	0.08	0.02	24.62
10	0.14	0.11	0.12	0.12	0.02	15.55
15	0.29	0.27	0.24	0.27	0.02	8.76
20	0.48	0.44	0.41	0.44	0.04	8.37
25	0.64	0.56	0.60	0.60	0.04	6.50
30	0.80	0.68	0.77	0.75	0.06	7.80
45	1.18	1.03	1.11	1.11	0.07	6.58
60	1.51	1.35	1.46	1.44	0.08	5.66
<b>Permeation rate (mg/min)</b>	0.028	0.025	0.027	0.026	0.001	5.506
<b>Lag time (min)</b>	3.23	3.79	4.46	3.83	0.62	16.12

**Table C22:** Amount of nicotine permeated (mg) from snus as a function of receptor to donor media volume ratio (4)

<b>Time (min)</b>	<b>1</b>	<b>2</b>	<b>3</b>	<b>Mean</b>	<b>SD</b>	<b>%RSD</b>
0	0	0	0	0	0	-
2.5	0.02	0.02	0.03	0.03	0.01	27.73
5	0.04	0.02	0.05	0.04	0.01	32.63
7.5	0.06	0.04	0.08	0.06	0.02	36.57
10	0.09	0.07	0.14	0.10	0.03	34.11
15	0.19	0.14	0.24	0.19	0.05	26.29
20	0.28	0.24	0.37	0.29	0.07	22.73
25	0.39	0.36	0.51	0.42	0.08	19.48
30	0.49	0.43	0.65	0.53	0.11	21.76
45	0.86	0.77	0.99	0.87	0.11	12.74
60	1.17	1.13	1.36	1.22	0.12	9.77
<b>Permeation rate (mg/min)</b>	0.022	0.021	0.025	0.022	0.002	8.476
<b>Lag time (min)</b>	6.11	7.59	4.42	6.04	1.59	26.26

**Table C23:** Amount of nicotine permeated (mg) from snus as a function of receptor to donor media volume ratio (8)

<b>Time (min)</b>	<b>1</b>	<b>2</b>	<b>3</b>	<b>Mean</b>	<b>SD</b>	<b>%RSD</b>
0	0	0	0	0	0	-
2.5	0.00	0.00	0.00	0.00	0.00	-
5	0.04	0.04	0.04	0.04	0.00	4.55
7.5	0.07	0.07	0.05	0.06	0.01	14.34
10	0.11	0.12	0.11	0.11	0.00	3.73
15	0.24	0.29	0.18	0.23	0.05	22.27
20	0.37	0.37	0.29	0.35	0.05	13.31
25	0.50	0.47	0.41	0.46	0.05	10.42
30	0.65	0.63	0.50	0.59	0.08	13.65
45	1.03	1.05	0.87	0.99	0.10	9.73
60	1.48	1.44	1.17	1.36	0.17	12.30
<b>Permeation rate (mg/min)</b>	0.027	0.026	0.022	0.025	0.003	11.490
<b>Lag time (min)</b>	5.94	5.36	5.78	5.69	0.30	5.30

**Table C24:** Amount of nicotine permeated (mg) from snus as a function of receptor dead volume (2.67 mL)

<b>Time (min)</b>	<b>1</b>	<b>2</b>	<b>3</b>	<b>4</b>	<b>5</b>	<b>Mean</b>	<b>SD</b>	<b>%RSD</b>
0	0	0	0	0	0	0	0	-
2.5	0.01	0.03	0.04	0.02	0.02	0.02	0.01	37.93
5	0.02	0.04	0.05	0.05	0.03	0.04	0.01	32.42
7.5	0.03	0.05	0.07	0.07	0.04	0.05	0.02	33.34
10	0.05	0.06	0.09	0.12	0.05	0.07	0.03	41.25
15	0.12	0.14	0.18	0.34	0.14	0.18	0.09	48.83
20	0.28	0.33	0.43	0.62	0.31	0.39	0.14	35.51
25	0.53	0.58	0.61	0.79	0.51	0.60	0.11	18.07
30	0.73	0.81	0.82	0.99	0.81	0.83	0.09	11.35
45	1.29	1.43	1.32	1.41	1.45	1.38	0.07	5.14
60	1.67	1.87	1.65	1.71	1.95	1.77	0.13	7.61
<b>Permeation rate (mg/min)</b>	0.035	0.045	0.038	0.040	0.044	0.040	0.004	10.256
<b>Lag Time (min)</b>	3.20	12.55	9.16	12.10	11.89	9.78	3.91	40.01

**Table C25:** Amount of nicotine permeated (mg) from snus as a function of receptor dead volume (5.15 mL)

<b>Time (min)</b>	<b>1</b>	<b>2</b>	<b>3</b>	<b>4</b>	<b>5</b>	<b>Mean</b>	<b>SD</b>	<b>%RSD</b>
0	0	0	0	0	0	0	0	-
2.5	0.01	0.02	0.03	0.04	0.02	0.02	0.01	42.47
5	0.03	0.03	0.04	0.04	0.03	0.03	0.01	23.41
7.5	0.05	0.04	0.06	0.05	0.04	0.05	0.01	13.26
10	0.06	0.06	0.08	0.05	0.07	0.06	0.01	16.92
15	0.10	0.10	0.15	0.07	0.14	0.11	0.03	29.42
20	0.20	0.19	0.29	0.11	0.31	0.22	0.08	36.86
25	0.32	0.32	0.43	0.22	0.56	0.37	0.13	34.90
30	0.46	0.40	0.60	0.39	0.77	0.52	0.16	31.05
45	0.94	0.71	1.01	0.82	1.35	0.97	0.24	25.25
60	1.24	1.00	1.26	1.14	1.76	1.28	0.28	22.21
<b>Permeation rate (mg/min)</b>	0.020	0.029	0.030	0.029	0.041	0.030	0.007	24.447
<b>Lag Time (min)</b>	11.66	9.86	13.97	16.59	10.10	12.43	2.84	22.85

**Table C26:** Amount of nicotine permeated (mg) from snus as a function of receptor dead volume (10 mL)

<b>Time (min)</b>	<b>1</b>	<b>2</b>	<b>3</b>	<b>4</b>	<b>5</b>	<b>Mean</b>	<b>SD</b>	<b>%RSD</b>
0	0	0	0	0	0	0	0	-
2.5	0.00	0.02	0.02	0.02	0.02	0.01	0.01	56.37
5	0.02	0.02	0.02	0.02	0.02	0.02	0.00	14.21
7.5	0.02	0.03	0.03	0.03	0.03	0.03	0.00	18.02
10	0.02	0.04	0.03	0.05	0.04	0.04	0.01	28.78
15	0.04	0.07	0.05	0.16	0.12	0.09	0.05	59.73
20	0.06	0.14	0.07	0.37	0.34	0.20	0.15	75.38
25	0.10	0.23	0.11	0.52	0.56	0.30	0.22	73.50
30	0.21	0.38	0.16	0.70	0.73	0.44	0.27	61.78
45	0.77	0.81	0.61	1.16	1.28	0.93	0.28	30.68
60	0.90	1.17	1.02	1.47	1.60	1.23	0.29	23.89
<b>Permeation rate (mg/min)</b>	0.035	0.029	0.026	0.032	0.036	0.032	0.004	13.095
<b>Lag Time (min)</b>	22.93	16.83	22.27	8.36	9.75	16.03	6.81	42.49



**Table C27:** Amount of nicotine permeated (mg) from snus as a function of media temperature (25°C)

<b>Time (min)</b>	<b>1</b>	<b>2</b>	<b>3</b>	<b>4</b>	<b>5</b>	<b>Mean</b>	<b>SD</b>	<b>%RSD</b>
0	0	0	0	0	0	0	0	-
2.5	0.03	0.02	0.03	0.02	0.01	0.02	0.01	36.43
5	0.05	0.04	0.08	0.04	0.03	0.05	0.02	36.66
7.5	0.10	0.08	0.12	0.07	0.07	0.09	0.02	23.46
10	0.15	0.12	0.16	0.12	0.13	0.14	0.02	12.68
15	0.24	0.24	0.26	0.24	0.25	0.25	0.01	4.68
20	0.35	0.33	0.38	0.40	0.40	0.37	0.03	8.94
25	0.44	0.43	0.49	0.51	0.49	0.47	0.03	7.15
30	0.54	0.54	0.61	0.64	0.67	0.60	0.06	9.49
45	0.85	0.78	0.92	1.07	0.95	0.91	0.11	11.83
60	1.12	1.10	1.26	1.38	1.25	1.22	0.11	9.27
<b>Permeation rate (mg/min)</b>	0.020	0.019	0.022	0.025	0.023	0.022	0.002	11.302
<b>Lag Time (min)</b>	2.31	3.08	2.28	4.48	3.49	3.13	0.92	29.31

**Table C28:** Amount of nicotine permeated (mg) from snus as a function of media temperature (37°C)

<b>Time (min)</b>	<b>1</b>	<b>2</b>	<b>3</b>	<b>4</b>	<b>5</b>	<b>Mean</b>	<b>SD</b>	<b>%RSD</b>
0	0	0	0	0	0	0	0	-
2.5	0.05	0.04	0.07	0.04	0.02	0.05	0.02	35.84
5	0.13	0.13	0.13	0.11	0.06	0.11	0.03	26.30
7.5	0.22	0.20	0.24	0.20	0.13	0.20	0.04	21.02
10	0.32	0.32	0.34	0.28	0.20	0.29	0.05	18.18
15	0.52	0.52	0.57	0.49	0.39	0.50	0.07	13.60
20	0.72	0.73	0.75	0.66	0.60	0.69	0.06	9.01
25	0.92	1.00	0.96	0.86	0.82	0.91	0.07	8.16
30	1.14	1.18	1.15	1.04	0.99	1.10	0.08	7.24
45	1.67	1.77	1.74	1.56	1.57	1.66	0.10	5.98
60	2.15	2.29	2.28	1.99	2.09	2.16	0.13	5.90
<b>Permeation rate (mg/min)</b>	0.037	0.040	0.039	0.035	0.038	0.038	0.002	5.459
<b>Lag Time (min)</b>	0.99	1.73	1.08	1.28	3.97	1.81	1.24	68.50

**Table C29:** Amount of nicotine permeated (mg) from snus as a function of media temperature (45°C)

<b>Time (min)</b>	<b>1</b>	<b>2</b>	<b>3</b>	<b>4</b>	<b>5</b>	<b>Mean</b>	<b>SD</b>	<b>%RSD</b>
0	0	0	0	0	0	0	0	-
2.5	0.06	0.14	0.05	0.04	0.06	0.07	0.04	59.18
5	0.16	0.27	0.13	0.09	0.13	0.16	0.07	43.06
7.5	0.28	0.43	0.22	0.19	0.24	0.27	0.09	34.30
10	0.41	0.57	0.35	0.29	0.34	0.39	0.11	27.11
15	0.68	0.85	0.64	0.50	0.58	0.65	0.13	20.49
20	0.90	1.13	0.86	0.73	0.79	0.88	0.16	17.65
25	1.19	1.36	1.11	0.90	0.99	1.11	0.18	16.18
30	1.36	1.58	1.31	1.12	1.21	1.32	0.17	13.08
45	2.21	2.22	1.95	1.65	1.77	1.96	0.26	13.04
60	2.57	2.53	2.52	2.12	2.19	2.39	0.21	8.83
<b>Permeation rate (mg/min)</b>	0.051	0.050	0.046	0.039	0.041	0.045	0.005	11.083
<b>Lag Time (min)</b>	1.83	0.00	1.81	2.15	1.27	1.41	0.85	60.18

**Table C30:** Amount of nicotine permeated (mg) from snus without agitation

<b>Time (min)</b>	<b>1</b>	<b>2</b>	<b>3</b>	<b>4</b>	<b>5</b>	<b>Mean</b>	<b>SD</b>	<b>%RSD</b>
0	0	0	0	0	0	0	0	-
2.5	0.03	0.02	0.07	0.03	0.01	0.03	0.02	69.50
5	0.05	0.03	0.08	0.04	0.02	0.04	0.03	61.49
7.5	0.05	0.03	0.11	0.06	0.02	0.05	0.03	62.63
10	0.06	0.04	0.12	0.07	0.03	0.06	0.04	59.05
15	0.08	0.06	0.17	0.09	0.04	0.09	0.05	54.37
20	0.20	0.11	0.28	0.19	0.08	0.17	0.08	46.70
25	0.36	0.20	0.48	0.36	0.16	0.31	0.13	41.85
30	0.58	0.36	0.66	0.59	0.27	0.49	0.17	33.51
45	1.17	0.92	1.34	1.27	0.74	1.09	0.25	22.85
60	1.56	1.35	1.93	1.72	1.25	1.56	0.27	17.51
<b>Permeation rate (mg/min)</b>	0.042	0.039	0.030	0.035	0.032	0.036	0.005	13.502
<b>Lag Time (min)</b>	13.57	15.06	19.25	13.87	17.76	15.90	2.50	15.72

**Table C31:** Amount of nicotine permeated (mg) from snus with agitation (1 agitation/min)

<b>Time (min)</b>	<b>1</b>	<b>2</b>	<b>3</b>	<b>4</b>	<b>5</b>	<b>Mean</b>	<b>SD</b>	<b>%RSD</b>
0	0	0	0	0	0	0	0	-
2.5	0.05	0.08	0.03	0.06	0.08	0.06	0.02	38.41
5	0.08	0.11	0.04	0.14	0.16	0.11	0.05	45.78
7.5	0.14	0.18	0.11	0.19	0.27	0.18	0.06	34.29
10	0.22	0.24	0.14	0.35	0.36	0.26	0.09	34.77
15	0.38	0.40	0.23	0.51	0.53	0.41	0.12	29.23
20	0.51	0.52	0.33	0.70	0.69	0.55	0.15	27.87
25	0.64	0.64	0.45	0.88	0.82	0.69	0.17	24.93
30	0.74	0.76	0.53	1.06	0.99	0.82	0.21	26.15
45	1.18	1.01	0.78	1.57	1.42	1.19	0.31	26.22
60	1.58	1.48	1.04	1.95	1.82	1.57	0.35	22.54
<b>Permeation rate (mg/min)</b>	0.034	0.030	0.027	0.024	0.018	0.027	0.006	22.944
<b>Lag Time (min)</b>	0.04	0.00	1.29	0.00	1.39	0.54	0.73	133.62

## **APPENDIX D**

### **REPLICATE AND MEAN DATA ON OPTIMIZATION OF THE IVIVR FOR SNUS REPORTED IN CHAPTER 5**

**Table D0:** Method for calculation of the amount of nicotine permeated\*\* as a function of SSSR (mL/min) and temperature (°C) over time

	Time (min) (A)	Dilution corrected concentration (mcg/mL) (B)*	Amount of nicotine in the volume of receptor media (25 mL) (mcg) [Bx25] (C)	Amount of nicotine in the volume of receptor media sampled (1 mL) [Cx1/25] (mcg) (D)	Amount of nicotine lost at each time point due to sampling (mcg) (E)	Cumulative amount of nicotine permeated [C+E] (mcg) (F)	Cumulative amount of nicotine swallowed [H/1000] (mg) (G)
1	0	0	0	0	0	0	0
2	2.5	B2	C2=B2x25	D2=(C2x1)/25	E2=0	F2=C2+E2	G2=F2/1000
3	5	B3	C3=B3x25	D3=(C3x1)/25	E3=Sum of D1 to D2	F3=C3+E3	G3=F3/1000
4	7.5	B4	C4=B4x25	D4=(C4x1)/25	E4=Sum of D1 to D3	F4=C4+E4	G4=F4/1000
5	10	B5	C5=B5x25	D5=(C5x1)/25	E5=Sum of D1 to D4	F5=C5+E5	G5=F5/1000
6	15	B6	C6=B6x25	D6=(C6x1)/25	E6=Sum of D1 to D5	F6=C6+E6	G6=F6/1000
7	20	B7	C7=B7x25	D7=(C7x1)/25	E7=Sum of D1 to D6	F7=C7+E7	G7=F7/1000
8	25	B8	C8=B8x25	D8=(C8x1)/25	E8=Sum of D1 to D7	F8=C8+E8	G8=F8/1000
9	30	B9	C9=B9x25	D9=(C9x1)/25	E9=Sum of D1 to D8	F9=C9+E9	G9=F9/1000
* Dilution corrected concentration = Concentration (mcg/mL) x Dilution factor							
** Amount permeated in both receptors calculated by the above method are added to obtain the total amount of nicotine permeated							

**Table D1:** Amount of nicotine permeated (mg) from snus as a function of SSSR 0.32 mL/min and media temperature 25 °C

<b>Time (min)</b>	<b>1</b>	<b>2</b>	<b>3</b>	<b>4</b>	<b>Mean</b>	<b>SD</b>	<b>%RSD</b>
0	0	0	0	0	0	0	-
2.5	0.15	0.06	0.17	0.11	0.12	0.05	38.96
5	0.20	0.10	0.21	0.17	0.17	0.05	27.39
7.5	0.26	0.16	0.26	0.23	0.23	0.05	20.11
10	0.33	0.23	0.30	0.31	0.29	0.05	15.99
15	0.47	0.35	0.38	0.44	0.41	0.06	13.36
20	0.60	0.46	0.49	0.58	0.53	0.07	12.97
25	0.66	0.58	0.55	0.72	0.63	0.08	12.57
30	0.77	0.64	0.59	0.86	0.72	0.12	16.75
<b>Permeation rate (mg/min)*</b>	0.022	0.022	0.015	0.028	0.022	0.005	23.104
<b>Ratio of rates**</b>	0.61	0.60	0.43	0.77	0.60	0.14	23.10

\* Permeation rate was calculated from the amount of nicotine permeated from 7.5 to 30 min

\*\* Ratio of rates is the ratio of *in vitro* nicotine permeation to the *in vivo* nicotine absorption rate (0.036 mg/min)

**Table D2:** Amount of nicotine permeated (mg) from snus as a function of SSSR 0.32 mL/min and media temperature 37 °C

<b>Time (min)</b>	<b>1</b>	<b>2</b>	<b>3</b>	<b>4</b>	<b>Mean</b>	<b>SD</b>	<b>%RSD</b>
0	0	0	0	0	0	0	-
2.5	0.11	0.08	0.12	0.14	0.12	0.02	21.66
5	0.19	0.15	0.19	0.22	0.19	0.03	15.12
7.5	0.29	0.26	0.29	0.32	0.29	0.02	8.24
10	0.42	0.35	0.37	0.40	0.38	0.03	7.86
15	0.62	0.55	0.57	0.54	0.57	0.04	6.66
20	0.82	0.71	0.73	0.75	0.75	0.05	6.16
25	0.94	0.87	0.87	0.88	0.89	0.04	3.95
30	1.11	0.99	0.98	0.97	1.01	0.06	6.30
<b>Permeation rate (mg/min)*</b>	0.036	0.033	0.031	0.030	0.033	0.002	7.627
<b>Ratio of rates**</b>	0.99	0.92	0.86	0.84	0.90	0.07	7.63

\* Permeation rate was calculated from the amount of nicotine permeated from 7.5 to 30 min

\*\* Ratio of rates is the ratio of *in vitro* nicotine permeation to the *in vivo* nicotine absorption rate (0.036 mg/min)

**Table D3:** Amount of nicotine permeated (mg) from snus as a function of SSSR 0.32 mL/min and media temperature 45 °C

Time (min)	1	2	3	4	Mean	SD	%RSD
0	0	0	0	0	0	0	-
2.5	0.19	0.32	0.25	0.14	0.23	0.08	35.14
5	0.36	0.52	0.37	0.29	0.39	0.10	25.05
7.5	0.48	0.66	0.53	0.43	0.53	0.10	19.08
10	0.64	0.82	0.68	0.56	0.67	0.11	16.45
15	0.89	1.05	0.93	0.77	0.91	0.11	12.47
20	1.13	1.31	1.17	1.00	1.15	0.13	11.22
25	1.32	1.48	1.38	1.17	1.34	0.13	9.78
30	1.49	1.65	1.58	1.33	1.51	0.14	9.33
<b>Permeation rate (mg/min)*</b>	0.045	0.044	0.047	0.040	0.044	0.003	6.323
<b>Ratio of rates**</b>	1.24	1.22	1.29	1.11	1.22	0.08	6.32

\* Permeation rate was calculated from the amount of nicotine permeated from 7.5 to 30 min

\*\* Ratio of rates is the ratio of *in vitro* nicotine permeation to the *in vivo* nicotine absorption rate (0.036 mg/min)

**Table D4:** Amount of nicotine permeated (mg) from snus as a function of SSSR 1.66 mL/min and media temperature 25 °C

Time (min)	1	2	3	4	Mean	SD	%RSD
0	0	0	0	0	0	0	-
2.5	0.09	0.12	0.05	0.08	0.08	0.03	33.69
5	0.14	0.19	0.08	0.13	0.14	0.04	32.20
7.5	0.18	0.24	0.12	0.19	0.18	0.05	27.31
10	0.22	0.28	0.15	0.22	0.22	0.05	24.35
15	0.28	0.36	0.22	0.28	0.29	0.06	20.10
20	0.35	0.44	0.27	0.35	0.35	0.07	18.85
25	0.39	0.50	0.32	0.40	0.40	0.07	18.16
30	0.43	0.56	0.36	0.44	0.45	0.08	18.10
<b>Permeation rate (mg/min)*</b>	0.011	0.014	0.011	0.011	0.012	0.002	13.301
<b>Ratio of rates**</b>	0.31	0.40	0.30	0.31	0.33	0.04	13.30

\* Permeation rate was calculated from the amount of nicotine permeated from 7.5 to 30 min

\*\* Ratio of rates is the ratio of *in vitro* nicotine permeation to the *in vivo* nicotine absorption rate (0.036 mg/min)

**Table D5:** Amount of nicotine permeated (mg) from snus as a function of SSSR 1.66 mL/min and media temperature 37 °C

Time (min)	1	2	3	4	Mean	SD	%RSD
0	0	0	0	0	0	0	-
2.5	0.10	0.09	0.09	0.08	0.09	0.01	9.22
5	0.18	0.16	0.15	0.14	0.16	0.02	10.62
7.5	0.27	0.24	0.21	0.19	0.23	0.03	15.34
10	0.33	0.30	0.25	0.26	0.29	0.04	13.11
15	0.44	0.41	0.35	0.34	0.39	0.05	12.02
20	0.54	0.48	0.43	0.41	0.46	0.06	13.00
25	0.61	0.53	0.49	0.49	0.53	0.06	10.65
30	0.66	0.57	0.56	0.54	0.58	0.05	8.95
<b>Permeation rate (mg/min)*</b>	0.018	0.015	0.016	0.015	0.016	0.001	7.763
<b>Ratio of rates**</b>	0.49	0.41	0.43	0.42	0.44	0.03	7.76

\* Permeation rate was calculated from the amount of nicotine permeated from 7.5 to 30 min

\*\* Ratio of rates is the ratio of *in vitro* nicotine permeation to the *in vivo* nicotine absorption rate (0.036 mg/min)

**Table D6:** Amount of nicotine permeated (mg) from snus as a function of SSSR 1.66 mL/min and media temperature 45 °C

Time (min)	1	2	3	4	Mean	SD	%RSD
0	0	0	0	0	0	0	-
2.5	0.16	0.30	0.24	0.27	0.24	0.06	25.64
5	0.27	0.46	0.36	0.38	0.37	0.08	21.43
7.5	0.36	0.61	0.50	0.52	0.50	0.10	21.02
10	0.46	0.70	0.62	0.61	0.60	0.10	17.03
15	0.58	0.85	0.79	0.78	0.75	0.12	15.48
20	0.71	0.96	0.95	0.87	0.87	0.12	13.38
25	0.78	1.03	1.01	0.94	0.94	0.11	12.04
30	0.84	1.12	1.08	1.02	1.01	0.12	12.30
<b>Permeation rate (mg/min)*</b>	0.021	0.022	0.026	0.022	0.023	0.002	8.707
<b>Ratio of rates**</b>	0.59	0.61	0.71	0.60	0.63	0.05	8.71

\* Permeation rate was calculated from the amount of nicotine permeated from 7.5 to 30 min

\*\* Ratio of rates is the ratio of *in vitro* nicotine permeation to the *in vivo* nicotine absorption rate (0.036 mg/min)



**Table D7:** Amount of nicotine permeated (mg) from snus as a function of SSSR 3 mL/min and media temperature 25 °C

Time (min)	1	2	3	4	Mean	SD	%RSD
0	0	0	0	0	0	0	-
2.5	0.09	0.04	0.06	0.05	0.06	0.02	31.75
5	0.13	0.08	0.09	0.10	0.10	0.02	22.91
7.5	0.17	0.12	0.13	0.11	0.13	0.03	20.17
10	0.21	0.15	0.16	0.15	0.17	0.03	17.83
15	0.26	0.20	0.23	0.21	0.23	0.03	11.90
20	0.31	0.25	0.28	0.24	0.27	0.03	11.98
25	0.33	0.27	0.32	0.26	0.30	0.03	10.79
30	0.34	0.29	0.34	0.28	0.31	0.03	10.68
<b>Permeation rate (mg/min)*</b>	0.007	0.008	0.010	0.007	0.008	0.001	14.565
<b>Ratio of rates**</b>	0.20	0.21	0.27	0.20	0.22	0.03	14.56

\* Permeation rate was calculated from the amount of nicotine permeated from 7.5 to 30 min

\*\* Ratio of rates is the ratio of *in vitro* nicotine permeation to the *in vivo* nicotine absorption rate (0.036 mg/min)

**Table D8:** Amount of nicotine permeated (mg) from snus as a function of SSSR 3 mL/min and media temperature 37 °C

Time (min)	1	2	3	4	Mean	SD	%RSD
0	0	0	0	0	0	0	-
2.5	0.13	0.13	0.12	0.06	0.11	0.03	31.62
5	0.24	0.21	0.20	0.13	0.19	0.05	24.54
7.5	0.29	0.30	0.26	0.19	0.26	0.05	18.47
10	0.34	0.36	0.33	0.25	0.32	0.05	15.00
15	0.43	0.44	0.41	0.34	0.40	0.04	10.81
20	0.47	0.49	0.47	0.40	0.46	0.04	9.02
25	0.50	0.51	0.49	0.43	0.48	0.04	7.38
30	0.51	0.53	0.51	0.44	0.50	0.04	7.79
<b>Permeation rate (mg/min)*</b>	0.010	0.010	0.011	0.011	0.010	0.001	6.350
<b>Ratio of rates**</b>	0.27	0.27	0.30	0.31	0.29	0.02	6.35

\* Permeation rate was calculated from the amount of nicotine permeated from 7.5 to 30 min

\*\* Ratio of rates is the ratio of *in vitro* nicotine permeation to the *in vivo* nicotine absorption rate (0.036 mg/min)

**Table D9:** Amount of nicotine permeated (mg) from snus as a function of SSSR 3 mL/min and media temperature 45 °C

<b>Time (min)</b>	<b>1</b>	<b>2</b>	<b>3</b>	<b>4</b>	<b>Mean</b>	<b>SD</b>	<b>%RSD</b>
0	0	0	0	0	0	0	-
2.5	0.18	0.19	0.14	0.13	0.16	0.03	18.31
5	0.28	0.27	0.24	0.22	0.25	0.03	10.17
7.5	0.35	0.36	0.35	0.29	0.34	0.03	9.38
10	0.42	0.42	0.41	0.36	0.40	0.03	7.03
15	0.51	0.50	0.51	0.45	0.49	0.03	5.58
20	0.56	0.55	0.55	0.51	0.54	0.02	4.51
25	0.60	0.59	0.58	0.53	0.57	0.03	4.97
30	0.61	0.59	0.59	0.55	0.59	0.02	4.17
<b>Permeation rate (mg/min)*</b>	0.012	0.011	0.010	0.012	0.011	0.001	6.079
<b>Ratio of rates**</b>	0.32	0.29	0.29	0.32	0.31	0.02	6.08

\* Permeation rate was calculated from the amount of nicotine permeated from 7.5 to 30 min

\*\* Ratio of rates is the ratio of *in vitro* nicotine permeation to the *in vivo* nicotine absorption rate (0.036 mg/min)

**Table D10:** Method for calculation of the amount of nicotine released as a function of SSSR (mL/min) and temperature (°C) over time

	Time (min) (A)	Amount of nicotine swallowed (mg) (B)*	$\Delta$ Amount of nicotine swallowed between two time intervals (mg) (C)	$\Delta$ Time interval between two sampling points (min) (D)	$\Delta$ Volume of media swallowed at $\Delta$ time [D x SSSR]** (mL) (E)	Concentration of nicotine in the volume of media swallowed at $\Delta$ Time [C/E] (mg/mL) (F)	Amount of nicotine released in the donor chamber of BTA [F x V]** (mg) (G)	Amount of nicotine swallowed from the donor chamber of BTA (mcg) (H)	Amount of nicotine permeated into the receptor chamber of BTA (mg) (I)****	Total amount of nicotine released in the donor chamber of BTA (G+H+I) (mg)
1	0	0	0	0	0	0	0	0	0	0
2	2.5	B2	C2=B2-B1	D2=A2-A1	E2=D2xSSSR	F2=C2/E2	G2=F2xV	H2=B2	I2	G2+H2+I2
3	5	B3	C3=B3-B2	D3=A3-A2	E3=D3xSSSR	F3=C3/E3	G3=F3xV	H3=B3	I3	G3+H3+I3
4	7.5	B4	C4=B4-B3	D4=A4-A3	E4=D4xSSSR	F4=C4/E4	G4=F4xV	H4=B4	I4	G4+H4+I4
5	10	B5	C5=B5-B4	D5=A5-A4	E5=D5xSSSR	F5=C5/E5	G5=F5xV	H5=B5	I5	G5+H5+I5
6	15	B6	C6=B6-B5	D6=A6-A5	E6=D6xSSSR	F6=C6/E6	G6=F6xV	H6=B6	I6	G6+H6+I6
7	20	B7	C7=B7-B6	D7=A7-A6	E7=D7xSSSR	F7=C7/E7	G7=F7xV	H7=B7	I7	G7+H7+I7
8	25	B8	C8=B8-B7	D8=A8-A7	E8=D8xSSSR	F8=C8/E8	G8=F8xV	H8=B8	I8	G8+H8+I8
9	30	B9	C9=B9-B8	D9=A9-A8	E9=D9xSSSR	F9=C9/E9	G9=F9xV	H9=B9	I9	G9+H9+I9
* Refer Table D22										
** SSSR = stimulated saliva swallowing rate = 0.32 or 1.66 or 3 mL/min										
*** V = Experimental volume of media available for release in the donor chamber = [Volume of swallowed media + Volume of donor chamber + Volume of tubing from the outlet of BTA to the reservoir collecting tobacco extract] – [Theoretical volume of swallowed media + Volume of donor chamber + Volume of tubing from the outlet of BTA to the reservoir collecting tobacco extract] + [Volume of donor chamber + Volume of tubing from the outlet of BTA to the reservoir collecting tobacco extract] <u>Volume of swallowed media</u> = observed volume collected in the reservoir of tobacco extract at the end of experiment; <u>Theoretical volume of swallowed media</u> = SSSR (mL/min) × 30 min <u>Volume of donor chamber</u> = 10 mL <u>Volume of tubing from the outlet of BTA to the reservoir collecting tobacco extract</u> = 2.67 mL										
**** Refer Table D0										

**Table D11:** Amount of nicotine released\* (mg) from snus as a function of SSSR 0.32 mL/min and media temperature 25 °C

Time (min)	1	2	3	4	Mean	SD	%RSD
0	0	0	0	0	0	0	-
2.5	0.40	0.97	0.33	0.26	0.49	0.33	66.70
5	0.59	0.80	0.39	0.37	0.54	0.20	37.07
7.5	0.69	1.41	0.46	0.49	0.77	0.44	57.96
10	1.08	1.85	0.69	0.68	1.07	0.55	51.29
15	2.05	3.14	1.17	1.10	1.86	0.96	51.32
20	3.92	4.52	2.71	2.36	3.38	1.01	29.91
25	3.32	6.39	3.73	3.44	4.22	1.46	34.52
30	4.17	5.87	3.96	3.01	4.25	1.19	28.02

\* Total nicotine released = nicotine permeated in receptor chambers (Table D1) + nicotine released in donor chamber + nicotine swallowed from donor chamber (Table D24)

**Table D12:** Amount of nicotine released\* (mg) from snus as a function of SSSR 0.32 mL/min and media temperature 37 °C

Time (min)	1	2	3	4	Mean	SD	%RSD
0	0	0	0	0	0	0	-
2.5	0.52	0.45	0.49	0.70	0.54	0.11	20.43
5	0.75	1.05	0.78	1.02	0.90	0.16	17.30
7.5	1.22	1.26	1.22	1.06	1.19	0.09	7.28
10	1.17	1.72	0.89	1.95	1.43	0.49	34.13
15	2.36	3.19	2.34	3.00	2.72	0.44	16.07
20	3.50	3.70	3.80	4.34	3.83	0.36	9.34
25	4.43	4.24	4.08	5.31	4.51	0.55	12.21
30	5.50	4.67	5.15	4.11	4.86	0.61	12.46

\* Total nicotine released = nicotine permeated in receptor chambers (Table D2) + nicotine released in donor chamber + nicotine swallowed from donor chamber (Table D25)

**Table D13:** Amount of nicotine released\* (mg) from snus as a function of SSSR 0.32 mL/min and media temperature 45 °C

<b>Time (min)</b>	<b>1</b>	<b>2</b>	<b>3</b>	<b>4</b>	<b>Mean</b>	<b>SD</b>	<b>%RSD</b>
0	0	0	0	0	0	0	-
2.5	1.57	1.05	1.06	1.67	1.34	0.33	24.47
5	1.68	2.08	1.27	2.46	1.87	0.52	27.60
7.5	2.37	1.82	1.48	2.71	2.09	0.55	26.31
10	3.23	3.04	2.14	3.50	2.98	0.59	19.85
15	4.91	3.74	2.74	4.35	3.94	0.93	23.63
20	6.54	5.36	4.59	3.92	5.10	1.12	22.02
25	7.39	5.59	5.08	5.65	5.93	1.01	16.99
30	6.95	6.62	5.43	6.35	6.34	0.66	10.35

\* Total nicotine released = nicotine permeated in receptor chambers (Table D3) + nicotine released in donor chamber + nicotine swallowed from donor chamber (Table D26)

**Table D14:** Amount of nicotine released\* (mg) from snus as a function of SSSR 1.66 mL/min and media temperature 25 °C

<b>Time (min)</b>	<b>1</b>	<b>2</b>	<b>3</b>	<b>4</b>	<b>Mean</b>	<b>SD</b>	<b>%RSD</b>
0	0	0	0	0	0	0	-
2.5	1.37	0.36	0.90	0.29	0.73	0.51	69.91
5	3.11	1.22	2.24	0.93	1.88	1.00	53.26
7.5	5.54	2.98	3.69	2.55	3.69	1.32	35.75
10	6.14	1.62	5.10	3.10	3.99	2.02	50.64
15	4.93	6.25	5.62	4.76	5.39	0.68	12.70
20	6.34	5.67	3.49	4.76	5.06	1.23	24.33
25	8.18	6.07	7.40	5.44	6.78	1.24	18.35
30	5.74	6.13	2.21	4.73	4.71	1.76	37.43

\* Total nicotine released = nicotine permeated in receptor chambers (Table D4) + nicotine released in donor chamber + nicotine swallowed from donor chamber (Table D27)

**Table D15:** Amount of nicotine released\* (mg) from snus as a function of SSSR 1.66 mL/min and media temperature 37 °C

<b>Time (min)</b>	<b>1</b>	<b>2</b>	<b>3</b>	<b>4</b>	<b>Mean</b>	<b>SD</b>	<b>%RSD</b>
0	0	0	0	0	0	0	-
2.5	0.98	0.76	1.63	1.01	1.10	0.38	34.29
5	1.70	1.80	2.15	1.83	1.87	0.20	10.55
7.5	3.34	3.60	4.15	3.28	3.59	0.40	11.06
10	5.04	4.32	4.10	3.47	4.23	0.65	15.37
15	5.34	5.05	4.79	5.73	5.23	0.41	7.77
20	6.50	5.26	5.75	4.51	5.50	0.84	15.24
25	5.27	5.17	5.01	5.49	5.23	0.20	3.80
30	6.29	6.42	5.97	4.55	5.81	0.86	14.77

\* Total nicotine released = nicotine permeated in receptor chambers (Table D5) + nicotine released in donor chamber + nicotine swallowed from donor chamber (Table D28)

**Table D16:** Amount of nicotine released\* (mg) from snus as a function of SSSR 1.66 mL/min and media temperature 45 °C

<b>Time (min)</b>	<b>1</b>	<b>2</b>	<b>3</b>	<b>4</b>	<b>Mean</b>	<b>SD</b>	<b>%RSD</b>
0	0	0	0	0	0	0	-
2.5	1.91	2.71	1.20	3.38	2.30	0.95	41.32
5	3.02	4.91	2.18	4.80	3.73	1.35	36.22
7.5	4.36	6.16	3.71	3.95	4.54	1.11	24.42
10	5.31	7.13	4.87	6.29	5.90	1.01	17.15
15	5.54	6.67	6.12	3.97	5.57	1.16	20.90
20	5.29	6.87	6.61	5.81	6.14	0.73	11.84
25	6.10	7.99	6.58	8.59	7.31	1.17	15.96
30	6.70	7.01	6.73	7.05	6.87	0.18	2.64

\* Total nicotine released = nicotine permeated in receptor chambers (Table D6) + nicotine released in donor chamber + nicotine swallowed from donor chamber (Table D29)

**Table D17:** Amount of nicotine released\* (mg) from snus as a function of SSSR 3 mL/min and media temperature 25 °C

<b>Time (min)</b>	<b>1</b>	<b>2</b>	<b>3</b>	<b>4</b>	<b>Mean</b>	<b>SD</b>	<b>%RSD</b>
0	0	0	0	0	0	0	-
2.5	1.92	1.07	0.55	0.68	1.06	0.61	58.14
5	5.44	4.76	2.15	3.54	3.97	1.45	36.46
7.5	5.77	5.28	4.32	3.66	4.76	0.95	19.94
10	6.07	5.02	4.51	4.52	5.03	0.73	14.54
15	6.71	5.50	6.17	5.12	5.88	0.71	12.04
20	6.53	5.55	5.98	6.08	6.04	0.40	6.64
25	6.56	5.80	6.81	6.24	6.35	0.44	6.86
30	5.89	6.65	7.77	5.09	6.35	1.14	17.99

\* Total nicotine released = nicotine permeated in receptor chambers (Table D7) + nicotine released in donor chamber + nicotine swallowed from donor chamber (Table D30)

**Table D18:** Amount of nicotine released\* (mg) from snus as a function of SSSR 3 mL/min and media temperature 37 °C

<b>Time (min)</b>	<b>1</b>	<b>2</b>	<b>3</b>	<b>4</b>	<b>Mean</b>	<b>SD</b>	<b>%RSD</b>
0	0	0	0	0	0	0	-
2.5	2.48	2.46	1.97	2.06	2.24	0.26	11.79
5	5.31	5.92	5.33	4.65	5.30	0.52	9.77
7.5	1.55	6.51	6.11	6.13	5.08	2.36	46.47
10	9.44	5.04	5.77	6.19	6.61	1.95	29.43
15	8.17	6.97	7.35	6.40	7.22	0.74	10.24
20	5.51	5.00	6.50	6.23	5.81	0.68	11.73
25	8.23	8.31	6.52	6.71	7.44	0.96	12.89
30	6.23	7.29	6.06	6.95	6.63	0.58	8.81

\* Total nicotine released = nicotine permeated in receptor chambers (Table D8) + nicotine released in donor chamber + nicotine swallowed from donor chamber (Table D31)

**Table D19:** Amount of nicotine released\* (mg) from snus as a function of SSSR 3 mL/min and media temperature 45 °C

<b>Time (min)</b>	<b>1</b>	<b>2</b>	<b>3</b>	<b>4</b>	<b>Mean</b>	<b>SD</b>	<b>%RSD</b>
0	0	0	0	0	0	0	-
2.5	3.42	2.52	2.40	3.88	3.05	0.72	23.44
5	6.08	5.79	6.27	4.73	5.72	0.69	11.98
7.5	6.03	6.55	7.12	6.65	6.59	0.45	6.77
10	6.41	6.64	7.12	4.96	6.28	0.93	14.83
15	6.87	6.53	7.07	5.82	6.57	0.55	8.37
20	6.32	7.02	7.09	5.49	6.48	0.75	11.51
25	7.64	6.69	7.83	6.87	7.26	0.56	7.77
30	7.91	5.55	8.56	4.94	6.74	1.76	26.16

\* Total nicotine released = nicotine permeated in receptor chambers (Table D9) + nicotine released in donor chamber + nicotine swallowed from donor chamber (Table D32)



**Table D20:** Amount of nicotine permeated (mg) from snus at optimal conditions of SSSR 0.55 mL/min and media temperature 43 °C

Time (min)	1	2	3	4	Mean	SD	%RSD
0	0	0	0	0	0	0	-
2.5	0.28	0.30	0.24	0.17	0.25	0.06	24.32
5	0.43	0.38	0.37	0.26	0.36	0.07	20.09
7.5	0.59	0.52	0.50	0.39	0.50	0.09	17.15
10	0.70	0.68	0.64	0.55	0.64	0.07	10.57
15	0.94	0.89	0.89	0.68	0.85	0.11	13.37
20	1.13	1.14	1.10	0.85	1.06	0.14	12.94
25	1.30	1.37	1.19	1.06	1.23	0.13	10.96
30	1.43	1.56	1.42	1.16	1.39	0.17	11.91
<b>Permeation rate (mg/min)*</b>	0.038	0.046	0.039	0.034	0.039	0.005	12.329
<b>Ratio of rates**</b>	1.05	1.27	1.09	0.94	1.09	0.13	12.33

\* Permeation rate was calculated from the amount of nicotine permeated from 7.5 to 30 min

\*\* Ratio of rates is the ratio of *in vitro* nicotine permeation to the *in vivo* nicotine absorption rate (0.036 mg/min)

**Table D21:** Amount of nicotine released\* (mg) from snus at optimal conditions of SSSR 0.55 mL/min and media temperature 43 °C

Time (min)	1	2	3	4	Mean	SD	%RSD
0	0	0	0	0	0	0	-
2.5	1.65	1.39	2.18	1.20	1.60	0.42	26.40
5	2.26	1.50	3.65	2.37	2.45	0.89	36.32
7.5	3.28	1.31	4.43	4.64	3.42	1.52	44.62
10	5.77	3.61	7.20	3.49	5.02	1.79	35.73
15	4.21	4.03	6.85	2.69	4.44	1.74	39.24
20	5.42	5.68	6.55	4.76	5.60	0.74	13.21
25	5.92	7.95	8.84	5.47	7.05	1.61	22.84
30	5.96	10.30	7.99	5.72	7.49	2.13	28.44

\* Total nicotine released = nicotine permeated in receptor chambers (Table D20) + nicotine released in donor chamber + nicotine swallowed from donor chamber (Table D23)

**Table D22:** Method for calculation of the amount of nicotine swallowed as a function of SSSR (mL/min) and temperature (°C) over time

	Time (min) (A)	Dilution corrected concentration (mcg/mL) (B)*	SSSR (mL/min) (C)**	Total volume of media swallowed (mL) [AxC] (D)	Amount of nicotine in the volume of media swallowed (mcg) [BxD] (E)	Amount of nicotine in the volume of media sampled (0.04 mL) [Bx0.04/1] (mcg) (F)	Amount of nicotine lost at each time point due to sampling (mcg) (G)	Cumulative amount of nicotine swallowed [E+G] (mcg) (H)	Cumulative amount of nicotine swallowed [H/1000] (mg) (I)
1	0	0	0	0	0	0	0	0	0
2	2.5	B2	C	D2=A2xC	E2=B2xD2	F2=B2x0.04	G2=0	H2=E2+G2	I2=H2/1000
3	5	B3	C	D3=A3xC	E3=B3xD3	F3=B2x0.04	G3=Sum of F1 to F2	H3=E3+G3	I3=H3/1000
4	7.5	B4	C	D4=A4xC	E4=B4xD4	F4=B2x0.04	G4=Sum of F1 to F3	H4=E4+G4	I4=H4/1000
5	10	B5	C	D5=A5xC	E5=B5xD5	F5=B2x0.04	G5=Sum of F1 to F4	H5=E5+G5	I5=H5/1000
6	15	B6	C	D6=A6xC	E6=B6xD6	F6=B2x0.04	G6=Sum of F1 to F5	H6=E6+G6	I6=H6/1000
7	20	B7	C	D7=A7xC	E7=B7xD7	F7=B2x0.04	G7=Sum of F1 to F6	H7=E7+G7	I7=H7/1000
8	25	B8	C	D8=A8xC	E8=B8xD8	F8=B2x0.04	G8=Sum of F1 to F7	H8=E8+G8	I8=H8/1000
9	30	B9	C	D9=A9xC	E9=B9xD9	F9=B2x0.04	G9=Sum of F1 to F8	H9=E9+G9	I9=H9/1000
* Dilution corrected concentration = Concentration (mcg/mL) x Dilution factor									
** SSSR = stimulated saliva swallowing rate = 0.32 or 1.66 or 3 mL/min									

**Table D23:** Amount of nicotine swallowed (mg) from snus at optimal conditions of SSSR 0.55 mL/min and media temperature 43 °C

Time (min)	1	2	3	4	Mean	SD	%RSD
0	0	0	0	0	0	0	-
2.5	0.09	0.08	0.13	0.08	0.10	0.03	28.02
5	0.21	0.16	0.35	0.22	0.24	0.08	34.99
7.5	0.39	0.20	0.60	0.52	0.43	0.17	40.74
10	0.71	0.40	1.01	0.69	0.70	0.25	35.45
15	1.04	0.77	1.65	0.87	1.08	0.39	36.40
20	1.46	1.28	2.14	1.28	1.54	0.41	26.53
25	1.87	2.00	2.86	1.71	2.11	0.51	24.27
30	2.22	2.92	3.34	2.10	2.64	0.59	22.26

**Table D24:** Amount of nicotine swallowed (mg) from snus as a function of SSSR 0.32 mL/min and media temperature 25 °C

Time (min)	1	2	3	4	Mean	SD	%RSD
0	0	0	0	0	0	0	-
2.5	0.01	0.03	0.01	0.01	0.01	0.01	99.16
5	0.02	0.05	0.01	0.01	0.02	0.02	80.96
7.5	0.03	0.10	0.02	0.02	0.04	0.04	85.11
10	0.06	0.15	0.03	0.03	0.07	0.05	81.26
15	0.16	0.32	0.08	0.07	0.16	0.12	72.58
20	0.36	0.57	0.23	0.19	0.34	0.17	51.04
25	0.51	0.92	0.44	0.36	0.56	0.25	45.35
30	0.69	1.21	0.64	0.48	0.75	0.32	41.99

**Table D25:** Amount of nicotine swallowed (mg) from snus as a function of SSSR 0.32 mL/min and media temperature 37 °C

<b>Time (min)</b>	<b>1</b>	<b>2</b>	<b>3</b>	<b>4</b>	<b>Mean</b>	<b>SD</b>	<b>%RSD</b>
0	0	0	0	0	0	0	-
2.5	0.02	0.01	0.01	0.02	0.02	0.00	20.95
5	0.04	0.05	0.04	0.05	0.04	0.01	17.50
7.5	0.07	0.08	0.07	0.08	0.07	0.01	8.33
10	0.10	0.13	0.09	0.13	0.11	0.02	21.34
15	0.21	0.31	0.21	0.30	0.26	0.06	21.36
20	0.39	0.51	0.42	0.54	0.46	0.07	15.16
25	0.62	0.72	0.62	0.82	0.69	0.10	13.99
30	0.89	0.93	0.88	0.99	0.92	0.05	5.44

**Table D26:** Amount of nicotine swallowed (mg) from snus as a function of SSSR 0.32 mL/min and media temperature 45 °C

<b>Time (min)</b>	<b>1</b>	<b>2</b>	<b>3</b>	<b>4</b>	<b>Mean</b>	<b>SD</b>	<b>%RSD</b>
0	0	0	0	0	0	0	-
2.5	0.04	0.03	0.03	0.06	0.04	0.01	36.91
5	0.08	0.08	0.06	0.13	0.09	0.03	35.26
7.5	0.14	0.12	0.09	0.21	0.14	0.05	37.22
10	0.22	0.19	0.14	0.31	0.21	0.07	33.83
15	0.45	0.36	0.25	0.54	0.40	0.12	31.26
20	0.76	0.60	0.46	0.70	0.63	0.13	20.81
25	1.09	0.84	0.68	0.96	0.89	0.18	19.77
30	1.36	1.11	0.89	1.25	1.15	0.20	17.57

**Table D27:** Amount of nicotine swallowed (mg) from snus as a function of SSSR 1.66 mL/min and media temperature 25 °C

<b>Time (min)</b>	<b>1</b>	<b>2</b>	<b>3</b>	<b>4</b>	<b>Mean</b>	<b>SD</b>	<b>%RSD</b>
0	0	0	0	0	0	0	-
2.5	0.18	0.04	0.14	0.04	0.10	0.07	73.52
5	0.58	0.21	0.47	0.16	0.36	0.20	56.36
7.5	1.25	0.64	0.98	0.54	0.85	0.33	38.30
10	1.91	0.76	1.63	0.94	1.31	0.55	41.97
15	2.59	2.26	2.69	1.97	2.38	0.33	13.85
20	3.43	3.12	2.84	2.68	3.02	0.33	10.97
25	4.51	3.83	4.03	3.37	3.94	0.47	12.02
30	4.71	4.34	3.42	3.64	4.03	0.60	14.94

**Table D28:** Amount of nicotine swallowed (mg) from snus as a function of SSSR 1.66 mL/min and media temperature 37 °C

<b>Time (min)</b>	<b>1</b>	<b>2</b>	<b>3</b>	<b>4</b>	<b>Mean</b>	<b>SD</b>	<b>%RSD</b>
0	0	0	0	0	0	0	-
2.5	0.16	0.14	0.27	0.16	0.18	0.06	34.99
5	0.40	0.44	0.58	0.42	0.46	0.08	18.17
7.5	0.87	1.04	1.18	0.87	0.99	0.15	14.92
10	1.55	1.64	1.65	1.27	1.53	0.18	11.67
15	2.57	2.66	2.49	2.47	2.55	0.08	3.32
20	3.59	3.38	3.35	2.95	3.32	0.27	8.11
25	3.91	3.80	3.70	3.54	3.74	0.16	4.19
30	4.43	4.50	4.22	3.68	4.21	0.37	8.80

**Table D29:** Amount of nicotine swallowed (mg) from snus as a function of SSSR 1.66 mL/min and media temperature 45 °C

<b>Time (min)</b>	<b>1</b>	<b>2</b>	<b>3</b>	<b>4</b>	<b>Mean</b>	<b>SD</b>	<b>%RSD</b>
0	0	0	0	0	0	0	-
2.5	0.31	0.47	0.23	0.74	0.44	0.23	51.73
5	0.75	1.24	0.61	1.62	1.06	0.47	44.29
7.5	1.32	2.08	1.23	2.06	1.67	0.46	27.40
10	1.95	2.93	1.95	2.92	2.44	0.56	23.04
15	2.86	3.87	3.25	3.02	3.25	0.44	13.58
20	3.38	4.53	4.18	3.76	3.96	0.50	12.64
25	3.96	5.32	4.72	5.26	4.82	0.63	13.07
30	4.54	5.50	5.08	5.56	5.17	0.47	9.15

**Table D30:** Amount of nicotine swallowed (mg) from snus as a function of SSSR 3 mL/min and media temperature 25 °C

<b>Time (min)</b>	<b>1</b>	<b>2</b>	<b>3</b>	<b>4</b>	<b>Mean</b>	<b>SD</b>	<b>%RSD</b>
0	0	0	0	0	0	0	-
2.5	0.39	0.24	0.15	0.17	0.24	0.11	45.32
5	1.43	1.30	0.71	1.06	1.12	0.32	28.05
7.5	2.31	2.22	1.73	1.74	2.00	0.31	15.29
10	3.06	2.85	2.50	2.46	2.72	0.29	10.54
15	4.24	3.79	4.07	3.51	3.90	0.32	8.23
20	4.93	4.37	4.81	4.51	4.66	0.26	5.57
25	5.38	4.82	5.57	5.14	5.23	0.33	6.26
30	5.44	5.41	6.42	5.00	5.57	0.60	10.83

**Table D31:** Amount of nicotine swallowed (mg) from snus as a function of SSSR 3 mL/min and media temperature 37 °C

<b>Time (min)</b>	<b>1</b>	<b>2</b>	<b>3</b>	<b>4</b>	<b>Mean</b>	<b>SD</b>	<b>%RSD</b>
0	0	0	0	0	0	0	-
2.5	0.54	0.54	0.43	0.46	0.49	0.06	11.49
5	1.59	1.73	1.51	1.40	1.56	0.14	8.87
7.5	1.51	2.76	2.52	2.45	2.31	0.55	23.74
10	3.26	3.21	3.19	3.25	3.23	0.04	1.11
15	4.94	4.45	4.60	4.31	4.57	0.27	5.96
20	4.98	4.48	5.14	4.88	4.87	0.28	5.78
25	6.01	5.72	5.47	5.40	5.65	0.28	4.89
30	5.90	6.11	5.50	5.82	5.83	0.25	4.37

**Table D32:** Amount of nicotine swallowed (mg) from snus as a function of SSSR 3 mL/min and media temperature 45 °C

<b>Time (min)</b>	<b>1</b>	<b>2</b>	<b>3</b>	<b>4</b>	<b>Mean</b>	<b>SD</b>	<b>%RSD</b>
0	0	0	0	0	0	0	-
2.5	0.75	0.54	0.52	0.87	0.67	0.17	25.03
5	1.92	1.69	1.79	1.71	1.78	0.10	5.88
7.5	2.79	2.73	2.94	2.78	2.81	0.09	3.25
10	3.53	3.53	3.81	3.20	3.52	0.25	7.06
15	4.59	4.47	4.84	4.01	4.48	0.35	7.73
20	5.03	5.22	5.47	4.38	5.02	0.47	9.34
25	5.78	5.55	6.14	5.11	5.65	0.43	7.66
30	6.35	5.33	6.83	4.84	5.84	0.91	15.64

## **APPENDIX E**

**REPLICATE AND MEAN DATA FOR NICOTINE RELEASE/PERMEATION, RATES  
AND LAG TIME OBTAINED WITH EXPERIMENTS REPORTED IN CHAPTER 6**



**Table E0:** Method for calculation of the amount of nicotine permeated<sup>\*\*</sup> from stonewall as a function of donor media flow rate (mL/min) and media temperature (°C) over time

	Time (min) (A)	Dilution corrected concentration (mcg/mL) (B)*	Amount of nicotine in the volume of receptor media (25 mL) (mcg) [Bx25] (C)	Amount of nicotine in the volume of receptor media sampled (1 mL) [Cx1/25] (mcg) (D)	Amount of nicotine lost at each time point due to sampling (mcg) (E)	Cumulative amount of nicotine permeated [C+E] (mcg) (F)	Cumulative amount of nicotine permeated [H/1000] (mg) (G)
1	0	0	0	0	0	0	0
2	A2	B2	$C2=B2 \times 25$	$D2=(C2 \times 1)/25$	$E2=0$	$F2=C2+E2$	$G2=F2/1000$
3	A3	B3	$C3=B3 \times 25$	$D3=(C3 \times 1)/25$	$E3=\text{Sum of D1 to D2}$	$F3=C3+E3$	$G3=F3/1000$
4	A4	B4	$C4=B4 \times 25$	$D4=(C4 \times 1)/25$	$E4=\text{Sum of D1 to D3}$	$F4=C4+E4$	$G4=F4/1000$
5	A5	B5	$C5=B5 \times 25$	$D5=(C5 \times 1)/25$	$E5=\text{Sum of D1 to D4}$	$F5=C5+E5$	$G5=F5/1000$
6	A6	B6	$C6=B6 \times 25$	$D6=(C6 \times 1)/25$	$E6=\text{Sum of D1 to D5}$	$F6=C6+E6$	$G6=F6/1000$
7	A7	B7	$C7=B7 \times 25$	$D7=(C7 \times 1)/25$	$E7=\text{Sum of D1 to D6}$	$F7=C7+E7$	$G7=F7/1000$
8	A8	B8	$C8=B8 \times 25$	$D8=(C8 \times 1)/25$	$E8=\text{Sum of D1 to D7}$	$F8=C8+E8$	$G8=F8/1000$
9	A9	B9	$C9=B9 \times 25$	$D9=(C9 \times 1)/25$	$E9=\text{Sum of D1 to D8}$	$F9=C9+E9$	$G9=F9/1000$
10	A10	B10	$C10=C10 \times 25$	$D10=(D10 \times 1)/25$	$E10=\text{Sum of D1 to D9}$	$F10=C10+E10$	$G10=G10/1000$
* Dilution corrected concentration = Concentration (mcg/mL) x Dilution factor							
** Amount permeated in both receptors calculated by the above method are added to obtain the total amount of nicotine permeated							

**Table E1:** Peak areas for nicotine analysis for the external standards and spiked *in vitro* donor samples for stonewall

<b>Nicotine external standards</b>						
<b>Nicotine concentration (µg/mL)</b>	<b>1</b>	<b>2</b>	<b>3</b>	<b>Mean</b>	<b>SD</b>	<b>%RSD</b>
0.5	7370	8507	7105	7661	744.83	9.72
1	19411	16673	15629	17238	1953.21	11.33
2	36222	35678	32805	34902	1836.03	5.26
4	69442	65280	69581	68101	2444.05	3.59
8	147358	142462	146844	145555	2690.63	1.85
16	284743	282572	285954	284423	1713.56	0.60
32	575295	564007	610972	583425	24515.23	4.20
<b>Spiked donor <i>in vitro</i> sample</b>						
<b>Nicotine concentration (µg/mL)</b>	<b>1</b>	<b>2</b>	<b>3</b>	<b>Mean</b>	<b>SD</b>	<b>%RSD</b>
0	97314	1317.7	1.35	97314	1317.7	1.35
0.5	105279	2463	2.34	105279	2463	2.34
1	117081	3132.9	2.68	117081	3132.9	2.68
2	138096	6615.8	4.79	138096	6615.8	4.79
4	164350	3513.9	2.14	164350	3513.9	2.14
8	237607	6885.5	2.90	237607	6885.5	2.90
16	385262	5334	1.38	385262	5334	1.38
32	650831	30923	4.75	650831	30923	4.75

**Table E2:** Peak areas for nicotine analysis for the external standards and spiked *in vitro* receptor samples for stonewall

<b>Nicotine external standards</b>						
<b>Nicotine concentration (µg/mL)</b>	<b>1</b>	<b>2</b>	<b>3</b>	<b>Mean</b>	<b>SD</b>	<b>%RSD</b>
0.5	7950	8177	7468	7865	362.06	4.60
1	16424	15837	16112	16124	293.69	1.82
2	33967	35183	33002	34051	1092.90	3.21
4	70672	69744	71528	70648	892.24	1.26
8	142075	139360	148622	143352	4761.29	3.32
16	280222	276443	288881	281849	6376.56	2.26
32	562462	562444	569165	564690	3875.19	0.69
<b>Spiked receptor <i>in vitro</i> sample</b>						
<b>Nicotine concentration (µg/mL)</b>	<b>1</b>	<b>2</b>	<b>3</b>	<b>Mean</b>	<b>SD</b>	<b>%RSD</b>
0	127117	127804	125265	126729	1313.3	1.04
0.5	134747	138090	136104	136314	1681.3	1.23
1	149875	147519	147446	148280	1381.8	0.93
2	170767	161327	166368	166154	4723.6	2.84
4	183983	183074	191951	186336	4883.9	2.62
8	240126	253030	263309	252155	11616	4.61
16	409831	405036	405467	406778	2652.7	0.65
32	623146	639680	696851	653226	38675	5.92

**Table E3:** Peak purity testing on the nicotine standards and *in vitro* donor sample for stonewall using the autothreshold method\*

		Purity Angle*			Threshold Angle*		
		Mean	SD	%RSD	Mean	SD	%RSD
<b>Nicotine standard (0.5 µg/mL)</b>	<b>1</b>	2.487			14.333		
	<b>2</b>	1.521	2.144	0.541	25.216	7.855	8.657
	<b>3</b>	2.425			3.784		61.452
<b>Nicotine standard (32 µg/mL)</b>	<b>1</b>	0.067			0.467		
	<b>2</b>	0.085	0.067	0.018	26.866	0.439	0.381
	<b>3</b>	0.049			0.237		32.937
<b>Donor sample at 60 min</b>	<b>1</b>	0.768			0.613		
	<b>2</b>	0.692	0.695	0.072	10.295	0.900	0.931
	<b>3</b>	0.625			1.281		35.981

\* Peak purity analysis was performed at the wavelength range of 250-270 nm

**Table E4:** Peak purity testing on the nicotine standards and *in vitro* receptor samples for stonewall using the autothreshold method\*

		Purity Angle*			Threshold Angle*		
		Mean	SD	%RSD	Mean	SD	%RSD
<b>Nicotine standard (0.5 µg/mL)</b>	<b>1</b>	1.474			5.670		
	<b>2</b>	1.256	1.642	0.492	29.964	3.988	4.258
	<b>3</b>	2.196			3.116		1.298
<b>Nicotine standard (32 µg/mL)</b>	<b>1</b>	0.051			0.237		
	<b>2</b>	0.058	0.054	0.004	7.055	0.257	0.285
	<b>3</b>	0.052			0.362		23.532
<b>Donor sample at 60 min</b>	<b>1</b>	0.433			0.480		
	<b>2</b>	0.394	0.408	0.021	5.254	0.553	0.487
	<b>3</b>	0.398			0.427		12.999

\* Peak purity analysis was performed at the wavelength range of 250-270 nm

**Table E5:** Amount of nicotine permeated (mg) from stonewall as a function of the donor media flow rate (1.66 mL/min) and media temperature (37 °C)

<b>Time (min)</b>	<b>1</b>	<b>2</b>	<b>3</b>	<b>4</b>	<b>5</b>	<b>Mean</b>	<b>SD</b>	<b>%RSD</b>
0	0	0	0	0	0	0	0	-
1	0.01	0.02	0.01	0.01	0.01	0.01	0.00	12.43
5	0.02	0.03	0.03	0.02	0.02	0.02	0.01	21.42
10	0.03	0.05	0.04	0.03	0.03	0.04	0.01	24.90
15	0.05	0.06	0.06	0.04	0.04	0.05	0.01	18.72
20	0.06	0.08	0.08	0.06	0.06	0.07	0.01	19.33
25	0.08	0.11	0.10	0.08	0.07	0.09	0.02	18.24
30	0.10	0.12	0.12	0.09	0.09	0.10	0.02	15.53
45	0.16	0.19	0.19	0.15	0.15	0.17	0.02	11.71
60	0.22	0.28	0.26	0.21	0.21	0.23	0.03	13.51
<b>Permeation rate (mg/min)*</b>	0.003	0.004	0.004	0.003	0.003	0.003	0.001	18.496
<b>Lag time (min)</b>	0	0	0	0	0	0	0	-
<b>Ratio of rates**</b>	0.03	0.04	0.04	0.03	0.03	0.04	0.01	18.50

\* Permeation rate was calculated from amount of nicotine permeated from 5 to 20 min

\*\* Ratio of rates is the ratio of *in vitro* nicotine permeation to *in vivo* nicotine absorption rate (0.083 mg/min)

**Table E6:** Amount of nicotine permeated (mg) from stonewall as a function of the donor media flow rate (16 mL/min) and media temperature (37 °C)

<b>Time (min)</b>	<b>1</b>	<b>2</b>	<b>3</b>	<b>Mean</b>	<b>SD</b>	<b>%RSD</b>
0	0	0	0	0	0	-
1	0.01	0.02	0.01	0.01	0.01	58.61
5	0.03	0.05	0.02	0.04	0.01	39.55
10	0.07	0.08	0.07	0.08	0.00	6.10
15	0.11	0.13	0.15	0.13	0.02	13.44
20	0.18	0.15	0.19	0.17	0.02	12.51
25	0.21	0.23	0.25	0.23	0.02	9.23
30	0.28	0.30	0.32	0.30	0.02	6.34
45	0.43	0.49	0.55	0.49	0.06	12.24
60	0.62	0.77	0.81	0.73	0.10	13.75
<b>Permeation rate (mg/min)*</b>	0.009	0.007	0.010	0.009	0.002	18.498
<b>Lag time (min)</b>	1.12	0.00	1.57	0.90	0.81	90.08
<b>Ratio of rates**</b>	0.11	0.08	0.12	0.10	0.02	18.50

\* Permeation rate was calculated from amount of nicotine permeated from 5 to 20 min

\*\* Ratio of rates is the ratio of *in vitro* nicotine permeation to *in vivo* nicotine absorption rate (0.083 mg/min)

**Table E7:** Amount of nicotine permeated (mg) from stonewall as a function of the donor media flow rate (16 mL/min) and media temperature (45 °C)

<b>Time (min)</b>	<b>1</b>	<b>2</b>	<b>3</b>	<b>4</b>	<b>5</b>	<b>Mean</b>	<b>SD</b>	<b>%RSD</b>
0	0	0	0	0	0	0	0	-
1	0.02	0.03	0.03	0.04	0.04	0.03	0.01	30.17
5	0.06	0.07	0.06	0.09	0.07	0.07	0.01	18.03
10	0.11	0.14	0.11	0.15	0.13	0.13	0.02	14.69
15	0.21	0.19	0.17	0.21	0.20	0.19	0.02	9.23
20	0.23	0.25	0.23	0.29	0.25	0.25	0.03	10.19
25	0.29	0.33	0.29	0.35	0.33	0.32	0.03	8.66
30	0.34	0.39	0.38	0.41	0.38	0.38	0.03	6.89
45	0.57	0.66	0.55	0.67	0.60	0.61	0.05	8.99
60	0.76	0.95	0.77	0.95	0.80	0.85	0.10	11.22
<b>Permeation rate (mg/min)*</b>	0.012	0.012	0.011	0.013	0.012	0.012	0.001	7.604
<b>Lag time (min)</b>	0.10	1.28	1.07	1.78	1.62	1.17	0.66	56.44
<b>Ratio of rates**</b>	0.14	0.14	0.13	0.16	0.14	0.14	0.01	7.60

\* Permeation rate was calculated from amount of nicotine permeated from 5 to 20 min

\*\* Ratio of rates is the ratio of *in vitro* nicotine permeation to *in vivo* nicotine absorption rate (0.083 mg/min)

**Table E8:** Amount of nicotine permeated (mg) from powdered stonewall as a function of the donor media flow rate (16 mL/min) and media temperature (37 °C)

<b>Time (min)</b>	<b>1</b>	<b>2</b>	<b>3</b>	<b>Mean</b>	<b>SD</b>	<b>%RSD</b>
0	0	0	0	0	0	-
1	0.15	0.13	0.10	0.13	0.02	19.57
5	0.27	0.27	0.25	0.26	0.01	5.14
10	0.38	0.40	0.39	0.39	0.01	1.84
15	0.52	0.53	0.50	0.52	0.01	2.90
20	0.63	0.65	0.62	0.63	0.02	2.76
25	0.67	0.73	0.70	0.70	0.03	4.79
30	0.75	0.79	0.76	0.76	0.02	2.83
45	0.87	0.99	1.03	0.96	0.08	8.69
60	1.09	1.14	1.19	1.14	0.05	4.55
<b>Permeation rate (mg/min)*</b>	0.025	0.026	0.025	0.025	0.001	2.042
<b>Lag time (min)</b>	0	0	0	0	0	-
<b>Ratio of rates**</b>	0.30	0.31	0.30	0.30	0.01	2.04

\* Permeation rate was calculated from amount of nicotine permeated from 5 to 20 min

\*\* Ratio of rates is the ratio of *in vitro* nicotine permeation to *in vivo* nicotine absorption rate (0.083 mg/min)



**Table E9:** Method for calculation of the amount of nicotine released from stonewall as a function of donor media flow rate (mL/min) and media temperature (°C) over time

	Time (min) (A)	Dilution corrected concentration (mcg/mL) (B)*	Amount of nicotine in the volume of donor media (25 mL) (mcg) [Bx25] (C)	Amount of nicotine in the volume of donor media sampled (0.04 mL) [Cx0.04/25] (mcg) (D)	Amount of nicotine lost at each time point due to sampling (mcg) (E)	Cumulative amount of nicotine released in the donor reservoir of BTA [C+E] (mcg) (F)	Cumulative amount of nicotine released in the donor reservoir of BTA [H/1000] (mg) (G)	Amount of nicotine permeated into the receptor chamber of BTA (mg) (H)**	Total amount of nicotine released in the donor chamber of BTA (G+H) (mg)
1	0	0	0	0	0	0	0	0	0
2	A2	B2	C2=B2x25	D2=(C2x0.04)/25	E2=0	F2=C2+E2	G2=F2/1000	I2	G2+H2
3	A3	B3	C3=B3x25	D3=(C3x0.04)/25	E3=Sum of D1 to D2	F3=C3+E3	G3=F3/1000	I3	G3+H3
4	A4	B4	C4=B4x25	D4=(C4x0.04)/25	E4=Sum of D1 to D3	F4=C4+E4	G4=F4/1000	I4	G4+H4
5	A5	B5	C5=B5x25	D5=(C5x0.04)/25	E5=Sum of D1 to D4	F5=C5+E5	G5=F5/1000	I5	G5+H5
6	A6	B6	C6=B6x25	D6=(C6x0.04)/25	E6=Sum of D1 to D5	F6=C6+E6	G6=F6/1000	I6	G6+H6
7	A7	B7	C7=B7x25	D7=(C7x0.04)/25	E7=Sum of D1 to D6	F7=C7+E7	G7=F7/1000	I7	G7+H7
8	A8	B8	C8=B8x25	D8=(C8x0.04)/25	E8=Sum of D1 to D7	F8=C8+E8	G8=F8/1000	I8	G8+H8
9	A9	B9	C9=B9x25	D9=(C9x0.04)/25	E9=Sum of D1 to D8	F9=C9+E9	G9=F9/1000	I9	G9+H9
10	A10	B10	C10=B10x25	D10=(C10x0.04)/25	E10=Sum of D1 to D9	F10=C10+E10	G10=F10/1000	I10	G10+H10
* Dilution corrected concentration = Concentration (mcg/mL) x Dilution factor									
** Refer Table E0									

**Table E10:** Amount of nicotine released (mg) from stonewall as a function of the donor media flow rate (1.66 mL/min) and media temperature (37 °C)

<b>Time (min)</b>	<b>1</b>	<b>2</b>	<b>3</b>	<b>Mean</b>	<b>SD</b>	<b>%RSD</b>
0	0	0	0	0	0	-
1	0.22	0.07	0.06	0.12	0.09	77.95
5	0.37	0.40	0.19	0.32	0.11	34.90
10	0.48	0.34	0.29	0.37	0.09	25.56
15	0.51	0.45	0.39	0.45	0.06	13.25
20	0.61	0.53	0.52	0.55	0.05	9.40
25	0.68	0.72	0.59	0.66	0.07	10.54
30	0.73	0.71	0.66	0.70	0.04	5.03
45	1.12	0.91	0.86	0.96	0.14	14.21
60	1.13	1.12	1.07	1.11	0.03	2.66
<b>Release rate (mg/min)*</b>	0.0157	0.016	0.0166	0.016	0.0005	2.846
<b>Lag time (min)</b>	0	0	0	0	0	-

\* Release rate was calculated from amount of nicotine released from 1 to 60 min

**Table E11:** Amount of nicotine released (mg) from stonewall as a function of the donor media flow rate (16 mL/min) and media temperature (37 °C)

<b>Time (min)</b>	<b>1</b>	<b>2</b>	<b>3</b>	<b>Mean</b>	<b>SD</b>	<b>%RSD</b>
0	0	0	0	0	0	-
1	0.23	0.35	0.19	0.26	0.08	32.11
5	0.44	0.53	0.41	0.46	0.06	13.59
10	0.60	0.71	0.71	0.67	0.07	9.79
15	0.79	0.89	0.95	0.88	0.08	8.92
20	0.91	1.06	1.10	1.03	0.10	9.92
25	0.93	1.23	1.35	1.17	0.22	18.37
30	1.11	1.42	1.65	1.39	0.27	19.54
45	1.38	1.87	1.99	1.75	0.33	18.62
60	1.76	2.42	2.53	2.23	0.42	18.71
<b>Release rate (mg/min)*</b>	0.024	0.034	0.039	0.032	0.008	23.369
<b>Lag time (min)</b>	0	0	0	0	0	-

\* Release rate was calculated from amount of nicotine released from 1 to 60 min

**Table E12:** Amount of nicotine released (mg) from stonewall as a function of the donor media flow rate (16 mL/min) and media temperature (45 °C)

<b>Time (min)</b>	<b>1</b>	<b>2</b>	<b>3</b>	<b>Mean</b>	<b>SD</b>	<b>%RSD</b>
0	0	0	0	0	0	-
1	0.36	0.32	0.26	0.31	0.05	16.41
5	0.66	0.59	0.56	0.60	0.05	8.51
10	0.97	0.78	0.74	0.83	0.12	15.08
15	1.13	0.98	0.94	1.02	0.10	9.62
20	1.39	1.15	1.15	1.23	0.14	11.33
25	1.68	1.32	1.29	1.43	0.21	15.03
30	1.93	1.50	1.45	1.63	0.26	16.25
45	2.72	2.14	2.08	2.31	0.35	15.32
60	3.48	2.91	2.53	2.97	0.48	15.99
<b>Release rate (mg/min)*</b>	0.052	0.042	0.038	0.044	0.007	16.907
<b>Lag time (min)</b>	0	0	0	0	0	-

\* Release rate was calculated from amount of nicotine released from 1 to 60 min

**Table E13:** Amount of nicotine released (mg) from powdered stonewall as a function of the donor media flow rate (16 mL/min) and media temperature (37 °C)

<b>Time (min)</b>	<b>1</b>	<b>2</b>	<b>3</b>	<b>Mean</b>	<b>SD</b>	<b>%RSD</b>
0	0	0	0	0	0	-
1	1.15	1.03	1.07	1.08	0.06	5.67
5	1.55	1.72	1.70	1.65	0.09	5.52
10	1.77	1.96	1.93	1.88	0.10	5.35
15	2.19	1.99	2.14	2.11	0.10	4.96
20	2.03	2.29	2.26	2.19	0.14	6.47
25	2.40	2.46	2.38	2.41	0.04	1.69
30	2.42	2.52	2.41	2.45	0.06	2.62
45	2.11	2.67	2.67	2.48	0.32	12.95
60	2.42	2.83	2.55	2.60	0.21	7.95
<b>Release rate (mg/min)*</b>	0.068	0.100	0.094	0.087	0.017	19.875
<b>Lag time (min)</b>	0	0	0	0	0	-

\* Release rate was calculated from amount of nicotine released from 1 to 10 min

## VITA

Poonam Delvadia was born on Feb 1, 1983 in Gujarat, India. She earned Bachelor's in Pharmacy in 2004 and Master's in Pharmaceutics and Pharmaceutical Technology in 2006 from Gujarat University, India. Following her graduation, Poonam worked as a formulation research scientist for the division of oral product development, Sun Pharma Advanced Research Centre, India, from 2006 to 2008. Poonam joined Ph.D. graduate program in the Department of Pharmaceutics, School of Pharmacy, Virginia Commonwealth University in Fall 2009. Her Ph.D. research is focused on the "Development and evaluation of a novel biorelevant *in vitro* device for oral transmucosal products". Her research resulted in three research papers (two published and one under preparation), two posters and two podium presentations. She also presented her research work at Pfizer Inc. (Richmond, VA), Teva Pharmaceuticals (Pomona, NY) and Centre of Research and Technology (Altria, Richmond, VA). Poonam was recipient of the John Wood Award (Spring 2013), the Joseph P Schwartz Award (Fall 2012) and the Thacker Award (Fall 2010) by the Department of Pharmaceutics, VCU. She also received Altria Group Tobacco Regulatory Science Fellowship (Spring 2012) to conduct research in the area of regulation of smokeless tobacco. She is the recipient of the Pfizer Consumer Healthcare R & D Leading for Innovation Award (Spring 2013). She also received APQ Graduate Student Symposium award at AAPS (American Association of Pharmaceutical Scientist) annual meeting (Fall 2012). She was inducted into Phi Kappa Phi and Alpha Epsilon Lambda Honor Societies and received Phi Kappa Phi Scholarship (Spring 2013). In addition to her academic and research accomplishment, Poonam has served as a Graduate Teaching Assistant for several Pharm.D courses. She has also served as secretary/treasurer of the VCU AAPS Student Chapter (2010-2011) and AAPS APQ student representative (2011-2012). She is the organizer and selected moderator for upcoming 2013 AAPS symposium on "Biorelevant *in vitro* testing of non-oral dosage forms".